UNIVERSITAT POLITÈCNICA DE VALÈNCIA

DOCTORADO EN INGENIERÍA Y PRODUCCIÓN INDUSTRIAL

TESIS DOCTORAL

"Desarrollo de formulaciones derivadas de ácido poliláctico (PLA), mediante plastificación e incorporación de aditivos de origen natural"

Autor:

José Miguel Ferri Azor

Dirigida por:

Dr. Rafael Antonio Balart Gimeno

Dr. Octavio Fenollar Gimeno

Julio 2017

UNIVERSITAT POLITÈCNICA DE VALÈNCIA

DOCTORADO EN INGENIERÍA Y PRODUCCIÓN INDUSTRIAL

TESIS DOCTORAL

"Desarrollo de formulaciones derivadas de ácido poliláctico (PLA), mediante plastificación e incorporación de aditivos de origen natural"

José Miguel Ferri Azor

El Dr. Rafael Antonio Balart Gimeno, Catedrático de Universidad y el Dr. Octavio Ángel Fenollar Gimeno, Profesor del Departamento de Ingeniería Mecánica y de Materiales de la Universitat Politècnica de València como Directores de la Tesis Doctoral (modalidad Doctorado Internacional) presentada por D. José Miguel Ferri Azor, con el título "**Desarrollo de formulaciones derivadas de ácido poliláctico (PLA), mediante plastificación e incorporación de aditivos de origen natural**".

CERTIFICAN

Que la presente memoria, "**Desarrollo de formulaciones derivadas de ácido poliláctico (PLA), mediante plastificación e incorporación de aditivos de origen natural**", para aspirar al grado de Doctor por la Universitat Politècnica de València constituye la tesis doctoral de D. José Miguel Ferri Azor (modalidad Doctorado Internacional) reúne las condiciones adecuadas para constituir su tesis doctoral.

Asímismo, certifican que la citada tesis doctoral se ha realizado en el Instituto de Tecnología de Materiales de la Universitat Politècnica de València y en la Facultad de ciencia de Materiales e Ingeniería, Universitatea Transilvania din Brasov (Rumania).

Y para que conste a los efectos oportunos, firma la presente en Alcoy a 12 de Mayo de 2017.

Fdo. Rafael Antonio Balart Gimeno Fdo. Octavio Ángel Fenollar Gimeno

A Isa

"Solo teniendo la voluntad de conseguir lo imposible
se realiza lo posible"

Henri Barbusse

Agradecimientos

En primer lugar, quiero agradecer de forma muy especial a mis Directores de tesis, el Catedrático Rafael Antonio Balart Gimeno y Octavio Ángel Fenollar "Tayo". Gracias "Rafa" por la confianza y seguridad que has mostrado en todo momento en la realización de esta tesis. Tu ayuda y seguimiento han sido muy importantes para el desarrollo de ésta. Gracias por el soporte científico-técnico, por tu positividad, generosidad, por el gran apoyo personal y por tu insistencia.

¡Muchas Gracias!

Gracias Tayo por tu colaboración, apoyo y aporte de conocimientos que en muchos momentos han sido de vital importancia. Gracias.

Al Ministerio de Economía y Competitividad por el soporte financiero de este trabajo (proyecto MAT2014-59242-C2-1-R).

A la Consellería d'Educació, Cultura y Esports por el soporte financiero de este trabajo (proyecto GV/2014/008).

Al Instituto de Tecnología de Materiales (ITM) de la Universitat Politècnica de València (UPV), donde se llevó a buen puerto la presente tesis.

A la beca concedida por el programa "Erasmus +" para realizar una estancia en el extranjero. A la profesora Dana Luca Motoc por su apoyo científico y su trato personal durante los meses que estuve trabajando en el departamento de la Universidad de Transilvania, Brasov. ¡Mulțumesc!

De forma también especial al Catedrático Juan López Martínez por su apoyo e insistencia. Por su grata compañía, sus consejos y positividad. Gracias Juan.

A los profesores David García Sanoguera, Lourdes Sánchez Nácher, Teodomiro Boronat y Emilio Rayón por sus aportaciones y colaboraciones. Muchas gracias a todos.

A los técnicos de laboratorio “Javi” Balart, “Matías” Monzó y “Rafa” Guarinós por sus apoyos técnicos.

A mis compañeros de laboratorio y amigos por ser como son. Tengo que agradecer de forma muy cariñosa a los mejores compañeros de trabajo que he tenido en mi vida. María Dolores Samper Madrigal, Daniel García García, Alfredo Carbonell Verdú y Vicent Fombuena. Además de excelentes personas, sois un apoyo muy importante en la consecución de los trabajos de laboratorio.

Al profesor quiteño recién llegado Miguel Aldas, a Marina, a la profesora mexicana Alondra Ortiz, a Jennifer, Ivet, a Luis Quiles, Néstor y el resto de personas que en algún momento han trabajado en el laboratorio.

Al grupo de investigación del profesor Alfonso Jiménez de la Universidad de Alicante por prestarme su equipamiento. En especial a Nuria Burgos por su ayuda y consejos.

A todos mis amigos por su apoyo fuera de los laboratorios. Gracias por los buenos momentos que me habéis hecho pasar. Franz, Nandez, El Pintor, Amando, Chals, Albu, Chechu, Serra, José “Abogado”, Vicentico, Mirian, Pucho, Laura, Victor, Ivonne, Robison, Pedro, Pepito, Roget y muchos más. ¡Gracias!

A Irene, en primer lugar, por tener que soportar los duros días de escritura de la tesis y por tu ayuda diaria. Por tu insistencia y comprensión. ¡Muchas Gracias!

A mi familia, en especial a mi madre, Isa, por hacer posible que yo haya llegado hasta aquí. Gracias por hacer que todo sea más fácil y por apoyar mis decisiones en todo momento. Por la gran confianza y la lucha incesante para que esto haya llegado a este punto. A Yaiza y a la “chacha Encarna” que a pesar de estar lejos, siempre ha estado tan cerca.

¡¡¡Muchísimas Gracias!!!

Para finalizar, quiero dar las gracias a otras personas que, además de ser un apoyo muy grande para mí y mi familia, han prestado un especial interés en que éste

momento llegara. Merecen su nombramiento en esta tesis, Ana García Segovia por su apoyo y ayuda incondicional y desinteresada sobre la defensa de los derechos de las personas. Gracias Ana por la ayuda que nos das en los malos momentos y por ser como eres. A María Ángeles Aguiñiga y su hijo Marcel por cuidar y ayudar a mi familia y por mostrarnos su interés y apoyo extraordinario. A Amparo Albors por ser un apoyo importante en la familia, por tu humildad y tu fuerza. A las tres, *Mil Gracias* por formar parte de mi familia.

!!!Muchas gracias a todos!!!

RESUMEN

"Desarrollo de formulaciones derivadas de ácido poliláctico (PLA), mediante plastificación e incorporación de aditivos de origen natural"

El objetivo principal de esta tesis doctoral es el estudio, desarrollo y caracterización de materiales biodegradables o biocompatibles de ácido poliláctico (PLA) con propiedades mejoradas para su aplicación en diversos sectores como el envasado de alimentos, sector médico, etc. Para modificar la ductilidad o rigidez del PLA y con ello su aptitud en los distintos campos, se lleva a cabo un estudio de la incorporación de diferentes cargas o aditivos, mediante mezclado por extrusión. Se han utilizado plastificantes derivados de aceites vegetales y ácidos grasos; en particular, un plastificante epoxidado derivado del ácido esteárico (epoxi estearato de octilo – OES) y un derivado maleinizado de aceite de linaza – MLO. Otra de las estrategias que se han abordado se ha centrado en el desarrollo de mezclas binarias con otros biopolímeros con mayor ductilidad como la policaprolactona (PCL) y el almidón termoplástico (TPS). Finalmente, se ha llevado a cabo la incorporación de cargas biocompatibles tipo ortofosfato cálcico ($Ca_3(PO_4)_2$) como el β-fosfato tricálcico (β-TCP) y la hidroxiapatita (HA) para ampliar el potencial de estos materiales basados en PLA en el sector médico.

En primer lugar, se realizan formulaciones base PLA mediante mezclas físicas o *blends* con polímeros biodegradables flexibles como la PCL y el TPS, con un contenido máximo de hasta un 30 wt% de éstos, mediante procesos de extrusión/compounding, seguidos de inyección. Los resultados obtenidos muestran ligeras diferencias sobre la ductilidad, ya que se trata de sistemas con una miscibilidad restringida. El alargamiento a la rotura es superior para el sistema de mezclas PLA/PCL. Sin embargo, la cristalinidad del PLA aumenta más cuando se incorporan pequeñas cantidades de TPS. Cabe destacar que la absorción de energía a impacto mejora para las mezclas con TPS y empeora sensiblemente con la incorporación de PCL. Este hecho se debe a la baja miscibilidad entre el PLA y la PCL. Si bien el almidón puro también es inmiscible con el PLA, el grado comercial empleado contiene plastificantes y un poliéster alifático/aromático biodegradable que mejora ligeramente la interacción

PLA/TPS. Debido a esta relativamente baja miscibilidad entre los componentes de las mezclas binarias PLA/PCL y PLA/TPS, las principales transiciones térmicas no se ven afectadas en gran medida.

En relación al empleo de plastificantes derivados de aceites vegetales y ácidos grasos, los resultados obtenidos muestran gran potencial para formulaciones de PLA con ductilidad mejorada para aplicaciones industriales. Con el empleo de un epoxi estearato de octilo (OES) se consigue una interesante reducción en la temperatura de transición vítrea (T_g), temperatura de cristalización fría (T_{cc}) así como un notable aumento del alargamiento a la rotura ($\varepsilon_{\%}$) y la capacidad de absorción de energía al impacto Charpy. Además, la cristalinidad aumenta como consecuencia de una mayor movilidad de las cadenas poliméricas. Estos materiales se han procesado en forma de film y ofrecen una menor permeabilidad al oxígeno y una mayor hidrofobicidad. Sobre la estabilidad térmica no se observaron cambios significativos. Por otro lado, el empleo de pequeñas cantidades de un plastificante maleinizado derivado del aceite de linaza (MLO) permite alcanzar niveles de alargamiento a la rotura superiores a los obtenidos con el plastificante OES, así como una mejora en las propiedades a impacto sin comprometer la rigidez de los materiales plastificados. El incremento de movilidad de las cadenas poliméricas que aporta el MLO permite reducir el valor de la T_g y el pico de la cristalización en frío y ello repercute en un incremento de la cristalinidad dando lugar a una serie de materiales con ductilidad y rigidez mejorada. Además de las excelentes propiedades de plastificación que aporta el MLO, se ha corroborado su función de compatibilización en el sistema PLA/TPS con cantidades de MLO comprendidas entre 2-8 phr. Estas mezclas compatibilizadas muestran una morfología homogénea y ofrecen una mejor absorción al impacto con el contenido en compatibilizante. En cuanto a las propiedades resistentes, se mantienen en niveles similares a los correspondientes a las mezclas sin compatibilizar. Todos los materiales basados en PLA con plastificantes y mezclas con polímeros más flexibles ofrecen propiedades de flexibilidad mejorada, lo cual amplía sus usos en el sector envase/embalaje.

Finalmente, se ha estudiado el efecto que ejercen varias cargas biocompatibles/bioabsorbibles de la familia de los ortofosfatos (β-TCP y HA) sobre las propiedades mecánicas, térmicas y termomecánicas del PLA con el fin de establecer su potencial en el sector médico. Ambos tipos de partículas muestran un efecto nucleante del proceso de cristalización en frío, lo que aporta una mayor rigidez a dichos composites. Aunque como refuerzo se comporten de forma similar, muestran diferencias sobre otras propiedades. En términos de estabilización térmica, la HA tiene un efecto positivo sobre el PLA, mientras que el β-TCP no solo no mejora, sino que en grandes proporciones empeora la estabilidad debido al carácter higroscópico que tienen estas últimas. Desde el punto de vista de las propiedades mecánicas, se consigue alta rigidez con composiciones en β-TCP y HA de hasta un 30% en peso.

Con esta tesis doctoral se amplían las posibilidades tecnológicas de las formulaciones de PLA para aplicaciones industriales en el sector envase-embalaje con plastificantes derivados de aceites vegetales y mezclas binarias con polímeros biodegradables flexibles como PCL y TPS. Por otro lado, la incorporación de cargas de ortofosfatos ofrece un grupo de materiales con amplias posibilidades en el sector médico debido a su bicompatibilidad y bioabsorción.

RESUM

"Desenvolupament de formulacions derivades d'àcid polilàctic (PLA), mitjançant plastificació i incorporació d'additius d'origen natural"

L'objectiu principal d'aquesta tesi doctoral és l'estudi, desenvolupament i caracterització de materials biodegradables i biocompatibles d'àcid polilàctic (PLA) amb propietats millorades per a la seua aplicació en diversos sectors com ara l'envasat d'aliments, sector mèdic, etc. Per tal de modificar la ductilitat o rigidesa del PLA, i amb això, la seua aptitud en els esmentats camps, s'ha fet un estudi de la incorporació de diferents càrregues o additius, mitjançant mesclat per extrusió. S'han utilitzat plastificants derivats d'olis vegetals i àcids grassos; en particular, un plastificant epoxidat derivat de l'àcid esteàric (epoxi estearat d'octil – OES) i un derivat maleinitzat d'oli llinós – MLO. Una altra estratègia que s'ha seguit s'ha centrat en el desenvolupament de mescles binàries amb altres polímers amb major ductilitat com ara la policaprolactona (PCL) i el midó termoplàstic (TPS). Finalment, s'ha dut a terme la incorporació de càrregues biocompatibles de tipus ortofosfat càlcic ($Ca_3(PO_4)_2$) com ara el β-fosfat tricàlcic (β-TCP) i la hidroxiapatita (HA) per tal d'ampliar el potencial d'aquests materials basats en PLA al sector mèdic.

En primer lloc, es realitzen formulacions amb base PLA mitjançant mescles físiques o *blends* amb d'altres polímers biodegradables flexibles com la PCL i el TPS, amb un contingut màxim de fins el 30% en pes d'aquests, utilitzant processos d'extrusió/*compounding* seguits de moldeig per injecció. Els resultats obtinguts mostren lleugeres diferències sobre la ductilitat, ja que es tracta de sistemes amb una miscibilitat restringida. L'allargament a la ruptura és superior per al sistema PLA/PCL. Malgrat això, la cristal·linitat del PLA augmenta més quan s'incorporen petites quantitats de TPS. Cal destacar que l'absorció d'energia a impacte millora per a les mescles amb TPS i empitjora sensiblement amb la incorporació de PCL. Aquest fet està lligat a la baixa miscibilitat entre el PLA i la PCL. Si bé el midó pur és també immiscible amb el PLA, el grau comercial utilitzat conté plastificants així com un polièster alifàtic/aromàtic biodegradable que milloren lleugerament la interacció

PLA/TPS. Com a conseqüència d'aquesta baixa miscibilitat entre els components de les mescles binàries PLA/PCL i PLA/TPS, les principals transicions tèrmiques no es veuen afectades en gran mesura.

Pel que fa a la utilització de plastificants derivats d'olis vegetals i àcids grassos, els resultats obtinguts demostren el gran potencial per a formulacions de PLA amb ductilitat millorada per a possibles aplicacions industrials. Amb la utilització d'un epoxi estearat d'octil (OES) s'aconsegueix una interessant reducció en la temperatura de transició vítria (T_g), temperatura de cristal·lització en gelat (T_{cc}) així com un notable augment de l'allargament a la ruptura ($\varepsilon_{\%}$) i la capacitat d'absorció d'energia d'impacte Charpy. A més a més, la cristal·linitat augmenta com a conseqüència d'una major mobilitat de les cadenes polimèriques. Aquests materials s'han processat en forma de pel·lícula i ofereixen una permeabilitat a l'oxigen reduïda així com una major hidrofobicidad. En relació a l'estabilitat tèrmica, no s'observen canvis significatius. Per altra banda, la utilització de petites quantitats d'un plastificant maleinitzat derivat de l'oli llinós (MLO) permet aconseguir nivells d'allargament a la ruptura superiors als obtinguts amb el plastificant OES, així com una millora en les propietats a impacte sense comprometre la rigidesa dels materials plastificats. L'increment de la mobilitat de les cadenes polimèriques que aporta el MLO permet reduir el valor de la T_g i el pic de temperatura corresponent a la cristal·lització en gelat i això condueix a una sèrie de materials amb ductilitat i rigidesa millorades. A més a més de les excel·lents propietats de plastificació que aporta el MLO, s'ha validat la seua funció com a compatibilitzador en el sistema PLA/TPS amb quantitats de MLO en el rang de 2-8 phr. Aquestes mescles compatibilitzades ofereixen una morfologia homogènia així com una absorció d'energia a l'impacte tant millor com més alt contingut en compatibilitzant. Tots aquests materials basats en PLA amb plastificants i mescles amb polímers més flexibles ofereixen propietats de flexibilitat millorada, la qual cosa amplia els seus potencials usos en el sector envàs/embalatge.

Finalment s'ha estudiat l'efecte que exerceixen diferents càrregues biocompatibles/bioabsorbibles de la família dels ortofosfats (β-TCP i HA) sobre les propietats mecàniques, tèrmiques i termomecàniques del PLA amb la finalitat

d'establir el seu potencial al sector mèdic. Ambdós tipus de partícules mostren un clar efecte nucleant del procés de cristal·lització en gelat, la qual cosa aporta una major rigidesa als esmentats compòsits. Malgrat que a nivell de reforç es comporten de forma similar, mostren algunes diferències en algunes propietats. En termes d'estabilització tèrmica, la HA té un efecte positiu sobre el PLA, mentre que el β-TCP no sols no millora, sinó que en grans proporcions, fins i tot empitjora l'estabilitat tèrmica com a conseqüència del seu caràcter higroscòpic. Des del punt de vista de les propietats mecàniques, s'aconsegueix una alta rigidesa amb composicions amb β-TCP i HA de fins un 30% en pes.

Amb aquesta tesi doctoral s'amplien les possibilitats tecnològiques de les formulacions de PLA per a aplicacions industrials en el sector de l'envàs-embalatge amb plastificants derivats d'olis vegetals i mescles binàries amb polímers biodegradables flexibles com ara la PCL i el TPS. D'altra banda, la incorporació de càrregues d'ortofosfats ofereix un grup de materials amb àmplies possibilitats al sector mèdic com a conseqüència de la seua biocompatibilitat i bioabsorció.

SUMMARY

"Development of polylactic acid (PLA)-derived formulations by plasticization and additives from renewable resources"

The main objective of this doctoral thesis is the study, development and characterization of biodegradable or biocompatible materials from poly(lactic acid) (PLA) with improved properties for uses in several sectors such as food packaging, medical sector, etc. In order to modify the ductility and the stiffness of PLA, with the subsequent effects on its potential uses in different sectors, different fillers and/or additives were incorporated to PLA formulations by extrusion. Several plasticizers derived from vegetable oils and fatty acids were used; particularly, an epoxidized plasticizer derived from stearic acid (octyl epoxy stearate – OES) and a maleinized linseed oil – MLO were used. Another strategy that has been used in this research has focused on the development of binary blends with other polymers with increased ductility such as polycaprolactone (PCL) and thermoplastic starch (TPS). Finally, incorporation of several biocompatible/resorbable fillers derived from calcium orthophosphate ($Ca_3(PO_4)_2$) such as β-tricalcium phosphate (β-TCP) and hydroxyapatite (HA), was carried out to widen the potential of these PLA-based materials in medical applications.

Initially, physical blends of PLA with flexible biodegradable polymers (PCL and TPS) with a maximum content of 30 wt% of them, were obtained by extrusion/compounding and subsequent processed by injection moulding. The obtained results suggest slight differences in ductility as both binary systems seen to show restricted miscibility. The elongation at break is higher for the system PLA/PCL. Nevertheless, PLA's crystallinity increases with small TPS loads. It is worthy to note that the energy absorption is better for the PLA/TPS system compared to the counterpart compositions of the PLA/PCL system. This phenomenon is directly related to the low miscibility of PLA and PCL. Although pure starch is also immiscible with PLA, its commercial thermoplastic form includes some plasticizers and an aliphatic/aromatic biodegradable polyester that contribute to improve PLA/TPS

interactions. As a consequence of this relatively low miscibility between binary PLA/PCL and PLA/TPS blends, the main thermal transitions do not change in a great extent.

Regarding the use of plasticizers from vegetable oils and fatty acids, the obtained results show interesting potential for industrial PLA formulations with improved ductility. By using octyl epoxy stearate (OES), a noticeable decrease in the glass transition temperature (T_g) and in the cold crystallization temperature (T_{cc}) occurs together with a remarkable increase in the elongation at break ($\varepsilon_{\%}$) and the energy absorption in a Charpy's test. In addition, the overall crystallinity increases due to the higher chain mobility. These materials have been also processed in a film form and show lower oxygen permeability and a higher hydrophobicity. No important changes in thermal stability were observed. On the other hand, slow amounts of maleinized derivative from linseed oil (MLO) allowed reaching higher elongation at break values than those obtained with OES, as well as a remarkable improvement on impact behavior without compromising the overall stiffness properties. The increase in chain mobility that MLO provides allows reducing the T_g and the cold crystallization peak temperature (T_{cc}) and this has a positive effect on crystallinity thus leading to materials with both improved ductility and stiffness. In addition to the excellent plasticization properties that MLO provides, this research assesses its potential as compatibilizer agent in the binary PLA/TPS blend with relatively low MLO amounts in the 2-8 phr. These compatibilized blends offer a homogeneous morphology and show a direct relationship between the overall impact-absorbed energy and MLO content. With regard to resistant properties, they keep almost constant with similar values to those of the uncompatibilized PLA/TPS blend. All these PLA-based materials with plasticizers and blends with other polymers offer interesting flexible properties, which widens its potential in the packaging industry.

Finally, the effect of different biocompatible/resorbable fillers from orthophosphates (β-TCP and HA) on mechanical, thermal and thermomechanical properties was evaluated with the aim of increasing the potential of these PLA-based formulations in the medical sector. Both particles show a nucleant effect on the cold

crystallization process thus leading to increased stiffness on composites. Although both reinforcing fillers offer similar performance, some differences can be seen regarding other properties. So, in terms of thermal stabilization, HA has a positive effect on PLA while β-TCP leads to lower thermal stability due to its high hygroscopic behavior. From a mechanical performance standpoint, good-balanced mechanical resistant properties are obtained with PLA formulations with 30 wt% β-TCP and HA.

With this doctoral thesis, the technologic potential of PLA formulations for industrial applications in the packaging industry is increased by using natural-derived plasticizers from vegetable oils and binary blends with flexible, biodegradable polymers such as PCL and TPS. On the other hand, addition of orthophosphate fillers into PLA matrix increases the potential of this polymer in the field of medical devices due to their biocompatibility and resorbability.

Tabla de contenidos

ECUACIONES.

$X_c\ (\%) = \frac{\Delta H_m - \Delta H_{cc}}{w\ \Delta H_m^0} 100$	$\mathbf{X_c}$ **=** grado de cristalinidad $\Delta\mathbf{H_m}$ **=** entalpía de fusión $\Delta\mathbf{H_{cc}}$ **=** entalpía de cristalización $\Delta\mathbf{H^0_m}$ **=** entalpía de fusión teórica material 100% cristalino w = fracción en masa del polímero
$D\ (\%) = \frac{m_i - m_f}{m_i} 100$	D = desintegración en porcentaje m_i = masa inicial m_f = masa final (tiempo de incubación)
$\Delta G = \Delta H - T \cdot \Delta S$	ΔG **=** variación de energía libre de Gibbs $\Delta\mathbf{H}$ **=** variación de la entalpía (mezclado) **T =** temperatura absoluta ΔS **=** entropía (mezclado)
$\delta = D \cdot \Sigma G\ /\ M_n$	δ **=** parámetro de solubilidad D **=** densidad ΣG **=** sum. de cte de atracción molar M_n **=** masa molar promedio en número por unidad repetitiva

ABREVIATURAS Y TÉRMINOS.

AAPE	copoliéster alifático aromático biodegradable
ABR	acetil butil ricinoleato
APS	aminopropiltrietoxisilano
ASA	anhídrido alquenil succinico
ASCs	células madre adiposas
ATEC	citrato de acetiltrietilo
ATBC	citrato de acetil-tri-n-butilo
BCP	fosfato bicálcico
BioPAs	biopoli(amidas)
BioPCs	biopoli(carbonatos)
BioPET	biopoli(etilen tereftalato)
b-HA	hidroxiapatita de hueso bovino
Ca/P	relación calcio/fosfato
CLTE	coeficiente térmico de expansión lineal
CNC	nanocristales de celulosa
CoCr	aleación metálica cromo cobalto
CoCrMo	aleación metálica de molibdeno cromo cobalto
CO	aceite de colza
D(%)	desintegración en porcentaje
D	densidad
DIDA	diisodecil adipato
DMA	análisis dinamo-mecánico
DMTA	análisis térmico y dinamomecánico
DOA	2 etilhexil adipato
DSA	analizador de forma de la gota
DSC	calorimetría diferencial de barrido
DTG	derivada de la masa frente a la temperatura
e	espesor
E	módulo elástico o de Young

ECO	aceite de ricino epoxidado
ECSO	aceite de semilla de algodón epoxidado
EG	etilen glicol
ELO	aceite de linaza epoxidado
EPO	aceite de palma epoxidado
ESBO (ESO)	aceite de soja epoxidado
ESFO	aceite de girasol epoxidado
EVOs	aceites vegetales epoxidados
FESEM	microscopía electrónica de barrido de emisión de campo
FS	resistencia a flexión
FTIR	espectroscopía infrarroja por transformada de Fourier
G	constantes de atracción molar
G′	módulo de almacenamiento
G″	módulo de pérdidas
GMA	glicidil metacrilato
HA	hidroxiapatita
HCl	ácido clorhídrico
HDI	hexametileno de diisocianato
HDT	temperatura de flexión bajo carga
HPMC	hidroxipropil metilcelulosa
HPLC	cromatografía líquida de alta resolución
HV	hidroxivalerato
IR	infrarrojos
LO	aceite de linaza
L/D	relación longitud/diámetro de husillo
$\mathbf{m_i}$	masa inicial de la muestra
$\mathbf{m_f}$	masa final de la muestra
$\mathbf{M_n}$	masa molar promedio
$\mathbf{M_w}$	peso molecular
MA	anhídrido maleíco
MCP	fosfato monocálcico

MCPM	fosfato monocálcico monohidratado
MFI	índice de fluidez
MLO	aceite de linaza maleinizado
MMA	metil metacrilato
MSCs	células madre mesenquimatosas
n-HA	nanopartículas de hidroxiapatita
OES	epoxi estearato de octilo (derivado del ácido esteárico)
OLAs	oligómeros de ácido láctico
OTR	velocidad de transmisión de oxígeno
OTR.e	velocidad de transmisión de oxígeno por el espesor del film
OXA	oxiapatita
PA	poli(amida)
PA6	poli(amida) 6
PA66	poli(amida) 66
PA610	poli(amida) 610
PBAT	poli(butileno adipato-co-tereftalato)
PBS	poli(butileno succinato)
PBSA	poli(butileno succinato-co-adipato)
PCL	poli(ε-caprolactona)
PDLA	poli(D-ácido láctico)
PE	poli(etileno)
PEA	poli(ester amidas)
PEG	poli(etilenglicol)
PEO	óxido de poli(etileno)
PET	poli(etileno tereftalato)
PGA	poli(ácido glicólico)
PHAs	poli(hidroxialcanoatos)
PHB	poli(hidroxibutirato)
PHV	poli(hidroxivalerato)
PHBV	poli(hidroxibutirato-co-valerato)
PLA	poli(ácido láctico)

PLACL	poli(ácido láctico)-co-poli(ε-caprolactona)
PLGA	poli(ácido láctico-co-glicólico**)**
PLLA	poli(L-ácido láctico)
PMMA	poli(metil metacrilato)
PO_4^{3-}	fosfato
PP	poli(propileno)
PPG	poli(propilen glicol)
PS	poli(estireno)
PU	poli(uretano)
PVC	poli(cloruro de vinilo)
PVOH	poli(vinil alcohol)
Py-GC/MS	pirólisis-cromatografía de gases/espectrometría de masas.
ROP	polimerización por apertura de anillo
SBO	aceite de semilla de soja
SEM	microscopía electrónica de barrido
SO	aceite de soja
SPLA	oligómero de ácido láctico terminado con sorbitol
sc-PLA	estereocomplejos de PLA
tan (δ)	tangente de la relación entre (G'') y (G')
T	temperatura absoluta
TBC	citrato de tributilo
TEC	citrato de trietilo
TGA	análisis termogravimétrico
TGA/SDTA	análisis termogravimétrico/termogravimétrico diferencial
Ti6Al4V	aleación metálica de titanio-aluminio-vanadio
TMA	análisis termomecánico
TMO	trimelitato de octilo
TPEO	almidón termoplástico mezclado con óxido de poli(etileno)
TPS	almidón termoplástico
TS	resistencia a la tracción
T_{cc}	temperatura de cristalización en frío

$\mathbf{T_g}$	temperatura de transición vítrea
$\mathbf{T_m}$	temperatura de fusión
$\mathbf{T_{max}}$	velocidad máxima de degradación
$\mathbf{T_{90}}$	temperatura a la que se pierde un 90% del peso por degradación
$\mathbf{T_5}$	temperatura a la que se pierde un 5% del peso por degradación
UV	ultravioleta
V	volumen
VOs	aceites vegetales
VST	temperatura de reblandecimiento Vicat
w	fracción en peso del PLA
β-TCP	fosfato tricálcico tipo β
α-TCP	fosfato tricálcico tipo α
α	coeficiente térmico de expansión lineal
$\Delta\mathbf{G}$	variación de la energía libre de Gibbs
$\Delta\mathbf{H}$	variación de la entalpía (calor de mezclado)
$\Delta\mathbf{H_{cc}}$	entalpía de cristalización en frío
$\Delta\mathbf{H_m}$	entalpía de fusión
$\Delta\mathbf{H^0_m}$	valor teórico de la ΔH_m suponiendo un χ_c del 100%
$\mathbf{\Delta S}$	variación de la entropía de mezclado
ε	alargamiento a la rotura
δ	parámetro de solubilidad
ν	coeficiente de Poisson
$\sum\mathbf{G}$	sumatorio de constantes de atracción molar
$\mathbf{\chi_c}$	grado de cristalinidad

LISTADO DE FIGURAS.

LISTADO DE TABLAS.

I. INTRODUCCIÓN

INTRODUCCIÓN

I.1. BIOPOLÍMEROS EN INGENIERÍA.

En la actualidad se presenta una grave problemática medioambiental en nuestro entorno debido a los residuos poliméricos de origen petroquímico generados. Cerca de 10 millones de toneladas de materiales no degradables se vierten a los océanos cada año, y las previsiones apuntan a un mayor crecimiento en los años venideros, debido al crecimiento de población a nivel mundial. Éste es el problema más visible que impacta a los expertos, ya que se generan grandes aglomeraciones de residuos en el océano, de los cuales, la mayoría son materiales poliméricos de degradación extremadamente lenta. Esta situación genera problemas en la biodiversidad, debido a que los animales quedan atrapados en estos residuos. Además, los plásticos liberan aditivos muy tóxicos que alteran el equilibrio de la cadena alimenticia del océano, ya que éstos tóxicos alteran la producción de plancton, que es la base de dicha cadena. Realmente aquí no termina el problema; además gran parte de los residuos generados son incinerados, enterrados y/o acumulados en vertederos controlados, con la consecuente liberación de gases tóxicos a la atmósfera, contaminación de aguas subterráneas e impacto visual generado.

Es por todo esto que los gobiernos están proponiendo estrategias comunes y generando nuevas normativas para, entre otras cosas, sustituir los materiales convencionales por otros que no generen impacto ambiental o se minimice.

Los materiales poliméricos biodegradables o polímeros verdes, así como los compuestos generados a partir de éstos ("*green composites*")[1-3], se presentan como una alternativa necesaria para frenar esta catástrofe natural creciente. Los polímeros obtenidos a partir de fuentes fósiles tienen una vida útil limitada en el ciclo de reciclado debido a su degradación durante el procesado, pero aún no reciclándose, las reservas de petróleo, precursor de éstos y muchos otros derivados, tienen también los años contados. Por tanto, se está llevando una intensa investigación enfocada, en gran parte, hacia la sustitución de éstos por otros obtenidos de fuentes naturales, de "un solo uso", que al final de su vida útil vuelvan a formar parte del entorno, cerrando el ciclo de vida. Para que esto pueda ocurrir dichos polímeros deben ser biodegradables y

compostables en condiciones ambientales en un tiempo relativamente corto. Más concretamente, se requiere que estos materiales sean desintegrables en condiciones de compost controlado, dando lugar a una completa desaparición del residuo plástico generado.

Los polímeros biodegradables son aquellos que se degradan a través de una acción enzimática y/ó reacciones químicas coligadas con determinados organismos vivos (bacterias, hongos, etc.) y sus productos intermedios. En esta definición, se consideran las reacciones abióticas (como pueden ser la fotooxidación, oxidación e hidrólisis) como reacciones que afectan al polímero antes, durante o en lugar de la biodegradación causada por los factores ambientales.

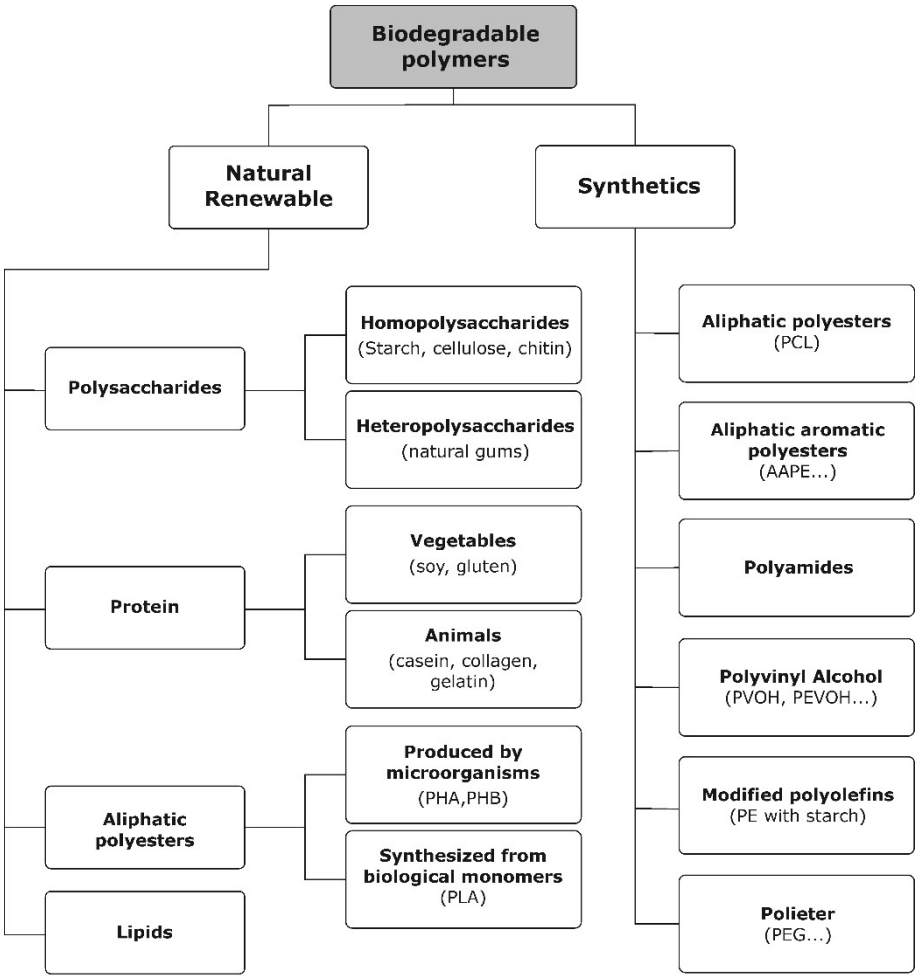

Figura I.1. Esquema de clasificación de polímeros biodegradables y biocompostables de origen natural y sintético.

Un material puede ser biodegradable y no compostable. Estos no interesan desde el punto de vista de la ingeniería y la industria. Los que cumplen un ciclo cerrado de vida son los compostables. Los materiales compostables [3–5] son, además de biodegradables en condiciones de compostaje con degradación controlada, los que cumplen con las especificaciones o estándares de calidad recogidos por la normativa al respecto [6]. En general estos materiales no deben generar residuos visibles, ecotoxicidad, tamaños y espesores mayores a los que determinan las normativas, contenidos de metales pesados, etc. Los materiales están sometidos a una evaluación por parámetros de calidad del compost y es de ésta forma como se determina su compostabilidad.

Los materiales biodegradables (**Figura I.1**) de acuerdo a su procedencia u origen se pueden clasificar como: polímeros **renovables** ó **naturales**, que son los polímeros obtenidos a partir de recursos naturales; y polímeros **sintéticos**, que son procedentes de fuentes fósiles/petroquímicas.

I.1.1. Polímeros de origen petroquímico biodegradables.

Los polímeros sintéticos biodegradables cuyo precursor es el petróleo tienen ciertas particularidades en su síntesis que los hacen biodegradables. Aunque realmente la síntesis de polímeros aporte una gran variedad de éstos, con propiedades casi a la carta, la fluctuación en el precio que dicho precursor tiene y su abundancia limitada los hace poco atractivos desde el punto de vista del investigador. Por ejemplo, los poliésteres alifáticos como la poli(caprolactona) -PCL, poliésteres alifático-aromáticos, poli(amidas) - PA66, PA6, PA610, etc. entre otras, poli(vinil alcohol) - PVOH, poliolefinas modificadas como los desarrollos con poli(etileno) modificado con almidón, y poliéteres tipo poli(etilén glicol) - PEG. Éstos no son los únicos polímeros de

origen petroquímico con propiedades de biodegradación. En general, los poliésteres alifáticos (e incluso algunos aromáticos), poseen las condiciones adecuadas para poder desintegrarse en condiciones de compost, fundamentalmente, debido a las reacciones de hidrólisis. Entre estos polímeros, destaca el uso crecience de poli(butilén succinato) – PBS, poli(butilén succinato-co-adipato) – PBSA, poli(butilén adipato-co-tereftalato) – PBAT, etc. cuya estructura química se muestra en la **Figura I.2** [135,136].

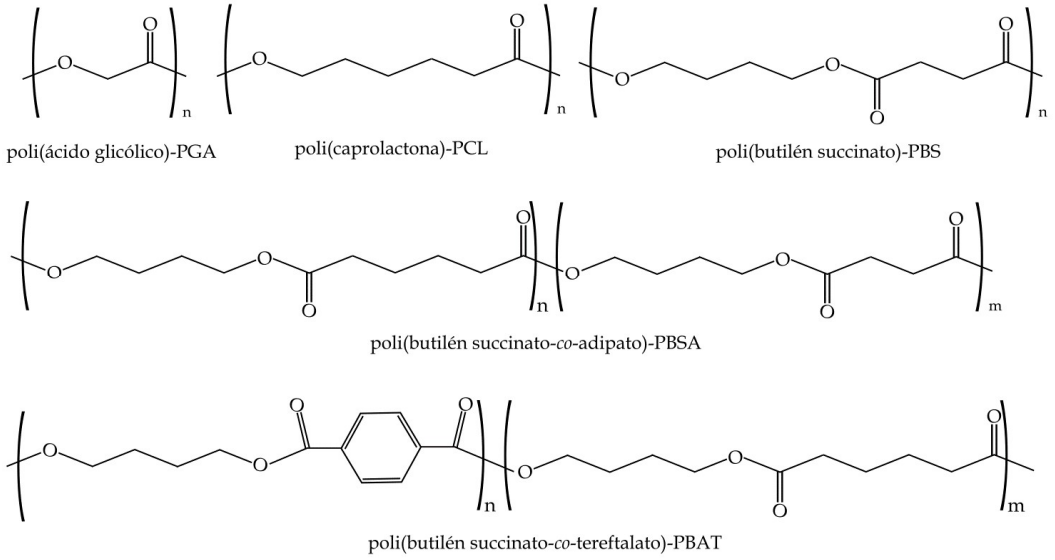

Figura I.2. Representación esquemática de la estructura de diversos poliésteres biodegradables (desintegrables en condiciones de compost) por reacciones de hidrólisis.

I.1.2. Polímeros de origen renovable, biodegradables y no biodegradables.

Se denominan polímeros de origen renovable a los producidos a partir de fuentes naturales o renovables. Los hay de muchos tipos y obtenidos de distintas fuentes naturales.

Dentro del grupo de polímeros naturales tenemos los *polisacáridos* que se dividen en homopolisacáridos y heteropolisacáridos. Los homopolisacáridos más utilizados son el almidón, celulosa y la quitina. Los heteropolisacáridos suelen ser gomas naturales (goma arábiga), pectinas, hemicelulosas, agar-agar, mucílagos, peptidoglucanos y glucosaminoglucanos (ácido hialurónico, heparina).

Las **proteínas** son otro grupo de polímeros naturales. Éstas se clasifican en dos grupos, las vegetales y las animales. Las primeras se obtienen de plantas, siendo los más comunes el gluten y soja. Las proteínas más conocidas y utilizadas de procedencia animal son la gelatina, caseína y colágeno.

Los **lípidos** están formados o bien por cadenas alifáticas o alifáticas con anillos aromáticos, pueden ser saturados o insaturados, hay una gran diversidad de tipos, entre ellos, las grasas, céridos, etc.

Finalmente existe un cuarto grupo, que son los **poliésteres alifáticos**. Éstos pueden producirse gracias a microorganismos (PHA, PHB) o a partir de la síntesis de monómeros naturales (PLA). La **Figura II.3** muestra un esquema de estos polímeros obtenidos a partir de la fermentación del almidón (PLA), o fermentación bacteriana (diversos PHAs).

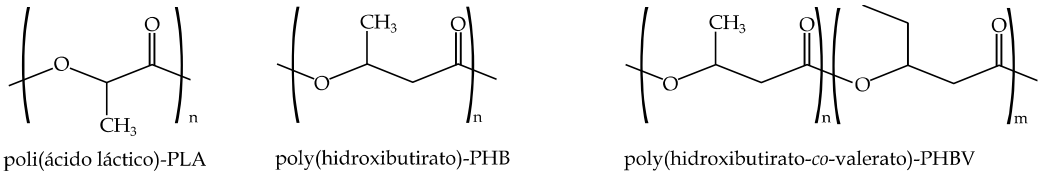

Figura I.3. Representación esquemática de la estructura de diversos poliésteres biodegradables de origen renovable.

Los polihidroxialcanoatos los producen bacterias específicas (ej: *Alcaligenes Eutrophus*); éstas se someten a unas condiciones ambientales específicas con glucosa para que se multipliquen y cuando se genera una cantidad suficiente se cambian las condiciones y se les vuelve a añadir glucosa. Bajo unas condiciones determinadas, las

bacterias dejan de reproducirse, se estresan, consumen e invierten dicha glucosa consumida para generar el polímero deseado.

Los polímeros producidos a partir de monómeros tipo L-ácido láctico o 2-hidroxiácido propanoico como la familia de los PLA, se sintetizan o bien por condensación/esterificación directa del ácido láctico, o bien por apertura del anillo del dímero cíclico láctico [7,8].

Por otra parte, también se pueden obtener polímeros a partir de fuentes naturales y éstos no ser degradables. Este es el caso del biopolietileno producido a partir de bioetanol. Otros polímeros de origen renovable (o cierto contenido renovable) pero que no presentan biodegradabilidad incluyen algunas poli(amidas) – BioPAs, poli(carbonatos) – BioPCs, poli(etilén tereftalato) – BioPET, etc. que paulatinamente se van incorporando a diversos mercados con cierta connotación medioambiental, pero sin alcanzar la biodegradación [133,134].

I.2. TECNOLOGÍA DE ÁCIDO POLILÁCTICO (PLA).

El PLA, es uno de los polímeros biodegradables tecnológicamente más desarrollado en los últimos años a nivel mundial y europeo [4]. Esto se debe principalmente a la abundancia de sus precursores, por su gran aplicabilidad en diferentes sectores industriales y por sus buenas características mecánicas. El monómero de partida necesario para la polimerización es el ácido láctico obtenido de la transformación del almidón extraído a partir de recursos renovables (alimentos o plantas), como el maíz [5-8], trigo [9], tapioca [10], patata [11], caña de azúcar[12], remolacha azucarera [7] y a partir de la celulosa extraída de bagazos como el de la caña de azúcar u otros [5, 13, 14] o incluso de la celulosa obtenida de árboles [15]. La buena procesabilidad del PLA [16], lo hace compatible para ser transformado en la maquinaria convencional de conformado de polímeros de uso común ("*commodities*") sintetizados a partir de fuentes fósiles.

Una vez finalizada su vida útil, los productos fabricados en base a PLA, gracias a su biodegradabilidad y capacidad de desintegración en condiciones de compostaje [17, 18], pueden recorrer varios caminos para ser aprovechados de alguna forma. Al igual que los polímeros convencionales, el PLA puede ser reciclado mecánicamente para volver a ser utilizado como polímero, aunque sus propiedades se ven mayormente afectadas que si se tratara de un polímero con origen fósil ya que la hidrólisis reduce el peso molecular del PLA a lo largo de su vida útil y en las acciones de reprocesado, ya que la temperatura favorece estas reacciones. Otra opción para ser utilizado, es a través del reciclado químico, mediante hidrólisis, consiguiendo ácido láctico y posteriormente volver a polimerizar [19]. Un segundo camino es, que el PLA pase a formar parte de la biomasa en las plantas de selección de residuos urbanos o industriales, por tratarse de un material compostable [20].

El PLA es un poliéster alifático resultado de la polimerización del ácido láctico, producto de la fermentación o síntesis química del almidón[5]. El ácido láctico es un

enantiómero o isómero óptico que tiene dos estereoisómeros: Levógiro-L(+) y Dextrógiro-D(-)[21-23] (**Figura I.4**).

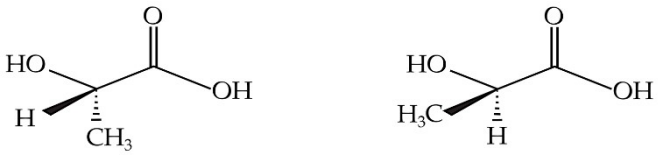

L-ácido láctico D-ácido láctico

Figura I.4. Representación esquemática de la estructura química de los enantiómeros del ácido láctico.

En la síntesis del PLA, se pueden obtener varios grados poliméricos; a partir del enantiomero L-ácido láctico, el poli(L-ácido láctico) (PLLA) y a partir del D-ácido láctico, el poli(D-ácido láctico) (PDLA). Aunque éstos son los básicos, existen gran variedad de polímeros diferentes, para aplicaciones diferentes y con propiedades diferentes [24]. En la **Figura I.5**, se muestra la unidad repetitiva del PLA.

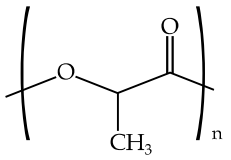

poli(ácido láctico)-PLA

Figura I.5. Representación esquemática de la estructura química de la unidad monomérica del ácido poliláctico.

La biodegradabilidad del PLA (más correctamente, su capacidad de desintegración en compost), está ligada a la sensibilidad del grupo éster por el agua, dando lugar a reacciones de hidrólisis. Las moléculas de agua presentes en el compost, producen la rotura de los grupos éster, reduciendo, progresivamente, el tamaño de las cadenas poliméricas (formando oligómeros de ácido láctico). Llega un momento en que el tamaño de las moléculas resultado de la hidrólisis, permite su incorporación en el

ciclo de alimentación de determinados microorganismos, dando lugar a la biodesintegración (**Figura I.6**).

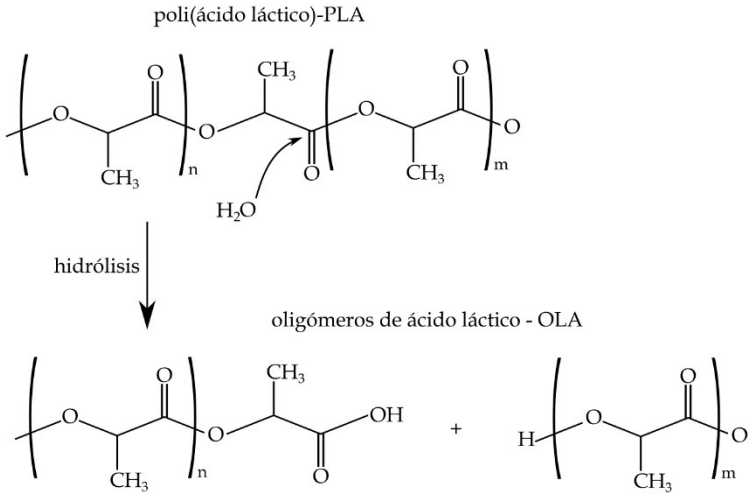

Figura I.6. Representación esquemática del proceso de rotura de los enlaces tipo éster mediante hidrólisis.

I.2.1. Obtención de ácido poliláctico.

A partir de determinados productos agrícolas o plantas ricas en carbohidratos, como es el caso de algunos cereales tipo maíz, se procede a la separación del almidón de otros componentes como pueden ser proteínas, grasas, fibras, cenizas y agua [25]. Una vez separados éstos, los polisacáridos se transforman en D-glucosa (**Figura I.7**) (dextrosa) a través de la hidrólisis enzimática cuya enzima es la amilasa (catalizador de la hidrólisis) [20]. Dicha enzima se produce en nuestro cuerpo, principalmente en las glándulas parótidas o glándulas salivales y en el páncreas, para transformar el almidón en azucares simples.

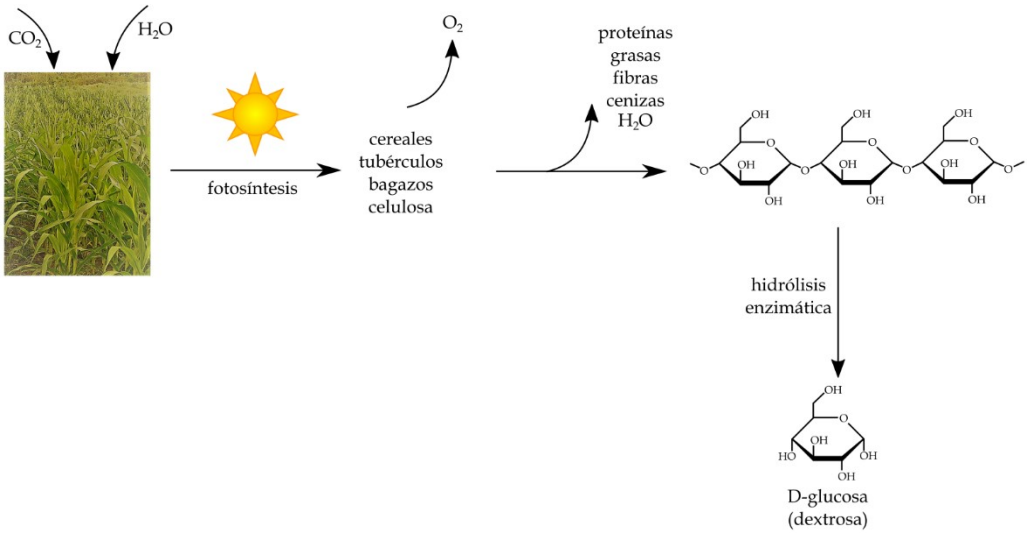

Figura I.7. Esquema del proceso de separación de almidón e hidrólisis enzimática para la obtención de dextrosa.

Posteriormente, el ácido láctico se puede producir mediante síntesis química, aunque tiene ciertas limitaciones: limitada producción, selectividad hacia el isómero L-láctico y altos costes de fabricación, que hacen inviable este método a nivel industrial [20]. El método mayormente utilizado por las grandes empresas productoras (NatureWorks LLC y Corbion) es el método de fermentación bacteriana de azúcares (**Figura I.8**) [23] a pH entre 5 y 7, a un rango de temperaturas de entre 38 y 42 ºC [20, 26]. Hay dos tipos de procesos de fermentación y se clasifican como métodos heterofermentativos y homofermentativos. Los heterofermentativos tienen menor conversión a ácido láctico produciendo grandes cantidades de otros metabolitos tales como etanol, glicerol, manitol, ácido acético y dióxido de carbono. Por el contrario, los métodos homofermentativos son los más utilizados por la industria debido a que tienen una mayor conversión a ácido láctico, aunque manteniendo la selectividad a los mismos subproductos [20, 23]. Las bacterias que se utilizan en el método homofermentativo provienen del género *Lactobacillus* y presentan gran variedad; *L. leichmannii, L. bulgaricus, L. amylophilus, L. delbrueckii* y otros [20, 25].

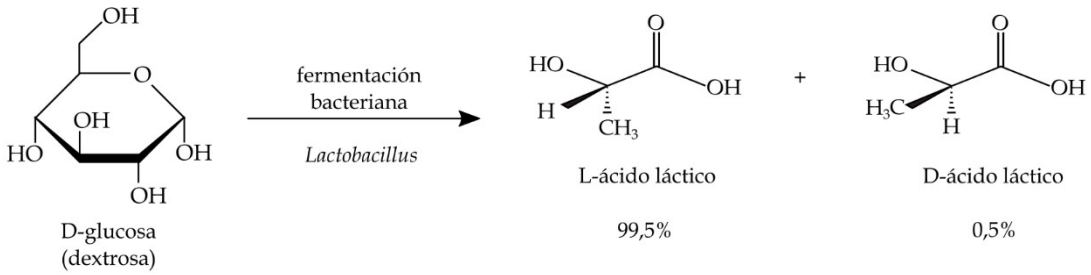

Figura I.8. Esquema del proceso de fermentación bacteriana para la producción de ácido láctico.

Existen tres principales rutas de síntesis del PLA a partir de ácido láctico que se resumen a continuación.

Condensación directa.

La polimerización por condensación directa (1) es el método de polimerización, para producir PLA de alto peso molecular M_w, más económico [20, 23].

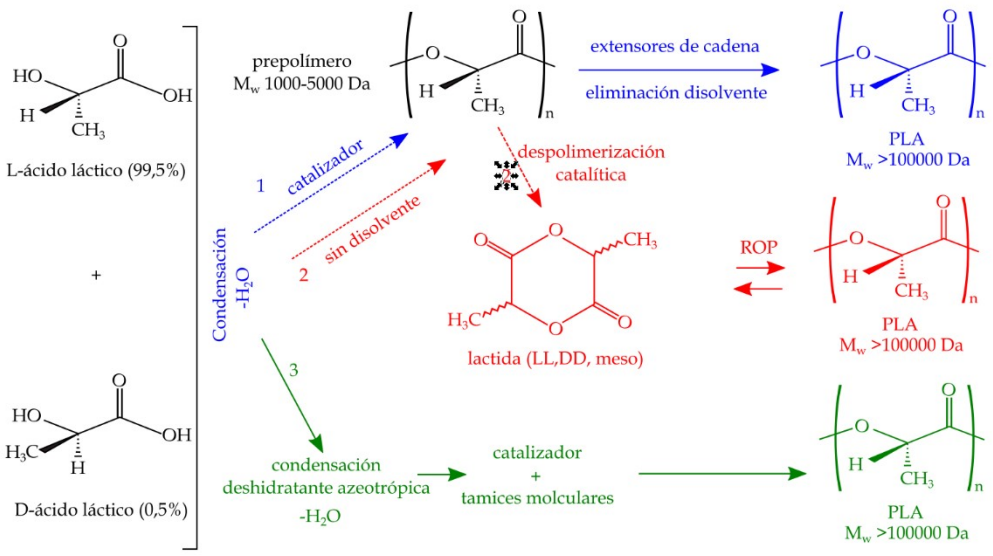

Figura I.9. Principales rutas de síntesis del PLA a partir de ácido láctico.

El monómero de partida (L-lactida, D-lactida o la combinación de éstos) se polimeriza directamente con la ayuda de un catalizador y un disolvente. Debido a que

la presencia de agua perjudica dicha síntesis, se aplica alto vacío y elevada temperatura para eliminar la humedad que se genera en la reacción de condensación [26]. La necesidad de obtener PLA libre de disolvente, hace que se tenga que añadir algún tipo de agente de acoplamiento. Esto aumenta la complejidad del proceso y en consecuencia su coste [23].

Apertura de anillo.

El método más usado por las grandes productoras en la síntesis de PLA de alta masa molecular es el de polimerización por apertura de anillo (método ROP – (2)) [20, 23]. La síntesis química mediante ROP puede controlar las propiedades resultantes de los polímeros, generando así diferentes grados con diferentes aplicaciones [22]. Partiendo de los enantiómeros L-láctico y D-láctico, por policondensación y sin usar disolvente se elimina el agua para generar un prepolímero de baja masa molar [26]. Seguidamente el prepolímero se despolimeriza de forma controlada en un dímero cíclico (lactida) [27]. Acto seguido se purifica mediante destilación [26] y se polimeriza mediante ROP en PLA de alto peso molecular, M_w [20, 22, 28-30]. El PLA generado por este método puede contener diferentes cantidades de L-láctico y D-láctico, aunque grandes cantidades de meso-láctico se producen en dicho proceso (**Figura I.9**). De estas cantidades en meso-láctico van a depender las propiedades del PLA, como la procesabilidad y cristalinidad.

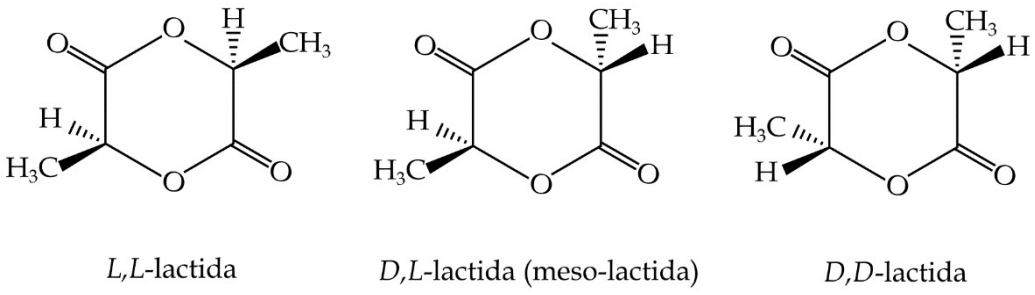

Figura I.10. Representación esquemática de las estructuras químicas de los diferentes estereoisómeros de la lactida.

Policondensación directa en solución azeotrópica.

La síntesis por policondensación directa en solución azeotrópica (3) se realiza mediante destilación a 130 °C durante 2-3 horas, eliminando gran cantidad de agua generada durante la reacción de condensación. Para ayudar a eliminar el agua se reduce la presión de destilación. A continuación, se añade el catalizador y recircula el disolvente a través de tamices moleculares de 3 Å a 130 °C, y durante 30-40 horas adicionales [20]. Como fase final, el polímero se separa o se disuelve-precipita una vez más con la intención de purificarlo para usos específicos donde se requiera gran pureza (por ejemplo, sector médico) [23].

I.2.2. Propiedades generales del ácido poliláctico.

I.2.2.1. Procesado.

Conocer bien las particularidades del PLA es importante a la hora de su procesado. Al igual que algunos polímeros obtenidos del petróleo como el PS o el PET, el PLA se puede procesar en equipos convencionales de transformación de polímeros [31] como la extrusión (films o hilos) [32], moldeo por inyección [33], moldeo por soplado [20], termoconformado y espumado [23, 30]. La temperatura de trabajo, el tiempo de residencia a la temperatura de trabajo, la temperatura de degradación, el secado previo antes de su transformación, el enfriamiento de los productos acabados, son parámetros que deben tenerse en cuenta a la hora de procesar el PLA [20, 22, 33]. Procesar PLA húmedo provoca la hidrólisis de las cadenas poliméricas y reduce por escisión la masa molecular de éste [31]. El secado previo al procesado a temperaturas inferiores a la temperatura de transición vítrea (T_g), (entre 43 °C y 60 °C) evita este fenómeno característico del PLA.

La temperatura de procesado depende de la estructura del PLA, si es amorfo o semicristalino. Para el PLA amorfo la temperatura debe ser superior a la de su T_g, mayor a 58 °C [5]. Para el caso del PLA semicristalino la temperatura de trabajo debe ser superior a la temperatura de fusión (T_m) [34], que depende del grado de cristalinidad y oscila en el rango comprendido entre 130 °C y 180 °C [23]. A su vez, la cristalinidad depende de la masa molecular y de la estereoquímica (cantidad de L, D y *meso*-lactida en la estructura) que son los parámetros que definen la velocidad de cristalización [22]. Si el PLA esta constituido por más de un 93% de L-ácido láctico, es semicristalino, mientras que si contiene entre 50 y 93% de L-ácido láctico es amorfo [23]. La cristalinidad influye en las propiedades mecánicas y térmicas de los polímeros como la dureza, módulo elástico, resistencia a la tracción, rigidez [5], transiciones térmicas (T_g, T_m).

I.2.2.2. Degradación.

El PLA experimenta diferentes procesos de degradación en diferentes ambientes a lo largo de su vida útil. Como consecuencia de la degradación se ven afectadas, en mayor o menor medida, sus propiedades, siendo estos cambios irreversibles. Estos procesos de degradación pueden ser consecuencia de la escisión que experimentan, resultado de diversos procesos tales como la hidrólisis [35], degradación microbiana, térmica, fotodegradación y degradación enzimática [36]. La degradación puede ser una ventaja si la aplicación del PLA va destinada a una prótesis bioabsorbible [37, 38] o si se aplica para la producción de films para cultivo de plantas [39]. Por el contrario, es una desventaja en la mayoría de aplicaciones, ya que la degradación disminuye, por escisión, la masa molecular de las cadenas, formando monómeros, dímeros y oligómeros que actúan, a su vez, de catalizador y acelerador del proceso de degradación [35].

La hidrólisis es un proceso de degradación del PLA cuando está expuesto a la humedad, rompiendo grupos éster [40]. La difusión de las moléculas de agua a través de las zonas amorfas da comienzo a la degradación, propagándose posteriormente a

las zonas cristalinas. En ambas fases la reacción con los grupos éster siguen el siguiente proceso:

$$-COO + H_2O \rightarrow -COOH + OH-$$

El pH [41], la temperatura y la exposición de determinadas sustancias en contacto con el PLA son parámetros que pueden acelerar el proceso de escisión de los grupos éster [35, 40]. Por tanto, determinados productos alimenticios como zumos [41] y bebidas alcoholicas [42], pueden facilitar dicho proceso. Es por ello que hay que tener en consideración este fenómeno al utilizar polímeros de PLA en el sector de la alimentación.

La degradación térmica es otro de los mecanismos en los que el PLA se ve sometido en el momento de su procesado. La temperatura y tiempo de exposición durante el procesado también afectan al PLA y se atribuye a la hidrólisis producida con la humedad residual existente [43]. Diferentes estudios demuestran que, además de los típicos compuestos derivados de la hidrólisis como la lactida, oligómeros cíclicos y monómeros, se generan otros productos de las reacciones de transesterificación, despolimerización, escisión y otras, como pueden ser CO_2, CO, acetaldehído y metil cetona [44].

La fotodegradación es otro de los mecanismos de pérdida de masa molecular que provoca la fragilización de los productos que están sometidos a una radiación con longitudes de onda en el rango UV de forma continuada, como pueden ser films para la agricultura. Dicha radiación es capaz de romper enlaces de la estructura molecular que conducen a la aceleración del proceso de degradación [45] ya que, en general, la energía asociada a las diferentes longitudes de onda correspondientes a la radiación UV, es superior a la mayoría de los enlaces que constituyen las cadenas poliméricas de PLA.

La biodegradación producida por microorganismos o por degradación enzimática son los procesos de degradación que aparecen durante o al final de la vida útil de los productos fabricados con PLA [46, 47]. Al principio de la degradación se rompen cadenas poliméricas por escisión, transesterificación o fotodegradación

formando moléculas de masa molecular más pequeñas [47]. Acto seguido, en condiciones de temperatura (58 ºC), humedad (50%) y aireación, los microorganismos se encargan de asimilar y transformar estas nuevas moléculas (de longitudes suficientemente cortas) para formar al final del proceso compost, CO_2, H_2O y minerales [20].

I.2.2.3. Propiedades mecánicas.

El PLA muestra diferente comportamiento mecánico para cada uno de los grados comerciales que las grandes empresas distribuyen [48, 49]. Tanto es así, que existen series de materiales basados en PLA que se utilizan para extrusión de film, inyección, producción de filamentos, etc. Estos grados tienen composiciones de L-ácido láctico y D-ácido láctico diferentes, masas molares diferentes y grados de cristalinidad distintos, evidentemente, como consecuencia de la composición. De ahí que las propiedades mecánicas del PLA dependan de la estereoquímica, M_w, del grado de cristalinidad [50] y en menor medida, pero no menos importante, del procesado.

Un PLA semicristalino permite alcanzar niveles de módulo de Young (E) y resistencia a tracción (TS) y flexión (FS) superior que los de un PLA amorfo. El contenido de D-ácido láctico en el PLA para que sea amorfo debe de ser mayor a 7%.

La producción de films y filamentos se fabrican con PLA de menor M_w y se prefieren grados de PLA amorfos, ya que esto facilita el procesado y aumenta la ductilidad del producto. Por el contrario, si se requieren propiedades mecánicas altas, se debe seleccionar un PLA semicristalino [22]. Por ejemplo, el grado de la serie 6000, concretamente el 6201D fabricado por NatureWorks, con un contenido cercano a 2% de D-ácido láctico es semicristalino, con un grado de cristalinidad de alrededor del 15%. Dicho PLA tiene valores de E entre 3500 y 4000 MPa, TS cercana a 70 MPa y un alargamiento a la rotura de alrededor del 7% [18]. Estos valores pueden ser superiores si se incrementa la cristalinidad.

Sin embargo, este polímero se caracteriza por su rigidez y fragilidad si se compara con el resto de polímeros de uso común. Para aumentar su ductilidad se está trabajando intensamente sobre su plastificación mediante el empleo de plastificantes naturales [51].

I.2.2.4. Propiedades barrera.

Los polímeros son relativamente permeables a las moléculas pequeñas, tales como gases, vapor de agua, vapores orgánicos y líquidos [52]. Debido a que el PLA se utiliza ampliamente en el sector envase y embalaje, es necesario describir sus propiedades barrera. Las paredes de los envases alimentarios son, a menudo, objeto de estudio, ya que están en contacto con líquidos y gases. El oxígeno es causante de la oxidación de los alimentos y es necesario que el alimento quede el mayor tiempo posible aislado de este gas. De la misma forma, el vapor de agua tiene afinidad para difundirse a través de las paredes de los envases, especialmente a través de la fase amorfa de éste, con lo que se acelera la degradación del mismo.

Determinados parámetros pueden ser objeto de modificación para disminuir la permeabilidad del agua y el oxígeno. La cristalinidad del PLA y las propiedades de barrera son temas ampliamente estudiados dada su repercusión en la aplicación final de los materiales derivados de PLA a escala industrial [53]. Algunos estudios muestran que no existe influencia de la cristalinidad en la permeabilidad al agua. Sin embargo, Guinault et al. concluyeron que la difusión de oxígeno y el coeficiente de solubilidad en función del grado de cristalinidad en muestras de PLA con diferente cristalinidad sí tenían influencia. Además, observaron que la permeabilidad depende del coeficiente de difusión [54].

I.2.3. Usos de ácido poliláctico en Ingeniería.

I.2.3.1. Sector médico.

Con el paso de los años, muchos estudios demuestran que las prótesis fabricadas a partir de aleaciones biocompatibles, no siempre lo son y producen metalosis (difusión de metales en el cuerpo) [55-58]. Además, incluso las menos susceptibles de ser rechazadas por el cuerpo, las aleaciones de Ti (Ti6Al4V), CoCr, CoCrMo y acero inoxidable, con el tiempo se deben retirar del cuerpo, ya que éste las concibe como un cuerpo extraño y con el tiempo tiende a reaccionar [55-58]. Solamente las prótesis de Mg resultan ser biocompatibles y bioabsorbibles por el cuerpo, aunque su problemática radica en la rápida disolución, que puede provocar infecciones. Para ello, se estudia el control de su disolución por medio de "*coatings*" o recubrimientos tales como óxidos o hidróxidos [59]. El uso de prótesis metálicas supone, como mínimo, una doble intervención por parte de los cirujanos, lo que genera unos gastos considerables y un riesgo de infección alto del paciente.

La necesidad de obtener nuevos materiales que carezcan de estos problemas hace que en los últimos años el PLA se esté investigando de forma intensa [37, 38, 60, 61]. Este presenta la ventaja de ser bioabsorbible por el organismo, ya que el ácido láctico forma parte de nuestro cuerpo, siendo fácilmente metabolizado por éste. Las propiedades mecánicas que el PLA presenta y su biocompatibilidad hacen de éste un material excelente para fabricar todo tipo de prótesis y piezas para sector médico tales como tornillos de interferencia [62, 63], puntos de sutura [63], placas de fijación para reparación de huesos [62, 64], etc. En el proceso de bioabsorción del ácido láctico se sustituye éste por tejido blando y posteriormente por tejido conectivo especializado [63, 65, 66].

Sin embargo, las prótesis de PLA no son osteoconductoras por sí solas y es necesario dotar a este material de un componente osteoconductor para poder regenerar

la zona afectada con hueso nuevo. La familia de ortofosfatos (HA, β-TCP, OXA, BCP, etc.) se presenta como la mejor opción para formar composites bioabsorbibles y biocompatibles. Gran cantidad de estudios demuestran que estos compuestos, además de tener propiedades químicas y mecánicas similares a la de los huesos reales, muestran la proliferación de células madre mesenquimatosas (MSCs), lo que a su vez permite una diferenciación a células madre adiposas (ASCs), que son las que se encargan de sintetizar el alimento necesario para el crecimiento celular, necesario para generar tejido blando que posteriormente pasa a transformarse en hueso nuevo [65, 66].

Otra de las ventajas que presenta el uso de ortofosfatos en las prótesis de PLA es que mineralizan (caso del β-TCP) la zona de crecimiento oseo y a su vez impiden la inflamación de la zona afectada ya que se disuelven fosfatos en el medio fisiológico que generan una solución tampón [67].

I.2.3.2. Sector envase-embalaje.

Como se ha comentado anteriormente, en la actualidad se detecta un gran interés por parte de la sociedad por reemplazar los plásticos convencionales no degradables por polímeros biodegradables y compostables que minimizan el impacto ambiental, siendo el envase y embalaje una de las aplicaciones que más residuos genera anualmente.

Gran variedad de productos destinados al envase de productos alimenticios tal como botellas, vasos, cubiertos, platos, tazas, tapas, pajitas de bebidas, bolsas, films [68], envases para fruta o vegetales, yogurts, bebidas con gas[23], se producen cada día más, gracias a los avances que la investigación en esta rama de la conservación de alimentos están obteniendo.

Los envases activos juegan un papel importante en estos avances para conservar los alimentos el mayor tiempo posible. El hecho de añadir antioxidantes al material del envase supone no añadirlo al alimento y ello genera un doble beneficio, el

comercial o de marketing por ofrecer alimentos libres de conservantes y antioxidantes y otro no menos importante, el que se minimice la ingesta de conservantes, lo que supone una alimentación más sana.

Técnicamente, los antioxidantes o conservantes son compuestos químicos que actúan de captadores o "*scavengers*" minimizando y frenando la oxidación de los alimentos durante un tiempo mayor, ya que reaccionan con los radicales libres que atraviesan las paredes de los envases. Otra de las ventajas que tienen estos antioxidantes es la estabilidad térmica que ofrecen al polímero durante el procesado, ya que permiten incrementar el tiempo de residencia del polímero a alta temperatura sin que éste ni el antioxidante se deterioren. Es importante que dichos conservantes pasen al alimento de forma progresiva y controlada. Los conservantes que están experimentando un mayor uso son los naturales. Un gran número de éstos se está utilizando con la intención de sustituir los convencionales. En la naturaleza encontramos un sinfín de compuestos fenólicos (de la familia de los flavonoides) obtenidos a partir de aceites esenciales que se pueden extraer de diversas plantas, entre ellas las hierbas aromáticas como el tomillo (timol), orégano (carvacrol), clavo (eugenol), té (catequinas), un gran número de vitaminas como la vitamina E (α-tocoferol), vitamina C (enantiómero-L de ácido ascórbico) que se utilizaba para prevenir el escorbuto, etc.

Un sistema para controlar la liberación de dichos antioxidantes es el uso de plastificantes. Los plastificantes naturales con mayor interés por su baja toxicidad y abundancia son los aceites naturales modificados. Entre ellos podemos encontrar una gran variedad que están siendo utilizados en aplicaciones alimentarias, como son los aceites epoxidados o maleinizados [69-73]. Los aceites modificados son más estables térmicamente como se ha demostrado en varios estudios científicos [74, 75]. Además, mejoran de forma considerable la plastificación del PLA [69-73].

I.2.3.3. Fibras textiles.

El sector textil está invirtiendo grandes esfuerzos en la mejora de la producción de fibras para el uso en tejidos y su posterior uso en cortinas, fundas de cojines, alfombras, etc [76-79]. Empresas de automoción también están haciendo grandes esfuerzos para utilizar este tipo de materiales ecológicos para aplicarlos en tapicería de vehículos, así como otras muchas piezas del automóvil que hoy en día se fabrican con PET y otros polímeros sintéticos como el PU. Aunque ya se fabrican telas basadas en PLA en algunas empresas, por cumplir con la mayoría de propiedades que los polímeros sintéticos poseen, todavía hay que mejorar ciertas propiedades como el índice de inflamación y la resistencia a la abrasión.

I.2.3.4. Sector de cultivos.

Uno de los campos más prometedores, donde el PLA tiene o tendrá un papel relevante es en el sector de la agricultura. Tradicionalmente se fabrican films de PE para proteger los cultivos del sol y de los animales e insectos, así como para proteger los suelos y retener su humedad. Actualmente, se está trabajando intensamente en la sustitución del PE por otros materiales biodegradables que cubran las funciones de éste.

Para ello se están fabricando films de PLA plastificado o blends de base PLA con otros polímeros biodegradables (PBAT [80], PHA [81, 82], almidón [83], etc.) que mejoren la biodegradación del PLA. Los PLA plastificados mejoran la biodegradación, ya que, al aumentar el volumen libre entre cadenas poliméricas, los microorganismos, así como las moléculas de agua pueden penetrar más fácilmente y, en consecuencia, acelerar su degradación. Esto conlleva una solución importante sobre la problemática del uso de films de PE, ya que es un producto que se genera en grandes cantidades, lo que a su vez genera grandes cantidades de residuos difícilmente reciclables. Al tratarse de un material biodegradable y compostable, el ciclo de vida de estos films se

completa, pasando a formar parte del compostaje o alimento que nuevos cultivos sintetizarán.

I.2.3.5. Otras aplicaciones.

Existen muchas más aplicaciones, aunque éstas no supongan un consumo de PLA tan importante como las aplicaciones descritas anteriormente. La fabricación de filamento para impresión 3D es cada vez más visible, ya que muchas empresas están empezando a utilizar este tipo de impresoras para hacer prototipado, piezas a medida, etc. Esta técnica tiene un interés creciente en el sector médico donde se pueden fabricar prótesis a medida, espumas a partir de filamentos cargados de nanopartículas osteoconductoras para la reconstrucción de la parte interna de un hueso, etc.

Filtros de cigarrillos, consumibles electrónicos, pinturas base acuosa, y un sinfín de aplicaciones van siendo objetivo de dicho material a medida que se van aportando mejoras en sus propiedades.

I.3. TECNOLOGÍAS DE MODIFICACIÓN DE FORMULACIONES DE POLÍMEROS.

I.3.1. Mezclado físico o "*blending*".

Un método sencillo, económico y uno de los más utilizados a nivel industrial para obtener características diferentes de un polímero concreto es el mezclado físico en fundido o "*blending*". En un sistema de mezclado físico, hay que tener en consideración varias características particulares de cada polímero constituyente de la mezcla. Conocer las temperaturas de fusión y de degradación de los polímeros permite seleccionar la temperatura de mezclado óptima sin que ninguno de sus componentes se degrade térmicamente. Las características finales del mezclado físico dependen de la afinidad entre polímeros, a lo que técnicamente se denomina la miscibilidad entre éstos. La miscibilidad depende de la polaridad intrínseca de cada uno de los componentes.

Si los polímeros constituyentes en una mezcla son totalmente inmiscibles, se obtiene un sistema bifásico, actuando como fase matriz el polímero mayoritario y como fase dispersa, el minoritario. Generalmente, estas mezclas no aportan las propiedades mecánicas esperadas, ya que la interacción molecular entre los dos polímeros es nula. Otra posibilidad es que los polímeros constituyentes sean parcialmente miscibles lo que nos aportaría propiedades intermedias o inferiores a las esperadas, aunque en este caso hay excepciones dependiendo de la propiedad. Cuando la miscibilidad es nula o pobre, la absorción de energía a impacto normalmente disminuye considerablemente [18]. Por el contrario, cuando la miscibilidad es total, la sinergia de propiedades que se desea obtener tiene una efectividad alta. En este caso, las proporciones de los polímeros en la mezcla son las que aportan los valores de las propiedades mecánicas o térmicas deseadas. [84].

A nivel industrial se suelen realizar mezclas de dos componentes (mezclas binarias) o mezclas de tres componentes (mezclas ternarias). El "*blending*" de más de

tres componentes puede suponer un coste demasiado elevado debido a la complejidad de la maquinaria de procesado y otros métodos de modificación de las propiedades de polímeros pueden entrar en juego.

Ciertos polímeros pueden actuar como plastificantes, aportando mayor ductilidad y procesabilidad al polímero mayoritario de la mezcla física. En determinadas aplicaciones donde no se permite una migración del plastificante, el mezclado físico se presenta como una excelente opción de modificación polimérica.

I.3.2. Plastificación.

I.3.2.1. Definiciones y clasificación.

El plastificante se define como una sustancia que se incorpora a un plástico para aumentar su flexibilidad o ductilidad y, en consecuencia, el objetivo a nivel tecnológico, facilitar su procesado. Normalmente el resultado de plastificar un polímero implica que la viscosidad del material disminuye y el índice de fluidez aumenta, por tanto, su procesabilidad, también mejora.

Tecnológicamente, lo que se pretende es disminuir las temperaturas de las principales transiciones térmicas, como la T_g, donde el material experimenta un reblandecimiento o la T_m, donde el material pasa a estar fundido. Un descenso de estas dos temperaturas implica un menor coste energético para la producción. Un aumento del índice de fluidez o descenso de la viscosidad implica maquinaria menos potente y, por tanto, un coste en recursos inferior.

A nivel molecular, un plastificante consiste en moléculas de bajo peso molecular que se posicionan entre las cadenas poliméricas disminuyendo la interacción entre éstas y facilitando su movimiento. La separación física supone una menor interacción debida a fuerzas atómicas débiles (Van der Waals o enlaces de hidrógeno)[85].

Existen cuatro tipos de teorías clásicas con las que se puede dar una explicación sobre los efectos de plastificación. Éstas se resumen a continuación.

Teoría de la lubricación.

En esta teoría se contempla el plastificante como un agente lubricante interno, lo que permite un deslizamiento más fácil de las cadenas. Al disminuir la fricción intermolecular las cadenas poliméricas se pueden mover fácilmente cuando el polímero se expone a algún tipo de esfuerzo.

Teoría del gel.

Es aplicable a polímeros amorfos. En ésta se afirma que el plastificante genera un debilitamiento en las fuerzas intermoleculares. En este caso, el plastificante enmascara los centros activos que tienen las cadenas polímericas para interactuar con las cadenas colindantes y ello dificulta o minimiza las interacciones moleculares. En consecuencia, las cadenas se pueden mover más fácilmente y el material polimérico se hace más dúctil y procesable.

Teoría mecánica.

Esta teoría de plastificación afirma que las moléculas de los plastificantes experimentan cierta fuerza de atracción por medio de centros activos y solamente éstas pueden ser sustituidas por otras moléculas de plastificante. Como resultado, las cadenas poliméricas quedan mayormente aisladas de la interacción entre otras cadenas y pueden moverse fácilmente.

Teoría del volumen libre.

En esta teoría el plastificante que se intercala entre las cadenas poliméricas genera, a su vez, un volumen libre. También cabe la posibilidad que las moléculas plastificantes reaccionen con las cadenas poliméricas (plastificante primario), formando un mayor volumen libre. Esto genera en cualquiera de los dos casos, que las cadenas se muevan más fácilmente.

La eficiencia de un plastificante depende de la estructura química de su molécula y su compatibilidad con la matriz polimérica. Por tanto, el plastificante y el polímero deben ser miscibles mostrando fuerzas intermoleculares similares. Sus solubilidades presentan gran similitud [86]. El parámetro de solubilidad (δ) depende en la energía libre de Gibbs (Ecuación 1).

$$\Delta G = \Delta H - T \cdot \Delta S \qquad \text{Ecuación 1}$$

donde ΔG es la variación en la energía libre de Gibbs, ΔH la variación de la entalpía (en este caso el calor necesario para el mezclado), T la temperatura absoluta y ΔS la entropía del mezclado.

Un valor negativo de ΔG sería indicativo de una buena disolución, ya que no se necesita un aporte externo de energía [87] y la entropía aumenta debido al desorden que genera el mezclado o disolución.

Una forma de calcular la solubilidad es mediante la formula de Small llevando a cabo el sumatorio de las constantes de atracción molar (G) tabuladas de varios tipos de moléculas o grupos funcionales simples. De esta forma, mediante la Ecuación 2 se calcula δ considerando el aporte que cada uno de los grupos hace a la estructura total de la molécula.

$$\delta = D \cdot \Sigma G / M_n \qquad \text{Ecuación 2}$$

siendo δ el parámetro de solubilidad medido en $(\text{cal cm}^{-3})^{1/2}$, D la densidad ($\text{g cm}^{-3}$), ΣG el sumatorio de constantes de atracción molar $[(\text{cal cm}^{-3})^{1/2}\ \text{mol}^{-1}]$ y M_n es la masa molar promedio en número por unidad repetitiva (g mol^{-1}). Este es un método

aproximado de calcular el parámetro de solubilidad de un polímero en un plastificante ya que este puede variar en función de la composición, la cristalinidad y la polaridad, entre otras [86]. Cuanto más cercanos sean los parámetros de solubilidad del polímero base y el plastificante, mayor será la compatibilidad y eficacia de plastificación.

Aunque la solubilidad es un parámetro indicativo de la eficiencia del plastificante, no siempre es así. Otros parámetros influyen en la eficiencia que un plastificante tiene sobre un polímero. Existen diferentes herramientas para diseñar un plastificante ideal según Bocqué y sus colaboradores. Para ello se dividen los diferentes grupos químicos en bloques, siendo tres tipos de bloques los que entran en juego. Un buen plastificante debe tener un componente espaciador que aumente el volumen libre, en este caso los grupos alifáticos o cadenas alifáticas (primer bloque) pueden aumentar éste. La longitud de cadenas alifáticas o su peso molecular no debe ser ni muy pequeño, para evitar ser volátil, ni muy grande, para facilitar la formulación y su difusión. Este primer bloque facilita la movilidad de las cadenas. El segundo bloque son los grupos éster que aportan cohesión ya que están constituidos por grupos funcionales que reaccionan con otros grupos de su entorno. Y finalmente, un tercer grupo, son los anillos aromáticos que hacen compatibles a los plastificantes con los polímeros [85].

I.3.2.2. Tipos de plastificantes según su acción.

Plastificantes primarios.

Los plastificantes primarios suelen ser moléculas compatibles con el polímero, lo que las hace capaces de mezclarse utilizando grandes cantidades de plastificante y se suele observar un gran efecto de plastificación. Dichos plastificantes suelen reaccionar con las cadenas poliméricas. Además, no se observa exudación en la superficie ni en el producto acabado dada la buena compatibilidad.

Plastificantes secundarios.

La compatibilidad del polímero con los plastificantes secundarios suele ser inferior y, en grandes cantidades, el polímero lo suele exudar de su seno. Cabe destacar que un plastificante puede comportarse como primario con un polímero determinado y en otros polímeros como secundario, pero cuando éstos se comportan como secundarios, se suele añadir un primario para reducir costes y mejorar las propiedades.

I.3.2.3. Tipos de plastificantes según su estructura.

Es bien sabido que un plastificante con un peso molecular bajo tiene mayor probabilidad de difundirse por el entramado de cadenas poliméricas, aunque esto no siempre es así y depende de su estructura química (grupos funcionales, polaridad, longitud de las cadenas, número de grupos hidroxilo, peso molecular, constante dieléctrica, etc.). Según la estructura y su peso molecular, los plastificantes se pueden clasificar en monoméricos, oligoméricos y poliméricos.

Plastificantes monoméricos.

Los plastificantes monómericos son moléculas de bajo peso molecular que tienen, por lo general, buena solubilidad, aunque una de sus desventajas es que también, en su mayoría, son volátiles o tienen baja resistencia a la migración. Por eso, según la aplicación a la que vaya destinado, será recomendable su uso o no. Actualmente, se utilizan en la mayoría de aplicaciones menos en las destinadas a alimentación; de ello va a depender si el plastificante está catalogado como tóxico o no.

Plastificantes oligoméricos.

Los plastificantes oligoméricos están formados por estructuras de cadenas basadas en diversos monómeros que presentan longitudes inferiores a las propias de los polímeros. En el caso concreto del PLA, han dado excelentes resultados los oligómeros del ácido láctico (OLA), que, con diversos pesos moleculares, permiten niveles de compatibilidad altos con las cadenas poliméricas de PLA y, en consecuencia, su eficacia como plastificante es muy elevada. Otros plastificantes oligoméricos se están obteniendo a partir de aceites o grasas naturales (triglicéridos) y tienen pesos moleculares mayores a los plastificantes monoméricos. La resistencia a la migración de los plastificantes oligoméricos aumenta considerablemente comparándolos con los monoméricos.

Plastificantes poliméricos.

Los plastificantes poliméricos, por el contrario, suelen tener pesos moleculares elevados o muy elevados. En este caso, el rango es mucho mayor que en los casos anteriores. Muchos polímeros pueden actuar de buenos plastificantes si la polaridad de ambos es similar; en consecuencia, la solubilidad (miscibilidad) de sus cadenas es alta y con ello pueden mejorar la ductilidad de los materiales poliméricos. Cabe destacar que, en este caso, si la miscibilidad de ambos polímeros es parcial o nula, también pueden mejorar determinadas propiedades relacionadas con la ductilidad (debido a la dispersión fina de una fase inmiscible altamente flexible en forma de micropartículas esféricas en el seno de la matriz), aunque otras pueden empeorar. En el caso de no miscibles, la absorción de energía a impacto suele empeorar.

I.3.2.4. Fenómenos de plastificación.

Los plastificantes pueden ser compatibles con un polímero o no serlo. La compatibilidad depende de la química de ambas moléculas y esto puede crear ciertos

fenómenos en la plastificación. Un plastificante totalmente compatible con el polímero, por regla general, aporta un efecto positivo en la plastificación, aunque todo polímero puede experimentar una saturación de éste en su entramado molecular.

De forma general, un polímero aditivado con un buen plastificante, experimenta saturación para bajos contenidos de éste y un polímero plastificado con un plastificante poco compatible con éste, satura con grandes contenidos de éste.

Cuando un polímero experimenta saturación de plastificante, su flexibilidad, alargamiento a la rotura, absorción de energía a impacto y dureza invierten su tendencia. Este fenómeno se llama "anti-plastificación" y se debe a la formación de dominios de plastificantes que generan una separación de fases en el seno del polímero. Varios son los indicios que nos indican la saturación de un plastificante en el seno de un polímero. Cuando se invierte la tendencia de absorción de energía al impacto, significa que se generan dominios de plastificante que actúan de concentradores de tensiones. Cuando el alargamiento de un material deja de aumentar para empezar a disminuir. En este caso es probable que el plastificante esté actuando como extensor de cadena, previo a la reacción química que experimenta con los grupos polares que tienen los polímeros. Cuando aumenta la dureza, aunque no en todos los casos, este indicador puede ser válido. Y cuando el exceso de plastificante aflora a la superficie de forma considerable.

I.3.3. Incorporación de cargas.

Se denomina carga o "*filler*" a cualquier compuesto sólido orgánico o inorgánico que se añade a una matriz polimérica con un objetivo concreto. En particular, en la industria de transformación de plásticos, se utilizan cargas para un sinfín de objetivos. Entre otros, para disminuir costes, aumentar la cristalinidad de un polímero ya que algunas partículas pueden actuar como agentes nucleantes, como refuerzos para aumentar las propiedades mecánicas, aumentar la estabilidad térmica, modificar las propiedades barrera, aumentar la absorción de la radiación ultravioleta (estabilidad

UV), como "*carrier*" para la liberación de sustancias de todo tipo como fármacos en aplicaciones médicas, estabilizantes poliméricos, conservantes, fungicidas, agentes antibacterianos, absorción de olores y sabores, como partículas osteoconductoras para uso en reparaciones oseas, diminuir densidad, etc.

Normalmente el tamaño de dichas cargas suele estar comprendido entre la nano y la macroescala. Se pueden utilizar partículas con una relación de aspecto cercana a 1 (partículas cerámicas tales como el carbonato cálcico - $CaCO_3$, talco-$Mg_3Si_4O_{10}(OH)_2$ de la familia de los silicatos, aluminosilicatos, ortofosfatos, feldespatos, partículas polimórficas del carbono como negros de humo, nanotubos de carbono, grafito, fullerenos, partículas metálicas como agentes antibacterianos (Ag, Zn, Cu, etc.) y como osteoconductores (Mg), etc) o mucho mayor, como podrían ser fibras naturales (yute, ramio, pita, lino, seda, sisal, etc.) o sintéticas (como fibras de carbono, aramida, basalto, etc).

El contenido de cargas que suelen añadirse va en función de la aplicación y del objetivo. La norma básica es incorporar la cantidad de carga adecuada que no comprometa el conjunto de propiedades necesarias para la aplicación del polímero. En ocasiones, se pueden incorporar hasta un 70% en peso del total. Es importante destacar la funcionalidad de las cargas. En general, las cargas no aportan ninguna función al polímero al que se incorporan; de hecho, la principal finalidad del uso de cargas es, precisamente, la reducción de costes. No obstante, las cargas, como se ha descrito previamente, también pueden aportar diversas funcionalidades. Así pues, en ocasiones se incorporan partículas cerámicas tipo talco o aluminosilicatos con el fin de actuar como agentes nucleantes de la cristalización, que a su vez aumentan la cristalinidad de la matriz y, en consecuencia, las propiedades mecánicas se ven notablemente mejoradas, junto con las propiedades barrera y estabilidad térmica.

En el caso de los materiales plásticos para el sector médico, generalmente se seleccionan cargas capaces de aportar cierta funcionalidad con el fin de facilitar la osteointegración. Un ejemplo claro sería cualquier tipo de prótesis fabricada para sustituir o reparar un hueso humano donde la parte dispersa (partículas de HA o β-TCP, entre otras) juegan un papel muy importante. Dichas partículas, con composición

química similar al hueso humano, actúan de agente nucleante en el crecimiento de nuevas células para la generación y mineralización del hueso. Además, queda bien demostrado que, gracias a estos ortofosfatos, existe la diferenciación a osteoblastos y células adiposas, lo que es beneficioso para la regeneración de huesos, cartílagos y tendones.

I.3.4. Otras modificaciones.

Técnicas como la copolimerización, el "*blending*" reactivo y el aditivado son otros métodos de modificación de las propiedades de los polímeros.

Los procesos de copolimerización son procesos de síntesis donde se polimerizan diferentes monómeros que permiten combinar características de los diferentes monómeros con un resultado excepcional y con unas prestaciones excelentes [84]. Se trata de un método más costoso, pero más efectivo. A escala industrial no es viable por su coste y solamente se lleva a cabo para aplicaciones donde el coste no es muy importante.

Un método complementario al "*blending*" y también económico es el mezclado reactivo. Este método de modificación es igual el mezclado físico, con la salvedad que en este caso se añaden radicales libres tipo peróxidos para que reaccionen sobre las cadenas polímericas constituyentes y generen modificaciones que deriven en una mayor polaridad con una consecuente unión entre dichas cadenas, durante el procesado de los materiales. El uso de esta técnica tiene sentido cuando se pretende mezclar polímeros con pobre o nula miscibilidad.

I.4. TECNOLOGÍAS DE PLASTIFICACIÓN EN POLÍMEROS BASE PLA.

I.4.1. Mecanismos de plastificación de PLA.

El PLA es uno de los polímeros con mayores perspectivas de consumo para la fabricación de productos del sector envase y embalaje [88-91], sector de la agricultura, sector médico, impresión 3D, etc. Éste presenta altas prestaciones mecánicas, buenas propiedades barrera [92], es inodoro, biocompatible y bioabsorbible en el organismo humano [31, 93, 94], además de económico. Algunas de sus desventajas son su hidrofilidad, su poca flexibilidad y alargamiento a la rotura. Para mejorar dichas desventajas, la ciencia de polímeros tiene varias posibilidades para hacer de un material frágil uno más dúctil. Como se ha descrito previamente, los plastificantes se pueden incorporar a los polímeros para aumentar el volumen libre entre cadenas poliméricas, lo que acaba disminuyendo la rigidez y permitiendo mayor movilidad, aportando mayor ductilidad [95]. En bibliografía se encuentran diversidad de plastificantes que ayudan a aumentar su ductilidad [96]. La potencial toxicidad asociada al empleo de algunos plastificantes convencionales, conduce hacia la selección de otros nuevos que no presenten este problema ya que, en muchas ocasiones (sector alimentario), el polímero plastificado entra en contacto directo con alimentos. Además, no solo se requiere la no toxicidad de éste, sino que también es necesario que los plastificantes sean compatibles, tengan carácter biodegradable, sean térmicamente estables durante el procesado [86], ofrezcan alta resistencia a la migración y presenten baja o nula volatilidad [21, 86], entre otros requisitos.

Los plastificantes de origen natural son una alternativa que evita estos problemas [97]. Los hay de diversos tipos. Destacan los aceites extraídos de semillas o moléculas amfifílicas (aceite de linaza-LO, aceite de colza-CO, aceite de ricino-CO, aceite de semilla de soja-SBO) [98]. Otro grupo está formado por los aceites vegetales

modificados como el aceite de linaza epoxidado-ELO, aceite de semilla de soja epoxidado-ESBO, aceite de ricino epoxidado-ECO, etc. así como ácidos grasos epoxidados como el epoxi octil estearato-EOS [99-102]. Entre los plastificantes monoméricos para PLA, destacan el acetil butil ricinoleato-ABR, acetil tributil citrato-ATBC, ácido ricinoleico, 2-etilhexil adipato-DOA, diisodecil adipato-DIDA, octil oleato, octil trimellitato-TMO, metil metacrilato-MMA, glicidil metacrilato-GMA [103-105].

En cuanto a los plastificantes de tipo polimérico destacan los poliésteres di alifático de ácidos carboxílicos, polipropilen glicol adipato y polímeros como almidón termoplástico-TPS o policaprolactona-PCL, etc. [28, 106-109]. El objetivo principal es añadir éstos plastificantes al polímero o polímeros constituidos como mezcla, grupos funcionales tipo hidroxilo, carbonilo u otros grupos polares como éster [110] que sirvan de puntos de anclaje o interacción química entre cadenas poliméricas del mismo polímero o de polímeros diferentes, mejorando la interfase de éstos y su consecuente miscibilidad.

Los indicadores usuales de que un plastificante tiene efecto sobre el polímero son la disminución de la T_g, T_m y un aumento del grado de cristalinidad. A menor masa molecular el plastificante aporta mayor disminución de la T_g del PLA, pero también su migración desde el material al alimento puede ser mayor que la de otros con mayor masa molecular [95].

Otros monómeros y oligómeros han sido investigados como plastificantes compatibles con el PLA. El poli(etilen glicol)-PEG y ésteres del ácido cítrico son comúnmente utilizados como plastificantes, tales como el citrato de trietilo (TEC), citrato de tributilo (TBC), citrato de acetiltrietilo (ATEC), y citrato de acetil-tri-n-butilo (ATBC)[21, 111, 112]. Marina et al. demostraron una notable mejora en la ductilidad del PLA añadiendo D-limoneno, lo que supuso un aumento de la movilidad de las cadenas y un descenso considerable de la T_g. Otros estudios similares demuestran que el uso de nuevos plastificantes obtenidos a partir de plantas aromáticas que contienen compuestos fenólicos, además de ofrecer mayor ductilidad también actúan de estabilizadores térmicos [132].

I.4.2. Aceites vegetales modificados.

El empleo de aceites vegetales es una vía económica y actualmente tiene especial interés para la plastificación de muchos polímeros biodegradables o de alto contenido bio [74, 113]. Los aceites vegetales se caracterizan por una baja toxicidad y se pueden modificar químicamente para mejorar propiedades como el índice de acidez [114]. Además, sus cadenas oligoméricas tienen relativa alta masa molecular y su migración es menor a la de otros plastificantes. Los ácidos grasos son los componentes principales de los aceites. Estos ácidos grasos, no suelen aparecer libres en los aceites vegetales, sino que se encuentran unidos a moléculas de glicerina formando las estructuras de los triglicéridos. La mayoría de los ácidos grasos que forman parte de los aceites vegetales están constituidos por una cadena de hidrocarbono con enlaces sencillos y, en determinados ácidos grasos, aparecen uno o varios dobles enlaces carbono-carbono o insaturaciones. La presencia de estos dobles enlaces desempeña un papel vital en las posibilidades de estos aceites vegetales en la obtención de resinas termoestables con aplicaciones en el campo de los materiales compuestos. En la **Tabla I.1** se muestran los contenidos en diversos tipos de ácidos grasos de diferentes tipos de aceites (los más interesantes desde el punto de vista de la obtención de materiales poliméricos), debido a la presencia de insaturaciones.

Tabla I.1. Resumen de composición en ácidos grasos de los principales tipos de aceites empleados en la obtención de polímeros para aplicaciones en Ingeniería.

Ácido graso	Designación (C_T:C=C)	canola	maíz	algodón	linaza	oliva	palma	colza	soja
Mirístico	14:0	0,1	0,1	0,7	0,0	0,0	1,0	0,1	0,1
Miristoleico	14:1	0,0	0,0	0,0	0,0	0,0	0,0	0,0	0,0
Palmítico	16:0	4,1	10,9	21,6	5,5	13,7	44,0	3,0	11,0
Palmitoleico	16:1	0,3	0,2	0,6	0,0	1,2	0,2	0,2	0,1
Margárico	17:0	0,1	0,1	0,1	0,0	0,0	0,1	0,0	0,0
Margaroleico	17:1	0,0	0,0	0,1	0,0	0,0	0,0	0,0	0,0
Esteárico	18:0	1,8	2,0	2,6	3,5	2,5	4,1	1,0	4,0
Oleico	18:1	60,9	25,4	18,6	19,1	71,1	39,3	13,2	23,4
Linoleico	18:2	21,0	59,6	54,4	15,3	10,0	10,0	13,2	53,2
Linolénico	18:3	8,8	1,2	0,7	56,6	0,6	0,4	9,0	7,8
Araquídico	20:0	0,7	0,4	0,3	0,0	0,9	0,3	0,5	0,3
Gadoleico	20:1	1,0	0,0	0,0	0,0	0,0	0,0	9,0	0,0
Eicosadienoico	20:2	0,0	0,0	0,0	0,0	0,0	0,0	0,7	0,0
Behénico	22:0	0,3	0,1	0,2	0,0	0,0	0,1	0,5	0,1
Erúcico	22:1	0,7	0,0	0,0	0,0	0,0	0,0	49,2	0,0
Lignocérico	22:0	0,2	0,0	0,0	0,0	0,0	0,0	1,2	0,0

En la **Figura I.11** se muestra la representación gráfica de las cadenas de algunos de los ácidos grasos listados en la **Tabla I.1**.

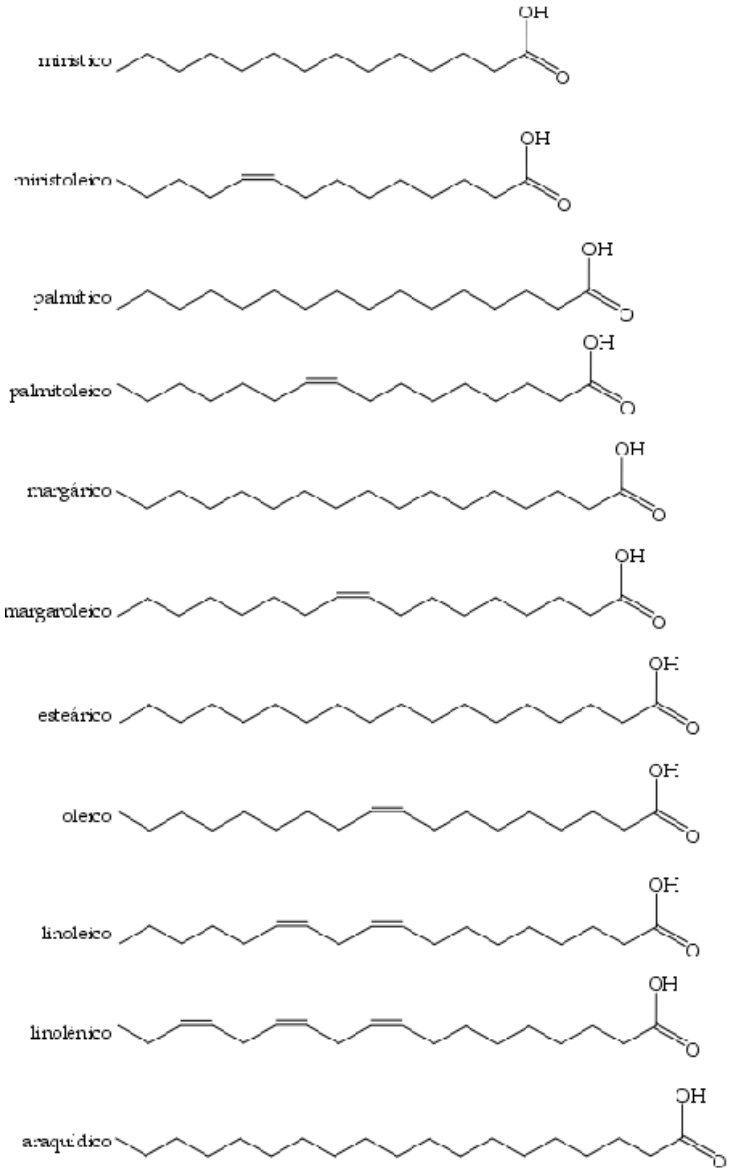

Figura I.11. Representación de la estructura de diferentes ácidos grasos que forman parte de las estructuras de los aceites vegetales.

Desde el punto de vista químico, merece la pena destacar los ácidos grasos insaturados. Entre estos ácidos grasos insaturados, el oleico, linoleico y linolénico con uno, dos y tres dobles enlaces respectivamente son los más habituales en los aceites

vegetales comunes. Es precisamente la reactividad de estas insaturaciones la que permite un amplio abanico de reacciones de modificación que abren las puertas a los aceites vegetales como materiales base en la síntesis de polímeros. La proporción relativa de cada uno de los ácidos grasos determina el tipo de aceite y sus posibilidades en el campo de los materiales en la formación de resinas para matrices termoestables, aditivos, modificadores, lubricantes, agentes de entrecruzamiento, tintas de curado UV, etc.

La epoxidación, alquilación, maleinización, etc. se presentan como métodos de modificación de los triglicéridos para aumentar su funcionalización y, en consecuencia, su reactividad con las cadenas poliméricas, si su objetivo es mejorar la ductilidad del PLA. Dependiendo de los niveles de insaturaciones que contengan los aceites vegetales, el grado de funcionalización es mayor o menor. En general, los EVO (aceites vegetales epoxidados) se usan extensivamente para plastificar aportando buenos resultados. Por ejemplo, el aceite de linaza, obtenido a partir de las semillas de lino *(Linum usitatissimum)*, es uno de los más interesantes para este propósito por su abundancia y alto grado de insaturaciones, junto con el aceite de soja-ESBO y el de ricino-ECO, fundamentalmente. Los aceites de linaza y de soja epoxidados son los que mayores posibilidades ofrecen en la preparación de plastificantes derivados de triglicéridos ya que el número de insaturaciones presentes en las estructuras es elevado y ello permite obtener elevados grados de epoxidación. Aunque se han descrito diversos procesos de epoxidación, el proceso más empleado a escala industrial emplea peroxiácidos generados in situ (**Figura I.12**).

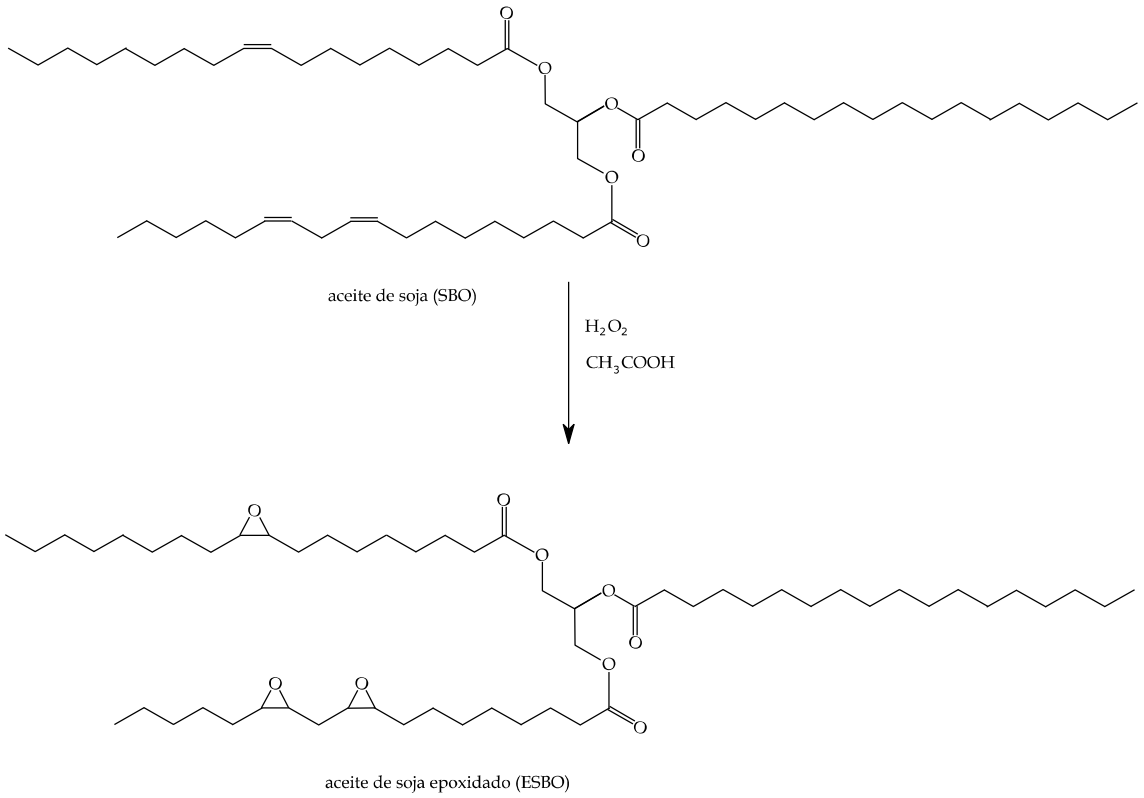

Figura I.12. Representación esquemática del proceso de epoxidación mediante el empleo de peroxiácidos.

Su baja estabilidad térmica hace necesaria su modificación química para mejorarla, modificando también su índice de acidez y así aumentar su eficacia en el proceso de entrecruzamiento, por medio de los grupos reactivos añadidos, o anexión a las cadenas poliméricas. En dicho proceso termo-químico se puede añadir anhídrido maleíco (MA) al aceite de linaza para obtener el aceite de linaza maleinizado (MLO). Los aceites maleinizados han demostrado su elevada eficacia en los procesos de compatibilización en mezclas de polímeros inmiscibles, como por ejemplo PLA y almidón termoplástico (TPS) [71]. Además, se puede someter a temperaturas altas (300 ^{o}C), siendo superior ésta a las temperaturas normales de procesado de productos para este tipo de polímeros. Adicionalmente, éste puede ser epoxidado o epoxidado acrilado (previa epoxidación se añade ácido acrílico y se somete durante un tiempo a temperatura y con un catalizador, para su funcionalización) y obtener diferentes propiedades, con diferentes niveles de plastificación para el PLA.

Prempeh et al. estudiaron y compararon las propiedades dúctiles adquiridas al plastificar el PLA con aceite de girasol epoxidado-ESFO y en paralelo con aceite de semilla de soja epoxidado-ESO [74]. En ambos casos se consiguió aumentar la estabilidad térmica y el alargamiento a la rotura del PLA, aunque mayormente con el uso del plastificante ESO. Por otra parte, Silverajah et al. plastificaron PLA con aceite de palma epoxidado-EPO, aumentando la estabilidad térmica y el alargamiento a la rotura en un 114%. El estudio mediante DSC y DMA demuestra que la movilidad de cadenas es mayor y por tanto la T_g para PLA-EPO disminuye. El plastificante basado en epoxi octil estearato-OES también muestra en un anterior trabajo [115] cómo, con tan solo con un 5 phr OES, se aumenta un 300% más el alargamiento a la rotura con respecto al alargamiento obtenido del PLA virgen. Además, la energía absorbida en impacto Charpy es un 75% mayor que la del PLA virgen. En otro estudio, Chieng et al [113] combinaron diferentes tipos de aceites vegetales epoxidados, EPO y ESO, consiguiendo un efecto sinérgico en las propiedades dúctiles que ambos aportan independientemente. En concreto para este caso, además de aumentar la estabilidad térmica, se consigue aumentar hasta un 220% el alargamiento a la rotura.

I.5. TECNOLOGÍAS DE MEZCLADO FÍSICO EN POLÍMEROS BASE PLA.

El PLA es uno de los polímeros biodegradables de mayor producción y de mayor aplicación, por sus buenas propiedades mecánicas, aunque su biodegradabilidad, propiedades barrera, estabilidad térmica, entre otras, hacen necesario el empleo de diversos mecanismos para mejorarlas.

Una forma sencilla y económica de mejorar éstas propiedades es el mezclado físico o "*blend*". Este procedimiento se realiza en la industria a través de las principales técnicas de conformado (inyección, extrusión, extrusión-soplado, termoconformado, etc.), donde, mediante el uso de unos tornillos especiales para mezclado, se funden los materiales poliméricos y se mezclan.

Para incrementar la resistencia a la difusión de oxígeno y humedad del PLA, este puede mezclarse con polihidroxibutirato-PHB ya que éste tiene muy buenas propiedades barrera. Un estudio realizado por Marina et al. en el que se añadió un 25% en peso de PHB al PLA, mostró un notable incremento en la cristalinidad y en consecuencia, disminuyó la permeabilidad al oxígeno y la humectabilidad de la superficie del PLA [82]. Sin embargo, teniendo en cuenta que el PHB es un material todavía más frágil que el PLA, la mezcla binaria tuvo que ser plastificada; en dicho trabajo se seleccionó el plastificante acetil tributil citrato-ATBC, consiguiendo aumentar la ductilidad y la desintegración en medio de compostaje.

Por otro lado, si lo que se pretende es aumentar, de forma considerable, la ductilidad del PLA, éste puede ser mezclado con diferentes polímeros dúctiles como son el almidón termoplástico-TPS, o poliésteres alifáticos (y/o aromáticos) como la poli(caprolactona)-PCL, el poli(butilén succinato)-PBS, poli(butilén adipato-*co*-tereftalato)-PBAT, poli(butilén succinato-*co*-adipato)-PBSA. Todos éstos aportan, en mayor o menor medida, mejoras en la ductilidad del PLA. Son varios los estudios de mezclas binarias que se han realizado. Añadiendo entre un 20 y un 25% de PCL a PLA se experimenta un descenso del módulo de Young y de su resistencia considerable,

aunque si se aumenta este contenido, el alargamiento a la rotura vuelve a disminuir experimentando un máximo en 22.5% [18]. Sin embargo, estos dos polímeros tienen muy baja o nula miscibilidad, lo que va en detrimento de la absorción de energía a impacto, ya que, según imágenes de microscopia electrónica, se observan esferas casi perfectas referentes a dominios de PCL finamente dispersos en la matriz de PLA.

Otro ejemplo de mezclas binarias que consigue aumentar considerablemente la ductilidad del PLA, es el TPS. El TPS en su producción se plastifica, ya que, en su forma natural, se trata de un material poco cohesionado. Los plastificante ampliamente utilizados son el glicerol y los derivados (EG, PEG) de éste, el agua, y otros alcoholes tipo, sorbitol, manitol, xilitol, etc. Aunque se han conseguido grandes avances con estos plastificantes, el almidón experimenta un proceso de envejecimiento llamado retrogradación y para evitar éste de forma temprana, las grandes empresas productoras de TPS lo modifican continuamente para conseguir mejorías. Este es el caso del TPS NF866 de la casa NOVAMONT, que añade un alto porcentaje de un poliéster arómático-alifático biodegradable (AAPE) que estabiliza el TPS, además de aumentar la resistencia a la retrogradación. Además, dicho poliéster es compatible con el PLA y le aporta un grado de plastificación bueno al TPS. Los aceites maleinizados han demostrado una buena compatibilización en mezclas de polímeros inmiscibles [71]. El PBSA y PBAT mezclados con el PLA muestran similares resultados que para las mezclas explicadas anteriormente [116, 117].

I.6. TECNOLOGÍAS DE INCORPORACIÓN DE CARGAS EN POLÍMEROS BASE PLA.

El PLA, por sí solo o aditivado, puede ser de aplicación para un sinfín de productos, aunque en algunas ocasiones necesita de determinadas cargas para mejorar ciertas propiedades.

Las cargas que se suelen utilizar para las formulaciones de PLA pueden ser de tipo orgánico o inorgánico. Para modificar sus propiedades barrera, se añaden cargas en porcentajes muy pequeños que actúan de agente nucleante de la cristalización en frío, lo que permite una mayor impermeabilidad a oxígeno y humedad. Cargas tipo talco, estearato de sodio y lactato de calcio, entre otras, pueden actuar de agente nucleante, aumentando la cristalinidad del PLA hasta un 40% [118]. Además, para mejorar la movilidad de las cadenas se pueden añadir plastificantes, como se ha visto anteriormente. Otras partículas como las montmorillonitas y su estructura exfoliada también aumentan el grado de cristalización y reducen la temperatura a la que da comienzo ésta sobre el seno de PLA [119]. Otros tipos de partículas inorgánicas también muestran ser agentes nucleantes, aunque las mayormente utilizadas suelen ser las que tienen un coste inferior, como es el caso del talco. Aunque la mayoría de agentes nucleantes son cargas inorgánicas debido a su abundancia y bajo coste, también las hay orgánicas [119].

El uso de cargas para aumentar las propiedades mecánicas del PLA también es de vital importancia, cuando se requiere de un grado de rigidez importante. En biomedicina, concretamente en la fabricación de tornillos de interferencia, espumas para la reconstrucción del hueso [120, 121], aplicaciones dentales [122] y otros tipos de fijaciones que necesiten de alta rígidez, se añaden partículas biocompatibles y en los últimos años preferiblemente bioabsorbibles. La familia de los fosfatos cálcicos se presenta como un grupo con excelentes propiedades por su similar estructura química. Varios estudios realizados con el fin de observar la biocompatibilidad del PLA, así como el crecimiento de células mesenquimatosas y adiposas, concluyen que los

ortofosfatos actúan de fuente de mineralización para la formación de hueso nuevo en la regeneración de éste y osteoconductoras, ya que facilitan dicha regeneración [121, 123]. Otras partículas inorgánicas como aluminosilicatos, Mg, Zn, etc, también se añaden con fines similares [124, 125]. Dependiendo del tipo de partículas y de su aplicación, se pueden añadir contenidos de hasta un 50% al PLA. Los procesos usuales de fabricación son los convencionales de extrusión, inyección, métodos de espumado, etc. Las propiedades resultantes de los materiales compuestos dependen del tipo de partículas utilizadas, ya que la química superficial de éstas difiere y ofrecen mayor o menor interacción con el PLA. La mojabilidad de ambas partes determina el comportamiento de los materiales compuestos. Otras cargas orgánicas, tales como fibras naturales o residuos orgánicos de diferentes frutos (cáscaras de almendra, avellana, nuez, etc.) sirven como refuerzo y se utilizan para la fabricación de materiales que simulan a la madera [69, 126].

Algunas de estas cargas también ejercen de estabilizantes térmicos [127] o a UV [128], aunque la tendencia para estabilizar el PLA, si su uso va a ser en aplicaciones del sector envase y embalaje, son el uso de estabilizantes orgánicos obtenidos de plantas aromáticas cuyos principios activos son compuestos fenólicos [129] . Algunos de éstos son previamente cargados en partículas porosas de naturaleza inorgánica u orgánica. Nanocápsulas de alginato, nanotubos de halloysita, zeolitas, bentonitas, cordieritas, sepiolitas, etc., son cargadas de forma física o química para actuar, además de refuerzo mecánico, de soporte de liberación de sustancias "*carrier*" [128, 130, 131]. En el sector médico se cargan estas partículas con determinados fármacos con eficaces controles de liberación, siempre y cuando dichos soportes sean biocompatibles con el cuerpo humano [130].

En el sector envase y embalaje, cada vez más, se utilizan partículas soporte de este tipo, siendo previamente cargadas con conservantes naturales, como pueden ser derivados de compuestos fenólicos provenientes de diferentes plantas aromáticas, que protegen un mayor tiempo el alimento. Por sí solas, utilizadas como cargas, ya demuestran una mejora en las propiedades barrera, dejando difundir menor cantidad de oxígeno y humedad a través de los composites basados en PLA.

REFERENCIAS

1. Samper, M.D., Petrucci, R., Sanchez-Nacher, L., Balart, R., and Kenny, J.M., *Effect of silane coupling agents on basalt fiber-epoxidized vegetable oil matrix composite materials analyzed by the single fiber fragmentation technique.* Polymer Composites, 2015. **36**(7): p. 1205-1212.
2. Samper, M.D., Petrucci, R., Sanchez-Nacher, L., Balart, R., and Kenny, J.M., *Properties of composite laminates based on basalt fibers with epoxidized vegetable oils.* Materials & Design, 2015. **72**: p. 9-15.
3. Samper, M.D., Petrucci, R., Sanchez-Nacher, L., Balart, R., and Kenny, J.M., *New environmentally friendly composite laminates with epoxidized linseed oil (ELO) and slate fiber fabrics.* Composites Part B-Engineering, 2015. **71**: p. 203-209.
4. GmbH, n.-I., *Market study and Database on Bio-based Polymers in the World: Capacities, Production and Applications: Status Quo and Trends towards 2020.* http://bio-based.eu/top-downloads/.
5. Jamshidian, M., Tehrany, E.A., Imran, M., Jacquot, M., and Desobry, S., *Poly-Lactic Acid: Production, Applications, Nanocomposites, and Release Studies.* Comprehensive Reviews in Food Science and Food Safety, 2010. **9**(5): p. 552-571.
6. Martino, V.P., Jimenez, A., Ruseckaite, R.A., and Averous, L., *Structure and properties of clay nano-biocomposites based on poly(lactic acid) plasticized with polyadipates.* Polymers for Advanced Technologies, 2011. **22**(12): p. 2206-2213.
7. Hwang, S.W., Shim, J.K., Selke, S.E.M., Soto-Valdez, H., Matuana, L., Rubino, M., and Auras, R., *Poly(L-lactic acid) with added a-tocopherol and resveratrol: optical, physical, thermal and mechanical properties.* Polymer International, 2012. **61**(3): p. 418-425.
8. Chavez Gutierrez, M., del Carmen Nunez-Santiago, M., Andrea Romero-Bastida, C., and Martinez-Bustos, F., *Effects of coconut oil concentration as a plasticizer and Yucca schidigera extract as a surfactant in the preparation of extruded corn starch films.* Starch-Starke, 2014. **66**(11-12): p. 1079-1088.
9. Schmitt, H., Prashantha, K., Soulestin, J., Lacrampe, M.F., and Krawczak, P., *Preparation and properties of novel melt-blended halloysite nanotubes/wheat starch nanocomposites.* Carbohydrate Polymers, 2012. **89**(3): p. 920-927.
10. Vásconez, M.B., Flores, S.K., Campos, C.A., Alvarado, J., and Gerschenson, L.N., *Antimicrobial activity and physical properties of chitosan–tapioca starch based edible films and coatings.* Food Research International, 2009. **42**(7): p. 762-769.

11. He, Y., Kong, W., Wang, W., Liu, T., Liu, Y., Gong, Q., and Gao, J., *Modified natural halloysite/potato starch composite films.* Carbohydrate Polymers, 2012. **87**(4): p. 2706-2711.
12. Chiellini, E., Cinelli, P., Chiellini, F., and Imam, S.H., *Environmentally Degradable Bio-Based Polymeric Blends and Composites.* Macromolecular Bioscience, 2004. **4**(3): p. 218-231.
13. Ghaderi, M., Mousavi, M., Yousefi, H., and Labbafi, M., *All-cellulose nanocomposite film made from bagasse cellulose nanofibers for food packaging application.* Carbohydrate Polymers, 2014. **104**: p. 59-65.
14. Vallejos, M.E., Curvelo, A.A.S., Teixeira, E.M., Mendes, F.M., Carvalho, A.J.F., Felissia, F.E., and Area, M.C., *Composite materials of thermoplastic starch and fibers from the ethanol–water fractionation of bagasse.* Industrial Crops and Products, 2011. **33**(3): p. 739-746.
15. Abdul Khalil, H.P.S., Bhat, A.H., and Ireana Yusra, A.F., *Green composites from sustainable cellulose nanofibrils: A review.* Carbohydrate Polymers, 2012. **87**(2): p. 963-979.
16. Scatto, M., Salmini, E., Castiello, S., Coltelli, M.-B., Conzatti, L., Stagnaro, P., Andreotti, L., and Bronco, S., *Plasticized and nanofilled poly(lactic acid)-based cast films: Effect of plasticizer and organoclay on processability and final properties.* Journal of Applied Polymer Science, 2013. **127**(6): p. 4947-4956.
17. Siracusa, V., Rocculi, P., Romani, S., and Rosa, M.D., *Biodegradable polymers for food packaging: a review.* Trends in Food Science & Technology, 2008. **19**(12): p. 634-643.
18. Ferri, J.M., Fenollar, O., Jorda-Vilaplana, A., García-Sanoguera, D., and Balart, R., *Effect of miscibility on mechanical and thermal properties of poly(lactic acid)/ polycaprolactone blends.* Polymer International, 2016. **65**(4): p. 453-463.
19. Auras, R., Harte, B., and Selke, S., *Polylactides. A new era of biodegradable polymers for packaging application.* Annual Technical Conference - ANTEC. , 2005a. Conference Proceedings, **8**: p. 320-324.
20. Castro-Aguirre, E., Iñiguez-Franco, F., Samsudin, H., Fang, X., and Auras, R., *Poly(lactic acid)-Mass production, processing, industrial applications, and end of life.* Advanced Drug Delivery Reviews, 2016. **107**(-): p. 333-366.
21. Liu, H. and Zhang, J., *Research progress in toughening modification of poly(lactic acid).* Journal of Polymer Science Part B: Polymer Physics, 2011. **49**(15): p. 1051-1083.
22. Sodergard, A. and Stolt, M., *Properties of lactic acid based polymers and their correlation with composition.* Progress in Polymer Science, 2002. **27**(6): p. 1123-1163.
23. Auras, R., Harte, B., and Selke, S., *An Overview of Polylactides as Packaging Materials.* Macromolecular Bioscience, 2004. **4**(9): p. 835-864.

24. Madhavan Nampoothiri, K., Nair, N.R., and John, R.P., *An overview of the recent developments in polylactide (PLA) research.* Bioresource Technology, 2010. **101**(22): p. 8493-8501.
25. Cheng, Y., Deng, S., Chen, P., and Ruan, R., *Polylactic acid (PLA) synthesis and modifications: a review*. Frontiers of Chemistry in China, 2009. **4**(3): p. 259-264.
26. Vink, E.T.H., Rábago, K.R., Glassner, D.A., and Gruber, P.R., *Applications of life cycle assessment to NatureWorks™ polylactide (PLA) production.* Polymer Degradation and Stability, 2003. **80**(3): p. 403-419.
27. Sinclair, R.G., *The case for polylactic acid as a commodity packaging plastic.* Journal of Macromolecular Science - Pure and Applied Chemistry, 1996. **33**(5): p. 585-597.
28. Averous, L., *Biodegradable multiphase systems based on plasticized starch: A review*. Journal of Macromolecular Science-Polymer Reviews, 2004. **C44**(3): p. 231-274.
29. Koller, M., Salerno, A., Dias, M., Reiterer, A., and Braunegg, G., *Modern Biotechnological Polymer Synthesis: A Review*. Food Technology and Biotechnology, 2010. **48**(3): p. 255-269.
30. Drumright, R.E., Gruber, P.R., and Henton, D.E., *Polylactic acid technology.* Advanced Materials, 2000. **12**(23): p. 1841-1846.
31. Carrasco, F., Pages, P., Gamez-Perez, J., Santana, O.O., and Maspoch, M.L., *Processing of poly(lactic acid): Characterization of chemical structure, thermal stability and mechanical properties.* Polymer Degradation and Stability, 2010. **95**(2): p. 116-125.
32. Gupta, B., Revagade, N., and Hilborn, J., *Poly(lactic acid) fiber: An overview.* Progress in Polymer Science, 2007. **32**(4): p. 455-482.
33. Lim, L.T., Auras, R., and Rubino, M., *Processing technologies for poly(lactic acid).* Progress in Polymer Science, 2008. **33**(8): p. 820-852.
34. Velazquez-Infante, J.C., *Relación estructura-propiedades de films de nanocompuestos de PLA*, in *Centre Català del Plastic*. 2012, Universitat Politècnica de Catalunya: Barcelona.
35. Auras, R., Lim, L-T., Selke, S. and Tsuji, H., *Hydrolytic Degradation*, in *Poly(Lactic Acid): Synthesis, Structures, Properties, Processing, and Applications*. 2010, John Wiley and Sons. p. 345-381.
36. Auras, R., Harte, B., and Selke, S., *An Overview of Polylactides as Packaging Materials.* Macromolecular Bioscience, 2004. **4**(9): p. 835-864.
37. Tayton, E., Purcell, M., Aarvold, A., Smith, J.O., Briscoe, A., Kanczler, J.M., Shakesheff, K.M., Howdle, S.M., Dunlop, D.G., and Oreffo, R.O.C., *A comparison of polymer and polymer-hydroxyapatite composite tissue engineered scaffolds for use in bone regeneration. An*

in vitro and in vivo study. Journal of Biomedical Materials Research Part A, 2014. **102**(8): p. 2613-2624.

38. Zhang, J.Y., Hua-Mo, Hsiao., Benjamin S.; Zhong, Gan-Ji. and Li, Zhong-Ming., *Biodegradable poly(lactic acid)-hydroxyl apatite 3D porous scaffolds using high-pressure molding and salt leaching.* Journal of Materials Science, 2014. **49**(4): p. 1648-1658.
39. Kasirajan, S. and Ngouajio, M., *Polyethylene and biodegradable mulches for agricultural applications: a review.* Agronomy for Sustainable Development, 2012. **32**(2): p. 501-529.
40. De Jong, S.J., Arias, E.R., Rijkers, D.T.S., Van Nostrum, C.F., Kettenes-Van Den Bosch, J.J., and Hennink, W.E., *New insights into the hydrolytic degradation of poly(lactic acid): Participation of the alcohol terminus.* Polymer, 2001. **42**(7): p. 2795-2802.
41. Jung, J.H., Ree, M., and Kim, H., *Acid- and base-catalyzed hydrolyses of aliphatic polycarbonates and polyesters.* Catalysis Today, 2006. **115**(1-4): p. 283-287.
42. Sato, S., Gondo, D., Wada, T., Kanehashi, S., and Nagai, K., *Effects of various liquid organic solvents on solvent-induced crystallization of amorphous poly(lactic acid) film.* Journal of Applied Polymer Science, 2013. **129**(3): p. 1607-1617.
43. Fukushima, K., Tabuani, D., Dottori, M., Armentano, I., Kenny, J.M., and Camino, G., *Effect of temperature and nanoparticle type on hydrolytic degradation of poly(lactic acid) nanocomposites.* Polymer Degradation and Stability, 2011. **96**(12): p. 2120-2129.
44. Zou, H., Yi, C., Wang, L., Liu, H., and Xu, W., *Thermal degradation of poly(lactic acid) measured by thermogravimetry coupled to Fourier transform infrared spectroscopy.* Journal of Thermal Analysis and Calorimetry, 2009. **97**(3): p. 929-935.
45. Santonja-Blasco, L., Ribes-Greus, A., and Alamo, R.G., *Comparative thermal, biological and photodegradation kinetics of polylactide and effect on crystallization rates.* Polymer Degradation and Stability, 2013. **98**(3): p. 771-784.
46. Ebadi-Dehaghani, H., Barikani, M., Borhani, S., Bolvardi, B., Khonakdar, H.A., Jafari, S.H., and Aarabi, A., *Biodegradation and hydrolysis studies on polypropylene/polylactide/organo-clay nanocomposites.* Polymer Bulletin, 2016. **73**(12): p. 3287-3304.
47. Pellis, A., Acero, E.H., Weber, H., Obersriebnig, M., Breinbauer, R., Srebotnik, E., and Guebitz, G.M., *Biocatalyzed approach for the surface functionalization of poly(L-lactic acid) films using hydrolytic enzymes.* Biotechnology Journal, 2015. **10**(11): p. 1739-1749.
48. NatureWorks. 2017; Available from: http://www.natureworksllc.com/Products.
49. Corbion, 2017.

50. Nascimento, L., Gamez-Perez, J., Santana, O.O., Velasco, J.I., Maspoch, M.L., and Franco-Urquiza, E., *Effect of the Recycling and Annealing on the Mechanical and Fracture Properties of Poly(Lactic Acid).* Journal of Polymers and the Environment, 2010. **18**(4): p. 654-660.
51. Arias, V., Hoglund, A., Odelius, K., and Albertsson, A.-C., *Polylactides with "green" plasticizers: Influence of isomer composition.* Journal of Applied Polymer Science, 2013. **130**(4): p. 2962-2970.
52. Auras, R.A., Singh, S.P., and Singh, J.J., *Evaluation of oriented poly(lactide) polymers vs. existing PET and oriented PS for fresh food service containers.* Packaging Technology and Science, 2005. **18**(4): p. 207-216.
53. Armentano, I., Bitinis, N., Fortunati, E., Mattioli, S., Rescignano, N., Verdejo, R., Lopez-Manchado, M.A., and Kenny, J.M., *Multifunctional nanostructured PLA materials for packaging and tissue engineering.* Progress in Polymer Science, 2013. **38**(10–11): p. 1720-1747.
54. Nassar, S.F., Guinault, A., Delpouve, N., Divry, V., Ducruet, V., Sollogoub, C., and Domenek, S., *Multi-scale analysis of the impact of polylactide morphology on gas barrier properties.* Polymer, 2017. **108**(-): p. 163-172.
55. La Verde, L., Fenga, D., Spinelli, M.S., Campo, F.R., Florio, M., and Rosa, M.A., *Catastrophic metallosis after tumoral knee prosthesis failure: A case report.* International Journal of Surgery Case Reports, 2017. **30**(-): p. 9-12.
56. Duarte, J., Correia, L., Simao, A., Figueiredo, A., and Carvalho, A., *Metallosis: A Rare Cause of Autoimmune Hemolytic Anemia.* Acta Medica Portuguesa, 2015. **28**(3): p. 386-389.
57. Heffernan, E.J., Alkubaidan, F.O., Nielsen, T.O., and Munk, P.L., *The imaging appearances of metallosis.* Skeletal Radiology, 2008. **37**(1): p. 59-62.
58. Panni, A.S., Vasso, M., Cerciello, S., and Maccauro, G., *Metallosis following knee arthroplasty: a histological and immunohistochemical study.* International Journal of Immunopathology and Pharmacology, 2011. **24**(3): p. 711-719.
59. Ferri, J.M., Molina, J.M., and Louis, E., *Fabrication of Mg foams for biomedical applications by means of a replica method based upon spherical carbon particles.* Biomedical Physics & Engineering Express, 2015. **1**(4): p. 045002.
60. Persson, M., Lorite, G.S., Kokkonen, H.E., Cho, S.-W., Lehenkari, P.P., Skrifvars, M., and Tuukkanen, J., *Effect of bioactive extruded PLA/HA composite films on focal adhesion.* Colloids and Surfaces B: Biointerfaces, 2014. **121**: p. 409-416.

61. Siqueira, L., Passador, F.R., Costa, M.M., Lobo, A.O., and Sousa, E., *Influence of the addition of β-TCP on the morphology, thermal properties and cell viability of poly (lactic acid) fibers obtained by electrospinning.* Materials Science and Engineering: C, 2015. **52**: p. 135-143.

62. Lewandrowski, K.-U., Bondre, S.P., Shea, M., Untch, C.M., Hayes, W.C., Hile, D.D., Wise, D.L., and Trantolo, D.J., *Composite polylactide-hydroxyapatite screws for fixation of osteochondral osteotomies. A morphometric, histologic and radiographic study in sheep.* Journal of Biomaterials Science, Polymer Edition, 2002. **13**(11): p. 1241-1258.

63. Suchenski, M., McCarthy, M.B., Chowaniec, D., Hansen, D., McKinnon, W., Apostolakos, J., Arciero, R., and Mazzocca, A.D., *Material Properties and Composition of Soft-Tissue Fixation.* Arthroscopy-the Journal of Arthroscopic and Related Surgery, 2010. **26**(6): p. 821-831.

64. Rokkanen, P.U., Bostman, O., Hirvensalo, E., Makela, E.A., Partio, E.K., Patiala, H., Vainionpaa, S., Vihtonen, K., and Tormala, P., *Bioabsorbable fixation in orthopaedic surgery and traumatology.* Biomaterials, 2000. **21**(24): p. 2607-2613.

65. Navarro, M., Engel, E., Planell, J.A., Amaral, I., Barbosa, M., and Ginebra, M.P., *Surface characterization and cell response of a PLA/CaP glass biodegradable composite material.* Journal of Biomedical Materials Research Part A, 2008. **85A**(2): p. 477-486.

66. Yanoso-Scholl, L., Jacobson, J.A., Bradica, G., Lerner, A.L., O'Keefe, R.J., Schwarz, E.M., Zuscik, M.J., and Awad, H.A., *Evaluation of dense polylactic acid/beta-tricalcium phosphate scaffolds for bone tissue engineering.* Journal of Biomedical Materials Research Part A, 2010. **95A**(3): p. 717-726.

67. Agrawal, C.M. and Athanasiou, K.A., *Technique to control pH in vicinity of biodegrading PLA-PGA implants.* Journal of Biomedical Materials Research, 1997. **38**(2): p. 105-114.

68. Conn, R.E., *Safety assessment of polylactide (PLA) for use as a food-contact polymer.* Food and Chemical Toxicology, 1995. **33**(4): p. 273-283.

69. Balart, J.F., Fombuena, V., Fenollar, O., Boronat, T., and Sánchez-Nacher, L., *Processing and characterization of high environmental efficiency composites based on PLA and hazelnut shell flour (HSF) with biobased plasticizers derived from epoxidized linseed oil (ELO).* Composites Part B, 2016. **86**: p. 168-177.

70. Carbonell-Verdu, A., Bernardi, L., Garcia-Garcia, D., Sanchez-Nacher, L., and Balart, R., *Development of environmentally friendly composite matrices from epoxidized cottonseed oil.* European Polymer Journal, 2015. **63**: p. 1-10.

71. Ferri, J.M., Garcia-Garcia, D., Sánchez-Nacher, L., Fenollar, O., and Balart, R., *The effect of maleinized linseed oil (MLO) on mechanical performance of poly(lactic acid)-thermoplastic starch (PLA-TPS) blends.* Carbohydrate Polymers, 2016. **147**(-): p. 60-68.

72. Mauck, S.C., Wang, S., Ding, W., Rohde, B.J., Fortune, C.K., Yang, G., Ahn, S.K., and Robertson, M.L., *Biorenewable Tough Blends of Polylactide and Acrylated Epoxidized Soybean Oil Compatibilized by a Polylactide Star Polymer.* Macromolecules, 2016. **49**(5): p. 1605-1615.

73. Santos, E.F., Oliveira, R.V.B., Reiznautt, Q.B., Samios, D., and Nachtigall, S.M.B., *Sunflower-oil biodiesel-oligoesters/polylactide blends: Plasticizing effect and ageing*. Polymer Testing, 2014. **39**: p. 23-29.

74. Prempeh, N., Li, J., Liu, D., Das, K., Maiti, S., and Zhang, Y., *Plasticizing Effects of Epoxidized Sun Flower Oil on Biodegradable Polylactide Films: A Comparative Study*. Polymer Science Series A, 2014. **56**(6): p. 856-863.

75. Silverajah, V.S.G., Ibrahim, N.A., Zainuddin, N., Yunus, W.M.Z.W., and Abu Hassan, H., *Mechanical, Thermal and Morphological Properties of Poly(lactic acid)/Epoxidized Palm Olein Blend*. Molecules, 2012. **17**(10): p. 11729-11747.

76. Baig, G.A. and Carr, C.M., *Surface and Structural Damage to PLA Fibres during Textile Pretreatments.* Fibres & Textiles in Eastern Europe, 2016. **24**(2): p. 52-58.

77. Cayla, A., Rault, F., Giraud, S., Salaun, F., Fierro, V., and Celzard, A., *PLA with Intumescent System Containing Lignin and Ammonium Polyphosphate for Flame Retardant Textile.* Polymers, 2016. **8**(9): p. 331-347.

78. Chang, T., *Analysis on PLA Textile Fiber Production Technology and Properties*, *in Advances in Mechanical Engineering, Pts 1-3*, M. Zhou, Editor. 2011. p. 2145-2150.

79. Saffari, M.R. and Miab, R.K., *Antibacterial property of PLA textiles coated by nano-TiO_2 through eco-friendly low-temperature plasma.* International Journal of Clothing Science and Technology, 2016. **28**(6): p. 830-840.

80. Correa, J.P., Bacigalupe, A., Maggi, J., and Eisenberg, P., *Biodegradable PLA/PBAT/Clay Nanocomposites: Morphological, Rheological and Thermomechanical Behavior.* Journal of Renewable Materials, 2016. **4**(4): p. 258-265.

81. Arrieta, M.P., Fortunati, E., Dominici, F., Rayon, E., Lopez, J., and Kenny, J.M., *PLA-PHB/cellulose based films: Mechanical, barrier and disintegration properties.* Polymer Degradation and Stability, 2014. **107**: p. 139-149.

82. Arrieta, M.P., Lopez, J., Rayon, E., and Jimenez, A., *Disintegrability under composting conditions of plasticized PLA-PHB blends.* Polymer Degradation and Stability, 2014. **108**: p. 307-318.

83. Swierz-Motysia, B., Jeziorska, R., Szadkowska, A., and Piotrowska, M., *Synthesis and properties of biodegradable polylactide and thermoplastic starch blends.* Polimery, 2011. **56**(4): p. 271-280.

84. Balart, R., López, J., Sánchez, L., and Nadal, A., eds. *Introducción a la ciencia e ingeniería de polímeros*. 2001, Alfagràfic S.A: Alcoy.

85. Bocque, M., Voirin, C., Lapinte, V., Caillol, S., and Robin, J.J., *Petro-Based and Bio-Based Plasticizers: Chemical Structures to Plasticizing Properties.* Journal of Polymer Science Part a-Polymer Chemistry, 2016. **54**(1): p. 11-33.

86. Murariu, M., Ferreira, A.D.S., Alexandre, M., and Dubois, P., *Polylactide (PLA) designed with desired end-use properties: 1. PLA compositions with low molecular weight ester-like plasticizers and related performances.* Polymers for Advanced Technologies, 2008. **19**(6): p. 636-646.

87. Auras, R.A., *Solubility of gases and vapors in polylactide polymers.* In Thermodynamics, Solubility and Environmental Issues, 2007. p. 343-368.

88. Cheng, H.-Y., Yang, Y.-J., Li, S.-C., Hong, J.-Y., and Jang, G.-W., *Modification and extrusion coating of polylactic acid films.* Journal of Applied Polymer Science, 2015. **132**(35).

89. Ingrao, C., Tricase, C., Cholewa-Wojcik, A., Kawecka, A., Rana, R., and Siracusa, V., *Polylactic acid trays for fresh-food packaging: A Carbon Footprint assessment.* Science of the Total Environment, 2015. **537**: p. 385-398.

90. Jost, V. and Kopitzky, R., *Blending of Polyhydroxybutyrate-co-valerate with Polylactic Acid for Packaging Applications - Reflections on Miscibility and Effects on the Mechanical and Barrier Properties.* Chemical and Biochemical Engineering Quarterly, 2015. **29**(2): p. 221-246.

91. Sanyang, M.L. and Sapuan, S.M., *Development of expert system for biobased polymer material selection: food packaging application.* Journal of Food Science and Technology, 2015. **52**(10): p. 6445-54.

92. Plackett, D.V., Holm, V.K., Johansen, P., Ndoni, S., Nielsen, P.V., Sipilainen-Malm, T., Sodergard, A., and Verstichel, S., *Characterization of L-polylactide and L-polylactide-polycaprolactone co-polymer films for use in cheese-packaging applications.* Packaging Technology and Science, 2006. **19**(1): p. 1-24.

93. Hutmacher, D.W., Goh, J.C.H., and Teoh, S.H., *An introduction to biodegradable materials for tissue engineering applications.* Annals Academy of Medicine Singapore, 2001. **30**(2): p. 183-191.

94. Maurus, P.B. and Kaeding, C.C., *Bioabsorbable implant material review.* Operative Techniques in Sports Medicine, 2004. **12**(3): p. 158-160.

95. Mekonnen, T., Mussone, P., Khalil, H., and Bressler, D., *Progress in bio-based plastics and plasticizing modifications.* Journal of Materials Chemistry A, 2013. **1**(43): p. 13379-13398.

96. Le Duigou, A., Deux, J.-M., Davies, P., and Baley, C., *PLLA/Flax Mat/Balsa Bio-Sandwich – Environmental Impact and Simplified Life Cycle Analysis.* Applied Composite Materials, 2012. **19**(3): p. 363-378.

97. Adeodato Vieira, M.G., da Silva, M.A., dos Santos, L.O., and Beppu, M.M., *Natural-based plasticizers and biopolymer films: A review.* European Polymer Journal, 2011. **47**(3): p. 254-263.

98. Yokesahachart, C. and Yoksan, R., *Effect of amphiphilic molecules on characteristics and tensile properties of thermoplastic starch and its blends with poly(lactic acid).* Carbohydrate Polymers, 2011. **83**(1): p. 22-31.

99. Jia, P., Zhang, M., Liu, C., Hu, L., and Zhou, Y.-H., *Properties of poly(vinyl chloride) incorporated with a novel soybean oil based secondary plasticizer containing a flame retardant group.* Journal of Applied Polymer Science, 2015. **132**(25).

100. Jia, P.-Y., Bo, C.-Y., Zhang, L.-Q., Hu, L.-H., Zhang, M., and Zhou, Y.-H., *Synthesis of castor oil based plasticizers containing flame retarded group and their application in poly (vinyl chloride) as secondary plasticizer.* Journal of Industrial and Engineering Chemistry, 2015. **28**: p. 217-224.

101. Mohammed, F.S., Conley, M., Saunders, S.R., Switzer, J., Jha, R., Cogen, J.M., Chaudhary, B.I., Pollet, P., Eckert, C.A., and Liotta, C.L., *Epoxidized linolenic acid salts as multifunctional additives for the thermal stability of plasticized PVC.* Journal of Applied Polymer Science, 2015. **132**(13): p. 42111-20.

102. Narute, P., Rao, G.R., Misra, S., and Palanisamy, A., *Modification of cottonseed oil for amine cured epoxy resin: Studies on thermo-mechanical, physico-chemical, morphological and antimicrobial properties.* Progress in Organic Coatings, 2015. **88**: p. 316-324.

103. Shi, Q., Chen, C., Gao, L., Jiao, L., Xu, H., and Guo, W., *Physical and degradation properties of binary or ternary blends composed of poly (lactic acid), thermoplastic starch and GMA grafted POE.* Polymer Degradation and Stability, 2011. **96**(1): p. 175-182.

104. Tsui, A., Wright, Z.C., and Frank, C.W., *Biodegradable Polyesters from Renewable Resources.* Annual Review of Chemical and Biomolecular Engineering. 2013. **4**: p. 143-170.

105. Reddy, M., Mohanty, A.K., and Misra, M., *Thermoplastics from Soy Protein: A Review on Processing, Blends and Composites.* Journal of Biobased Materials and Bioenergy, 2010. **4**(4): p. 298-316.

106. Mittal, V., Akhtar, T., and Matsko, N., *Mechanical, Thermal, Rheological and Morphological Properties of Binary and Ternary Blends of PLA, TPS and PCL.* Macromolecular Materials and Engineering, 2015. **300**(4): p. 423-435.

107. Oromiehie, A.R., Lari, T.T., and Rabiee, A., *Physical and thermal mechanical properties of corn starch/LDPE composites.* Journal of Applied Polymer Science, 2013. **127**(2): p. 1128-1134.

108. Ren, J., Fu, H., Ren, T., and Yuan, W., *Preparation, characterization and properties of binary and ternary blends with thermoplastic starch, poly(lactic acid) and poly(butylene adipate-co-terephthalate).* Carbohydrate Polymers, 2009. **77**(3): p. 576-582.

109. Sarazin, P., Li, G., Orts, W.J., and Favis, B.D., *Binary and ternary blends of polylactide, polycaprolactone and thermoplastic starch.* Polymer, 2008. **49**(2): p. 599-609.

110. Niazi, M.B.K., Zijlstra, M., and Broekhuis, A.A., *Influence of plasticizer with different functional groups on thermoplastic starch.* Journal of Applied Polymer Science, 2015. **132**(22): p. 42012.

111. Courgneau, C., Domenek, S., Guinault, A., Averous, L., and Ducruet, V., *Analysis of the Structure-Properties Relationships of Different Multiphase Systems Based on Plasticized Poly(Lactic Acid).* Journal of Polymers and the Environment, 2011. **19**(2): p. 362-371.

112. Martin, O. and Averous, L., *Poly(lactic acid): plasticization and properties of biodegradable multiphase systems.* Polymer, 2001. **42**(14): p. 6209-6219.

113. Chieng, B.W., Ibrahim, N.A., Then, Y.Y., and Loo, Y.Y., *Epoxidized Vegetable Oils Plasticized Poly(lactic acid) Biocomposites: Mechanical, Thermal and Morphology Properties.* Molecules, 2014. **19**(10): p. 16024-16038.

114. Ford, E.N.J., Rawlins, J.W., Mendon, S.K., and Thames, S.F., *Effect of acid value on the esterification mechanism of maleinized soybean oil with cotton.* Journal of Coatings Technology and Research, 2012. **9**(5): p. 637-641.

115. Ferri, J.M., Samper, M.D., García-Sanoguera, D., Reig, M.J., Fenollar, O., and Balart, R., *Plasticizing effect of biobased epoxidized fatty acid esters on mechanical and thermal properties of poly(lactic acid).* Journal of Materials Science, 2016. **51**(11): p. 5356-5366.

116. Ojijo, V., Sinha Ray, S., and Sadiku, R., *Toughening of Biodegradable Polylactide/Poly(butylene succinate-co-adipate) Blends via in Situ Reactive Compatibilization.* ACS Applied Materials & Interfaces, 2013. **5**(10): p. 4266-4276.

117. Weng, Y.-X., Jin, Y.-J., Meng, Q.-Y., Wang, L., Zhang, M., and Wang, Y.-Z., *Biodegradation behavior of poly(butylene adipate-co-terephthalate) (PBAT), poly(lactic acid) (PLA), and their blend under soil conditions.* Polymer Testing, 2013. **32**(5): p. 918-926.

118. Li, H. and Huneault, M.A., *Effect of Chain Extension on the Properties of PLA/TPS Blends.* Journal of Applied Polymer Science, 2011. **122**(1): p. 134-141.

119. Saeidlou, S., Huneault, N.A., Li, H., and Park, C.B., *Poly(lactic acid) crystallization*. Progress in Polymer Science, 2012. **37**(12): p. 1657-1677.

120. Aurelio Salerno, A.F.-G., M.; San Roman del Barrio, J.; Pascuala, C. D., *Macroporous and nanometre scale fibrous PLA and PLA–HA composite scaffolds fabricated by a bio safe strategy*. RSC Advances, 2014. **4**(106): p. 61491-61502.

121. Chae, T., Yang, H., Ko, F., and Troczynski, T., *Bio-inspired dicalcium phosphate anhydrate/poly(lactic acid) nanocomposite fibrous scaffolds for hard tissue regeneration: In situ synthesis and electrospinning*. Journal of Biomedical Materials Research Part A, 2014. **102**(2): p. 514-522.

122. Hu, H.-T., Lee, S.-Y., Chen, C.-C., Yang, Y.-C., and Yang, J.-C., *Processing and properties of hydrophilic electrospun polylactic acid/beta-tricalcium phosphate membrane for dental applications.* Polymer Engineering and Science, 2013. **53**(4): p. 833-842.

123. Danoux, C.B., Barbieri, D., Yuan, H., de Bruijn, J.D., van Blitterswijk, C.A., and Habibovic, P., *In vitro and in vivo bioactivity assessment of a polylactic acid/hydroxyapatite composite for bone regeneration.* Biomatter, 2014. **4**(1): e27664.

124. Ishikawa, K., Akasaka, T., Abe, S., Yawaka, Y., Suzuki, M., and Watari, F., *Application of imogolite, alumino-silicate nanotube, as scaffold for the mineralization of osteoblasts.* Bioceramics Development and Applications, 2011. **1:** p. 1-3.

125. Abdullayev, E. and Lvov, Y., *Halloysite clay nanotubes as a ceramic "skeleton" for functional biopolymer composites with sustained drug release.* Journal of materials chemistry B, 2013. **1**(23): p. 2894-2903.

126. Balart, J.F., García-Sanoguera, D., Balart, R., Boronat, T., and Sánchez-Nacher, L., *Manufacturing and properties of biobased thermoplastic composites from poly(lactid acid) and hazelnut shell wastes.* Polymer Composites, 2016.

127. Ferri, J., Gisbert, I., García-Sanoguera, D., Reig, M.J., and Balart, R., *The effect of beta-tricalcium phosphate on mechanical and thermal performances of poly(lactic acid)*. Journal of Composite Materials, 2016. **50**(30): p. 4189-4198.

128. Lvov, Y.M., Shchukin, D.G., Mohwald, H., and Price, R.R., *Halloysite clay nanotubes for controlled release of protective agents.* Acs Nano, 2008. **2**(5): p. 814-820.

129. Sahnoun, S., Boutahala, M., Zaghouane-Boudiaf, H., and Zerroual, L., *Trichlorophenol removal from aqueous solutions by modified halloysite: kinetic and equilibrium studies.* Desalination and Water Treatment, 2016. **57**(34): p. 15941-15951.

130. Tan, D., Yuan, P., Annabi-Bergaya, F., Yu, H., Liu, D., Liu, H., and He, H., *Natural halloysite nanotubes as mesoporous carriers for the loading of ibuprofen.* Microporous and Mesoporous Materials, 2013. **179**: p. 89-98.

131. Xi, L., Xiaojie, J., Rui, X., Jiang, M., Jie, W., and Liangyin, C., *Halloysite nanotube composited thermo-responsive hydrogel system for controlled-release.* Chinese Journal of Chemical Engineering, 2013. **21**(9): p. 991-998.

132. Hassouna, F., Mihai, I., Fetzer, L., Fouquet, T., Raquez, J. M., Laachachi, A., Ibn Al Ahrach, H., Dubois, P., *Design of New Cardanol Derivative: Synthesis and Application as Potential Biobased Plasticizer for Poly(lactide).* Macromolecular Materials and Engineering, 2016. **301**(10): p. 1267-1278.

133. Torres-Huerta, A.M., Palma-Ramirez, D., Dominguez-Crespo, M.A., Del Angel-López, D., and de la Fuente, D., *Comparative assessment of miscibility and degradability on PET/PLA and PET/chitosan blends*. European Polymer Journal, 2014. **61**: p. 285-299.

134. Non-Biodegradable Bioplastic. *http://www.bioplastics.guide/ref/bioplastics/non-biodegradable-bioplastics/.*

135. Muroi, F., Tachibana, Y., Soulenthone, P., Yamamoto, K., Mizuno, T., Sakurai, T., Kobayashi, Y., and Kasuya, K., *Characterization of a poly(butylene adipate-co-terephthalate) hydrolase from the aerobic mesophilic bacterium Bacillus pumilus*. Polymer Degradation and Stability, 2017. **137**: p. 11-22.

136. Siracusa, V., Lotti, N., Murani, A., and Marco Dalla, R., *Poly(butylene succinate) and poly(butylene succinate-co-adipate) for food packaging applications: Gas barrier properties after stressed treatments*. Polymer Degradation and Stability, 2015. **119**: p. 35-45.

II. OBJETIVOS

OBJETIVOS

II.1. OBJETIVOS GENERALES

El objetivo general del presente trabajo es el de mejorar la aplicabilidad en diferentes sectores (envase-embalaje y médico, entre otros) de materiales biodegradables en base a PLA mezclado en fundido con aceites naturales modificados, o bien con otros polímeros biodegradables como PCL y/o TPS o con ortofosfatos del tipo HA y β-TCP. Dicha aplicabilidad depende de la modificación sobre la ductilidad o la rigidez del material base.

II.2. OBJETIVOS ESPECÍFICOS.

Dicho objetivo general se ha desglosado en una serie de objetivos específicos que se detallan a continuación:

- Evaluación del efecto de la incorporación de otros polímeros biodegradables como el TPS y/o PCL sobre las propiedades mecánicas y térmicas aportadas al PLA.
- Evaluación de la miscibilidad entre PLA-PCL y PLA-TPS en las diferentes mezclas realizadas, así como la mejora mediante la incorporación de MLO como agente compatibilizante.
- Estudio de la biodegradación-desintegración de los blends PLA-PCL en condiciones de compostaje.
- Evaluación del efecto de la incorporación de diferentes aceites naturales modificados (OES, MLO) sobre las propiedades mecánicas y térmicas del PLA destinadas al envasado alimentario.
- Estudio y evaluación de las propiedades barrera como la permeabilidad al oxígeno y la mojabilidad del PLA-OES.

- Evaluación de las saturaciones y su efecto antiplastificante de los aceites OES y MLO sobre las propiedades mecánicas.
- Evaluación del efecto de OES y MLO sobre la cristalinidad del PLA.
- Evaluación del efecto de la incorporación de HA y β-TCP sobre las propiedades mecánicas y térmicas aportadas al PLA.

Para alcanzar estos objetivos, se contempla la siguiente planificación.

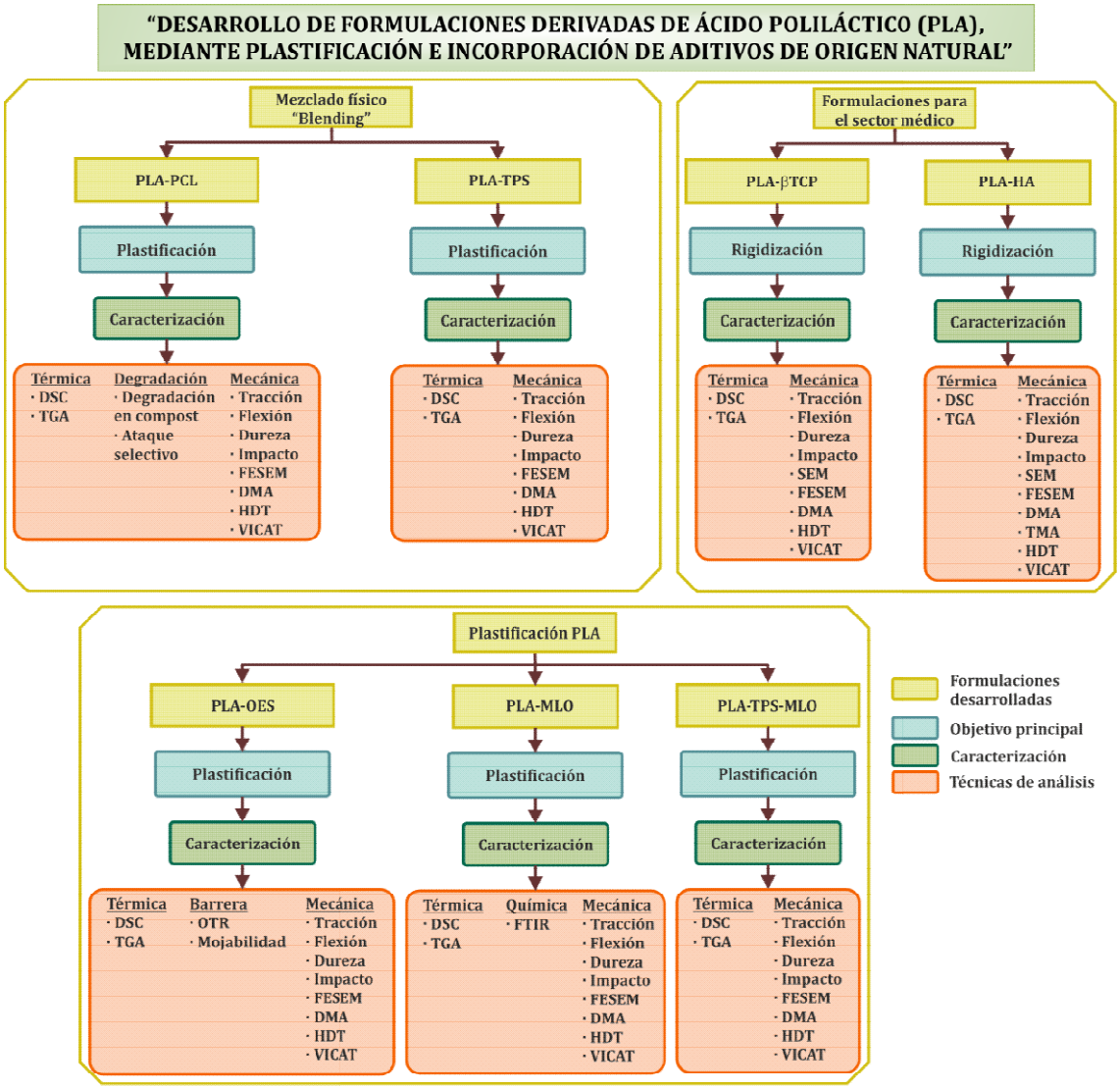

III. RESULTS AND DISCUSSION

RESULTS AND DISCUSSION

SUMMARY

This block shows the most relevant results regarding PLA-improved formulations. The block is structured into seven chapters corresponding to different papers/manuscripts. The information herein shown is divided into three different thematics depending on the strategy to optimize the PLA behaviour: physical blending with other polymers, plasticization strategies with biobased and modified vegetable oils and, finally, use of orthophosphate fillers for uses in the medical sector.

PLA-improved formulations by physical blending.

Chapter III.1

Effect of miscibility on mechanical and thermal properties of poly(lactic acid)-poly(caprolactone) blends.

Chapter III.2

Poly(lactic acid) formulations with improved toughness by physical blending with thermoplastic starch.

PLA-improved formulations by plasticizer.

Chapter III.3

Plasticizing effect of biobased epoxidized fatty acid esters on mechanical and thermal properties of poly(lactic acid).

Chapter III.4

The effect of maleinized linseed oil as biobased plasticizer in poly(lactic acid)-based formulations.

Chapter III.5

The effect of maleinized linseed oil (MLO) on mechanical performance of poly(lactic acid)-thermoplastic starch (PLA-TPS) blends.

PLA-improved formulations for medical applications.

Chapter III.6

The effect of beta-tricalcium phosphate on mechanical and thermal performance of poly(lactic acid).

Chapter III.7

Manufacturing and characterization of poly(lactic acid) composites with hydroxyapatite.

Chapter III.1

Chapter III.1. Effect of miscibility on mechanical and thermal properties of poly(lactic acid)-poly(caprolactone) blends.

“Effect of miscibility on mechanical and thermal properties of poly(lactic acid)-poly(caprolactone) blends”

J.M. Ferri, O. Fenollar, A. Jorda-Vilaplana, D. García-Sanoguera, R. Balart

Instituto de Tecnología de Materiales (ITM)

Universitat Politècnica de València (UPV)

Plaza Ferrandiz y Carbonell 1, 03801, Alcoy, Alicante (Spain)

Polymer International 65: 453-463 (2016)

Abstract.

Binary blends based on poly(lactic acid) (PLA) and polycaprolactone (PCL) were prepared by melt mixing in a twin-screw co-rotating extruder in order to increase the low intrinsic elongation at break of PLA for packaging applications. Although PLA and PCL show low miscibility, the presence of PCL leads to a marked improvement in the ductile properties of PLA. Various mechanical properties were evaluated in terms of PCL content up to 30 wt% PCL. In addition to tensile and flexural properties, Poisson's ratio was obtained using biaxial extensometry to evaluate transversal deformations when axial loads are applied. Very slight changes in the melt temperature and glass transition temperature of PLA are observed thus indicating the low miscibility of the PLA-PCL system. Field emission scanning electron microscopy reveals some interactions between the two components of the blend since the morphology is characterized by non-spherical polycaprolactone drops dispersed into the PLA matrix. In addition to the improvement of mechanical ductile properties, PCL provides higher degradation rates of blends under conditions of composting for contents below 22.5% PCL.

Keywords: poly(lactic acid) (PLA); polycaprolactone (PCL); binary blends; FESEM; mechanical properties; degradability.

Introduction.

Nowadays, polymers find a broad number of applications in the fields of packaging, medical and automotive industries due to an excellent balance between processing and overall properties [1]. Among all these polymers, aliphatic polyesters from both renewable and/or fossil fuel resources [2] such as poly(lactic acid) (PLA), polycaprolactone (PCL), poly(ester amide) (PEA), polyhydroxybutyrate, thermoplastic starch (TPS), etc., and their copolymers such as poly(lactic acid)-co-poly(ε-caprolactone) (PLACL), poly(hydroxybutyrate-co-hydroxyvalerate) (PHBV), etc., are increasingly used in the medical[3] and packaging fields due to their easy processing[1] and quick degradability in various environments [4-6]. Some of their uses include films, bottles, homewares, packages, etc. Most of these polymers offer attractive degradation rates in controlled environments, thus avoiding permanent environmental impact. On the other hand, their thermoplastic nature enables easy processing by conventional processes such as melt spinning [7, 8], injection moulding [9], extrusion [1], etc., or other advanced manufacturing processes such as electrospinning [10-12], three-dimensional printing [13-15], etc.

PLA is one of the most used biocompostable polymers in packaging applications due to its good mechanical performance and balanced barrier properties [16, 17]. PLA is widely used in the manufacturing of biodegradable/biocompostable films for food applications. The main drawback related to PLA is its high intrinsic fragility that is still accentuated as degradation occurs. PLA has low ductility at room temperature because its glass transition temperature (T_g) is located at around 60 ^oC; so that, below its T_g, it behaves as a glass characterized by high mechanical resistance and modulus and high fragility together with low elongation at break (due to restricted polymer chain mobility below T_g). Conventional plasticizers could potentially be used to allow some elongation at break but typical plasticizers can migrate and this could be responsible for toxicity as well as deterioration in mechanical properties [18-20]. Another alternative is copolymerization. By using copolymerization processes with appropriately selected monomers it is possible to tailor PLA properties to desired

performance. Some examples of PLA-based copolymers are PLACL, poly[(lactic acid-co-ethylene glycol)], PHBV, etc [21, 22]. Nevertheless these copolymers are expensive. One attractive solution is the manufacturing of binary or ternary PLA-based blends. The use of a flexible polymer can lead to improved ductile properties with effects similar to those of a plasticizer.

Polymeric plasticizers thus provide improved elongation to PLA. Additionally, by controlling the blend composition it is possible to tailor desired properties such as toughness, ductility, elongation at break, mechanical strength, etc.

PCL is partially compatible with PLA, as they are aliphatic polyesters. PCL is characterized by a very low T_g of about -60 ^oC [23] which makes it very flexible at room temperature. On the other hand, it melts at relatively low temperatures close to 60 ^oC, markedly lower than the melt temperature of PLA located at about 170 ^oC, so that it can provide features similar to those of polymeric plasticizers when processed in conjunction with PLA. PCL can provide flexibility and elongation ability depending on the total PCL content. Although PLA and PCL are compatible, some research studies have demonstrated that there are very weak interactions between them when melt blended [23, 24]. Broz et al. observed that stronger interactions are detected for PCL contents higher than 50%. Also they conducted comparative studies with the Kerner-Uemura-Takayangi mathematical model to compare their results [25]. Yeh et al. demonstrated using dynamic mechanical thermal analysis (DMTA) studies that increased interactions or miscibility occur for a mixing ratio of PLA70/PCL30 [23]. Lopez-Rodriguez et al. also observed from DMTA studies that there is a weak interaction between these two polymers [26]. The poor interactions are demonstrated by DSC and DMTA studies of PLA/PCL blends, showing two T_g values at positions close to those of the raw components revealing a clear phase separation.

The aim of the study reported here was to evaluate the influence of PCL as minor component in PLA/PCL blends. The effect of PCL content in the 0 – 30 wt% range was evaluated in terms of mechanical properties (tensile, flexural, impact, hardness tests) and thermal properties using DSC, TGA and DMTA in torsion mode. Qualitative assessment of miscibility/interactions was carried out by characterizing

surface morphology of PLA/PCL blends with field emission scanning electron microscopy (FESEM).

Experimental.

Materials.

PLA from renewable resources, Ingeo™ Biopolymer 6201D supplied by NatureWorks LLC (Minnetonka, USA) was used as base polymer. This polymer is characterized by a 2% D-lactic acid content with overall density of 1.24 g cm^{-3} and a melt flow index of 15-30 g $(10\ min)^{-1}$ at 210 ^{o}C. A commercial grade of PCL, Capa™ 6500 supplied by Perstorp (Warrington, UK) was used to provide ductile properties to PLA. This PCL grade is characterized by a melt flow index of 5.60-7.90 g $(10\ min)^{-1}$ at 160 ^{o}C, a density of 1.1 g cm^{-3} and a molecular weight of 50,000 g mol^{-1}. Its melt point is located in the range 58-60 ^{o}C and it offers a high elongation at break of more than 800%.

PLA/PCL blend manufacturing.

Four different PLA/PCL blend compositions were defined, PLA being the major component. **Table III.1.1** summarizes the compositions and labelling of each PLA/PCL blend. PLA and PCL pellets were previously dried in an oven at 60 and 40 °C respectively, for 24 h before melt blending. Appropriate amounts of PLA and PCL were manually mixed in pellet form in a zip bag, and then mixtures were melt compounded in a twin screw co-rotating extruder at a rotating speed of 60 rpm. The temperature profile was 25, 175, 177.5 and 180 ^{o}C from the hopper to the die. After cooling, the material was pelletized and subsequently injection moulded using a Mateu & Solé model Meteor 270/75 (Barcelona, Spain) at a temperature of 180 ^{o}C.

Mechanical characterization of PLA/PCL blends.

Mechanical properties of PLA/PCL blends were measured with tensile, flexural, impact and hardness tests at time zero and after 8 months. Samples were not stored under special conditions. Tensile and flexural properties were obtained using a universal test machine (SAE Ibertest model ELIB 30, Madrid, Spain) at room temperature by following the guidelines of ISO 527-5 and ISO 178, respectively, with a load cell of 5 kN and a crosshead speed of 10 mm min^{-1}. At least five different samples were tested in tensile and flexural tests and average values of the relevant parameters were calculated. In addition, elastic modulus and Poisson's ratio were accurately determined by using biaxial (longitudinal and transversal) extensometers (SAE Ibertest model IB/MFQ-R2, Madrid, Spain) coupled to the universal test machine.

Hardness of PLA/PCL blends was obtained using a Shore D durometer from Instrumentos J Bot SA, model 673-D (Barcelona, Spain) as recommended in UNE-EN-ISO 868.

Impact absorbed energy values were measured on unnotched samples with a Charpy pendulum (6 J) from Metrotec SA (San Sebastián, Spain) as indicated in the ISO 179:1993 standard. The impact test was carried out on five different samples and average values of the impact absorbed energy were calculated.

Table III.1.1. Summary of the compositions of PLA/PCL blends and labelling.

Sample	PLA (wt%)	PCL (wt%)
PLA	100	-
PLA/7.5PCL	92.5	7.5
PLA/15PCL	85	15
PLA/22.5PCL	77.5	22.5
PLA/30PCL	70	30

Characterization of surface morphology of PLA/PCL blends.

All PLA/PCL composites were subjected to a cryofracture process with liquid nitrogen and samples were observed using a FESEM instrument (Zeiss ULTRA55 from Oxford Instruments, Oxford, UK) at an acceleration voltage of 2 kV. Samples for FESEM observation were subjected to a sputtering process with platinum to obtain detailed information of the blend morphology. Cryofractured PLA/PCL samples were also subjected to selective extraction with acetone to selectively remove PCL from the surface thus leading to detailed observation of the blend morphology. The samples were immersed in acetone for 12 h then placed in an oven at 40 °C for 1 h to evaporate the solvent.

DMTA of PLA/PCL blends.

DMTA was carried out in torsion-shear mode with an oscillatory rheometer (TA Instruments, model AR G2, New Castle, USA) equipped with a torsion clamp accessory for solid samples. Rectangular samples of size 40x10x4 mm^3 were subjected to a temperature ramp from -80 up to 130 ^oC at a constant heating rate of 2 $^oC\ min^{-1}$. A frequency of 1 Hz was used for all tests and the maximum deformation (γ) was set at 0.1%.

Thermal characterization of PLA/PCL blends.

Thermal properties of PLA/PCL blends were studied using DSC and TGA. TGA was conducted using a TGA/SDTA 851 thermobalance (Mettler-Toledo Inc., Schwerzenbach, Switzerland) with a temperature programme from 30 to 700 ^oC at a heating rate of 20 $^oC\ min^{-1}$ and nitrogen gas atmosphere (66 mL min^{-1}). The main thermal transitions were investigated using a differential scanning calorimeter (DSC 821 from Mettler-Toledo Inc., Schwerzenbach, Switzerland) in air atmosphere. The

heating programme for DSC runs was from 30 to 350 °C at a heating rate of 10 °C min^{-1}. The percentage crystallinity of PLA was calculated by means of the following equation:

$$\boldsymbol{X_c}\ (\%) = \frac{\boldsymbol{\Delta H_m - \Delta H_c}}{\boldsymbol{w\ \Delta H_m^0}} 100 \qquad (1)$$

where ΔH_m and ΔH_c are the experimental melting enthalpy and cold crystallization enthalpy of PLA, respectively, and w is the weight fraction of PLA. A value of ΔH^0_m = 93 J g^{-1} was used according to a reported enthalpy of melting of 100% crystalline PLA [23]. The percentage cristallinity of PCL was 46.4%. Neat PCL had no cold crystallization peak and a value of ΔH^0_m = 139 J g^{-1} was used according to a reported melt enthalpy of 100% crystalline PCL [26].

Degradability under composting conditions.

The disintegration of PLA and PLA/PCL blends under composting conditions was investigated according to the ISO 20200 standard. The composition of the solid synthetic waste was prepared by mixing 40% sawdust, 30% rabbit food, 10% mature compost supplied by BCM-BRICOLAGE SA, 10% starch, 5% sugar, 4% corn oil and 1% urea. The water content was set to 55 wt% and aerobic conditions were guaranteed by appropriate and vigorous mixing. Sheets of size 25 x 25 mm^2 were initially weighed and buried at 4 - 6 cm depth inside perforated polystyrene boxes containing the prepared mix. The incubation temperature was maintained constant at 58 °C. Each sample was extracted from the boxes at regular periods of 3, 7, 14, 21, 28, 35 and 42 days of disintegration; extracted samples were cleaned gently with distilled water, dried in an oven at 37 °C during 24 h and finally, reweighed. The degree of disintegration was calculated by referring the sample weight at different days of incubation to the initial weight. The equation to calculate the disintegration in percentage is:

$$\boldsymbol{D}\ (\%) = \frac{\boldsymbol{m_i - m_f}}{\boldsymbol{m_i}} 100 \qquad (2)$$

where m_i is the initial weight of the sample and m_f is the weight of the same sample after the corresponding incubation period.

Results and discussion.

Effect of PCL on mechanical properties of PLA/PCL binary blends.

One of the main drawbacks related to PLA is its low intrinsic ductility with low elongation at break values; this is an important issue to be taken into account when used in packaging applications. **Figure III.1.1** shows the evolution of the tensile properties of PLA/PCL blends in terms of the PCL content. As expected, PCL provides improved ductile properties (with similar effect to plasticizers) that lead to lower tensile strength. The tensile strength of unblended PLA is close to 64 MPa and the addition of only 7.5 wt% PCL leads to a value of 56.8 MPa (a decrease of 12.7%). As the PCL content increases, tensile strength decreases to 45.8 MPa for a PLA/PCL blend with 30 wt% PCL, representing a decrease of about 28.4%. The plasticization effect that PCL provides to PLA is evident. Similar tendency is observed with regard to the tensile modulus. With regard to elongation at break, it clearly shows an improvement. PLA is a quite brittle polymer with a low elongation at break of 8.6%. Addition of 7.5 wt% of PCL leads to an elongation at break of 19.1% which represents an increase of 122%. Higher PCL contents lead to elongation at break values higher than 70% for compositions containing 22.5 wt% PCL which represents an increase of more than 715% with regard to PLA alone. For higher contents over 22.5 wt% PCL, elongation decreases. When polymers are immiscible, with the growth of the minority polymer domains (in this case the PCL rich phase), the continuous phase (in this case the PLA

rich matrix) shows a clear phase separation. This phase separation is responsible for the interruption of the blend elongation as observed by other authors [27]. As we have previously described, PLA is a stiff polymer with a tensile modulus of about 3594 MPa. Tensile modulus is defined as the ratio between the strength and the strain values in the linear region. As we have seen, tensile strength decreases with the PCL content, but the decrease in elongation at break is markedly higher and this leads to lower stress/strain ratios, which leads to lower tensile modulus as observed in Figure 1. The tensile modulus of PLA alone is reduced to values lower than 3000 MPa for PLA/PCL blends with a PCL content of 22.5 wt% and higher.

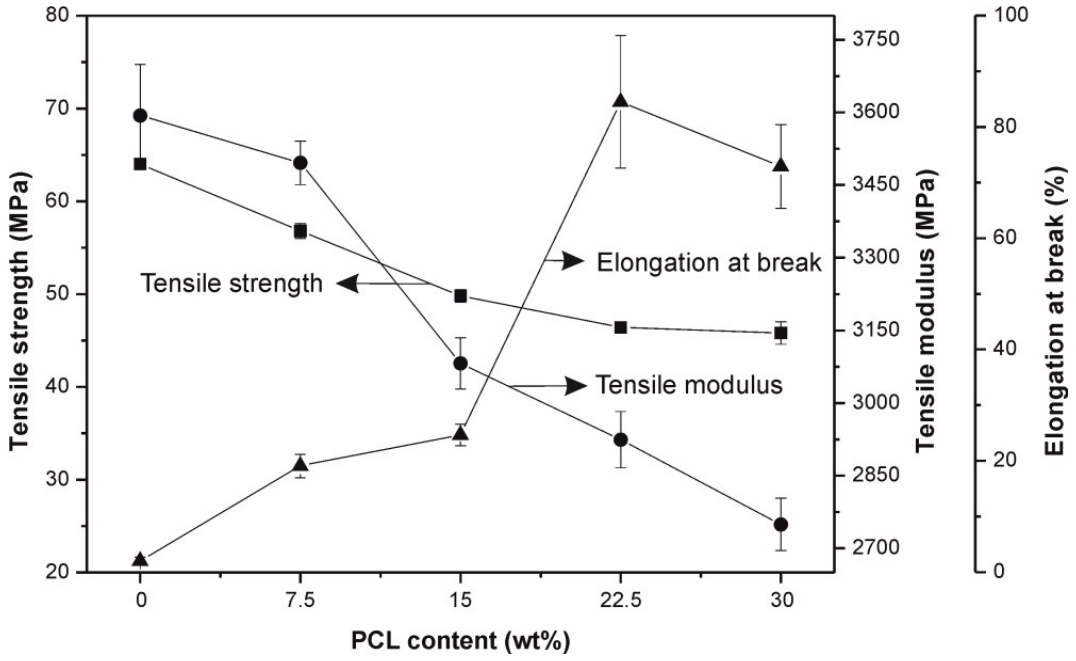

Figure III.1.1. Evolution of mechanical properties from tensile tests (tensile strength, elongation at break and tensile modulus) in terms of the PCL content.

The evolution of the flexural properties is similar to that of the tensile properties (**Figure III.1.2**). As the PCL content increases both flexural modulus and flexural strength decreases due to the plasticization effect provided by PCL. The flexural strength of unblended PLA is 116.3 MPa and we observe a decrease to 91.3 and 86.7 MPa for PLA/PCL blends with 22.5 and 30 wt%, respectively (21.5 and 25.45% lower values, respectively). With regard to the flexural modulus, it represents the ratio

between the flexural stress and flexural deformation. In a similar way to tensile modulus, the decrease in flexural stress is lower than the deflection due to increased deformation provided by PCL and this leads to lower flexural modulus. So that the PLA flexural modulus of 3273 MPa is reduced to 2701 MPa for PLA/PCL blends with 30 wt% PCL.

The ability for energy absorption is also reduced with increasing PCL content (Table 2). The absorbed energy is directly related to deformation and mechanical resistance. As we have described previously, both tensile and flexural strength are reduced (mechanical resistant properties) while the elongation at break (deformation property) increases to a great extent. These changes lead to lower impact absorbed energy values as evident from Table III.1.2.

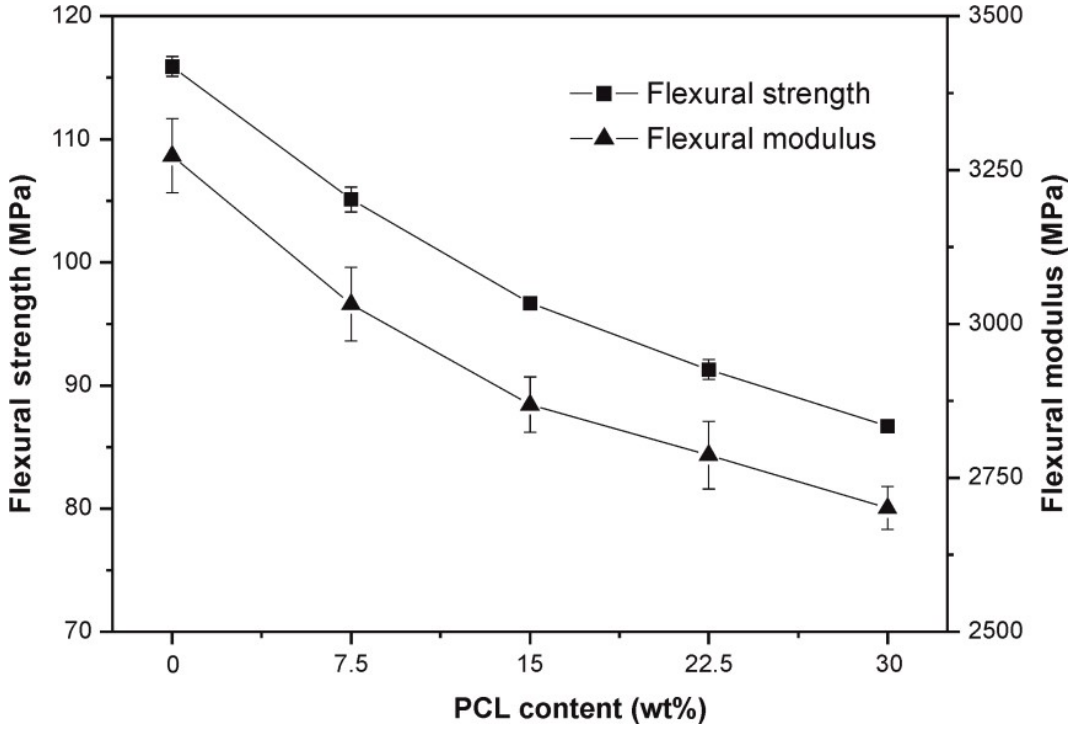

Figure III.1.2. Evolution of mechanical properties from flexural tests (flexural strength and flexural modulus) in terms of the PCL content.

Unblended PLA offers an absorbed energy value of 30.9 kJ m^{-2} due to the combination of high mechanical resistance and very low deformation; as the PCL

content in PLA/PCL blends increases, we observe a decrease in the absorbed energy values due to the plasticization effect of PCL which contributes to higher deformation but lower mechanical resistance. The maximum decrease in the absorbed energy value is found for PLA/PCL blend containing 30 wt% PCL with a value of 23.1 kJ m^{-2} which represents a decrease of almost 25%. With regard to the hardness (Shore D), the evolution is identical to that observed for other mechanical resistance properties such as strength and modulus. We observe a decreasing tendency in Shore D hardness values as the PCL content increases. As we have described previously, Poisson's ratio is an important parameter from a design point of view and it is a key parameter for dimensioning plastic parts with potential application in the packaging industry. For this reason, the influence of PCL content on Poisson's ratio ν has been evaluated. **Table III.1.2** gives Poisson's ratios with varying PCL content in PLA/PCL blends. Unblended PLA shows Poisson ratio of 0.43 [28, 29] and this value does not change in a marked way with varying PCL content. This could be related to the high PLA content in PLA/PCL blends which maintains transversal deformations in the same range as for unblended PLA.

Table III.1.2. Summary of some mechanical properties: impact absorbed energy, hardness and Poisson´s ratio of PLA/PCL blends in terms of the PCL content.

	PCL content (wt%)				
Property	**0**	**7.5**	**15**	**22.5**	**30**
Charpy impact energy (kJ m^{-2})	30.9 ± 0.8	28.3 ± 1.8	26.6 ± 0.6	24.9 ± 0.4	23.1 ± 0.4
Hardness (Shore D)	73.9 ± 0.8	71.1 ± 1.0	69.1 ± 0.6	68.2 ± 1.1	66.3 ± 1.2
Poisson´s ratio, ν	0.43	0.42	0.43	0.42	0.43

Figure III.1.3 shows FESEM images of fractured surfaces from impact tests corresponding to PLA/PCL blends with various PCL contents. Fracture surface of unblended PLA (Figure 3(a)) is smooth as typical of fragile polymers due to very low

deformation as indicated by the very low elongation at break values. As the PCL content increases, we observe rougher surfaces with some voids, flake structure and some filaments giving some evidence of plastic deformation provided by PCL.

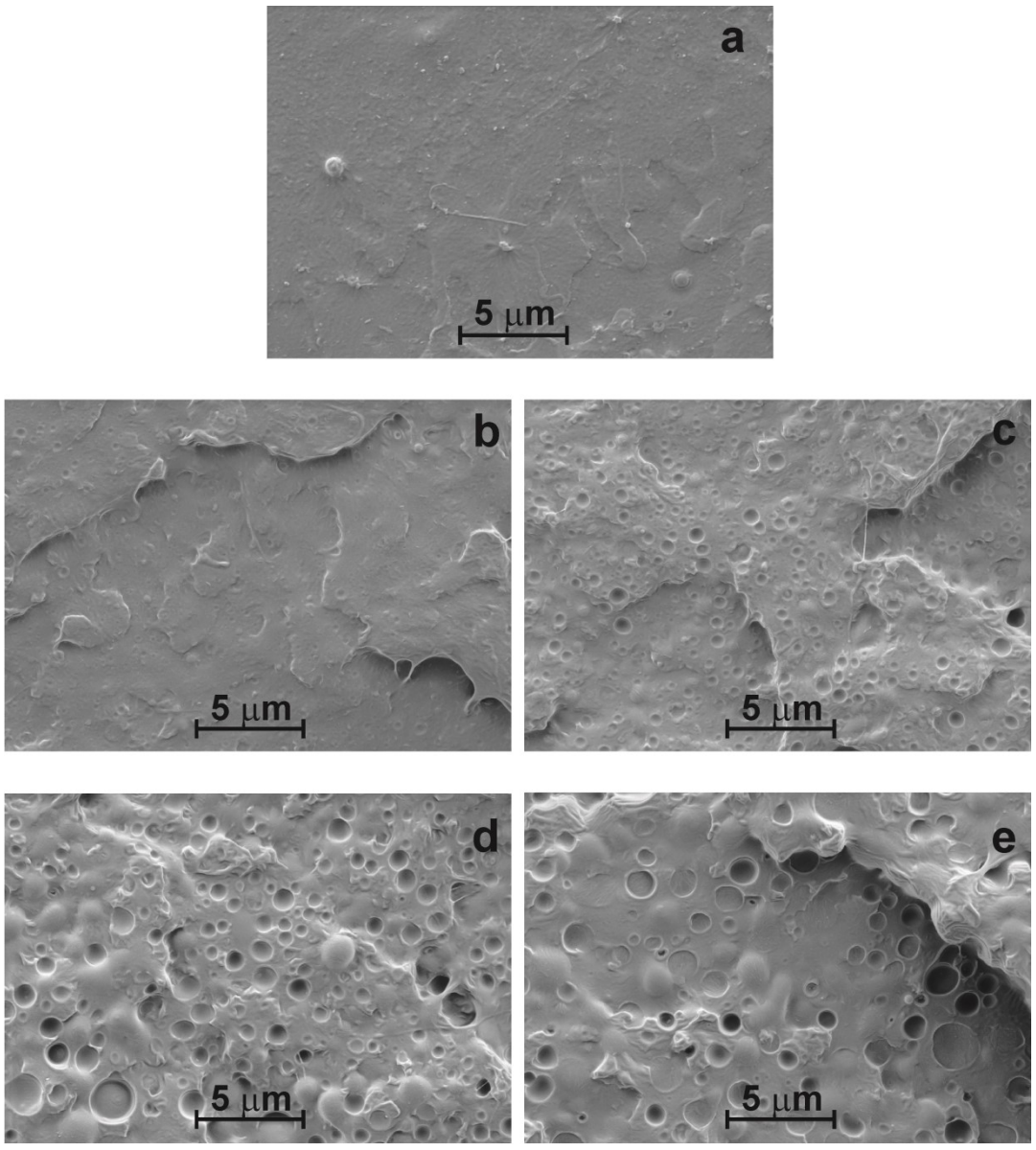

Figure III.1.3. FESEM images of fractured surfaces from impact tests of PLA/PCL blends with various PCL contents at x 5000: (a) 0 wt%; (b) 7.5 wt%; (c) 15.0 wt%; (d) 22.5 wt%; (e) 30.0 wt%.

These filament structures are related to the plastic deformation of PCL immersed in the PLA matrix. The morphological structure can be identified and phase separation due to immiscibility between PLA and PCL is clearly detectable.

Table III.1.3 summarizes the potential change in mechanical properties 8 months after the injection moulding to demonstrate how they changed over time. The obtained results show that the tensile and flexural properties, impact absorbed energy and hardness of virgin PLA and PLA/PCL formulations only vary less than ± 5%. This means that values are into typical error range and do not show an important variation. Only the elongation at break shows an important reduction being up to 25% lower for PLA/PCL blends with 22.5 wt% PCL.

Table III.1.3. Summary of tensile and flexural tests, impact absorbed energy and hardness of PLA/PCL blends in terms of the PCL content, aged at room temperature for 8 months.

	Samples (8 months)				
Property	**PLA**	**PLA/7.5PCL**	**PLA/15PCL**	**PLA/22.5PCL**	**PLA/30PCL**
Tensile strength (MPa)	61.4 ± 1.4	55.4 ± 0.4	51.8 ± 0.9	48.5 ±1.5	46.8 ± 0.8
Tensile modulus (MPa)	3453 ± 128	3555 ± 21	3131 ± 110	3113 ± 34	2687 ± 62
Flexural strength (MPa)	105.9 ± 0.7	101.2 ± 0.8	95.2 ± 0.6	87.3 ± 0.9	82.2 ± 0.2
Flexural modulus (MPa)	3374 ± 65	3185 ± 68	2758 ± 49	2798 ± 67	2691 ± 80
Elongation at break (%)	7.8 ± 0.7	18.2 ± 2.6	18.0 ± 1.0	64.5 ± 7.8	54.6 ± 8.0
Charpy impact energy (J m^{-2})	29.3 ± 0.7	27.2 ± 1.1	25.0 ± 0.9	22.7 ± 0.6	21.1 ± 0.5
Hardness (Shore D)	74.7 ± 0.7	72.1 ± 1.1	70.5 ± 0.8	68.9 ± 0.9	67.3 ± 1.0

Effect of PCL content on thermal and thermomechanical properties of PLA/PCL blends.

Figure III.1.4 shows a comparative plot of typical DSC curves of PLA/PCL blends with varying PCL content. Three different thermal transitions can be identified for unblended PLA. $T_{g\ PLA}$ is located in the range 55 – 65 ^{o}C. The typical cold crystallization process of PLA is located in the range 85 – 115 ^{o}C with a peak ($T_{cc\ PLA}$) at about 100 ^{o}C. Finally, the melt process comprises a temperature range from 155 to 175 ^{o}C with a peak ($T_{m\ PLA}$) at 168 ^{o}C. With regard to PCL, the melt process is located between 45 and 65^{o}C with a peak at 59 ^{o}C; T_g for PCL ($T_{g\ PCL}$) cannot be seen in these DSC traces because the temperature programme starts from room temperature and the typical $T_{g\ PCL}$ values are close to -60 ^{o}C. DSC curves of PLA/PCL blends are very interesting for assessing the miscibility between these two components. As we can see, the DSC curves of PLA/PCL blends between 30 ^{o}C and 210 ^{o}C show the same thermal transitions as individual polymers. **Table III.1.4** summarizes the main thermal parameters obtained from DSC curves. T_m PLA does not change with PCL addition with values around 168 ^{o}C. With regard to the melt peak of PCL ($T_{m\ PCL}$), it is located at about 59 ^{o}C and it is overlapped with $T_{g\ PLA}$, which is located in the same temperature range. Nevertheless, the melt peak of PCL does not change with varying PCL and it remains at 59 ^{o}C as for PCL alone. With regard to $T_{cc\ PLA}$, it does not change with the PCL content and remains constant at about 101 ^{o}C. The fact that all the thermal transitions of PLA and PCL in PLA/PCL blends appear at the same typical temperatures as those of the corresponding individual polymers is representative for a lack of (or very weak) interactions between these two polymers which indicates no (or poor) miscibility [23-26]. Furthermore, the crystallization enthalpy of PLA decreases with increasing PCL content. Nevertheless, the degree of crystallinity (X_c) of PLA increases with a PCL content of 22.5%. Higher PCL content does not allow growth of PLA spherulites. An excess of PCL can block or restrict molecular motions of PLA chains and interrupt the growth of PLA spherulites [23].

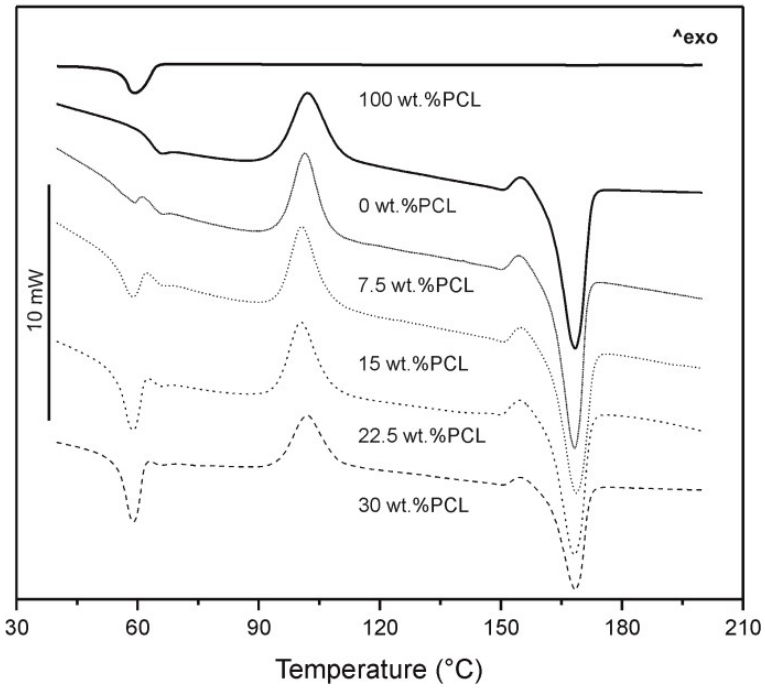

Figure III.1.4. Comparative plot of DSC curves of unblended PLA and PCL and PLA/PCL blends with various PCL contents showing the main thermal transitions.

Figure III.1.5 shows a comparative plot of the TGA degradation curves of individual PCL and PLA together with the TGA curves of PLA/PCL blends with various PCL contents. Although the thermal performance of PCL is not high due to low melt and glass transition temperatures, PCL is characterized by extraordinary thermal stability at high temperaturas [30], even more so than other biodegradable polymers. In fact, PCL degrades at higher temperatures than PLA (**Figure III.1.5**).

Addition of PCL to PLA gives more stable materials. We can see that thermal degradation of PLA/PCL blends occur in two stages: one is located between 300 ^{o}C and 370 ^{o}C that is attributable to PLA degradation; the second degradation step with typical weight loss in the range 370 – 440 ^{o}C is attributable to PCL degradation. This situation is also representative of poor or lack of polymer interactions thus leading to a blend of immiscible polymers as validated by DSC.

Table III.1.4. Summary of thermal parameters of PLA/PCL blends with various PCL content obtained using DSC.

	PLA thermal properties				
PCL wt%	**Melt temperature, $T_{m\ PLA}$ (°C)**	**Crystallization peak, $T_{cc\ PLA}$ (°C)**	**Crystallization enthalpy, $\Delta H_{cc\ PLA}$ (J g^{-1})**	**Melt enthalpy, $\Delta H_{m\ PLA}$ (J g^{-1})**	**Degree crystallinity, $X_{c\ PLA}$ (%)**
0	168.3	102.1	24.3	39.7	16.5
7.5	168.2	101.5	25.3	38.6	15.5
15.0	168.6	100.6	22.7	36.8	17.8
22.5	168.3	100.5	20.9	33.3	17.2
30.0	168.5	102.2	20.2	29.4	14.1

	PCL thermal properties		
PCL wt%	**Melt temperature, $T_{m\ PCL}$ (°C)**	**Melt enthalpy, $\Delta H_{m\ PCL}$ (J g^{-1})**	**Degree crystallinity, $X_{c\ PCL}$ (%)**
0	-	-	-
7.5	59.2	0.9	8.6
15.0	58.8	4.8	23.0
22.5	58.9	8.3	26.5
30.0	59.0	11.1	26.6

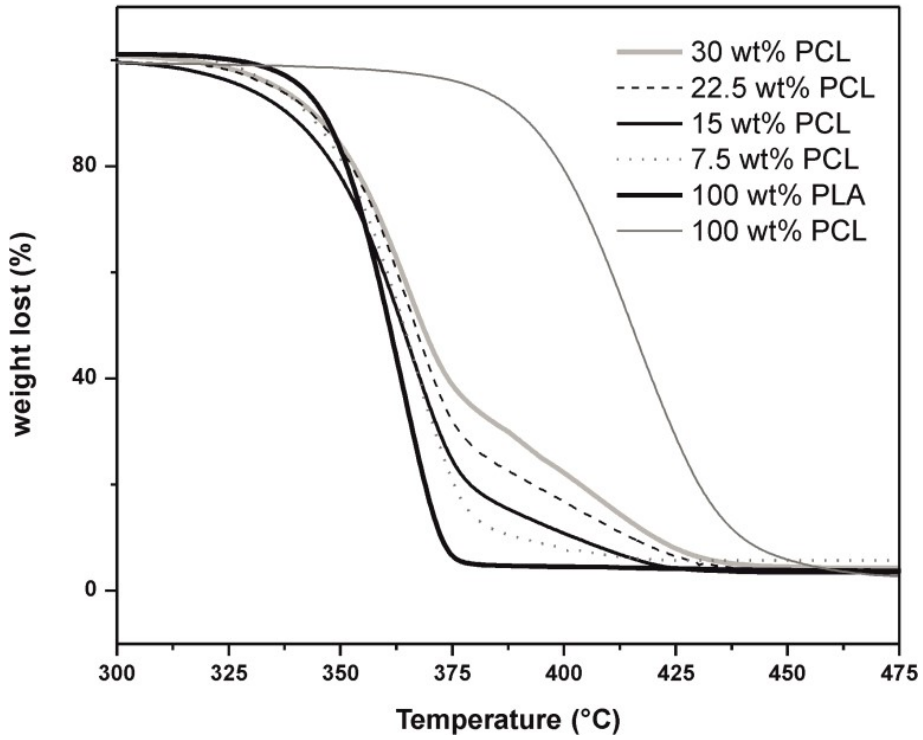

Figure III.1.5. Comparative plot of TGA curves of unblended PLA, PCL and PLA/PCL blends with various PCL contents.

DSC and TGA studies reveal poor interactions between the two polymers as both components in PLA/PCL blends maintain their typical thermal transitions. With regard to the combined effect of mechanical loads and temperature, **Table III.1.5** summarizes the evolution of the Vicat softening temperature (VST) and heat deflection temperature (HDT) of PLA/PCL with varying PCL content. As PCL is markedly more flexible than PLA, addition of PCL leads to a decrease in VST and HDT values due to the plasticization effect provided by PCL, but, in general terms, the variation in VST and HDT is not high.

Table III.1.5. Thermomechanical properties (Vicat softening temperature (VST) and heat deflection temperature (HDT)) of PLA/PCL blends.

	PCL content (wt%)				
Property	**0**	**7.5**	**15**	**22.5**	**30**
VST (ºC)	52.8	52.4	51.4	51.2	51.0
HDT (ºC)	47.6	46.4	45.4	44.4	44.2

Figure III.1.6 shows the evolution of the storage modulus (G´) of PLA and PLA/PCL blends with varying PCL content.

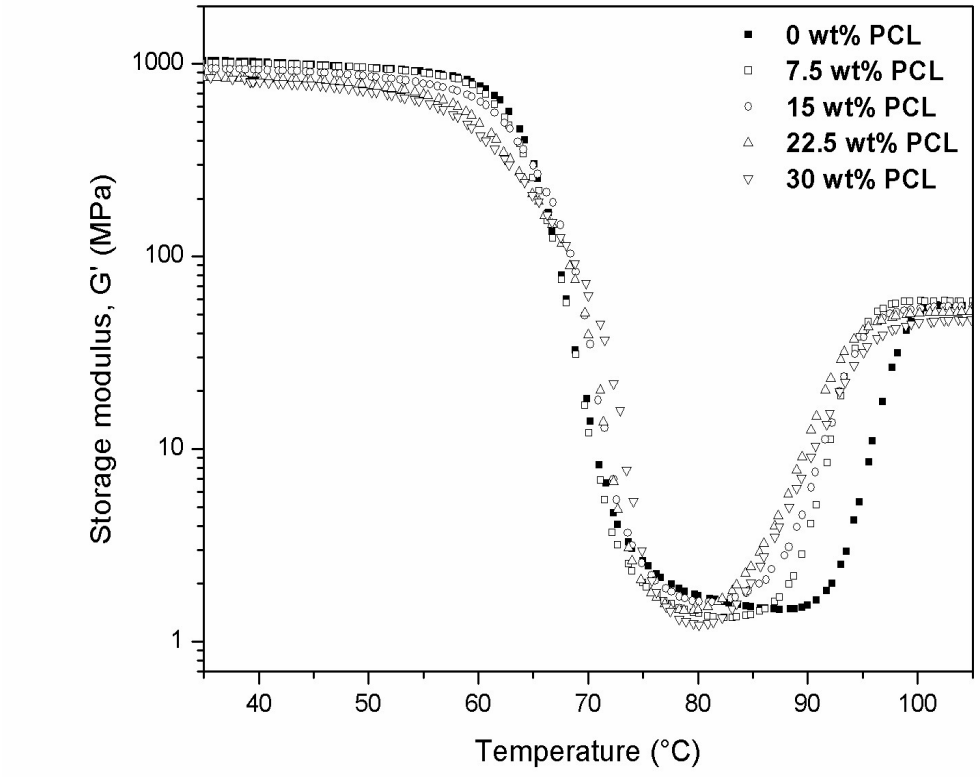

Figure III.1.6. Evolution of storage modulus, G´ with temperature for PLA/PCL blends with various PCL contents.

The plasticizing effect provided by PCL is proportional to the total PCL content and this can be observed in **Figure III.1.6** from the displacement of the G´ curve to

lower temperatures. At 37 ºC, unblended PLA has G´ of 1035 MPa. The addition of only 7.5 wt% PCL gives a reduction in G´ to 1010 MPa which represents a decrease of about 2.4%. As the PCL content increases, we observe a decreasing tendency in G´ to 835 MPa for PLA/PCL blends containing 30 wt% PCL with a reduction of about 19.3%. A marked decrease in G´ (threefold) occurs between 60 and 75 ºC that is attributable to T_g PLA. Finally, at 80 –100 ºC, G´ increases again due to the cold crystallization process of PLA; the crystallization process leads to a more packed structure that improve mechanical elastic behavior. As we can see, PCL addition leads to lower crystallization temperatures [23].

Morphology of PLA/PCL blends.

Fracture analysis by FESEM gives some evidences of the fracture type as described before but it does not give evidence of polymer phase separation due to immiscibility. For this reason, PLA/PCL blends were subjected to a cryofracture process and subsequent observation using FESEM. As described previously, PLA and PCL are not miscible polymers; thermal analysis gives some evidence of this lack of miscibility. By observing FESEM images of cryofractured surfaces of PLA/PCL blends (**Figure III.1.7**), PCL appears in the form of circular shapes dispersed in a predominant PLA matrix. The geometry of dispersed PCL is in the form of regular or irregular spheres but the cryofracture process gives a circular cross-section to these spheres so that FESEM observation offers these circular shapes. We can also observe how the sphere size increases with increasing PCL content.

For a 7.5 wt% content of PCL in the blends, the particle size is lower than 0.5 μm (**Figs. III.1.7(a) and III.1.7(b)**). In addition we observe some evidence of the plasticization effect through some filament structures representative for plastic deformation. PLA/PCL blends with 15 wt% PCL show similar structure with a predominant PLA matrix in which PCL spherical shapes are immersed. For this composition, PCL spheres are characterized by a sphere size of 0.5 – 1.0 μm (**Figs. III.1.7(c) and III.1.7(d)**).

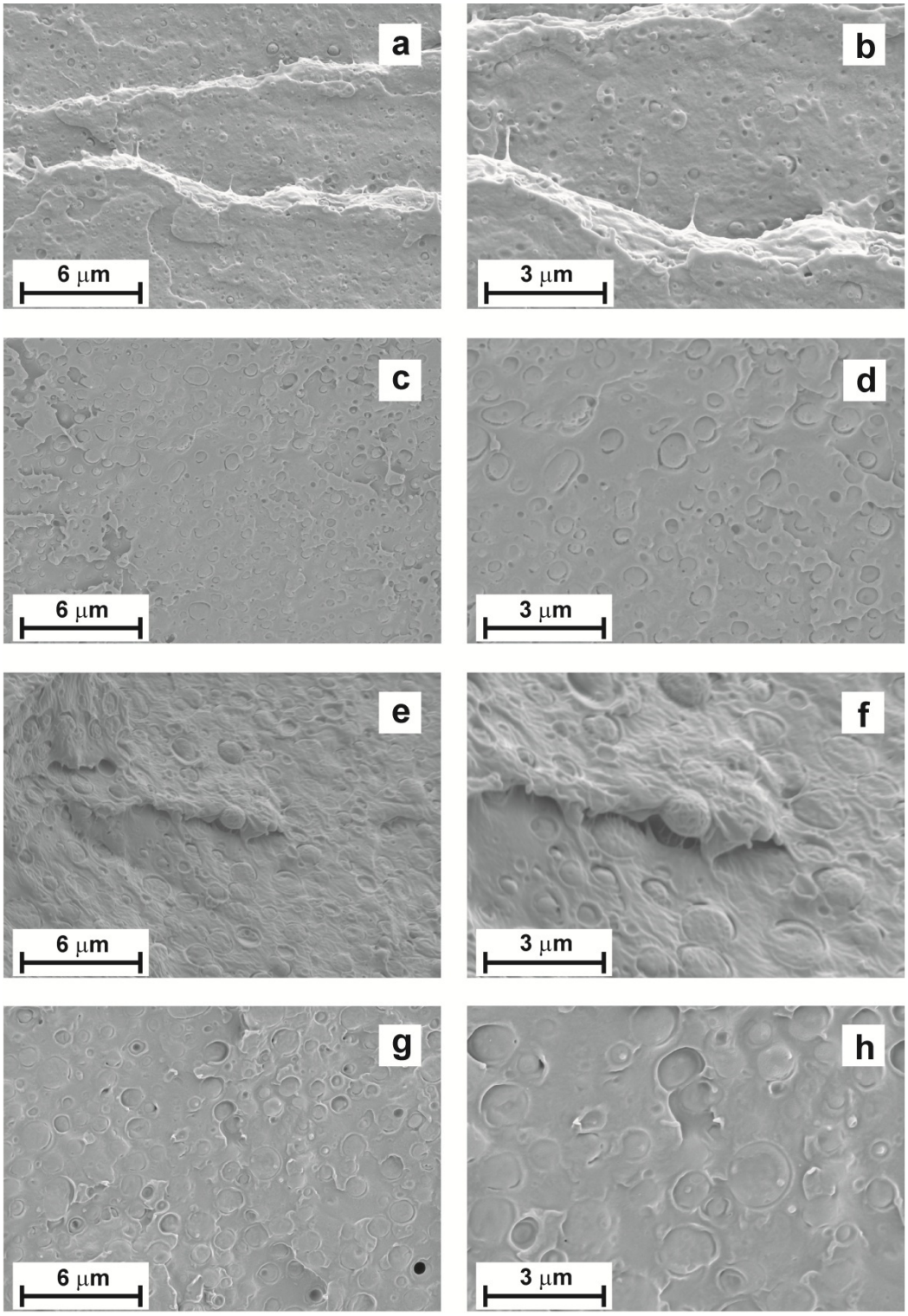

Figure III.1.7. FESEM images of cryofractured surfaces of PLA/PCL blends with various PCL contents and magnifications: (a) 7.5 wt% PCL, x5000; (b) 7.5 wt% PCL, x10000; (c) 15 wt% PCL, x5000; (d) 15 wt% PCL, x10000; (e) 22.5 wt% PCL, x5000; (f) 22.5 wt% PCL, x10000; (g) 30 wt% PCL, x5000; (h) 30 wt% PCL, x10000.

This size is even larger for PLA/PCL blends containing 30 wt% PCL with an average size of 1.5 – 2.0 μm (**Figs. III.1.7(g) and III.1.7(h)**). The phase separation between these two biodegradable polymers is evident for the whole composition range in this study, thus giving clear evidence of immiscibility (or very low miscibility). The plasticization effect can be observed in PLA/PCL blends with 22.5 wt% PCL at x 10000 (**Figure III.1.7(f)**) with a PCL sphere linked to the surrounding PLA matrix through different filament formations thus giving evidence of some weak interactions between the two polymers.

Cryofractured samples from PLA/PCL blends were also subjected to selective extraction with acetone. This solvent causes PCL extraction but also some swelling on PLA occurs (probably due to some PCL domains being dissolved in the PLA matrix). This situation can be observed in **Figure III.1.8**. The selective extraction of PCL leads to a porous structure of PLA because the spherical PCL domains have been removed by the action of acetone. We also observe the same for cryofractured images in **Figure III.1.7**: the sphere diameter increases with increasing PCL content in PLA/PCL blends. FESEM gives clear evidence of phase separation so that PCL and PLA are immiscible to a great extent but the plasticizing effect of PCL leads to attractive elongation at break values as described previously with regard to tensile properties.

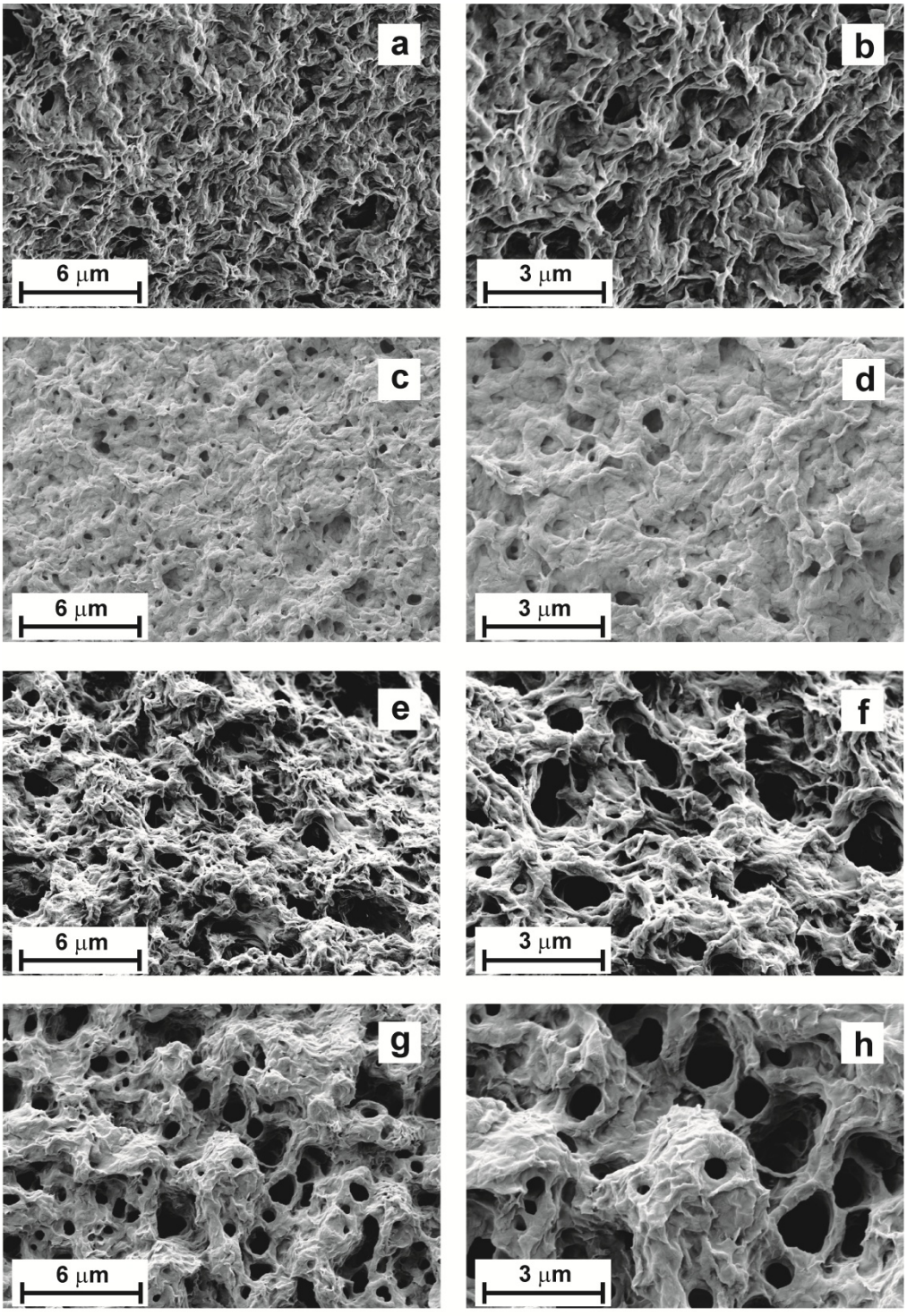

Figure III.1.8. FESEM images of cryofractured surfaces of PLA/PCL blends with various PCL contents and magnifications after selective extraction with acetone: (a) 7.5 wt% PCL, x5000; (b) 7.5 wt% PCL, x10000; (c) 15 wt% PCL, x5000; (d) 15 wt% PCL, x10000; (e) 22.5 wt% PCL, x5000; (f) 22.5 wt% PCL, x10000; (g) 30 wt% PCL, x5000; (h) 30 wt% PCL, x10000.

Disintegration under composting.

Figure III.1.9 shows the visual appearance of PLA and PLA/PCL blends before and after various times of disintegration in composting conditions; clearly evident is the biodegradable character of all the formulations studied.

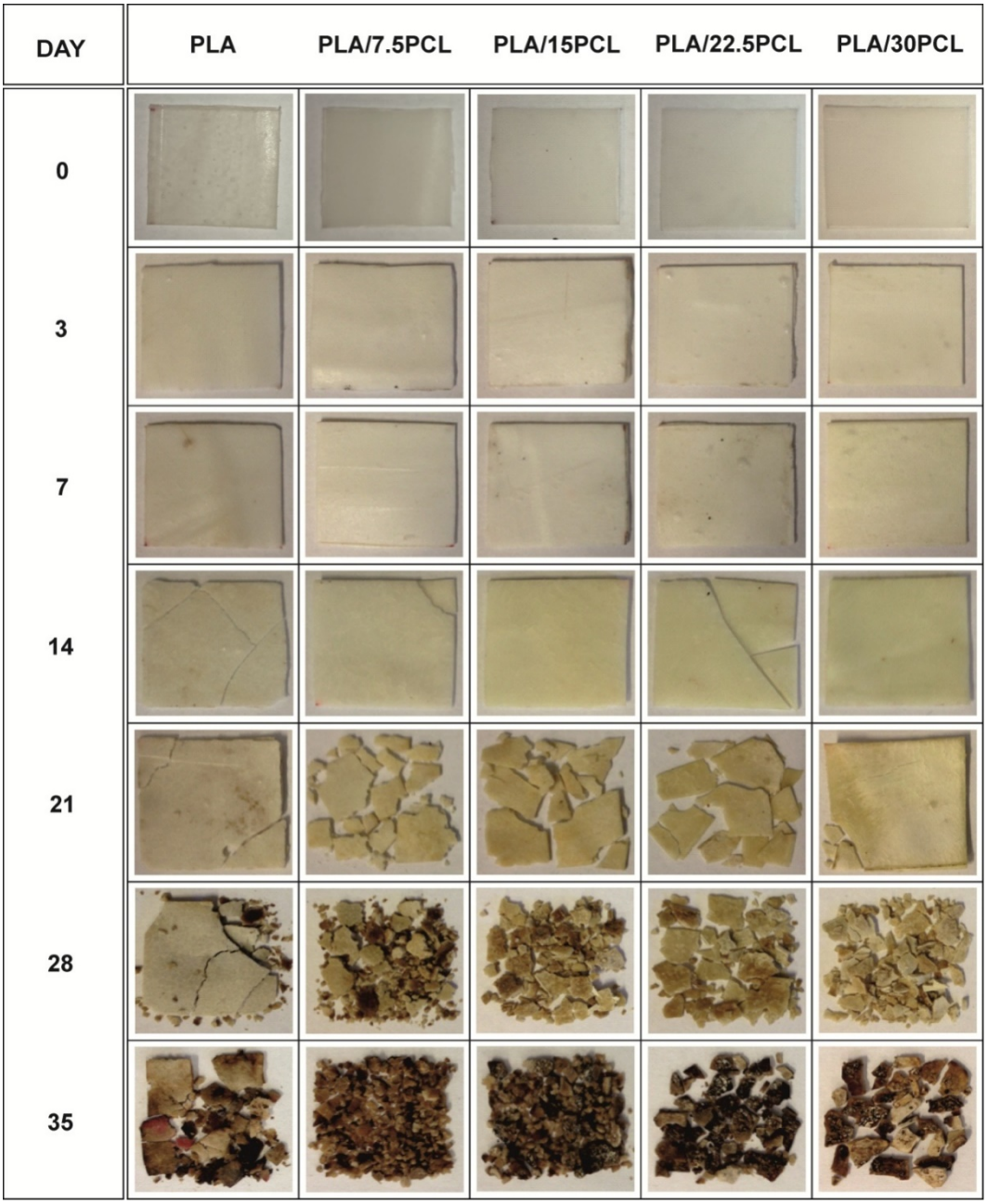

Figure III.1.9. Visual appearance of PLA and PLA/PCL samples before and after various incubation times under composting conditions.

Before placing the samples in composting conditions, we observed that neat PLA is transparent and PLA/PCL blends have a whitish color. After 3 days of incubation PLA sample becomes opaque thus giving evidence of the hydrolysis process [6, 31, 32]. For an incubation period of 14 days, samples become brittle and acquire a light yellow hue. After this time, the degradation process is accelerated in a marked way. At an incubation period of 21 days, the neat PLA shows less degradation than all PLA/PCL blends. It is clear that the higher PCL content the blend contains, the less the degradation. This is because the PCL degrades less than PLA [33]. The PCL acts as a nucleating agent for the degradation process. In fact, the samples with minor percentage of PCL are more liable to degradation than those with higher percentage of PCL. For further degradation time, samples acquire a light brown hue and the pieces are increasingly smaller. For an incubation period of 42 days, PLA and PLA/PCL blends are totally disintegrated. PLA with 7.5 wt% PCL is the blend composition with higher disintegration rate as detected by visual appearance.

Furthermore, the mass loss as a function of incubation time of neat PLA and PLA/PCL blends was evaluated (**Figure III.1.10**). It can be seen that from day 14 the mass loss increases significantly. At an incubation period of about 35 days, almost 50% of the initial mass is lost. After an incubation period of 42 days, all samples are completely disintegrated. In Figure **III.1.10** one can see that degradation is lower at higher PCL contents. In fact, from 0 to 28 days mass loss is lower than for neat PLA. The nucleating effect of the PCL in the PLA crystallization decreases the degradation rate of PLA/PCL samples due to an increase in the degree of crystallinity.

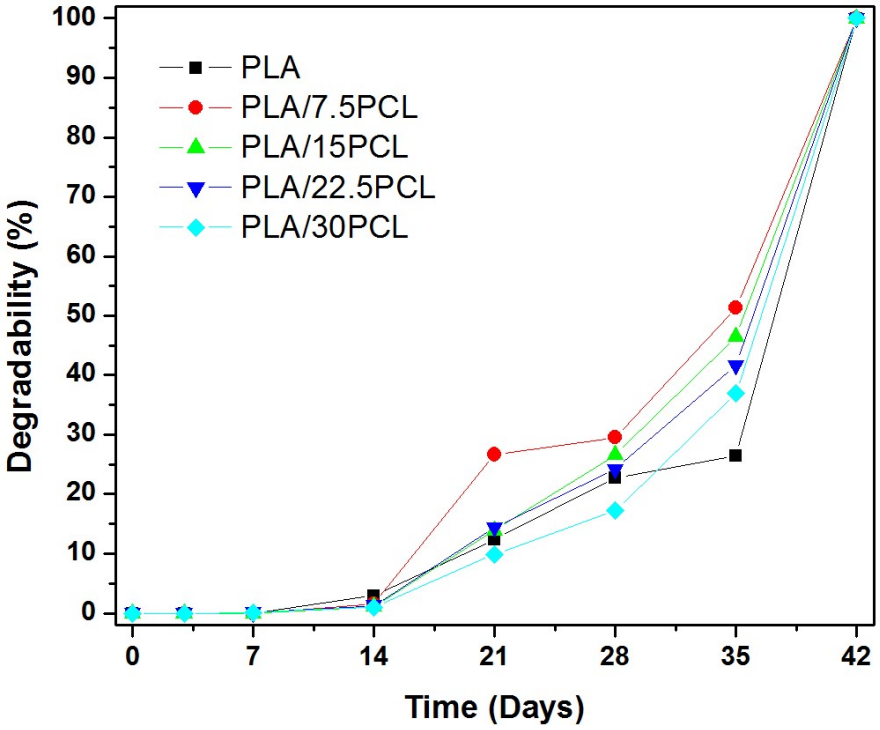

Figure III.1.10. Degradability of neat PLA and PLA/PCL blends under composting conditions as a function of time.

Conclusions.

The results show that PCL provides attractive ductile properties to PLA with a marked increase in elongation at break values from 8% for unblended PLA up to values higher than 70% for PLA/PCL blends with 20-30 wt% PCL. Although these two polymers seem to be highly immiscible, the improvement in ductile properties is quite good without compromising mechanical resistance properties. Thermal analysis by DSC revealed high immiscibility of both polymers since the main thermal transitions for PLA and PCL in PLA/PCL blends are independent of the blend composition. FESEM analysis of cryofractured samples from PLA/PCL blends revealed a morphology with a clear phase separation; PCL appears in the form of variable-size spheres dispersed in the predominant PLA matrix. The size of PCL phase domains changes from 0.5 μm for PLA/PCL blends with 7.5 wt% PCL up to values of 1.5-2 μm for blends containing 30 wt% PCL. With regard to mechanical properties, the

plasticizing effect of PCL leads to lower tensile and flexural strength and modulus values. Overall, addition of PCL to PLA provides PLA with enough flexibility to be used in packaging for applications such as those that require flexible materials to be adapted to different geometries (homewares) or to extrude films for food product conservation. Furthermore PLA/PCL blends under composting conditions have a mass loss higher than neat PLA. This is due to PCL acting as a nucleating agent to accelerate the degradation process for lower PCL content. Nevertheless, for contents over 22.5 wt% PCL the mass loss is less than that of neat PLA.

Acknowledgements.

This research was supported by the Ministry of Economy and Competitiveness - MINECO, ref: MAT2014-59242-C2-1-R. The authors also thank the Conselleria d'Educació, Cultura i Esport - Generalitat Valenciana, ref. GV/2014/008 for financial support.

References.

1. Mathieu, L.M., Bourban, P.E., and Manson, J.A.E., *Processing of homogeneous ceramic/polymer blends for bioresorbable composites*. Composites Science and Technology, 2006. **66**(11-12): p. 1606-1614.

2. Vroman, I., and Tighzert, L., *Biodegradable Polymers*. Materials, 2009. **2**(2): p. 307-344.

3. Fortunati, E., Latterini, L., Rinaldi, S., Kenny, J.M., and Armentano, I., *PLGA/Ag nanocomposites: in vitro degradation study and silver ion release*. Journal of Materials Science-Materials in Medicine, 2011. **22**(12): p. 2735-2744.

4. Arrieta, M.P., Lopez, J., Hernandez, A., and Rayon, E., *Ternary PLA-PHB-Limonene blends intended for biodegradable food packaging applications*. European Polymer Journal, 2014. **50**: p. 255-270.

5. Arrieta, M.P., Samper, M.D., Lopez, J., and Jimenez, A., *Combined Effect of Poly(hydroxybutyrate) and Plasticizers on Polylactic acid Properties for Film Intended for Food Packaging*. Journal of Polymers and the Environment, 2014. **22**(4): p. 460-470.

6. Arrieta, M.P., Lopez, J., Rayon, E., and Jimenez, A., *Disintegrability under composting conditions of plasticized PLA-PHB blends*. Polymer Degradation and Stability, 2014. **108**: p. 307-318.

7. Doumbia, A.S., Vezin, H., Ferreira, M., Campagne, C., and Devaux, E., *Studies of polylactide/zinc oxide nanocomposites: influence of surface treatment on zinc oxide antibacterial activities in textile nanocomposites*. Journal of Applied Polymer Science, 2015. **132**(17): 41776.

8. Pivsa-Art, W., Pivsa-Art, S., Fujii, K., Nomura, K., Ishimoto, K., Aso, Y., Yamane, H., and Ohara, H., *Compression molding and melt-spinning of the blends of poly(lactic acid) and poly(butylene succinate-co-adipate)*. Journal of Applied Polymer Science, 2015. **132**(16): 41856.

9. Awal, A., Rana, M., and Sain, M., *Thermorheological and mechanical properties of cellulose reinforced PLA bio-composites*. Mechanics of Materials, 2015. **80**, Part A: p. 87-95.

10. Baek, J., Chen, X., Sovani, S., Jin, S., Grogan, S.P., and D'Lima, D.D., *Meniscus tissue engineering using a novel combination of electrospun scaffolds and human meniscus cells embedded within an extracellular matrix hydrogel*. Journal of orthopaedic research: official publication of the Orthopaedic Research Society, 2015. **33**(4): p. 572-83.

11. Han, W.-P., Huang, Y.-Y., Yu, M., Zhang, J.-C., Yan, X., Yu, G.-F., Zhang, H.-D., Yan, S.-Y., and Long, Y.-Z., *Self-powered electrospinning apparatus based on a hand-operated Wimshurst generator*. Nanoscale, 2015. **7**(13): p. 5603-6.

12. Valarezo, E., Tammaro, L., Malagon, O., Gonzalez, S., Armijos, C., and Vittoria, V., *Fabrication and Characterization of Poly(lactic acid)/Poly(epsilon-caprolactone) Blend Electrospun Fibers Loaded with Amoxicillin for Tunable Delivering*. Journal of Nanoscience and Nanotechnology, 2015. **15**(6): p. 4706-4712.

13. Farahani, R.D., Chizari, K., and Therriault, D., *Three-dimensional printing of freeform helical microstructures: a review*. Nanoscale, 2014. **6**(18): p. 10470-10485.

14. Shaffer, S., Yang, K., Vargas, J., Di Prima, M.A., and Voit, W., *On reducing anisotropy in 3D printed polymers via ionizing radiation*. Polymer, 2014. **55**(23): p. 5969-5979.

15. Water, J.J., Bohr, A., Boetker, J., Aho, J., Sandler, N., Nielsen, H.M., and Rantanen, J., *Three-Dimensional Printing of Drug-Eluting Implants: Preparation of an Antimicrobial Polylactide Feedstock Material*. Journal of Pharmaceutical Sciences, 2015. **104**(3): p. 1099-1107.

16. Plackett, D.V., Holm, V.K., Johansen, P., Ndoni, S., Nielsen, P.V., Sipilainen-Malm, T., Sodergard, A., and Verstichel, S., *Characterization of L-potylactide and L-polylactide-polycaprolactone co-polymer films for use in cheese-packaging applications*. Packaging Technology and Science, 2006. **19**(1): p. 1-24.

17. Thellen, C., Orroth, C., Froio, D., Ziegler, D., Lucciarini, J., Farrell, R., D'Souza, N.A., and Ratto, J.A., *Influence of montmorillonite layered silicate on plasticized poly(L-lactide) blown films*. Polymer, 2005. **46**(25): p. 11716-11727.

18. Rahman, M. and Brazel, C.S., *The plasticizer market: an assessment of traditional plasticizers and research trends to meet new challenges*. Progress in Polymer Science, 2004. **29**(12): p. 1223-1248.

19. Adeodato Vieira, M.G., da Silva, M.A., dos Santos, L.O., and Beppu, M.M., *Natural-based plasticizers and biopolymer films: A review*. European Polymer Journal, 2011. **47**(3): p. 254-263.

20. Averous, L., *Biodegradable multiphase systems based on plasticized starch: A review*. Journal of Macromolecular Science-Polymer Reviews, 2004. **C44**(3): p. 231-274.

21. Gigli, M., Lotti, N., Gazzano, M., Siracusa, V., Finelli, L., Munari, A., and Dalla Rosa, M., *Biodegradable aliphatic copolyesters containing PEG-like sequences for sustainable food packaging applications*. Polymer Degradation and Stability, 2014. **105**: p. 96-106.

22. Arvanitoyannis, I., Nikolaou, E., and Yamamoto, N., *Novel biodegradable copolyamides based on adipic acid, isophorone diamine and alpha-amino-acids .3. Synhesis, study of properties and evaluation of their biodegradability for food-packaging applications*. Angewandte Makromolekulare Chemie, 1994. **221**: p. 67-90.

23. Jen-Taut Yeh, C.-J.W., Chi-Hui Tsou, Wan-Lan Chai, Jing-Dong Chow, Chi-Yuan Huang, Kan-Nan Chen, Chin-San Wu, *Study on the Crystallization, Miscibility, Morphology, Properties of Poly(lactic acid)/Poly(ε-caprolactone) Blends*. Polymer Plastics Technology and Engineering, 2009. **48**(6): p. 571-578.

24. Zhang, L.L., Xiong, C.D., and Deng, X.M., *Biodegradable polyester blends for biomedical application*. Journal of Applied Polymer Science, 1995. **56**(1): p. 103-112.

25. Broz M.E, V.D.L., Washburn N.R., *Structure and mechanical properties of poly(d,l-lactic acid)/poly(e-caprolactone) blends*. Biomaterials, 2003. **24**: p. 4181-4190.

26. Lopez-Rodriguez, N., Lopez-Arraiza, A., Meaurio, E., and Sarasua, J.R., *Crystallization, morphology, and mechanical behavior of polylactide/poly(epsilon-caprolactone) blends*. Polymer Engineering and Science, 2006. **46**(9): p. 1299-1308.

27. Kim, Y.J., Kang, G.D., Yoon, K.C., and Park, O.O., *Comparison of Mechanical Properties of Blended and Synthesized Biodegradable Polyesters*. Macromolecular Research, 2014. **22**(4): p. 382-387.

28. Sami Ben Brahim, R.B.C., *Influence of fibre orientation and volume fraction on the tensile properties of unidirectional Alfa-polyester composite*. Composites Science and Technology, 2007. **67**(1): p. 140-147.

29. Pillin, I., Montrelay, N., Bourmaud, A., and Grohens, Y., *Effect of thermo-mechanical cycles on the physico-chemical properties of poly(lactic acid)*. Polymer Degradation and Stability, 2008. **93**(2): p. 321-328.

30. Sivalingam, G., and Giridhar,.M., *Thermal degradation of binary physical mixtures and copolymers of poly(3-caprolactone), poly(D, L-lactide), poly(glycolide)*. Polymer Degradation and Stability 2004. **84**: p. 393-398.

31. Husarova, L., Pekarova, S., Stloukal, P., Kucharczyk, P., Verney, V., Commereuc, S., Ramone, A., and Koutny, M., *Identification of important abiotic and biotic factors in the biodegradation of poly(L-lactic acid)*. International Journal of Biological Macromolecules, 2014. **71**: p. 155-162.

32. Sikorska, W., Musiol, M., Nowak, B., Pajak, J., Labuzek, S., Kowalczuk, M., and Adamus, G., *Degradability of polylactide and its blend with poly (R,S)-3-hydroxybutyrate in industrial composting and compost extract*. International Biodeterioration & Biodegradation, 2015. **101**: p. 32-41.

33. Fukushima, K., Tabuani, D., Abbate, C., Arena, M., and Ferreri, L., *Effect of sepiolite on the biodegradation of poly(lactic acid) and polycaprolactone*. Polymer Degradation and Stability, 2010. **95**(10): p. 2049-2056.

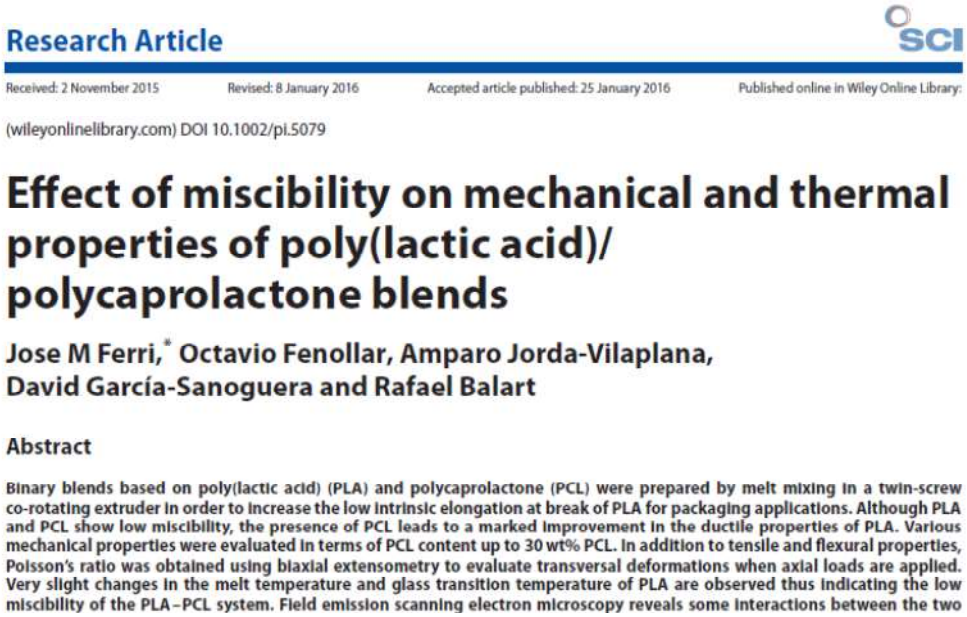

Research Article

SCI

Received: 2 November 2015 Revised: 8 January 2016 Accepted article published: 25 January 2016 Published online in Wiley Online Library:

(wileyonlinelibrary.com) DOI 10.1002/pi.5079

Effect of miscibility on mechanical and thermal properties of poly(lactic acid)/ polycaprolactone blends

Jose M Ferri,* Octavio Fenollar, Amparo Jorda-Vilaplana, David García-Sanoguera and Rafael Balart

Abstract

Binary blends based on poly(lactic acid) (PLA) and polycaprolactone (PCL) were prepared by melt mixing in a twin-screw co-rotating extruder in order to increase the low intrinsic elongation at break of PLA for packaging applications. Although PLA and PCL show low miscibility, the presence of PCL leads to a marked improvement in the ductile properties of PLA. Various mechanical properties were evaluated in terms of PCL content up to 30 wt% PCL. In addition to tensile and flexural properties, Poisson's ratio was obtained using biaxial extensometry to evaluate transversal deformations when axial loads are applied. Very slight changes in the melt temperature and glass transition temperature of PLA are observed thus indicating the low miscibility of the PLA–PCL system. Field emission scanning electron microscopy reveals some interactions between the two

Chapter III.2

Chapter III.2. 1. Poly(lactic acid) formulations with improved toughness by physical blending with thermoplastic starch.

“Poly(lactic acid) formulations with improved toughness by physical blending with thermoplastic starch”

J.M. Ferri, D. Garcia-Garcia, A. Carbonell, O. Fenollar, R. Balart

Instituto de Tecnología de Materiales (ITM)

Universitat Politècnica de València (UPV)

Plaza Ferrandiz y Carbonell 1, 03801, Alcoy, Alicante (Spain)

Journal of Applied Polymer Science (enviado)

Abstract.

This work focuses on poly(lactic acid) (PLA) formulations with improved toughness by physical blending with thermoplastic maize starch (TPS) plasticized with aliphatic-aromatic copolyester (AAPE) up to 30 wt%. A noticeable increase in toughness is observed, due to the finely dispersed spherical TPS domains in the PLA matrix. It is worth to note the remarkable increase in the elongation at break that changes from 7% (neat PLA) up to 21.5% for PLA with 30 wt% TPS. The impact-absorbed energy is markedly improved from the relatively low values of neat PLA (1.6 J m^{-2}) up to more than three times. Although TPS is less thermally stable than PLA due to its plasticizer content, in general, PLA/TPS blends offer good balanced thermal stability. The morphology reveals high immiscibility in PLA/TPS blends, with TPS-rich domains with an average size of 1 μm, finely dispersed which, in turn, is responsible for the improved toughness.

Keywords: thermoplastic starch, physical blending, poly(lactic acid),plasticized.

Introduction.

The packaging industry is facing an important challenge, which is the increasing use of environmentally friendly materials to avoid waste generation. For this reason, the use of biodegradable (disintegrable in controlled compost conditions) polymers is continuously growing. Biodegradable polymers include some petroleum-based polyesters such as poly(caprolactone) (PCL) [1], poly(butylene succinate) (PBS) [2], poly(butylene succinate–co–adipate) (PBSA) [3], poly(butylene adipate-co-terephthalate) (PBAT) [4], etc, among others. In addition, some biodegradable polymers can be obtained from renewable resources as it is the case of poly(lactic acid) (PLA) [5], bacterial polyesters such as poly(hydroxybutyrate) (PHB)[6], poly(hydroxybutyrate-co-valerate) (PHBV)[7], protein-based polymers (gluten, casein, soy protein, etc.), and polysaccharide polymers (chitosan, cellulose, starch, etc.).

PLA offers good perspectives at present and in the near future for use in the packaging industry [8-11]. Its possesses good mechanical properties, together with balanced barrier properties; in addition, it can be disintegrated in soil compost [12]. All these features, along with its increasingly competitive price, have led PLA to an advantageous position against other biodegradable polymers. PLA can be obtained from starch-rich materials such as some cereals (wheat, corn) and some roods (beetroot, cassava, yucca, etc.) [13, 14]. However, not all are advantages; some of its disadvantages are related to its low elongation at break, low flexibility and toughness. To overcome these drawbacks, different strategies have been proposed. Copolymerization is highly interesting from a technical standpoint but it is not a cost-effective solution. Plasticization is a cost-effective approach but it is important to take into account the plasticizer migration. For these reasons, new strategies are being investigated. Physical blending with ductile and flexible polymers is an interesting solution but there are some issues related with the miscibility between the components that must be addressed to obtain optimum properties. Blending with thermoplastic starch (TPS) is a cost-effective solution as it can provide increased flexibility, elongation at break and, subsequently, a marked improvement on toughness can be achieved [13,

15]. TPS is obtained from starch-rich plants or foods such as pea, corn, sorghum, barley, amaranth, yucca, sweet potato, etc. [16], etc. Industrial formulations of TPS contain certain amounts of a plasticizer such as water [17, 18], glycerol, sorbitol, xylitol, glucose or combinations [19, 20] to improve ductility, elongation at break and resistance to retrogradation as well as to increase the overall thermal stability [21, 22]. Starch is chemically constituted of two types of polysaccharides: amylose and amylopectin and, in a less extent, some lipids. Depending on the origin, the amylose/amylopectin ratio varies and this has a direct influence on mechanical properties [23-25]. Furthermore, the degree of crystallinity of starch can vary in the 15-45% range as a consequence of the abovementioned ratio and may change in time due to retrogradation phenomena [22]. The plasticizer type and content can also influence the degree of crystallinity of starch in industrial TPS formulations [21]. TPS is poorly miscible with hydrophobic polymers as it is the case of PLA [26, 27]. For this reason, new starch plasticizers are being investigated to allow somewhat interactions with other polymers.

This work explores the potential of a thermoplastic starch, plasticized with a biodegradable aliphatic/aromatic copolyester (AAPE), to obtain high toughness PLA formulations by physical blending [28]. The effect of TPS content (0 – 30 wt%) in PLA/TPS blends is evaluated in terms of mechanical and thermal properties as well as morphology.

Experimental.

Materials.

A commercial PLA grade IngeoTM Biopolymer 6201D was obtained in pellet form from NatureWorks LLC (Minnetonka, USA). This PLA grade contains 2% D-lactic acid and possesses a density of 1.24 g cm^{-3} at 23 ^{o}C and a melt flow index comprised in the 15-20 g/(10 min) range at 210 ^{o}C. A TPS grade Mater-Bi® NF 866 was supplied by Novamont (Novara, Italy). This TPS is obtained from maize starch and is characterized by a melt flow index of 3.5 g/(10 min) at 150 ^{o}C and a density of 1.27 g cm^{-3} at 23 ^{o}C. Its

melting peak temperature is comprised between 110 – 120 ºC and contains more than 50% of AAPE [28]. With regard to the base starch, it is composed of 73% amylopectin and 23% amylose.

Preparation of PLA/TPS blends.

The TPS content in PLA/TPS varied in the range 0 – 30 wt% as summarized in Table 1. Initially all materials were dried at 60 ºC for 24 h, weighed in the appropriate proportions and mechanically pre-mixed in a zipper bag. Then, the materials were compounded in a twin-screw co-rotating extruder from Dupra (Castalla, Spain) at 60 rpm. The temperature profile was set to 165 ºC (feeding), 170 ºC, 172.5 ºC y 175 ºC (die). After cooling, the compounded materials were pelletized and subsequently processed by injection moulding in a Meteor 270/75 from Mateu&Solé (Barcelona, Spain) at an injection temperature of 175 ºC.

Table III.2.1. Summary of compositions and labelling of PLA/TPS formulations.

Code	PLA (wt%)	TPS (wt%)
TPS	-	100
PLA	-	100
PLA /7.5TPS	92.5	7.5
PLA /15TPS	85	15
PLA /22.5TPS	77.5	22.5
PLA /30TPS	70	30

Mechanical characterization of PLA/TPS blends.

Tensile and flexural tests were carried out in a universal testing machine ELIB 30 from S.A.E. Ibertest (Madrid, Spain) at room temperature according to ISO 527-5 and ISO 178 respectively at a crosshead speed of 10 mm min^{-1}. At least, five different samples were tested and average values of tensile strength (σ), modulus (E) and elongation at break (ε_b) were calculated. Moreover, an axial extensometer (SAE Ibertest model IB/MFQ-R2, Madrid, Spain) was used to obtain the Young's modulus in a more accurate way. Hardness measurements were obtained in a Shore D durometer model 673-D from Instrumentos J. Bot S.A. (Barcelona, Spain) following ISO 868. Impact-absorbed energy was obtained in a Charpy's pendulum from Metrotec S.A. (San Sebastián, Spain) with an energy of 1 J, as indicated in ISO 179:1993. Five different notched (notch type A) samples were tested and average values were calculated. The notch was done in a notch machine from HOYTOM S.L. (Leioa, Bizkaia, Spain) with a background radius of 0.25±0.05, a remaining width of 8.0±0.2 and a notch angle of 45º± 1º.

Dynamic mechanical thermal characterization (DMTA) was carried out using an oscillatory rheometer AR G2 from TA Instruments (New Castle, USA) equipped with a special clamp system to test solid samples in a torsion/shear mode. The samples sized 40x10x4 mm^3 and were subjected to a heating program from -80 ºC up to 130 ºC at a constant heating rate of 2 ºC min^{-1}. The selected frequency was 1 Hz and the maximum shear deformation percentage (%γ) was set to 0.1%.

Morphology characterization by FESEM.

A field emission scanning electron microscope (FESEM) model ZEISS ULTRA55 from Oxford Instruments (Abingdon, United Kingdom) was used to characterize the morphology of the fractured surfaces from impact tests. The acceleration voltage was set to 2 kV. Prior to observation by FESEM, all surfaces were covered with an ultrathin

platinum layer by a high vacuum sputtering process in a EM MED020 sputter coater from Leica Microsystems (Wetzlar, Germany).

Results and discussion.

Influence of TPS content on mechanical properties of PLA/TPS blends.

Fig. III.2.1 and **Fig. III.2.2** show the evolution of tensile and flexural properties of the PLA/TPS system as a function of the TPS content. Neat PLA possesses a tensile strength of 64 MPa. This decreases almost linearly down to values of 41.5 MPa for the PLA/TPS blend containing 30 wt% TPS. In a similar way, tensile modulus also offers a decreasing tendency with increasing TPS content. The initial tensile modulus of neat PLA is close to 3.6 GPa and decreases down to values of about 2.5 GPa (PLA/TPS blend with 30 wt% TPS). This phenomenon is typical of plasticized PLA formulations. Silverajah et al. reported that 5 wt% EPO plasticizer in PLA formulations led to lower tensile strength values by 26.3% with regard to neat PLA. Moreover, they reported a decrease in Young's modulus of EPO-plasticized PLA of 7% by adding 5 wt% EPO [29]. Despite this decrease in mechanical resistant properties for PLA/TPS blends with high TPS content, both tensile strength and modulus are still superior to most commodity plastics. With regard to the ductile properties, TPS has a very positive effect. Whilst PLA is characterized by a very low elongation at break value of about 7%, the addition of TPS raises this up to values of 18% and 21.5% for PLA/TPS blends containing 22.5 wt% and 30 wt% TPS, respectively. It seems to be a threshold in the range 15-22.5 wt% TPS. It is clearly observed that the elongation at break does not increase in a marked way below this threshold whilst a noticeable rise is detected over this threshold value. This could be related to the plasticizer content in TPS with a clear effect above this threshold point. It has been reported a similar effect by using PCL with an increase in elongation at break of 85% in PLA/PCL blends with 22.5 wt% PCL [30]. Nevertheless, TPS is a more cost-effective solution to PCL due to its lower cost compared to PCL and other polyester polymers. In a first approach, TPS offers

restricted miscibility with PLA [26, 27]. Nevertheless, the results herein shown, indicate a synergistic effect that could be related with the particular plasticizer in TPS as it is a copolyester-type that could interact with the polyester structure of PLA chains.

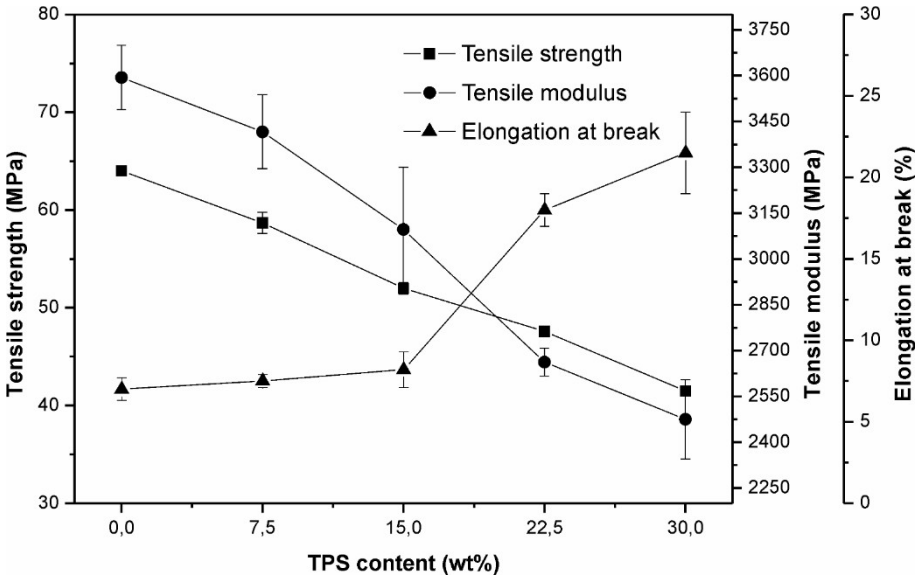

Figure III.2.1. Plot evolution of mechanical properties from tensile tests as a function of the weight % TPS.

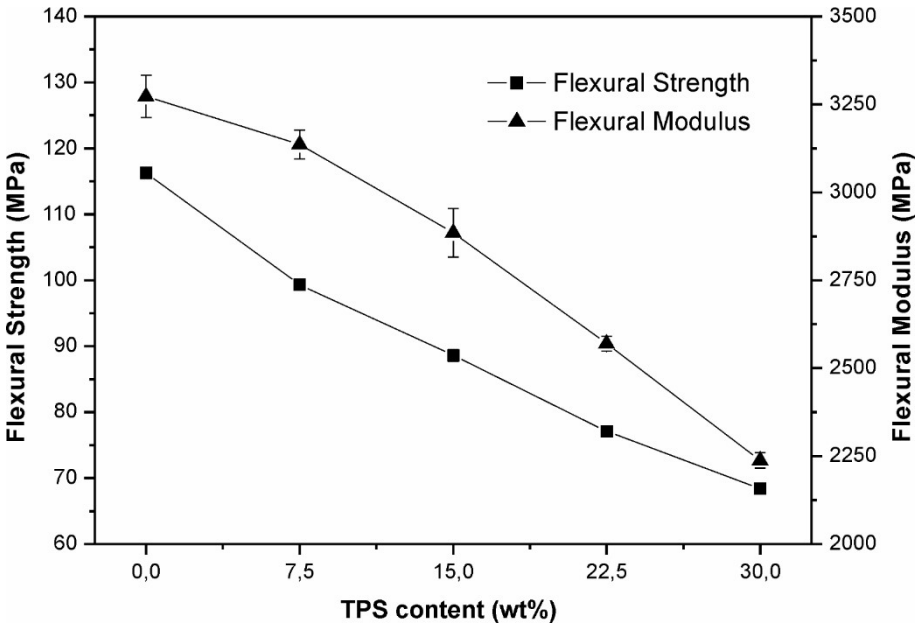

Figure III.2.2. Plot evolution of flexural strength and flexural modulus from PLA/TPS blends as a function of the weight % TPS.

Similar tendency can be observed for flexural properties (**Fig. III.2.2**). The flexural strength and modulus of neat PLA, 116.3 MPa and 3.27 GPa, respectively, decrease down to values of 64.8 MPa and 2.24 GPa respectively in the PLA/TPS blend with 30 wt% TPS. Although the plasticizing effect of TPS is not so pronounced as is discussed in the thermal analysis section, the effects on mechanical properties are quite similar and this could be related to the particular structure of this biphasic polymer system with a fragile matrix of PLA in which, spherical particles of a very flexible polymer (TPS) are finely dispersed.

As expected, as the TPS content increases, Shore D hardness values are lower as observed in **Table III.2.2**. It is worthy to note the positive effect of TPS on PLA/TPS blends toughness. Neat PLA is characterized by an extremely low toughness, directly related to its intrinsic fragility. As we have described previously, addition of TPS to PLA, leads to decreased mechanical resistant properties and a marked increase in the elongation at break which is directly related to the ability of the material to absorb energy. For this reason, the impact-absorbed energy change from 1.6 kJ m^{-2} (neat PLA) up to more than 3 times higher values of 5.3 kJ m^{-2} for PLA/TPS blends with 30 wt% TPS. Once again, although it is not expected a high miscibility between PLA and TPS, it is possible that the particular biphasic structure of the PLA/TPS systems contributes to improved toughness. Ojijo *et al.* observed a high increase in toughness of PLA by blending with poly(butylene succinate-co-adipate)(PBSA). Adding 30 wt% of PBSA, the absorption of energy to the impact increased 21.4%. Regarding thermomechanical properties, VST and HDT values do not change in a marked way and no clear tendency can be detected since the standard deviation is within the typical variation range.

Table III.2.2. Impact-absorbed energy, Shore D hardness and thermomechanical properties of PLA/TPS blends as a function of the weight % TPS.

wt% TPS	Charpy's impact-absorbed energy (kJ m^{-2})	Shore D hardness	Vicat softening temperature, VST (°C)	Heat deflection temperature, HDT (°C)
0	1.6 ± 0.3	76.0 ± 0.5	52.8 ± 1.4	47.6 ± 1.0
7.5	1.9 ± 0.3	73.8 ± 0.3	52.6 ± 1.2	49.2 ± 1.2
15	2.8 ± 0.3	72.5 ± 0.7	52.4 ± 0.6	49.0 ± 0.8
22.5	3.7 ± 0.1	69.9 ± 0.9	51.4 ± 0.8	49.2 ± 1.0
30	5.3 ± 0.1	68.2 ± 0.6	50.6 ± 1.0	49.4 ± 0.8

Effect of TPS content on thermal properties of PLA/TPS blends.

Fig. III.2.3 shows a comparative plot of the DSC curves of neat PLA, TPS and their blends. Regarding neat PLA, its glass transition temperature (T_g) is close to 60 °C and is clearly detectable by a change in slope. The exothermic peak comprised between 90 – 110 °C is related to the cold crystallization process and, finally, the endothermic peak between 150 - 180 °C corresponds to the melting process. TPS addition has a slight effect on the glass transition temperature thus showing a poor plasticization effect. The T_g of PLA is 65.4 °C and it is decreased by 3 °C whatever the TPS content as it can be seen in **Table III.2.3**, which gathers the main thermal transitions and parameters of PLA and its blends with TPS. This slight decrease in T_g is representative for poor miscibility between PLA and TPS [26, 27]. This poor plasticization effect is also assessed by the slight decrease in the cold crystallization peak which changes from 102 °C for neat PLA down to 98 - 99 °C for almost all PLA/TPS blends. However, López-Rodriguez et al. reported a decrease of almost 20 °C by the addition of 40 wt% of PCL.

On the other hand, PLA plasticized by oligomeric plasticizers revealed a decrease in T_{cc} in a range of 10 to 15 °C. This low decrease in the cold crystallization peak could be related to the slight plasticization effect that TPS could provide, thus allowing increased chain mobility [26].

Table III.2.3. Summary of the main thermal transitions and parameters of PLA/TPS blends obtained by DSC.

wt% TPS	T_g (°C)	T_{cc} (°C)	ΔH_{cc} (J g^{-1})	T_m (°C)	ΔH_m (J g^{-1})	%X
0	65.4	102	26.71	168.3	40.19	14.5
7.5	62.4	98.7	16.53	170.4	36.31	23.0
15	62.1	99.0	15.42	170.4	30.51	19.1
22.5	61.5	98.6	16.47	170.1	27.92	15.9
30	62.8	98.5	16.64	170.3	26.25	14.7

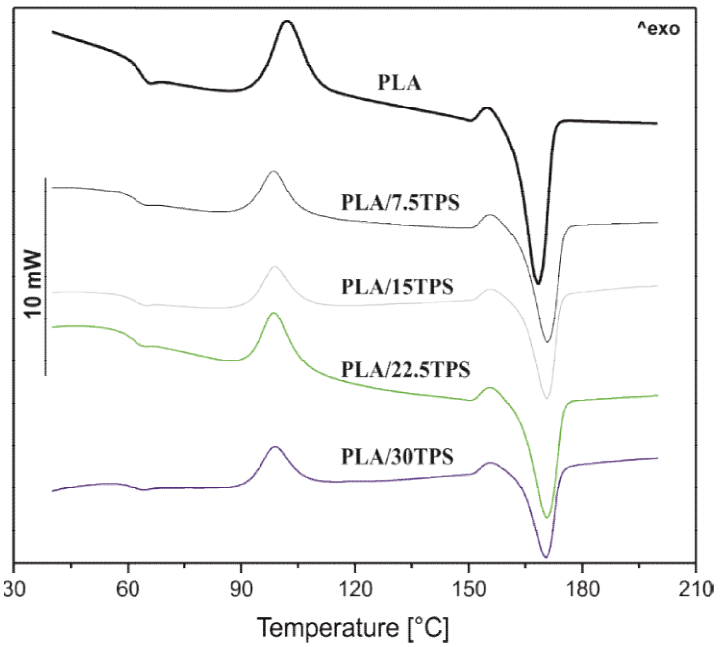

Figure III.2.3. Comparative DSC thermograms of neat PLA and PLA/TPS blends with different weight % TPS.

With regard to the degree of crystallinity (%X) of the PLA-rich domain, low TPS addition provides elevated %X values of almost 23% which is noticeably higher than that observed for neat PLA (14.5%). Nevertheless, this effect is lost as the TPS content increases to 30 wt% TPS thus leading to similar crystallinity to neat PLA. Similar behavior has been reported by Shin BY et al. [31]. Adding 20% of modified TPS to PLLA 2002D, the %X increased from 0.2% to 24%.

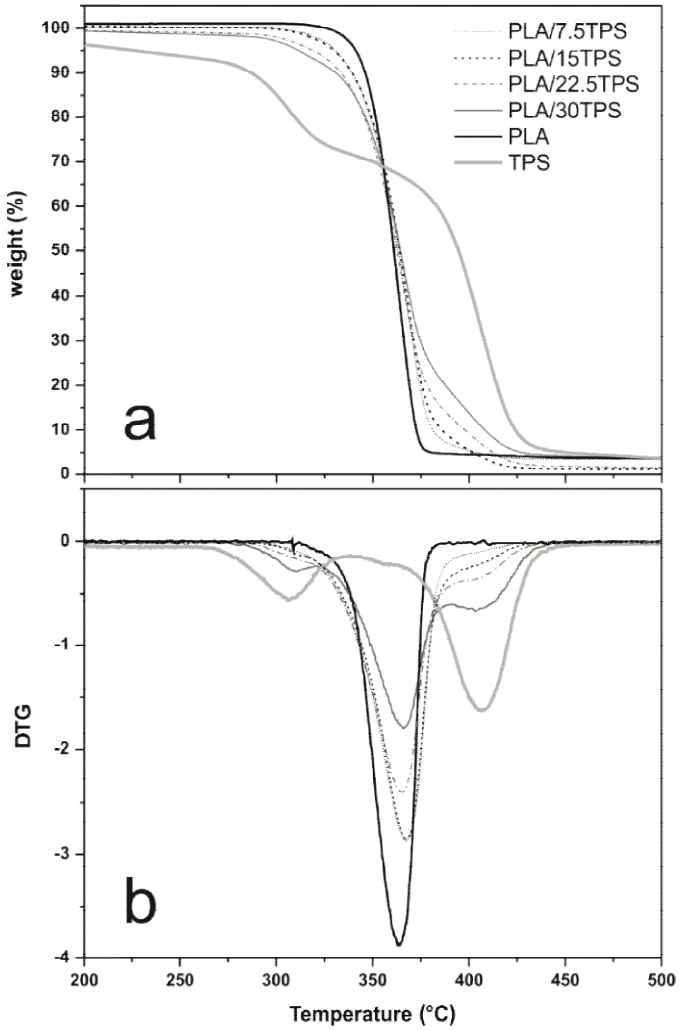

Figure III.2.4. a) Thermogravimetric (TG) and b) derivative thermogravimetric curves (DTG) of neat PLA, TPS and their blends with different TPS content.

With regard to the thermal stability at high temperatures, **Fig. III.2.4** shows a comparative plot of the TGA curves of neat PLA and TPS and their corresponding

blends. PLA degrades in a single step process with onset degradation temperature of 310 ºC. Regarding TPS, its degradation process occurs in two main stages. The first one occurs in the 300 – 360 ºC range with a weight loss of about 29%; this degradation stage could be attributed to the starch pyrolysis [32]. The second stage is comprised between 360 – 500 ºC with a weight loss of 61% which is related to the decomposition of the biodegradable copolyester component in TPS [33].

Table III.2.4 shows some parameters related to the thermal degradation. In particular, the temperature at which a 5% and 90% weight loss occurs ($T_{5\%}$, $T_{90\%}$) and the maximum degradation rate temperature (T_{max}), are summarized. Although slight decrease in $T_{5\%}$ can be detected, in general, the thermal stability is not highly affected by presence of TPS. In fact, as we can observe, a slight increase in $T_{90\%}$ is detected but in both cases, the change is not significative.

Table III.2.4. Thermal parameters of unplasticized PLA and PLA/TPS blends with various TPS content.

wt% TPS	**TGA**		
	$T_{5\%}$ (ºC)	**$T_{90\%}$ (ºC)**	**T_{max} (ºC)**
0	336.9	365.1	363.5
7.5	330.7	381.1	365.0
15	329.9	385.8	364.5
22.5	319.0	397.7	364.6
30	311.5	427.2	365.1

Effect of TPS content on dynamic-mechanical thermal behaviour of PLA/TPS blends.

Fig. III.2.5 shows the evolution of the storage modulus (G′) as a function of increasing temperature for both neat materials, PLA and TPS and their corresponding blends. As the TPS content increase, the characteristic G′ curve moves to lower G′ values. This also corroborates more flexible materials as previously described in the mechanical characterization. As it can be seen for neat PLA, G′ suffers a noticeable decrease in the temperature range comprised between 55 – 70 ºC (more than two fold). This is directly related to its glass transition relaxation (T_g). If we compare the G′ values at 25 ºC, the effect of TPS become clearly evident with a marked decreasing tendency. Neat PLA shows a G′ value of 1.34 GPa; addition of 7.5 wt% leads to a G′ value of 1.08 GPa. G′ is slightly reduced in PLA/TPS blends with 15-22.5 wt% TPS, with values in the 0.95-1.0 GPa whilst minimum values of 0.6 GPa are obtained in blends with 30 wt% TPS.

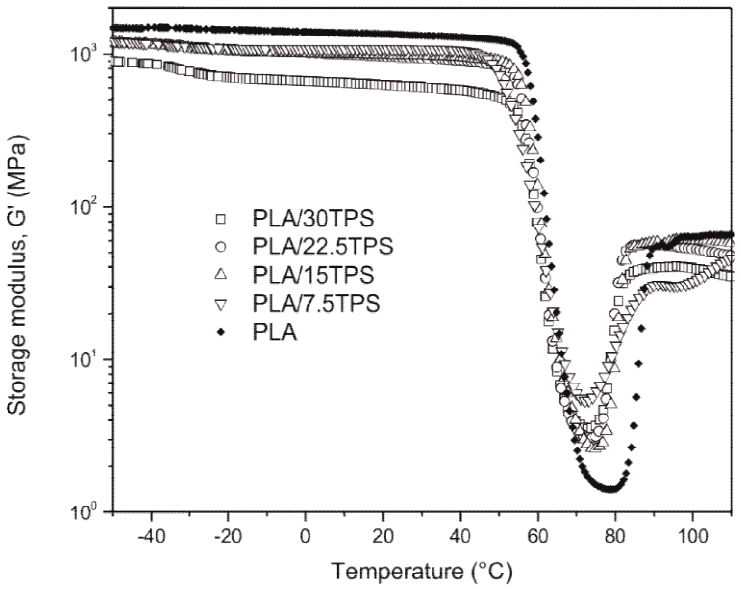

Figure III.2.5. Plot evolution of the storage modulus (G′) of neat PLA and PLA/TPS blends vs temperature for various TPS contents.

The evolution of G' in the glass transition relaxation zone, also indicates poor plasticization effects as the typical curves are not highly moved to lower temperatures thus indicating a slight decrease in T_g values as observed in DSC analysis. Another important transition of neat PLA is the cold crystallization process with occurs in the 80-90 ºC range. During the cold crystallization, amorphous domains in PLA tend to rearrange in a packed structure to form crystalline zones that contribute to increase its mechanical resistance and rigidity (almost two fold higher regarding the minimum values achieved after the glass transition relaxation). As it has been previously described in the DSC analysis, the cold crystallization process occurs at lower temperatures in PLA/TPS blends, due to the slightly increased chain mobility that TPS provides. For this reason, characteristic curves are shifted by almost 10 ºC to the left with regard to neat PLA. This is in total accordance with the results shown in the DSC analysis and it is in agreement with some other Works [29, 34].

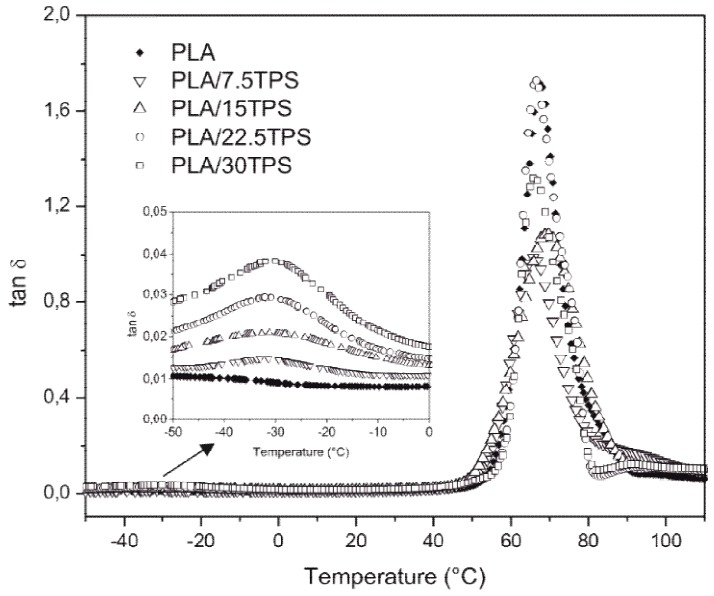

Figure III.2.6. Plot evolution of the damping factor (tan δ) of neat PLA and PLA/TPS blends vs temperature for various TPS contents.

The change in the glass transition temperature (T_g) is more clearly detectable by analysing the evolution of the damping factor (tan δ) with temperature (**Fig. III.2.6**). By

taking the damping factor peak as the criterion to estimate the T_g, neat PLA possesses a T_g value of about 68 ^oC and this is reduced by not more than 2 ^oC for PLA/TPS blends with 15-22.5 wt% TPS. This means poor plasticization effect due to restricted miscibility between these two polymers. Neat TPS shows a wide relaxation temperature range comprised between -50 ^oC and -5 ^oC with a peak (T_g) value of -28.3 ^oC as it can be seen if **Fig. III.2.6**. Although the miscibility between PLA and TPS is restricted, some PLA chains enter TPS domains and contribute to slightly decrease its characteristic T_g value by 4-5 ^oC. Similarly, it occurs in the work of Ojijo et al. where they modify PBSA by adding triphenyl phosphite (TPP). In this way, the interaction between the PLA and PBSA improves significantly contributing a greater tenacity to the binary mixture.

Effect of TPS content on the morphology of PLA/TPS blends.

Fig. III.2.7 gathers typical FESEM images of cryofractured samples of both neat PLA and TPS at different magnifications.

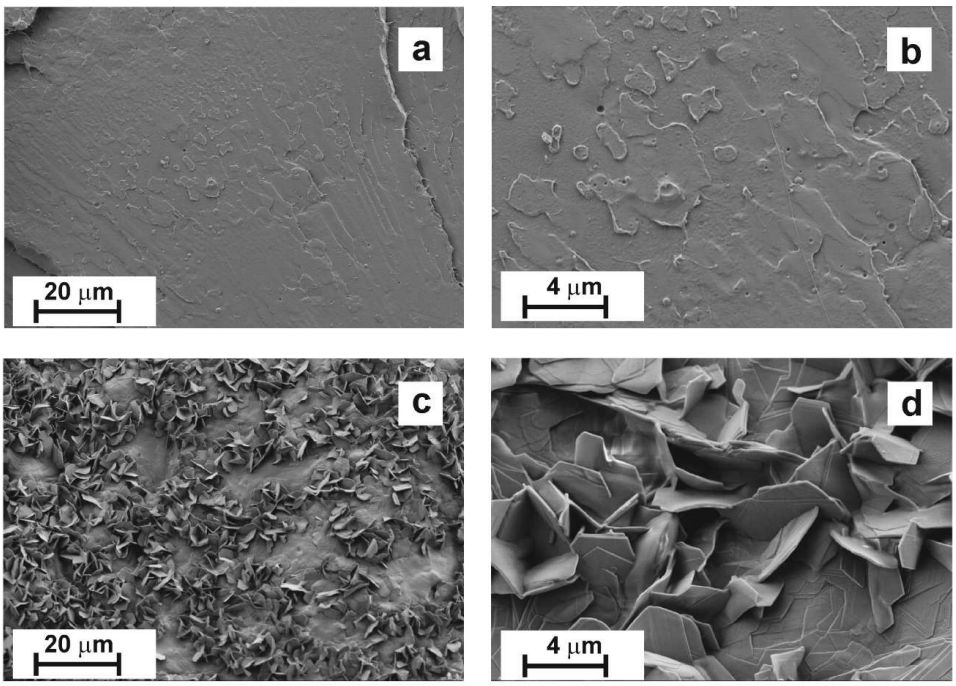

Figure III.2.7. FESEM images of cryofractured samples of neat PLA (a and b) and TPS (c and d) at different magnifications, 1000x (a and c) and 5000x (b and d).

PLA (**Fig. III.2.7a** and **Fig. III.2.7b**) shows a typical fragile fracture surface with no evidence of plastic deformation and a homogenous smooth surface. On the other hand, TPS (**Fig. III.2.7c** and **Fig. III.2.7d**) shows a different fracture with flake formation typical of the growth of crystalline planes in maize starch (crystalline lamellae) which are oriented randomly during the fracture process. These planes are stacked in a parallel way due to the growth of starch A-type from the seeds. These stacked planes from small blocks and the aggregate of blocks form granules that are separated from the amorphous zones in which, amylose and plasticizers are located [35].

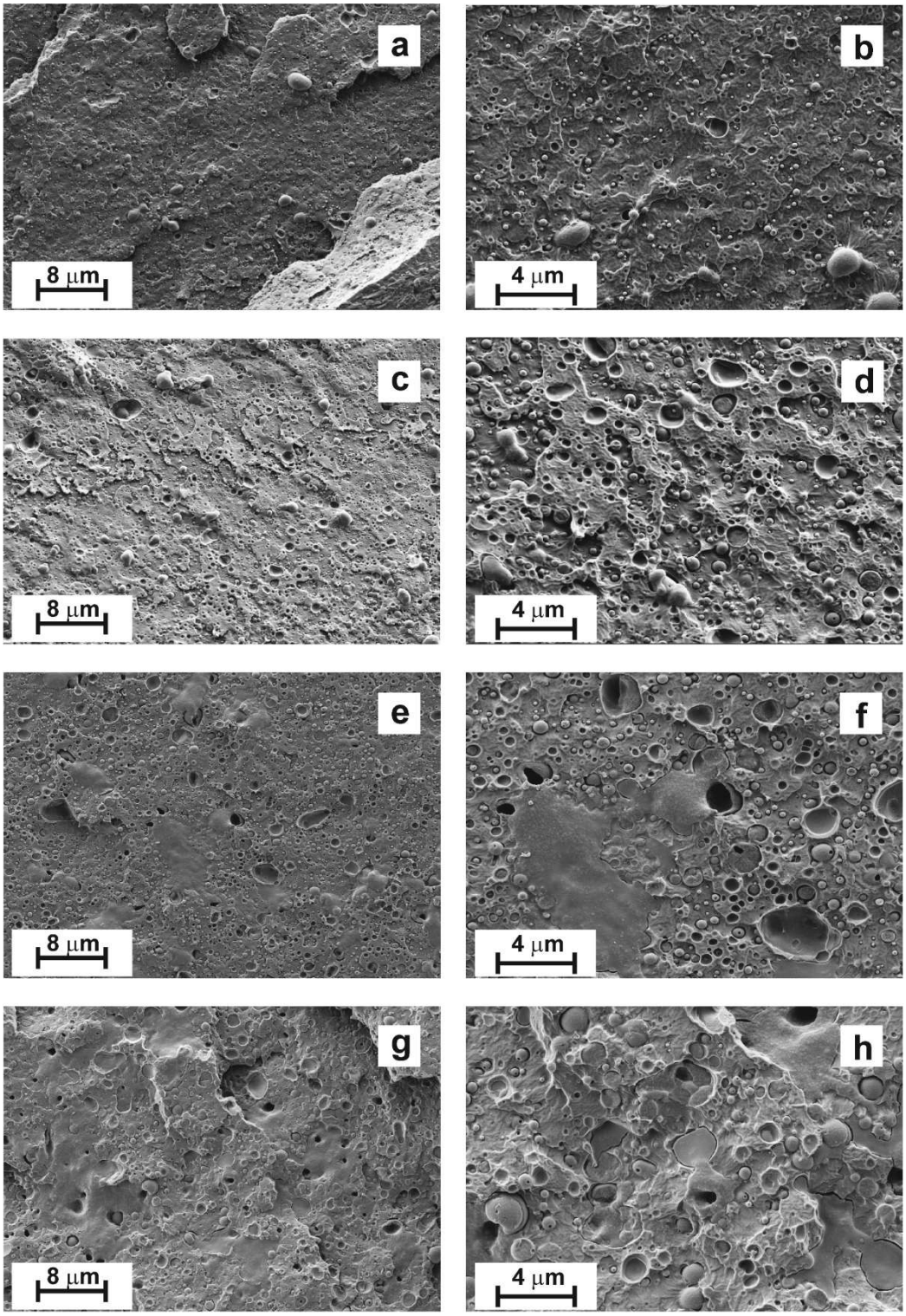

Figure III.2.8. FESEM images of cryofractured samples of PLA/TPS blends with different TPS content: a-b) 7.5 wt%, c-d) 15.0 wt%, e-f) 22.5 wt% and g-h) 30 wt% at different magnifications, 1000x (a, c, e and g) and 5000x (b, d, f and h).

Fig. III.2.8 reveals in a clear way, the biphasic structure of the PLA/TPS system, through FESEM images of cryofractured samples. All formulations offer a biphasic structure with a PLA-rich matrix in which TPS-rich domains appear randomly dispersed. The TPS-rich domains offer different size as the TPS content increases. So that, the TPS-rich domains change from 0.2 – 0.4 μm (in PLA/TPS blends with 7.5 wt% TPS) up to 1 – 2 μm (in PLA/TPS blend with 30 wt% TPS). A similar result has been reported by Mittal V et al. In that work, the authors studied binary and ternary blends and showed TPS-rich domains with sizes comprised between 0.5-2 μm in a PLA/TPS blend with 50 wt% TPS. As the particle size increases we can also observe the lack (or very poor) miscibility between PLA and TPS as some spherical voids appear, thus indicating that some TPS-rich domains have been pulled out during the cryofracture process. This particular morphology, with TPS-rich domains with a size ranging from 0.2 to 2 μm, positively contributes to improved toughness as it has been described previously.

Conclusions.

Addition of TPS is a cost-effective method to improve the low intrinsic ductile behaviour of PLA with improved toughness. This widens its uses at industrial scale as its fragility is markedly reduced. Indeed, the elongation at break improves from 7.0% (neat PLA) up to values of 21.5% in PLA/TPS blend with 30 wt% TPS, which represents a percentage increase by more than 300%. It is worthy to note that the impact-absorbed energy is increased up to 5.3 J m^{-2} (PLA/TPS blend with 30 wt% TPS) which is more than three times the value of neat PLA (1.6 J m-2). Thermal analysis has revealed a poor miscibility between PLA and TPS. In fact, DSC and DMTA revealed a reduction of 2-3 ^{o}C in T_g thus showing a restricted miscibility between these polymers. The plasticization effects that TPS can provide are restricted duo to the lack of miscibility. Nevertheless, the particular biphasic structure revealed by FESEM, with small spherical TPS-rich domains (with a size ranging between 0.2 to 2 μm) finely dispersed in the rigid PLA-rich matrix, has a positive effect on toughness and energy-

absorption. As a general conclusion, blending PLA with TPS represents a cost-effective and environmentally friendly solution to widen the uses of PLA way by improving its toughness and ductile properties.

Acknowledgements.

This research was supported by the Ministry of Economy and Competitiveness - MINECO, Ref: MAT2014-59242-C2-1-R. Authors also thank to "Conselleria d'Educació, Cultura i Esport" - Generalitat Valenciana, Ref: GV/2014/008 for financial support.

References.

1. Tsuji, H. and Ishizaka, T., *Blends of aliphatic polyesters. VI. Lipase-catalyzed hydrolysis and visualized phase structure of biodegradable blends from poly(ε-caprolactone) and poly(l-lactide)*. International Journal of Biological Macromolecules, 2001. **29**(2): p. 83-89.

2. Genovese, L., Lotti, N., Gazzano, M., Siracusa, V., Dalla Rosa, M., and Munari, A., *Novel biodegradable aliphatic copolyesters based on poly(butylene succinate) containing thioether-linkages for sustainable food packaging applications*. Polymer Degradation and Stability, 2016. **132**(-): p. 191-201.

3. Ojijo, V., Sinha Ray, S., and Sadiku, R., *Toughening of Biodegradable Polylactide/Poly(butylene succinate-co-adipate) Blends via in Situ Reactive Compatibilization*. ACS Applied Materials & Interfaces, 2013. **5**(10): p. 4266-4276.

4. Weng, Y.-X., Jin, Y.-J., Meng, Q.-Y., Wang, L., Zhang, M., and Wang, Y.-Z., *Biodegradation behavior of poly(butylene adipate-co-terephthalate) (PBAT), poly(lactic acid) (PLA), and their blend under soil conditions*. Polymer Testing, 2013. **32**(5): p. 918-926.

5. Balart, J.F., Fombuena, V., Fenollar, O., Boronat, T., and Sánchez-Nacher, L., *Processing and characterization of high environmental efficiency composites based on PLA and hazelnut shell flour (HSF) with biobased plasticizers derived from epoxidized linseed oil (ELO)*. Composites Part B, 2016. **86**: p. 168-177.

6. Garcia-Garcia, D., Ferri, J.M., Boronat, T., Lopez-Martinez, J., and Balart, R., *Processing and characterization of binary poly(hydroxybutyrate) (PHB) and poly(caprolactone) (PCL) blends with improved impact properties*. Polymer Bulletin, 2016. **73**(12): p. 3333-3350.

7. Nair, M.B., Baranwal, G., Vijayan, P., Keyan, K.S., and Jayakumar, R., *Composite hydrogel of chitosan–poly(hydroxybutyrate-co-valerate) with chondroitin sulfate nanoparticles for nucleus pulposus tissue engineering*. Colloids and Surfaces B: Biointerfaces, 2015. **136**(-): p. 84-92.

8. Cheng, H.-Y., Yang, Y.-J., Li, S.-C., Hong, J.-Y., and Jang, G.-W., *Modification and extrusion coating of polylactic acid films*. Journal of Applied Polymer Science, 2015. **132**(35): 42472.

9. Ingrao, C., Tricase, C., Cholewa-Wojcik, A., Kawecka, A., Rana, R., and Siracusa, V., *Polylactic acid trays for fresh-food packaging: A Carbon Footprint assessment*. Science of the Total Environment, 2015. **537**: p. 385-398.

10. Jost, V. and Kopitzky, R., *Blending of Polyhydroxybutyrate-co-valerate with Polylactic Acid for Packaging Applications - Reflections on Miscibility and Effects on the Mechanical and Barrier Properties*. Chemical and Biochemical Engineering Quarterly, 2015. **29**(2): p. 221-246.

11. Sanyang, M.L. and Sapuan, S.M., *Development of expert system for biobased polymer material selection: food packaging application*. Journal of Food Science and Technology, 2015. **52**(10): p. 6445-54.

12. Plackett, D.V., Holm, V.K., Johansen, P., Ndoni, S., Nielsen, P.V., Sipilainen-Malm, T., Sodergard, A., and Verstichel, S., *Characterization of L-polylactide and L-polylactide-polycaprolactone co-polymer films for use in cheese-packaging applications*. Packaging Technology and Science, 2006. **19**(1): p. 1-24.

13. Averous, L., *Biodegradable multiphase systems based on plasticized starch: A review*. Journal of Macromolecular Science-Polymer Reviews, 2004. **C44**(3): p. 231-274.

14. Lasprilla, A.J.R., Martinez, G.A.R., Lunelli, B.H., Jardini, A.L., and Maciel Filho, R., *Poly-lactic acid synthesis for application in biomedical devices - A review*. Biotechnology Advances, 2012. **30**(1): p. 321-328.

15. Boonprasith, P., Wootthikanokkhan, J., and Nimitsiriwat, N., *Mechanical, thermal, and barrier properties of nanocomposites based on poly(butylene succinate)/thermoplastic starch blends containing different types of clay*. Journal of Applied Polymer Science, 2013. **130**(2): p. 1114-1123.

16. Sahari, J., Sapuan, S.M., Zainudin, E.S., and Maleque, M.A., *Thermo-mechanical behaviors of thermoplastic starch derived from sugar palm tree (Arenga pinnata)*. Carbohydrate Polymers, 2013. **92**(2): p. 1711-1716.

17. Mahieu, A., Terrie, C., and Youssef, B., *Thermoplastic starch films and thermoplastic starch/polycaprolactone blends with oxygen-scavenging properties: Influence of water content*. Industrial Crops and Products, 2015. **72**: p. 192-199.

18. Chocyk, D., Gladyszewska, B., Ciupak, A., Oniszczuk, T., Moscicki, L., and Rejak, A., *Influence of water addition on mechanical properties of thermoplastic starch foils*. International Agrophysics, 2015. **29**(3): p. 267-273.

19. Li, H. and Huneault, M.A., *Effect of Chain Extension on the Properties of PLA/TPS Blends*. Journal of Applied Polymer Science, 2011. **122**(1): p. 134-141.

20. Mikus, P.Y., Alix, S., Soulestin, J., Lacrampe, M.F., Krawczak, P., Coqueret, X., and Dole, P., *Deformation mechanisms of plasticized starch materials*. Carbohydrate Polymers, 2014. **114**: p. 450-457.

21. Schmitt, H., Guidez, A., Prashantha, K., Soulestin, J., Lacrampe, M.F., and Krawczak, P., *Studies on the effect of storage time and plasticizers on the structural variations in thermoplastic starch*. Carbohydrate Polymers, 2015. **115**: p. 364-372.

22. Zhang, Y., Rempel, C., and Liu, Q., *Thermoplastic Starch Processing and Characteristics-A Review*. Critical Reviews in Food Science and Nutrition, 2014. **54**(10): p. 1353-1370.

23. Chaudhary, A.L., Miler, M., Torley, P.J., Sopade, P.A., and Halley, P.J., *Amylose content and chemical modification effects on the extrusion of thermoplastic starch from maize*. Carbohydrate Polymers, 2008. **74**(4): p. 907-913.

24. Chaudhary, A.L., Torley, P.J., Halley, P.J., McCaffery, N., and Chaudhary, D.S., *Amylose content and chemical modification effects on thermoplastic starch from maize - Processing and characterisation using conventional polymer equipment*. Carbohydrate Polymers, 2009. **78**(4): p. 917-925.

25. Pang, M.M., Pun, M.Y., and Ishak, Z.A.M., *Thermal, mechanical, and morphological characterization of biobased thermoplastic starch from agricultural waste/polypropylene blends*. Polymer Engineering and Science, 2014. **54**(6): p. 1357-1365.

26. Teixeira, E.d.M., Curvelo, A.A.S., Correa, A.C., Marconcini, J.M., Glenn, G.M., and Mattoso, L.H.C., *Properties of thermoplastic starch from cassava bagasse and cassava starch and their blends with poly (lactic acid)*. Industrial Crops and Products, 2012. **37**(1): p. 61-68.

27. Mittal, V., Akhtar, T., and Matsko, N., *Mechanical, Thermal, Rheological and Morphological Properties of Binary and Ternary Blends of PLA, TPS and PCL*. Macromolecular Materials and Engineering, 2015. **300**(4): p. 423-435.

28. NOVAMONT. Copoliéster alifático/aromático biodegradable (AAPE). 2010; Available from: http://patentados.com/invento/poliesteres-alifaticos-aromaticos-biodegradables.html.

29. Ferri, J.M., Samper, M.D., García-Sanoguera, D., Reig, M.J., Fenollar, O., and Balart, R., *Plasticizing effect of biobased epoxidized fatty acid esters on mechanical and thermal properties of poly(lactic acid)*. Journal of Materials Science, 2016. **51**(11): p. 5356-5366.

30. Lopez-Rodriguez, N., Lopez-Arraiza, A., Meaurio, E., and Sarasua, J.R., *Crystallization, morphology, and mechanical behavior of polylactide/poly(epsilon-caprolactone) blends*. Polymer Engineering and Science, 2006. **46**(9): p. 1299-1308.

31. Shin, B.Y., Jang, S.H., and Kim, B.S., *Thermal, Morphological, and Mechanical Properties of Biobased and Biodegradable Blends of Poly(lactic acid) and Chemically Modified Thermoplastic Starch*. Polymer Engineering and Science, 2011. **51**(5): p. 826-834.

32. Mano, J.F., Koniarova, D., and Reis, R.L., *Thermal properties of thermoplastic starch/synthetic polymer blends with potential biomedical applicability*. Journal of Materials Science: Materials in Medicine, 2003. **14**(2): p. 127-135.

33. Alvarez, V.A. and Vázquez, A., *Thermal degradation of cellulose derivatives/starch blends and sisal fibre biocomposites*. Polymer Degradation and Stability, 2004. **84**(1): p. 13-21.

34. Yu, Y., Cheng, Y., Ren, J., Cao, E., Fu, X., and Guo, W., *Plasticizing effect of poly(ethylene glycol)s with different molecular weights in poly(lactic acid)/starch blends*. Journal of Applied Polymer Science, 2015. **132**(16): 41808.

35. Hee-Young Kim, S.S.P., Seung-Taik Lim, *Preparation, characterization and utilization of starch nanoparticles*. Colloids and Surfaces B: Biointerfaces, 2014. **126**: p. 607-620.

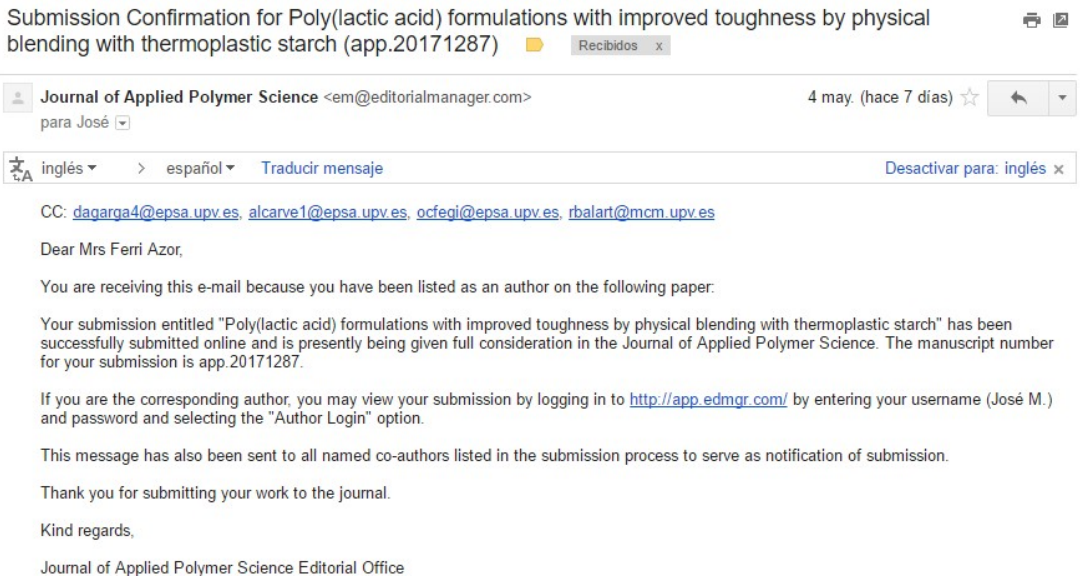

Submission Confirmation for Poly(lactic acid) formulations with improved toughness by physical blending with thermoplastic starch (app.20171287) Recibidos x

Journal of Applied Polymer Science <em@editorialmanager.com> 4 may. (hace 7 días)
para José

inglés > español Traducir mensaje Desactivar para: inglés ×

CC: dagarga4@epsa.upv.es, alcarve1@epsa.upv.es, ocfegi@epsa.upv.es, rbalart@mcm.upv.es

Dear Mrs Ferri Azor,

You are receiving this e-mail because you have been listed as an author on the following paper:

Your submission entitled "Poly(lactic acid) formulations with improved toughness by physical blending with thermoplastic starch" has been successfully submitted online and is presently being given full consideration in the Journal of Applied Polymer Science. The manuscript number for your submission is app.20171287.

If you are the corresponding author, you may view your submission by logging in to http://app.edmgr.com/ by entering your username (José M.) and password and selecting the "Author Login" option.

This message has also been sent to all named co-authors listed in the submission process to serve as notification of submission.

Thank you for submitting your work to the journal.

Kind regards,

Journal of Applied Polymer Science Editorial Office

Chapter III.3

Chapter III.3. Plasticizing effect of biobased epoxidized fatty acid esters on mechanical and thermal properties of poly(lactic acid).

“Plasticizing effect of biobased epoxidized fatty acid esters on mechanical and thermal properties of poly(lactic acid)”

J.M. Ferri, M.D. Samper, D. García-Sanoguera, M.J. Reig, O., Fenollar, R. Balart

Instituto de Tecnología de Materiales (ITM)

Universitat Politècnica de València (UPV)

Plaza Ferrandiz y Carbonell 1, 03801, Alcoy, Alicante (Spain)

Journal of Materials Science 51:5356-5366 (2016)

Abstract.

Poly(lactic acid), PLA, is a polyester that can be produced from lactic acid derived from renewable resources. This polymer offers attracting uses in packaging industry due to its biodegradability and high tensile strength. However, PLA is quite brittle, which limits its applications. To overcome this drawback, PLA was plasticized with epoxy-type plasticizer derived from a fatty acid, octyl epoxy stearate (OES) at different loadings (1, 3, 5, 10, 15, and 20 phr). The addition of OES decreases the glass transition temperature and provides a remarkable increase in elongation at break and impact-absorbed energy. Plasticizer saturation occurs at relatively low concentrations of about 5 phr OES; higher concentration leads to phase separation as observed by field emission scanning electron microscopy (FESEM). Optimum balanced mechanical properties are obtained at relatively low concentrations of OES (5 phr) thus indicating the usefulness of this material as environmentally friendly plasticizer for PLA industrial formulations.

Keywords: Plasticized, PLA, EVO, fatty acid esters.

Introduction.

Poly(lactic acid), PLA, is a linear aliphatic polyester that is produced from lactic acid derived from renewable resources through a fermentation process of corn starch, wheat starch, sugar bagasse, and other starch-rich products. This biobased polymer possesses attracting properties such as biodegradability, biocompatibility, easy processing, and overall good mechanical properties. For these reasons, it is the selected candidate for a wide variety of applications as, in addition, it is shiny and transparent, moisture and fat resistant, and offers similar flavor and odor barrier properties to poly(ethylene terephthalate), PET. All these features make PLA highly useful for food packaging [1, 2]. Furthermore, due to its high UV stability and low flammability, it is widely used in non-discoloring textiles and fabrics for uses in agricultural applications [3, 4]. PLA is also biocompatible and resorbable so that it finds increasing applications in the medical sector for controlled drug delivery [5] and tissue engineering [6-10].

Nevertheless, its high stiffness and brittleness restrict some uses in engineering applications. To overcome this, several environmentally friendly approaches have been proposed. One of these approaches is blending PLA with other polymers such as poly(hydroxybutyrate), PHB [2, 11-13], poly(caprolactone), PCL [14], acetylated thermoplastic starch [15], etc. which can lead to tailored properties in terms of mechanical response, biodegradation rate, etc. Another interesting approach is the use of environmentally friendly and non-toxic plasticizers such as poly(ethylene glycol), PEG [16-18], poly(propylene glycol), PPG [19], oligomeric lactic acid, OLA [20], citrates such as acetyl tributyl citrate (ATBC) [21-23] or tributyl citrate (TBC) [22, 24-26].

Vegetable oils are cost-effective products (or in some cases, by-products) characterized by high availability; in addition, they can be chemically modified to improve some properties or attach selected functionalities. Raw or modified vegetable oils find new and attracting uses as plasticizers or raw materials for polymer synthesis. Vegetable oils can be converted into epoxidized oils (EVOs) by conventional epoxidation processes. These epoxidized vegetable oils can be successfully used as high environmentally friendly epoxy resins [27-30] as well as plasticizers for poly(vinyl

chloride), PVC industrial formulations due to its high compatibility with PVC resins [31-35]. Epoxidized vegetable oils also have been used as plasticizers for PLA. Chieng et al. used epoxidized palm oil (EPO) and a mixture of epoxidized oils (palm-EPO and soybean-ESBO) as plasticizers for PLA and both plasticizers systems contributed to a remarkable increase in elongation at break and a parallel decrease in stiffness [36]. Prempeh et al. compared the effectiveness of epoxidized sunflower oil (ESFO) with regard to epoxidized soybean oil (ESBO) as plasticizers for PLA formulations. ESFO gave a remarkable increase in elongation at break. In addition, the glass transition temperature (T_g) was decreased by 3 ºC and the overall thermal stability of PLA was improved [37]. The results reported by Santos et al. showed a remarkable increase in mechanical ductile properties of PLA together with a decrease in T_g, by using 20% plasticizer coming from biodiesel derived from sunflower oil. This was attributed to an increase in polymer chain mobility due to the internal lubricating effect provided by the plasticizer [38]. Finally, Alam et al. studied the effect of epoxidized linseed oil (ELO) on mechanical performance of PLA with addition of carbon nanotubes; addition of ELO led to an increase in elongation at break, a reduction of the T_g and a thermal stabilization effect [1].

The aim of this work is to improve the ductile properties of PLA by using an epoxy plasticizer derived from a fatty acid, octyl epoxy stearate (OES). The work has focused on the effect of this plasticizer on thermal and mechanical performance of PLA with different amounts of OES to obtain balanced properties and overcome the intrinsic fragility of PLA polymers.

Experimental.

Materials.

Poly(lactic acid) resin commercial grade, IngeoTM Biopolymer 6201D was supplied by NatureWorks LLC (Minnetonka, USA). Its density is 1.24 g cm^{-3} and contains about 2% D-isomer. The selected plasticizer was an octyl epoxy stearate (OES) with tradename "plasticizer 201", supplied by Traquisa S.L. (Barcelona, Spain). It is characterized by an epoxide oxygen content in the 3.1-3.3% range, a viscosity of 20-30 cP at 20 ^{o}C, and a molecular weight of 408 g mol^{-1}. A schematic representation of the chemical structure of OES is shown in **Figure III.3.1**, and the presence of one epoxide ring per molecule can be observed.

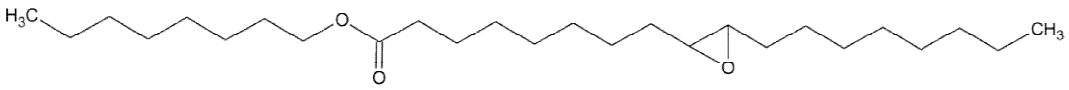

Figure III.3.1. Schematic representation of the chemical structure of octyl epoxy stearate (OES) plasticizer.

Processing of OES-plasticized PLA.

Initially, PLA pellets were dried at 60 ^{o}C for 24 h for further processing operations. After this, PLA pellets and the corresponding amounts of OES plasticizer were mechanically mixed in a zipper bag. **Table III.3.1** summarizes all the compositions tested in this work as well as their labelling. PLA-OES mixtures were melt blended in a twin screw co-rotating extruder at a rotating speed of 60 rpm and temperature profile in the 172 ^{o}C (hopper) – 180 ^{o}C (die) range and subsequently pelletized. After this, plasticized PLA pellets were molded by injection molding in a Meteor 270/75 from Mateu & Solé (Barcelona, Spain) at an injection temperature of 180 ^{o}C and standard samples for tensile tests and rectangular samples sizing 80 x 10 x 4 mm^3 were obtained. The formulation with best-balanced properties was selected for

film formation by using a cast film equipment from EuroTech S.A.S (San Martino in Riu, Italy). The extrusion temperature was set to 210 ºC, and film of 200 mm wide and 200 μm thick was obtained.

Code	Plasticizer amount (phr – per hundred PLA resin)
PLA	-
PLA-1 OES	1
PLA-3 OES	3
PLA-5 OES	5
PLA-10 OES	10
PLA-15 OES	15
PLA-20 OES	20

Table III.3.1. Summary of the compositions and coding of poly(lactic acid), PLA with different amounts of octyl epoxy stearate (OES) plasticizer.

Mechanical characterization of OES-plasticized PLA.

Mechanical characterization was carried out with tensile and impact tests. Tensile tests were done in a universal test machine ELIB 30 from S.A.E. Ibertest (Madrid, Spain) at room temperature according to the ISO 527 standard. A 5 kN load cell and a crosshead speed of 10 mm min^{-1} were used. At least five different samples were tested and average values were calculated. In addition, an axial extensometer from Ibertest was coupled to the longitudinal section to obtain the Young's modulus in a more accurate way.

To evaluate the ability of the PLA-OES materials to absorb energy, the Charpy impact test was carried out in a Charpy pendulum (6 J) from Metrotec S.A. (San Sebastián, Spain) following the guidelines of the ISO 197:1993. At least five different specimens of each sample were tested and average values were calculated.

Surface characterization of the fractured samples from impact tests was carried out by field emission scanning electron microscopy (FESEM) in a Zeiss ULTRA

microscope at an accelerating voltage of 2 kV. Samples were previously covered with a thin platinum layer in a high vacuum sputter EM MED020 from Leica Microsystems.

Thermo-mechanical characterization of OES-plasticized PLA.

The effect of temperature on mechanical properties was studied by conventional heat deflection temperature (HDT) and Vicat softening temperature (VST) tests. In addition, dynamic mechanical thermal analysis (DMTA) was carried on PLA-OES materials.

Dynamic mechanical thermal analysis (DMTA) was carried out in rectangular torsion mode in an oscillatory rheometer AR G2 from TA Instruments (New Castle, USA), equipped with a torsion clamp system for rectangular solid samples. Samples sizing 40x10x4 mm^3 were subjected to a temperature sweep program from 20 up to 130 ^oC at a constant heating rate of 2 $^oC\ min^{-1}$ in air atmosphere. The selected frequency was 1 Hz and the maximum deformation (γ) was set to 0.1%.

The heat deflection temperature (HDT) was determined by the A method according to ISO 75 which recommends a load of 1.8 MPa and a heating rate of 120 $^oC\ h^{-1}$. Vicat softening temperature (VST) was done using the B method as recommended by the ISO 306 with a load of 50 N and a heating rate of 50 $^oC\ h^{-1}$. Both tests were carried out in a VICAT/HDT station DEFLEX 687-A2 from Metrotec S.A. (San Sebastián, Spain).

Thermal characterization of OES-plasticized PLA.

Thermal properties of PLA and PLA plasticized with octyl epoxy stearate (OES) were obtained by differential scanning calorimetry (DSC) and thermogravimetric analysis (TGA). Thermogravimetric (TGA) tests were carried out in a TGA/SDTA 851

thermobalance from Mettler-Toledo Inc. (Schwerzenbach, Switzerland) with a heating program from 30 to 500 ^{o}C at a heating rate of 20 ^{o}C min^{-1} in nitrogen atmosphere (66 mL min^{-1}). Differential scanning calorimetry (DSC) was conducted in a Mettler-Toledo 821 calorimeter (Schwerzenbach, Switzerland) in nitrogen atmosphere (66 mL min^{-1}); the heating program was from 30 to 190 ^{o}C at a heating rate of 10 ^{o}C min^{-1}.

Oxygen permeability measurement of OES-plasticized PLA.

Oxygen transmission rate (OTR) measurements were carried out using an oxygen permeation analyzer from Systech Instruments Model 8500 (Metrotec S.A, Spain) at a pressure of 2.5 atm. Measurements were conducted at room temperature. Films were clamped in the diffusion chamber and pure oxygen (99.9% purity) was flowed through the upper half of the sample chamber, while nitrogen was flowed through the lower half of the chamber. Three measurements were made to obtain an average value, and the results were expressed as oxygen transmission rate per film thickness (OTR · e). Thickness was accurately measured at 25 ^{o}C using a Digimatic Micrometer Series 293 MDC-Lite (Mitutoyo, Japan) with an error of 0.001 mm. Ten readings were taken at random positions over the 14 cm diameter circle films.

Wettability of OES-plasticized PLA.

The wetting properties of the film surface were measured by water contact angle at room temperature with an Easy Drop Standard goniometer FM140 (KRÜSS GmbH, Hamburg, Germany). It is equipped with a stroboscopic camera and an analyzer program (Drop Shape Analysis SW21; DSA1). Ten contact angles were measured randomly using distilled water as contact liquid onto the surface film with a micro syringe. Five measurements were carried out for each drop, and the average values were calculated.

Results and discussion.

Mechanical properties of OES-plasticized PLA.

Mechanical properties are very sensitive to the presence of plasticizers. **Figure III.3.2** shows the evolution of the tensile strength and Young's modulus. We can see a clear plasticization effect as the tensile strength of unplasticized PLA (64.0 MPa) is reduced up to values of 61.3, 55.2, and 43 MPa (a percentage decrease of 33%) for PLA-OES compositions containing 1, 3 and 5 phr OES, respectively. With regard to the maximum OES content, the tensile strength is reduced up to 40.5 MPa (percentage decrease of 37%). This could be related to the formation of a separated phase structure. Regarding to the Young's modulus, no significant changes are observed. The modulus of unplasticized PLA is close to 3600 MPa. Low amounts of OES plasticizer lead to a slight increase up to values of 3829 and 3729 MPa for OES-plasticized PLA containing 1 and 3 phr, respectively. However, an increase of OES plasticizer leads to a decrease in Young's modulus to values of 3473 and 3445 MPa for samples containing 5 and 10 phr OES, respectively. Higher OES contents leads to slightly increased modulus in the 5-7% range (probably due to a decrease in elongation at break).

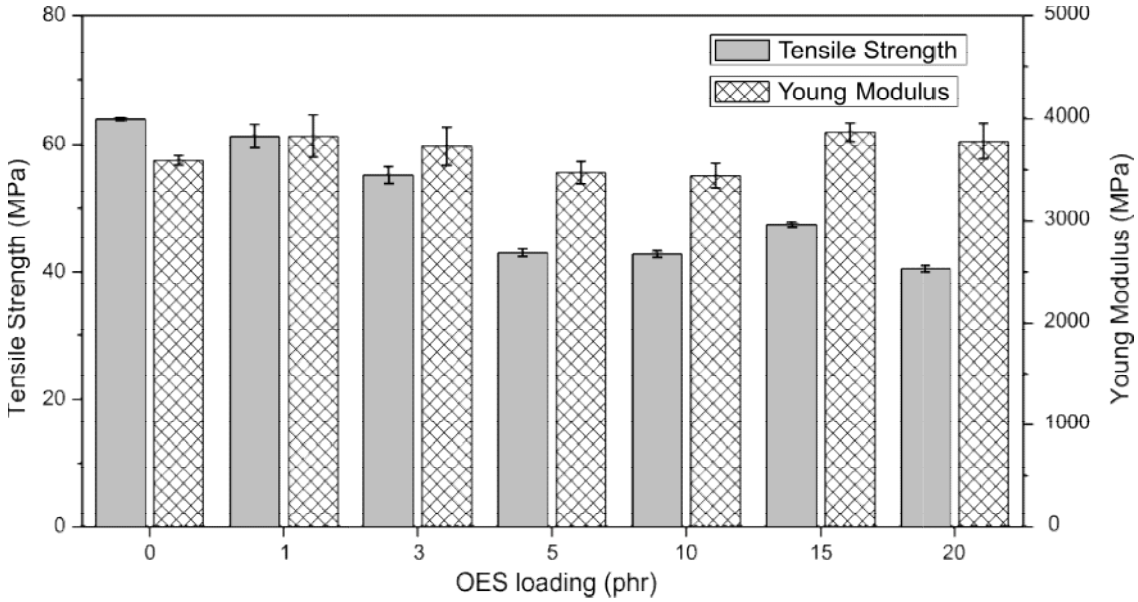

Figure III.3.2. Variation of tensile strength and Young's modulus of OES-plasticized PLA.

Regarding mechanical ductile properties, **Figure III.3.3** shows the plot evolution of the elongation at break from tensile tests and the impact-absorbed energy from Charpy's tests. We can see that for low OES plasticizer content (1 and 3 phr OES), both elongation at break and impact-absorbed energy are slightly increased. However, an increase in the plasticizer content up to 5 phr OES clearly enhances both properties. The elongation at break of unplasticized PLA is close to 8.6% and this is increased up to values of 40.6% (a percentage increase of almost 300%) for PLA-OES formulations containing 5 phr OES.

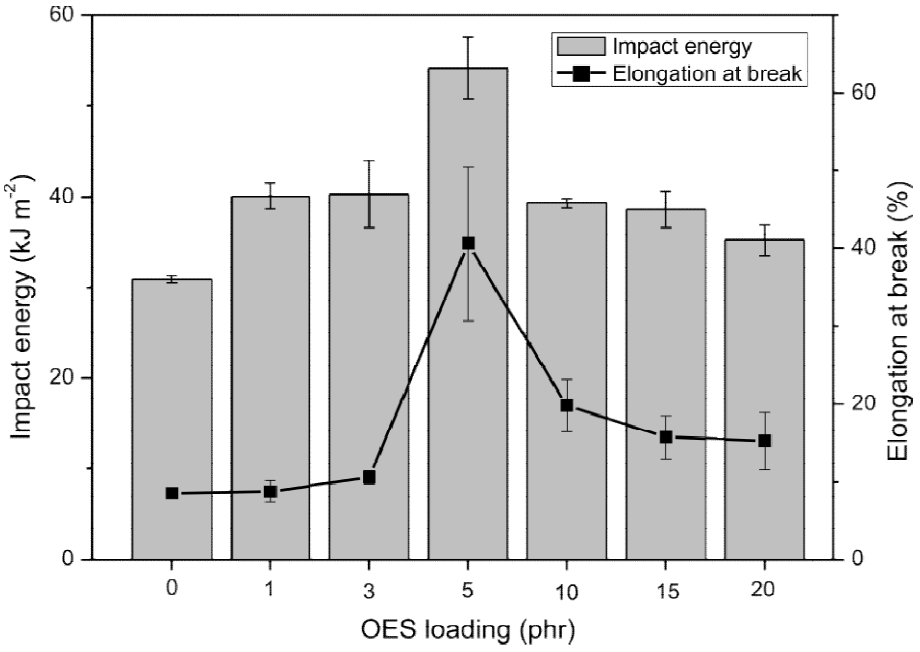

Figure III.3.3. Variation of elongation at break and impact-absorbed energy of OES-plasticized PLA.

Similar tendency can be found for impact absorbed energy as unplasticized PLA is characterized by a relatively low value around 30.9 kJ m^{-2} and this is increased up to (54.2 kJ m^{-2}) which represents a percentage increase of about 75%. OES contents higher than 5 phr leads to a decrease in both ductile properties to constant values of about 15% for elongation at break and 38 kJ m^{-2} for impact-absorbed energy. This fact could be related to a plasticizer saturation close to 5 phr OES. Higher OES plasticizer

content can lead to a phase separation that is responsible for a decrease in ductile properties.

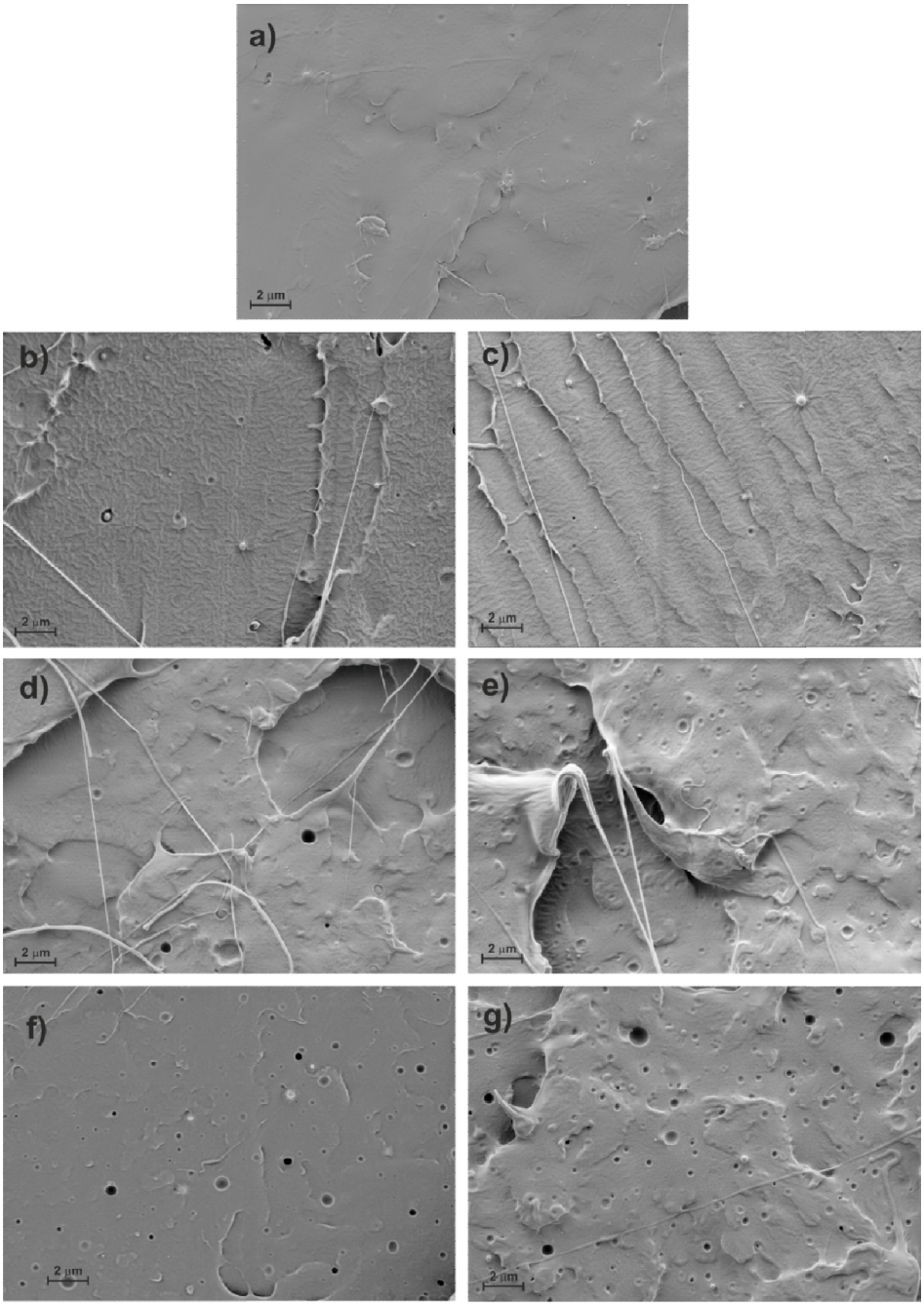

Figure III.3.4. FESEM images at 5000x of fractured samples from impact tests corresponding to **a** unplasticized PLA, **b** OES-plasticized PLA with 1 phr OES, **c** OES-plasticized PLA with 3 phr OES, **d** OES-plasticized PLA with 5 phr OES, **e** OES-plasticized PLA with 10 phr OES, **f** OES-plasticized PLA with 15 phr OES and **g** OES-plasticized PLA with 20 phr OES.

Surface analysis of fractured samples from impact tests was carried out by field emission scanning electron microscopy (FESEM). **Figure III.3.4a** shows the fracture surface of unplasticized PLA, which is mainly smooth and homogeneous with some voids related to porosity. In general, this is the typical surface appearance of a fractured brittle material. If we observe **Figure III.3.4b**, the appearance is different; this corresponds to OES-plasticized PLA with 1 phr OES. We can see typical fracture surface of a ductile material characterized by a rough surface, the presence of filaments due to plastic deformation, and the presence of voids (probably due to phase separation between the base polymer and excess plasticizer). **Figure III.3.4c-g** corresponds to fractured surfaces of OES-plasticized PLA with 3, 5, 10, 15, and 20 phr OES, respectively. As the amount of OES increases, we can clearly see increased presence of voids in the surface, especially over 5 phr OES. This indicates that PLA is saturated with the plasticizer and phase separation occurs. The excess plasticizer appears in the form of spherical shapes and this has a negative effect on overall mechanical properties as described previously (mainly in ductile properties).

Thermo-mechanical properties of OES-plasticized PLA.

Figure III.3.5 shows the plot evolution of the storage modulus (G´) and the phase angle (δ) as a function of temperature for unplasticized PLA and OES-plasticized PLA with different plasticizer contents. PLA is a semicrystalline polymer and as it can be observed in **Figure III.3.5b**, it shows relatively high G´ values around 1.3 GPa. In the glass transition temperature range, the storage modulus is remarkably reduced up to values of about 1.4 MPa and at about 84 ^{o}C the storage modulus increases again (up to 60 MPa) due to the cold crystallization process. OES-plasticized materials show similar behavior, but both the glass transition temperature (T_g) and the cold crystallization (T_{cc}) are moved to lower temperatures as the plasticizer enables chain mobility. The storage modulus (G´) of the OES-plasticized PLA samples starts at about 1.2 GPa and after the glass transition (a few degrees lower than in unplasticized PLA) decreases to 2 MPa. The cold crystallization in OES-plasticized PLA samples starts

before than unplasticized PLA; in particular, the cold crystallization process for samples containing 1 and 3 phr OES start at about 82 ºC but when the OES content increases (samples with 5, 10, 15 and 20 phr of OES) the cold crystallization starts at lower temperatures of about 73-74 ºC.

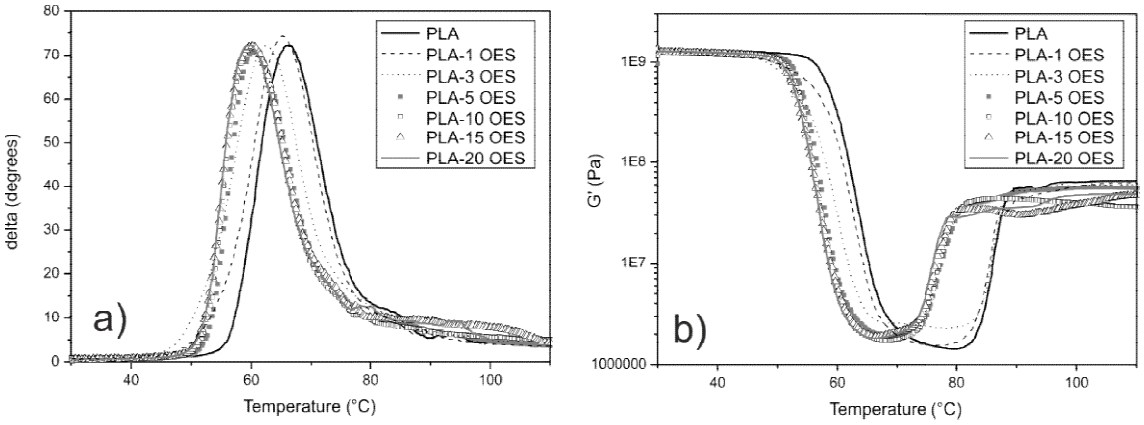

Figure III.3.5. Plot evolution of **a** the phase angle (δ) and **b** storage modulus (G') in terms of temperature for unplasticized PLA and OES-plasticized PLA with different OES loads.

The glass transition was estimated as the phase angle peak (or *tan δ* peak). As we can see in **Figure III.3.5a**, the T_g changes from 65.9 ºC for unplasticized PLA up to slightly lower values of 65.2 ºC (1 phr OES), 62.4 ºC (3 phr OES). As the OES content increases, the T_g is still lower with values of 60.4 ºC (5 phr OES), 60.1 ºC (10-15 phr OES) and 59.7 ºC (20 phr OES). This decrease in T_g is a clear evidence of the plasticizing effect that OES provides; nevertheless, no important changes are observed with increasing OES content over 5 phr thus indicating that PLA gets saturated with relatively low plasticizer contents.

Octyl epoxy stearate plasticizer has also effects on thermo-mechanical properties as observed in **Table III.3.2** that summarizes the values of the heat deflection temperature (HDT) and Vicat softening temperature (VST). The VST of unplasticized PLA (52.8 ºC) decreases up to values of 47.2 ºC for a plasticizer content of 1 phr and minimum values of 46 ºC are obtained for a plasticizer content of 20 phr. Variation of HDT is less accentuated with values of 47.6 ºC for unplasticized PLA and values in the 46.0 – 46.8 ºC for OES-plasticized PLA.

Table III.3.2. Results of the heat deflection temperature (HDT) and Vicat softening temperature (VST) of OES-plasticized PLA with different OES loads.

Sample	VST (ºC)	HDT (ºC)
PLA	52.8	47.6
PLA-1 OES	47.2	46.8
PLA-3 OES	47.6	46.6
PLA-5 OES	47.8	46.4
PLA-10 OES	47.0	46.0
PLA-15 OES	46.6	46.6
PLA-20 OES	46.0	46.6

Thermal properties of OES-plasticized PLA.

Differential scanning calorimetry (DSC) thermograms show three different thermal transitions as expected. The glass transition temperature (T_g) is located between 55 and 65 ºC; the exothermic peak located between 80 and 100 ºC corresponds to the cold crystallization process; and finally, the endothermic peak located at 170 – 175 ºC which corresponds to PLA melting. The decrease in T_g is a clear evidence of the plasticization effect. OES plasticizers allow chain mobility due to the free volume and reduced chain interactions [39]. In good agreement with previously described DMTA behavior, DSC shows a clear decrease in T_g with OES plasticizer. The glass transition temperature of the unplasticized PLA is close to 64.2 ºC as obtained by DSC. This value decreases up to values of 55.5 ºC for OES-plasticized PLA with 5 phr OES which is in total accordance with previous results. This also indicates that plasticizer saturation occurs for relatively low plasticizer content. Regarding the cold crystallization process, we observe a decrease in its typical temperatures (onset, peak, and endset). This indicates that OES plasticizer allows chain motion, which has a positive effect on cold crystallization [38]; these results are in total agreement with DMTA results which show a decrease of about 10 ºC in the cold crystallization process. In addition, if we compare the cold crystallization enthalpy (ΔH_{cc}) and the melt enthalpy (ΔH_m), we observe that ΔH_m is much higher than ΔH_{cc} thus indicating the semicrystalline nature of PLA at

room temperature. The presence of OES plasticizer leads to increased enthalpy difference (ΔH_m-ΔH_{cc}) thus indicating higher crystallinity.

Thermal stability of raw PLA and OES-plasticized PLA was evaluated by means of thermogravimetric analysis (TGA). **Table III.3.3** also shows some parameters related to the thermal degradation. In particular, the temperature at which a 5% weight loss occurs ($T_{5\%}$) and the maximum degradation rate temperature (T_{max}), are summarized. Although slight decrease in $T_{5\%}$ can be detected, in general, the thermal stability is not highly affected by the presence of OES plasticizer. In fact, as we can observe, a slight increase in T_{max} is detected but in both cases, the change is not significative.

Table III.3.3. Thermal parameters of unplasticized PLA and OES plasticized PLA obtained by differential scanning calorimetry (DSC) and thermogravimetric analysis (TGA) in terms of the plasticizer content.

OES (phr)	DSC					
	T_g (°C)	T_{cc} (°C)	ΔH_{cc} (J g^{-1})	T_m(°C)	ΔH_m (J g^{-1})	ΔH_m-ΔH_{cc}(J g^{-1})
0	64.2	98.4	18.2	175.0	40.8	22.6
1	64.5	98.5	15.9	174.3	40.2	24.3
3	61.9	94.0	22.6	174.3	47.9	25.3
5	55.5	85.9	14.2	173.6	41.5	27.3
10	57.0	83.9	11.1	171.2	37.9	26.8
15	57.5	83.8	9.2	173.6	37.7	28.5
20	56.4	81.5	10.7	170.4	41.9	31.2

OES (phr)	TGA	
	$T_{5\%}$(°C)	T_{max}(°C)
0	336.9	363.5
1	338.3	373.4
3	336.7	373.3
5	329.2	368.4
10	333.2	371.7
15	327.5	366.6
20	331.9	368.3

Oxygen permeability measurement of OES-plasticized PLA films.

As optimum balanced properties were obtained for an OES content of 5 phr, this formulations was selected for an in depth study in the film form. The oxygen transmission rate (OTR) of neat is around 44.4 ± 0.9 $cm^3 \cdot mm \cdot m^{-2} \cdot day^{-1}$ [40, 41], while the OTR for the OES-plasticized PLA film is 23.2 ± 0.2 $cm^3 \cdot mm \cdot m^{-2} \cdot day^{-1}$. The lower oxygen transmission rate is due to increased crystallinity. As we have previously observed by dynamic mechanical thermal analysis (DMTA) and differential scanning calorimetry (DSC), presence of plasticizer leads to increased polymer chain mobility and this leads to increased crystallinity. In general, the addition of plasticizers to polymers leads to an increase in gas permeability due to the free volume they provide. However, in this case, this phenomenon is overlapped with the decreased gas permeability effect because of the increased crystallinity being the overall result a decrease in gas permeation properties.

Surface wettability of OES-plasticized PLA films.

The surface wetting properties of 5 OES-plasticized PLA films containing 5 phr OES were investigated by water contact angle measurement. By adding 5 phr OES into the PLA matrix, the water contact angle increased from 58º to approximately 66º showing an increase in hydrophobicity. It is evident that the contact angle of plasticized PLA is higher than neat PLA as the plasticizer is an oil type with remarked hydrophobicity. Therefore, PLA films containing 5 phr OES are also expected to have higher resistance to water adsorption than neat PLA film. For these reasons, PLA films plasticized with OES can offer attracting uses in the packaging industry.

Conclusions.

In the present work, thermal and mechanical properties of PLA plasticized with octyl epoxy stearate (OES) were evaluated. Samples with 5 phr of octyl epoxy stearate showed the best results in terms of ductile properties such as elongation and impact properties. If compared to unplasticized PLA, OES addition leads to a percentage increase in elongation at break of about 300 and 75% regarding impact-absorbed energy. This behavior validated by surface analysis of fractured samples by FESEM images with clear evidences of plastic deformation in OES-plasticized PLA materials.

Moreover, DSC results showed that OES causes a decrease in the T_g of the PLA; in particular, the sample containing 5 phr of OES showed a T_g of 55.5 ^oC, while unplasticized PLA shows a T_g located at 64.2 ^oC. Additionally, the cold crystallization process moves to lower temperatures when OES is added to PLA, more than 10 ^oC for the plasticized samples with 5 phr OES. From DMTA results, a decrease in T_g and cold crystallization is also observed, which is consistent with the DSC results. Furthermore, oxygen permeability and wettability tests on PLA films plasticized with 5 phr OES showed attracting properties for the packaging industry as the oxygen transmission rate (OTR) changed from 44.4 $cm^3 \cdot mm \cdot m^{-2} \cdot day^{-1}$ for neat PLA to 23.2 $cm^3 \cdot mm \cdot m^{-2} \cdot day^{-1}$ for sample of PLA plasticized with 5 phr OES. In addition, OES-plasticized PLA is more hydrophobic than neat PLA which has a positive effect on water resistance.

We can conclude that octyl epoxy stearate (OES) can be used as an effective plasticizer for PLA and good results are obtained for relatively low OES load of about 5 phr. This fact could be related to a plasticizer saturation close to 5 phr OES. Higher OES plasticizer content can lead to a phase separation that is responsible for a decrease in ductile properties due to an antiplasticization process. Octyl epoxy stearate represents an environmentally friendly material that can positively contribute to obtain high environmental efficient PLA formulations for industrial applications.

Acknowledgements.

This research was supported by the Ministry of Economy and Competitiveness -MINECO, Ref: MAT2014-59242-C2-1-R. Authors also thank to "Conselleria d'Educació, Cultura i Esport" - Generalitat Valenciana, Ref: GV/2014/008 for financial support.

References.

1. Alam, J., Alam, M., Raja, M., Abduljaleel, Z., and Dass, L.A., *MWCNTs-Reinforced Epoxidized Linseed Oil Plasticized Polylactic Acid Nanocomposite and Its Electroactive Shape Memory Behaviour*. International Journal of Molecular Sciences, 2014. **15**(11): p. 19924-19937.

2. Arrieta, M.P., Fortunati, E., Dominici, F., Lopez, J., and Kenny, J.M., *Bionanocomposite films based on plasticized PLA-PHB/cellulose nanocrystal blends*. Carbohydrate Polymers, 2015. **121**: p. 265-275.

3. Dharmalingam, S., Hayes, D.G., Wadsworth, L.C., Dunlap, R.N., DeBruyn, J.M., Lee, J., and Wszelaki, A.L., *Soil Degradation of Polylactic Acid/Polyhydroxyalkanoate-Based Nonwoven Mulches*. Journal of Polymers and the Environment, 2015. **23**(3): p. 302-315.

4. Lin, C.-M., Lin, C.-H., Huang, Y.-T., Lou, C.-W., and Lin, J.-H., *Mechanical and Electrical Properties of the Polyaniline (PANI)/Polylactic acid (PLA) Nonwoven Fabric*, in Machine Design and Manufacturing Engineering II, Pts 1 and 2, K. Kida, Editor. 2013. p. 1074-1077.

5. Serafini Immich, A.P., Lis Arias, M., Carreras, N., Luis Boemo, R., and Tornero, J.A., *Drug delivery systems using sandwich configurations of electrospun poly(lactic acid) nanofiber membranes and ibuprofen*. Materials Science & Engineering C-Materials for Biological Applications, 2013. **33**(7): p. 4002-4008.

6. Llorens, E., Calderon, S., del Valle, L.J., and Puiggali, J., *Polybiguanide (PHMB) loaded in PLA scaffolds displaying high hydrophobic, biocompatibility and antibacterial properties*. Materials Science & Engineering C-Materials for Biological Applications, 2015. **50**: p. 74-84.

7. Nainar, S.M.M., Begum, S., Ansari, M.N.M., Hoque, M.E., Aini, S.S., Ng, M.H., and Ruszymah, B.H.I., *Effect of compatibilizers on in vitro biocompatibility of PLA-HA bioscaffold*. Bioinspired Biomimetic and Nanobiomaterials, 2014. **3**(4): p. 208-216.

8. Huang, R., Zhu, X., Tu, H., and Wan, A., *The crystallization behavior of porous poly(lactic acid) prepared by modified solvent casting/particulate leaching technique for potential use of tissue engineering scaffold*. Materials Letters, 2014. **136**: p. 126-129.

9. Yesid Gomez-Pachon, E., Manuel Sanchez-Arevalo, F., Sabina, F.J., Maciel-Cerda, A., Montiel Campos, R., Batina, N., Morales-Reyes, I., and Vera-Graziano, R., *Characterization and modelling of the elastic properties of poly(lactic acid) nanofibre scaffolds*. Journal of Materials Science, 2013. **48(**23): p. 8308-8319.

10. Zhang, J., Yin, H.-M., Hsiao, B.S., Zhong, G.-J., and Li, Z.-M., *Biodegradable poly(lactic acid)/hydroxyl apatite 3D porous scaffolds using high-pressure molding and salt leaching*. Journal of Materials Science, 2014. **49**(4): p. 1648-1658.

11. Armentano, I., Fortunati, E., Burgos, N., Dominici, F., Luzi, F., Fiori, S., Jimenez, A., Yoon, K., Ahn, J., Kang, S., and Kenny, J.M., *Processing and characterization of plasticized PLA/PHB blends for biodegradable multiphase systems*. Express Polymer Letters, 2015. **9**(7): p. 583-596.

12. Patricia Arrieta, M., del Mar Castro-Lopez, M., Rayon, E., Fernando Barral-Losada, L., Manuel Lopez-Vilarino, J., Lopez, J., and Victoria Gonzalez-Rodriguez, M., *Plasticized Poly(lactic acid)-Poly(hydroxybutyrate) (PLA-PHB) Blends Incorporated with Catechin Intended for Active Food-Packaging Applications*. Journal of Agricultural and Food Chemistry, 2014. **62**(41): p. 10170-10180.

13. He, Y., Hu, Z., Ren, M., Ding, C., Chen, P., Gu, Q., and Wu, Q., *Evaluation of PHBHHx and PHBV/PLA fibers used as medical sutures*. Journal of Materials Science-Materials in Medicine, 2014. **25**(2): p. 561-571.

14. Vieira, A.C., Vieira, J.C., Ferra, J.M., Magalhaes, F.D., Guedes, R.M., and Marques, A.T., *Mechanical study of PLA-PCL fibers during in vitro degradation*. Journal of the Mechanical Behavior of Biomedical Materials, 2011. **4**(3): p. 451-460.

15. Zhang, K.-y., Ran, X.-h., Zhuang, Y.-g., Yao, B., and Dong, L.-s., *Blends of Poly(lactic acid) with Thermoplastic Acetylated Starch*. Chemical Research in Chinese Universities, 2009. **25**(5): p. 748-753.

16. Chieng, B.W., Ibrahim, N.A., Yunus, W.M.Z.W., and Hussein, M.Z., *Plasticized Poly(lactic acid) with Low Molecular Weight Poly(ethylene glycol): Mechanical, Thermal, and Morphology Properties*. Journal of Applied Polymer Science, 2013. **130**(6): p. 4576-4580.

17. Yu, Y., Cheng, Y., Ren, J., Cao, E., Fu, X., and Guo, W., *Plasticizing effect of poly(ethylene glycol)s with different molecular weights in poly(lactic acid)/starch blends*. Journal of Applied Polymer Science, 2015. **132**(16).

18. Nazari, T. and Garmabi, H., *Polylactic acid/polyethylene glycol blend fibres prepared via melt electrospinning: effect of polyethylene glycol content*. Micro & Nano Letters, 2014. **9**(10): p. 686-690.

19. Piorkowska, E., Kulinski, Z., Galeski, A., and Masirek, R., *Plasticization of semicrystalline poly(L-lactide) with poly(propylene glycol)*. Polymer, 2006. **47**(20): p. 7178-7188.

20. Burgos, N., Martino, V.P., and Jimenez, A., *Characterization and ageing study of poly(lactic acid) films plasticized with oligomeric lactic acid*. Polymer Degradation and Stability, 2013. **98**(2): p. 651-658.

21. Dobircau, L., Delpouve, N., Herbinet, R., Domenek, S., Le Pluart, L., Delbreilh, L., Ducruet, V., and Dargent, E., *Molecular Mobility and Physical Ageing of Plasticized Poly(lactide)*. Polymer Engineering and Science, 2015. **55**(4): p. 858-865.

22. Hassouna, F., Raquez, J.-M., Addiego, F., Toniazzo, V., Dubois, P., and Ruch, D., *New development on plasticized poly(lactide): Chemical grafting of citrate on PLA by reactive extrusion*. European Polymer Journal, 2012. **48**(2): p. 404-415.

23. Tsou, C.-H., Suen, M.-C., Yao, W.-H., Yeh, J.-T., Wu, C.-S., Tsou, C.-Y., Chiu, S.-H., Chen, J.-C., Wang, R.Y., Lin, S.-M., Hung, W.-S., De Guzman, M., Hu, C.-C., and Lee, K.-R., *Preparation and Characterization of Bioplastic-Based Green Renewable Composites from Tapioca with Acetyl Tributyl Citrate as a Plasticizer*. Materials, 2014. **7**(8): p. 5617-5632.

24. Jing, J., Qiao, Q.a., Jin, Y., Ma, C., Cai, H., Meng, Y., Cai, Z., and Feng, D., *Molecular and Mesoscopic Dynamics Simulations on the Compatibility of PLA/Plasticizer Blends*. Chinese Journal of Chemistry, 2012. **30**(1): p. 133-138.

25. Ljungberg, N. and Wesslen, B., *Tributyl citrate oligomers as plasticizers for poly (lactic acid): thermo-mechanical film properties and aging*. Polymer, 2003. **44**(25): p. 7679-7688.

26. Notta-Cuvier, D., Murariu, M., Odent, J., Delille, R., Bouzouita, A., Raquez, J.-M., Lauro, F., and Dubois, P., *Tailoring Polylactide Properties for Automotive Applications: Effects of Co-Addition of Halloysite Nanotubes and Selected Plasticizer*. Macromolecular Materials and Engineering, 2015. **300**(7): p. 684-698.

27. Carbonell-Verdu, A., Bernardi, L., Garcia-Garcia, D., Sanchez-Nacher, L., and Balart, R., *Development of environmentally friendly composite matrices from epoxidized cottonseed oil*. European Polymer Journal, 2015. **63**: p. 1-10.

28. Samper, M.D., Fombuena, V., Boronat, T., Garcia-Sanoguera, D., and Balart, R., *Thermal and Mechanical Characterization of Epoxy Resins (ELO and ESO) Cured with Anhydrides*. Journal of the American Oil Chemists Society, 2012. **89**(8): p. 1521-1528.

29. Samper, M.D., Petrucci, R., Sanchez-Nacher, L., Balart, R., and Kenny, J.M., *Properties of composite laminates based on basalt fibers with epoxidized vegetable oils*. Materials & Design, 2015. **72**: p. 9-15.

30. Samper, M.D., Petrucci, R., Sanchez-Nacher, L., Balart, R., and Kenny, J.M., *New environmentally friendly composite laminates with epoxidized linseed oil (ELO) and slate fiber fabrics*. Composites Part B-Engineering, 2015. **71**: p. 203-209.

31. Bueno-Ferrer, C., Garrigos, M.C., and Jimenez, A., *Characterization and thermal stability of poly(vinyl chloride) plasticized with epoxidized soybean oil for food packaging*. Polymer Degradation and Stability, 2010. **95**(11): p. 2207-2212.

32. Bueno-Ferrer, C., Jimenez, A., and Garrigos, M.C., *Migration analysis of epoxidized soybean oil and other plasticizers in commercial lids for food packaging by gas chromatography-mass spectrometry*. Food Additives and Contaminants Part a-Chemistry Analysis Control Exposure & Risk Assessment, 2010. **27**(10): p. 1469-1477.

33. Fenollar, O., Garcia-Sanoguera, D., Sanchez-Nacher, L., Lopez, J., and Balart, R., *Effect of the epoxidized linseed oil concentration as natural plasticizer in vinyl plastisols*. Journal of Materials Science, 2010. **45**(16): p. 4406-4413.

34. Fenollar, O., Garcia-Sanoguera, D., Sanchez-Nacher, L., Lopez, J., and Balart, R., *Characterization of the curing process of vinyl plastisols with epoxidized linseed oil as a natural-based plasticizer*. Journal of Applied Polymer Science, 2012. **124**(3): p. 2550-2557.

35. Semsarzadeh, M.A., Mehrabzadeh, M., and Arabshahi, S.S., *Mechanical and thermal properties of the plasticized PVC-ESBO*. Iranian Polymer Journal, 2005. **14**(9): p. 769-773.

36. Chieng, B.W., Ibrahim, N.A., Then, Y.Y., and Loo, Y.Y., *Epoxidized Vegetable Oils Plasticized Poly(lactic acid) Biocomposites: Mechanical, Thermal and Morphology Properties*. Molecules, 2014. **19**(10): p. 16024-16038.

37. Prempeh, N., Li, J., Liu, D., Das, K., Maiti, S., and Zhang, Y., *Plasticizing Effects of Epoxidized Sun Flower Oil on Biodegradable Polylactide Films: A Comparative Study*. Polymer Science Series A, 2014. **56**(6): p. 856-863.

38. Santos, E.F., Oliveira, R.V.B., Reiznautt, Q.B., Samios, D., and Nachtigall, S.M.B., *Sunflower-oil biodiesel-oligoesters/polylactide blends: Plasticizing effect and ageing*. Polymer Testing, 2014. **39**: p. 23-29.

39. Li, H. and Huneault, M.A., *Effect of nucleation and plasticization on the crystallization of poly(lactic acid)*. Polymer, 2007. **48**(23): p. 6855-6866.

40. Arrieta, M.P., Lopez, J., Ferrandiz, S., and Peltzer, M.A., *Characterization of PLA-limonene blends for food packaging applications*. Polymer Testing, 2013. **32**(4): p. 760-768.

41. Arrieta, M.P., Samper, M.D., Lopez, J., and Jimenez, A., *Combined Effect of Poly(hydroxybutyrate) and Plasticizers on Polylactic acid Properties for Film Intended for Food Packaging*. Journal of Polymers and the Environment, 2014. **22**(4): p. 460-470.

J Mater Sci

Plasticizing effect of biobased epoxidized fatty acid esters on mechanical and thermal properties of poly(lactic acid)

J. M. Ferri[1], M. D. Samper[1,*], D. García-Sanoguera[1], M. J. Reig[1], O. Fenollar[1], and R. Balart[1]

[1] Instituto de Tecnología de Materiales (ITM), Universitat Politècnica de València (UPV), Plaza Ferrándiz y Carbonell s/n, 03801 Alcoy, Alicante, Spain

Received: 23 November 2015
Accepted: 15 February 2016

ABSTRACT

Poly(lactic acid), PLA, is a polyester that can be produced from lactic acid derived from renewable resources. This polymer offers attracting uses in packaging industry due to its biodegradability and high tensile strength. However, PLA is quite brittle, which limits its applications. To overcome this drawback, PLA was plasticized with epoxy-type plasticizer derived from a fatty acid, octyl epoxy stearate (OES) at different loadings (1, 3, 5, 10, 15, and 20 phr). The addition of OES decreases the glass transition temperature and provides a remarkable increase in elongation at break and impact-absorbed energy. Plasticizer saturation occurs at relatively low concentrations of about 5 phr OES; higher concentration leads to phase separation as observed by field emission scanning electron microscopy (FESEM). Optimum balanced mechanical properties are obtained at relatively low concentrations of OES (5 phr), thus indicating the usefulness of this material as environmentally friendly plasticizer for PLA industrial formulations.

Chapter III.4

Chapter III.4. The effect of maleinized linseed oil as biobased plasticizer in poly(lactic acid)-based formulations

“The effect of maleinized linseed oil as biobased plasticizer in poly(lactic acid)-based formulations”

J.M. Ferri, D. Garcia-Garcia, N. Montanes, O. Fenollar, R. Balart

Instituto de Tecnología de Materiales (ITM)

Universitat Politècnica de València (UPV)

Plaza Ferrandiz y Carbonell 1, 03801, Alcoy, Alicante (Spain)

Polymer International 66: 882-891 (2017)

Abstract.

The use of maleinized linseed oil (MLO) as a potential biobased plasticizer for poly(lactic acid) (PLA) industrial formulations with improved toughness was evaluated. MLO content varied in the range 0 – 20 phr (parts by weight of MLO per hundred parts by weight of PLA). Mechanical, thermal and morphological characterizations were used to assess the potential of MLO as an environmentally friendly plasticizer for PLA formulations. Dynamic mechanical thermal analysis and differential scanning calorimetry revealed a noticeable decrease in the glass transition temperature of about 6.5 ºC compared to neat PLA. In addition, the cold crystallization process was favoured with MLO content due to the increased chain mobility that the plasticizer provides. PLA toughness was markedly improved in formulations with 5 phr MLO, while maximum elongation at break was obtained for PLA formulations plasticized with MLO content in the range 15 – 20 phr. Scanning electron microscopy revealed evidence of plastic deformation. Nevertheless, phase separation was detected in plasticized PLA formulations with high MLO content (above 15-20 phr MLO), which had a negative effect on overall toughness.

Keywords: poly(lactic acid); PLA; plasticizers; environmentally friendly; maleinized linseed oil (MLO); anti-plasticization effects

Introduction.

The increasing concern about the environment and sustainable development is currently leading the search and development of new materials. Today, a wide variety of biobased and/or biodegradable polymers with potential use at an industrial scale can be obtained from renewable resources [1]. These polymers could be used as environmentally friendly solutions as against conventional petroleum-based and non-biodegradable polymers in blend formulations [2], disposable products [3, 4], medical devices [5], packaging [6, 7], green composites [8-13], etc. It is worth noting the increasing use of aliphatic polyesters [14], polysaccharides [15] and protein-derived polymers [16, 17]. Despite the wide variety of biobased polymers, poly(lactic acid) (PLA) is one of the most promising polymers due to its excellent balance between mechanical, barrier and processing properties, and an increasingly competitive price. It is obtained from lactic acid derived from several cereals and tubers, mainly from corn, wheat, beetroot, potato and other starch-rich products. Its biodegradability in natural media makes it the ideal choice for a wide range of disposable products that can undergo disintegration by hydrolysis and enzymatic degradation in controlled conditions (moisture, temperature, bacterial growth, etc.) [18-20]. Moreover, PLA is characterized by high biocompatibility and a good balance of mechanical properties, thus widening its uses in the medical sector [21], such as in resorbable interference screws and prostheses subjected to moderate mechanical stresses [22]. In addition to this, its relatively good resistance to moisture and fats, together with overall balanced barrier properties to flavours and odours, makes PLA a good candidate for the food packaging industry. One important drawback of PLA is its extremely high stiffness, which leads to high fragility, and this fact restricts some engineering uses that require high toughness behaviour. To overcome this drawback, various approaches have been explored in the last few years. New flexible copolyesters have been investigated as toughened alternatives to brittle PLA formulations [23, 24]. In these works, the results showed increased elongation at break values and a marked improvement in ductile properties. A wide variety of conventional plasticizers have been reported to greatly increase PLA ductility [25], but the potential toxic risks associated to some of these

plasticizers, restrict their use in some sectors such as food packaging, medical devices, toys, etc. For this reason, new plasticizers are continually being demanded by industry with the aim of reducing the toxic risk related to plasticizer migration [26, 27].

Vegetable oils such as those obtained from linseed, rape, soybean and cottonseed, among others, offer a natural source of chemicals for the polymer industry [28, 29]. They can readily be converted into their corresponding epoxidized oils by epoxidation, leading to materials with potential use as biobased plasticizers and matrices for green composites. Several epoxidized vegetable oils such as epoxidized linseed oil (ELO) [30], epoxidized soybean oil (ESBO), epoxidized castor oil (ECO), epoxy octyl stearate (EOS) [31] and epoxidized cottonseed oil (ECSO) [32-36] have been reported as environmentally friendly plasticizers for a wide variety of polymers [32, 37]. The use of monomeric and polymeric plasticizers has also been reported in the last decade. Monomeric plasticizers such as acetylbutyl ricinoleate (ABR), acetyltributyl citrate (ATBC), ricinoleic acid, adipate 2-ethylhexyl (DOA), diisodecyl adipate (DIDA), octyl oleate, octyl trimellitate (TMO), methyl methacrylate (MMA) and glycidyl methacrylate (GMA), among others [14, 16, 38], have given interesting results in PLA plasticization. Also, several polymeric plasticizers such as aliphatic polyesters from dicarboxylic acids, polypropylene glycol adipate, thermoplastic starch (TPS), polycaprolactone (PCL), etc., [2, 39-44] have proved their efficiency in plasticizing PLA formulations.

The use of plasticizers from vegetable oils is a cost-effective alternative [45, 46]. Unmodified vegetable oils are not suitable for most polymers due to the lack of compatibility. For example, the solubility parameter for soybean oil has been reported to be close to 16 $MPa^{1/2}$,[47] whilst some epoxidized compounds derived from soybean oil achieve a solubility parameter of 19-19.5 $MPa^{1/2}$ [48]. Considering that the solubility parameter of PLA is between 19.5 and 20.5 $MPa^{1/2}$ [49], chemically modified vegetable oils are preferable as their corresponding solubility parameters are closer compared to those of unmodified vegetable oils. For this reason, the majority of vegetable oil-based plasticizers consist of chemically modified vegetable oils with increased polarity to achieve improved interactions with polymers. The final performance of a vegetable oil

can be tailored to specific properties by chemical modification [50]. Prempeh et al. studied the effect of epoxidized sunflower oil (ESFO) and ESBO on ductile properties of PLA [45]. Our previous study revealed that addition of 5 phr epoxy octyl stearate to PLA led to a marked increase in elongation at break by 300% compared to neat PLA; the toughness was also improved by 75% [31]. Finally, Chieng et al. [46] combined various epoxidized vegetable oils, i.e. epoxidized palm oil (EPO) and ESBO, and reported synergistic effects on ductile properties.

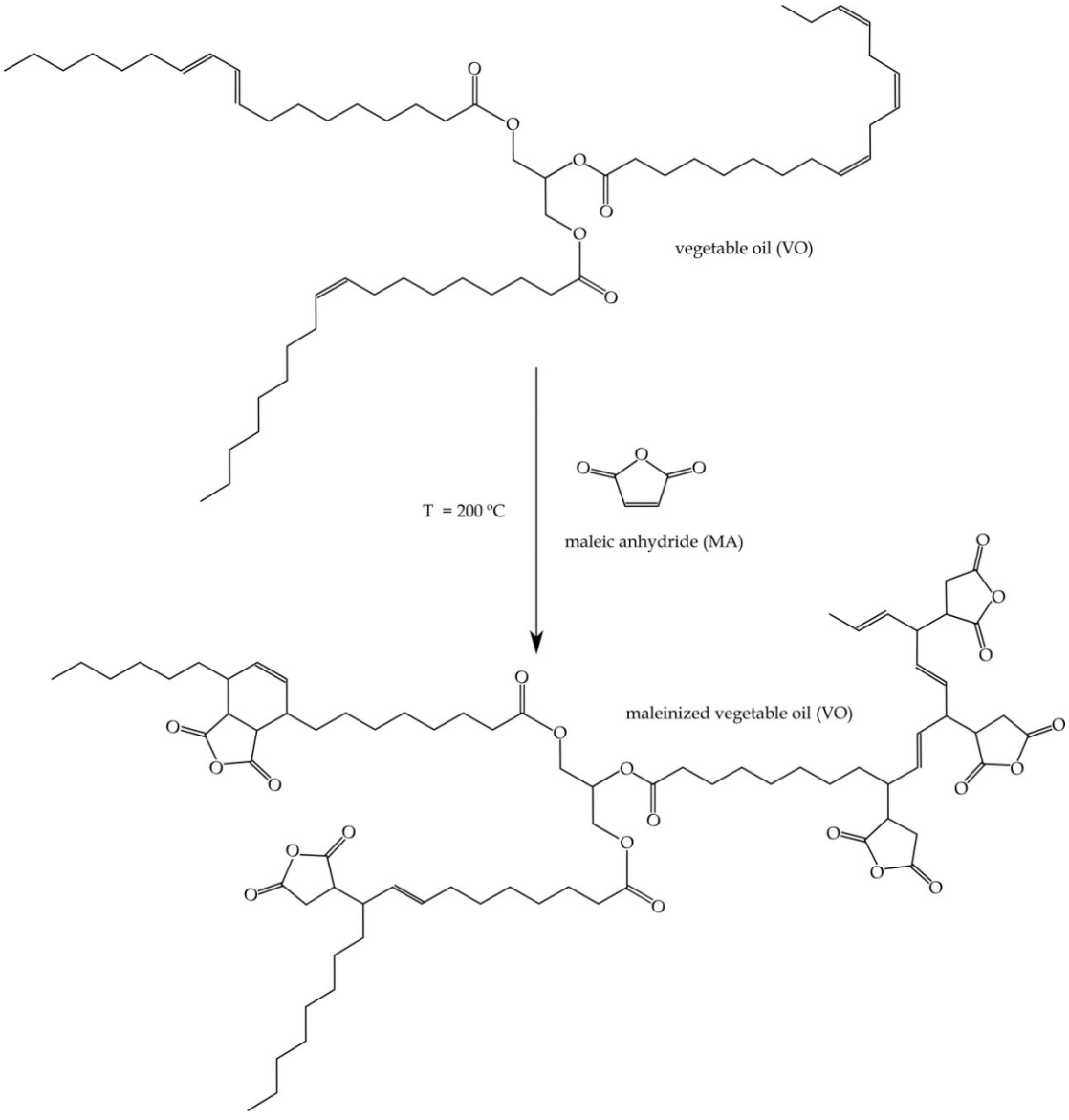

Figure III.4.1. Scheme of the maleinization process of linseed oil by Diels-Alder and "*ene*" reactions.

In addition to epoxidized vegetable oils, new plasticizers derived from vegetable oils are being investigated. Maleinization represents an interesting and easy way to chemically modify a vegetable oil. In such thermochemical process, maleic anhydride is chemically attached to a triglyceride by "*ene*" reactions, and, in some cases, by Diels-Alder condensation (in the case of conjugated unsaturations in a fatty acid) as it can be seen in **Figure III.4.1**. Maleinized vegetable oils and other petrochemical oils are widely used in the field of cosmetics [51], detergents [52], cleaning products [53], lubricants [54], coatings [55], etc. [56, 57].

The reactivity of maleinized vegetable oils is much higher than that of unmodified vegetable oils due to maleic anhydride polarity. Recently, this has been reported to provide good compatibilizing and chain extension effects in immiscible polymer blends such as those from PLA and thermoplastic starch [58]. Wiyono et al. reported that chemical modification of pimaric rosins with maleic anhydride and fumaric acid led to materials with potential use as fruit coatings with good antioxidant and barrier properties [59].

In addition, maleinized vegetable oils offer high thermal stability and can be subjected to temperatures up to 300 ^{o}C without any degradation. The cyclic anhydride functionality can readily react with hydroxyl groups to form monoesters. This feature has been widely exploited in the paper industry to provide hydrophobizing properties by using various chemicals such as alkenyl succinic anhydrides [60].

This reaction could be conducted with polymers with terminal hydroxyl groups as is the case of biobased polyesters. Maleic anhydride could react with hydroxyl groups to provide a plasticization effect combined to a chain extension phenomenon due to the multifunctionality of maleinized vegetable oil as shown in **Figure III.4.2**.

The work presented here explored the potential of maleinized linseed oil (MLO) as a bio-derived plasticizer for PLA formulations with improved toughness. The effect of MLO content on the mechanical properties of PLA formulations was evaluated using standard tests: tensile, impact and hardness. The thermal stabilization effect was assessed using thermal analysis: DSC and TGA. Dynamic properties were studied

using dynamic mechanical thermal analysis (DMTA) and the morphology of the formulations was observed using field emission SEM (FESEM).

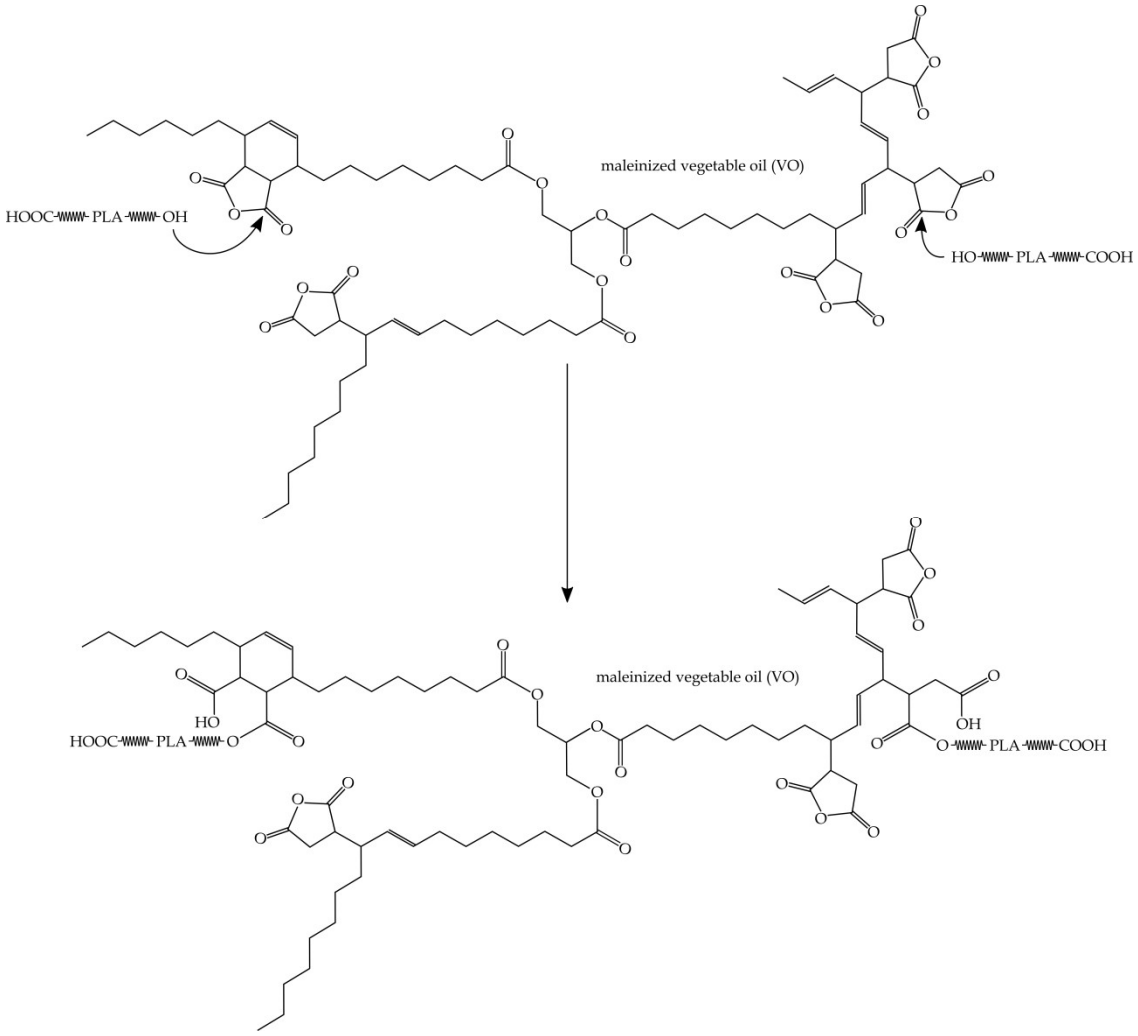

Figure III.4.2. Proposed mechanism for a chain extension effect that MLO could provide by reaction with hydroxyl terminal groups in PLA.

Experimental.

Materials.

PLA (commercial grade IngeoTM Biopolymer 6201D) was supplied by NatureWorks LLC (Minnetonka, USA). This PLA grade contains around 2% D-lactic acid. Its density is 1.24 g cm^{-3} and its melt flow index is between 15 and 30 g $(10\ min)^{-1}$ at 210 ^{o}C. MLO (commercial grade Veomer Lin) was supplied by Vandeputte (Mouscron, Belgium). Its viscosity at 20 ^{o}C is 10 dPa s and its acid value is 105-130 mg KOH g^{-1} as a consequence of the maleinization process. Typical acid values of unmodified linseed oil are lower than 1 mg KOH g^{-1} and this value is markedly increased in the corresponding maleinized oil due to presence of attached cyclic anhydride groups.

Preparation of PLA formulations plasticized with MLO.

Four different PLA formulations were manufactured with MLO as an environmentally friendly plasticizer (**Table III.4.1**). The MLO content varied in the range 0-20 phr (parts by weight of MLO with respect to 100 parts by weight of PLA). As PLA is rather sensitive to moisture, it was dried overnight at 60 ^{o}C in an air-circulating oven. The procedure for sample preparation was as follows. Initially, the required amounts of both PLA and MLO were weighed and mechanically pre-mixed in a zipper bag. After this stage, the mixture was extruded in a twin-screw co-rotating extruder (with diameter D of 25 mm and L/D ratio of 24) from DUPRA SL (Castalla, Spain) with a temperature profile of 165 ^{o}C (feed), 170 ^{o}C, 172.5 ^{o}C and 175 ^{o}C (die), and subsequently pelletized after cooling. Further processing was carried out by injection molding with a Meteor 270/75 from Mateu & Solé (Barcelona, Spain) at an injection temperature of 175 ^{o}C and normalized samples for testing were obtained.

Table III.4.1. Summary of compositions and labelling of PLA formulations plasticized with MLO.

Poly (lactic acid)-PLA, phr	Maleinized linseed oil (MLO), phr	Code
100	-	PLA
100	5	PLA/5MLO
100	10	PLA/10MLO
100	15	PLA/15MLO
100	20	PLA/20MLO

Mechanical characterization of PLA formulations plasticized with MLO.

The effect of MLO content on mechanical properties was studied using standardized tensile, flexural, hardness and impact tests. Tensile and flexural tests were conducted with an Ibertest ELIB 30 universal test machine from SAE Ibertest (Madrid, Spain) at room temperature. The load cell was 5 kN and the crosshead rate was set to 10 mm min^{-1} for both tests as recommended by the ISO 527-5 and ISO 178 standards for tensile and flexural characterization, respectively. Tests were carried out on five different specimens and the average values of the main parameters were calculated. Additionally, for a correct determination of the Young's modulus, an axial extensometer was used. Shore D hardness values were obtained using a Shore D model 673-D durometer from Instrumentos J Bot SA (Barcelona, Spain) as recommended by the ISO 868 standard. The impact-absorbed energy was characterized using a 6 J Charpy pendulum from Metrotec SA (San Sebastián, Spain) on unnotched samples following the ISO 179:1993 standard. Five different measurements of each property were obtained and averaged.

Morphology of PLA formulations plasticized with MLO.

A high-resolution FESEM instrument (Zeiss ULTRA55 from Oxford Instruments, Oxford, UK) operated at an accelerating voltage of 2 kV was used to characterize the surface morphology. Fractured samples from impact tests were subjected to a metallization process in vacuum conditions with a high-vacuum sputter (EM MED020 from Leica Microsystems, Wetzlar, Germany).

Thermal analysis of PLA formulations plasticized with MLO.

Thermal transitions of PLA and PLA formulations plasticized with various MLO loads were obtained using DSC with a Mettler Toledo DSC 821 calorimeter (Schwerzenbach, Switzerland). The thermal programme consisted of a heating ramp from 30 to 350 ^{o}C at a heating rate of 10 ^{o}C min^{-1} in nitrogen atmosphere with a constant flow rate of 66 mL min^{-1}. The percentage crystallinity of PLA and plasticized formulations was calculated with the following equation:

$$\boldsymbol{X_c}\ (\%) = \frac{\boldsymbol{\Delta H_m - \Delta H_{cc}}}{\boldsymbol{w\ \Delta H_m^0}} 100 \qquad \text{(Equation 1)}$$

where ΔH_m and ΔH_{cc} represent the experimental melt and cold crystallization enthalpies, respectively, and w is the weight fraction of PLA. ΔH_m^0 is the melt enthalpy for a theoretical fully crystalline PLA structure, and was assumed to be 93 J g^{-1} as reported in the literature [20].

Thermal degradation/decomposition of PLA and PLA formulations plasticized with MLO was assessed using TGA with a TGA/SDTA 851 thermobalance from Mettler Toledo (Schwerzenbach, Switzerland). Samples with an average weight of 8-10 mg were subjected to a heating ramp from 30 to 500 ^{o}C at a heating rate of 20 ^{o}C min^{-1} in nitrogen atmosphere with a constant flow of 66 mL min^{-1}.

DMTA in torsion mode of neat PLA and plasticized PLA formulations was carried out in an AR G2 oscillatory rheometer from TA Instruments (New Castle, USA), equipped with a clamp accessory for solid samples. Rectangular samples of dimensions 40x10x4 mm^3 were subjected to a temperature ramp from 30 to 130 ^oC at a heating rate of 2^oC min^{-1}. The maximum deformation (γ) was 0.1% and all samples were tested at a constant frequency of 1 Hz.

Results and Discussion.

Effect of MLO on mechanical properties of plasticized PLA formulations.

Figure III.4.3 compares the infrared (IR) spectra of linseed oil and MLO with clear evidence of increased functionality through the cyclic anhydride.

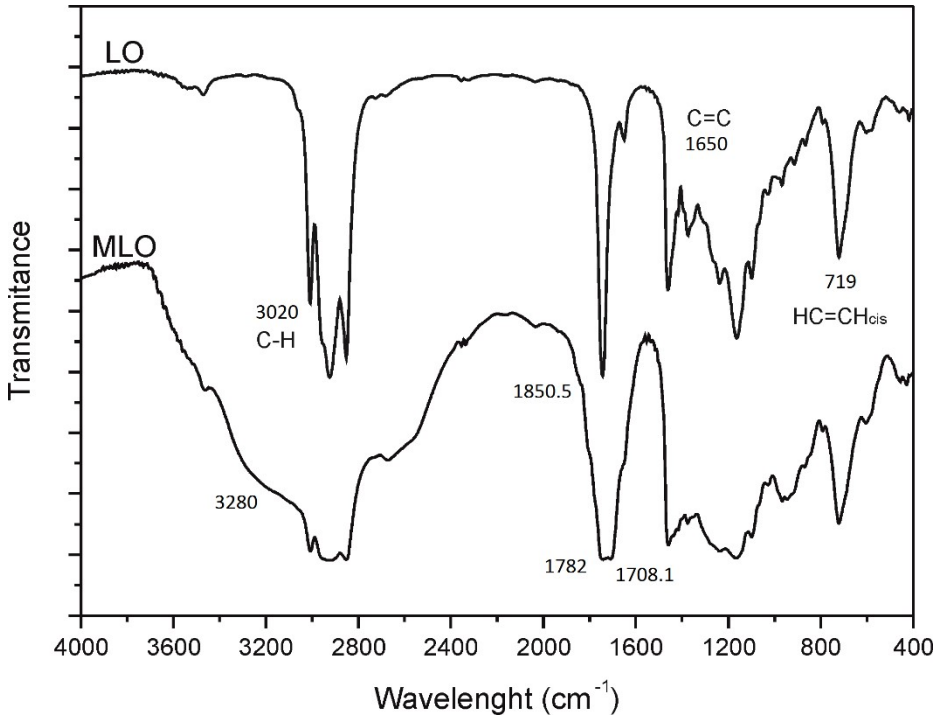

Figure III.4.3. Comparison of IR spectra of linseed oil (LO) and MLO.

The IR spectrum of linseed oil is characterized by peaks at 3020, 1650 and 719 cm^{-1} which are attributed to the stretching vibration of C-H bond of a sp^2 carbon atom, stretching vibration of C=C and angular deformation of cis-CH=CH moieties, respectively [61]. On the other hand, Eren et al. reported a band located at 1708.5 cm^{-1} that corresponds to the carbonyl functional group. This peak can also be observed in the IR spectrum of MLO [62]. Moreover, as pointed out by Balsamo et al. in research work concerning maleinized copolymers, two peaks located at 1780 and 1857 cm^{-1} can be assigned to carbonyl stretching [63].

Figure III.4.4 shows the evolution of the tensile strength of plasticized PLA formulations as a function of MLO content. As expected, MLO provides improved ductile properties (with similar effect as some epoxidized vegetable oils) that lead to lower tensile strength. Tensile strength and tensile modulus decrease in all formulations with increasing MLO content. Specifically, the plasticized formulation containing 20 phr MLO (16.67 wt%) offers a decrease in tensile strength of 21.1% with regard to unplasticized PLA while the tensile modulus is slightly reduced (no clear percentage value can be set due to the deviation of the results, but possibly, this decrease could be close to 3%) for the same formulation in comparison to neat PLA. Similar findings were reported by Silverajah et al. [64]. They reported that 5 wt% EPO plasticizer in PLA formulations led to lower tensile strength values by 26.3% with regard to neat PLA. In a previous work, we reported a decrease of 37% in the tensile strength of neat PLA by the addition of 20 phr of octyl epoxy stearate [31]. In a similar way, Silverajah et al. reported a decrease in Young's modulus of EPO-plasticized PLA of 7% by adding 5 wt% EPO [31]. MLO facilitates crystallization [65], as it provides increased chain mobility and free volume. Increasing the crystallinity of a polymer also increases its rigidity, although in this case it is counteracted with the ductility offered by the MLO in PLA.

MLO has a positive effect on ductile properties. PLA is quite a brittle polymer with very low elongation at break (about 7%). This is noticeably improved by MLO addition. In a previous work, the elongation at break of neat PLA was improved up to 40.5% [31] by the addition of only 5 phr of octyl epoxy stearate, which was the highest

elongation at break achieved with this plasticizer in the range 5-20 phr. Over 5 phr octyl epoxy stearate, phase separation occurs, and this resulted in lower elongation at break values. This phase separation has been reported for other plasticized systems [66]. Xu and Qu reported a marked increase in elongation at break of neat PLA using ESBO (36% increase on addition of 15 wt% ESBO) [67]. The PLA formulation plasticized with 20 phr MLO provides a high elongation at break value of 78.4% which represents an increase of 1020% with regard to neat PLA. This can be indicative of good compatibility between PLA and MLO, which can minimize the negative effects of phase separation. The plasticization effects that MLO provides to PLA are noticeable, increasing the ductility in the same way (or even a greater extent) as some other plasticizers from renewable resources. This can be explained by three different combined effects. Firstly, MLO exerts a lubricant effect which increases chain mobility. Secondly, the gel theory suggests that the plasticizer contributes to weaker polymer-polymer interactions (hydrogen bonds, Van der Waals or ionic forces, etc.) as MLO molecules are placed between PLA chains. This phenomenon also has a positive effect on chain mobility. Finally, the plasticizer increases the free volume and, subsequently, chain interactions decrease, thus leading to improved intermolecular mobility [68].

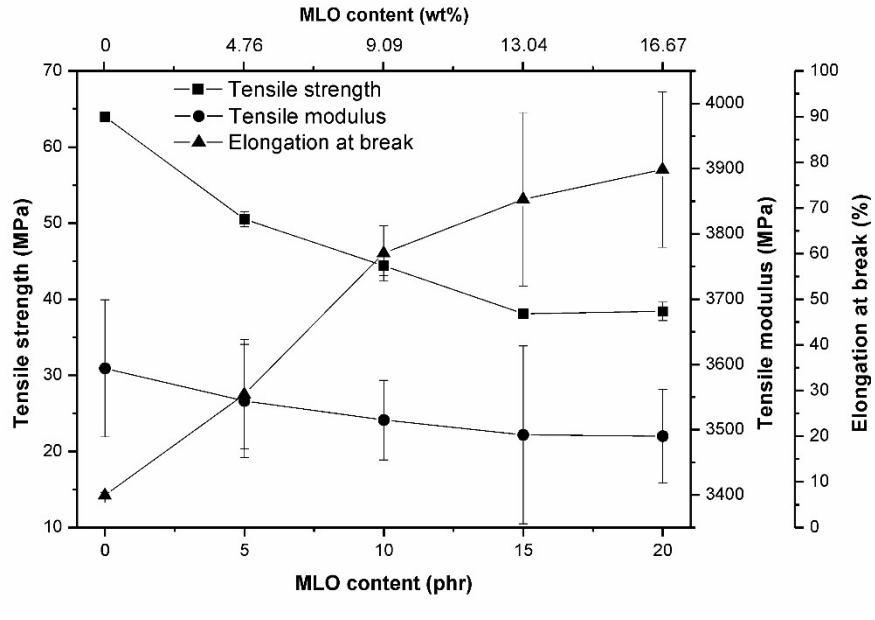

Figure III.4.4. Plot of evolution of tensile mechanical properties of PLA formulations plasticized with various contents of MLO.

In a parallel way, **Figure III.4.5** shows a noticeable decrease in the flexural strength, even for formulations with low MLO content. As the MLO content increases, a decreasing tendency in flexural strength is detected. Nevertheless, the maximum decrease (24% with regard to neat PLA) is achieved by the addition of 5 phr MLO while no marked changes are obtained for higher MLO loads. In fact, flexural strength tends to stabilize at MLO concentrations of 15-20 phr, which could be a sign of plasticizer saturation. Some authors have described an anti-plasticization effect once plasticizer saturation occurs [66]. This anti-plasticization phenomenon could lead to an increase in mechanical resistant properties. Anti-plasticization effects were observed by Gutierrez-Villarreal and Rodriguez-Velazquez when citrate esters were used to plasticize poly(methyl methacrylate) [69]. They reported this effect at a low plasticizer concentration of about 13 wt%. Vidotti et al. suggested that the anti-plasticization effect can be due to a free volume reduction [70]. When this free volume becomes full of plasticizer this effect may appear. The increase in tensile strength related to the anti-plasticization phenomenon can also be explained by taking into account crystallinity considerations, as plasticizer enhances chain mobility, and thus the crystallization tendency is clearly favoured. The anti-plasticization effect depends on molecular weight and concentration of the diluent and is specific for each polymer–plasticizer system [71]. The plasticization threshold for the PLA-MLO system could be located near the 15-20 phr MLO composition as no clear evidence of anti-plasticization is observed in the studied range. As can be seen in **Figs III.4.4** and **III.4.5**, the evolution of mechanical resistance properties tends to stabilize to constant values for PLA formulations plasticized with 15-20 phr MLO. This fact is in accordance with plasticizer saturation as no further plasticization effects can be achieved with plasticizer contents over this range.

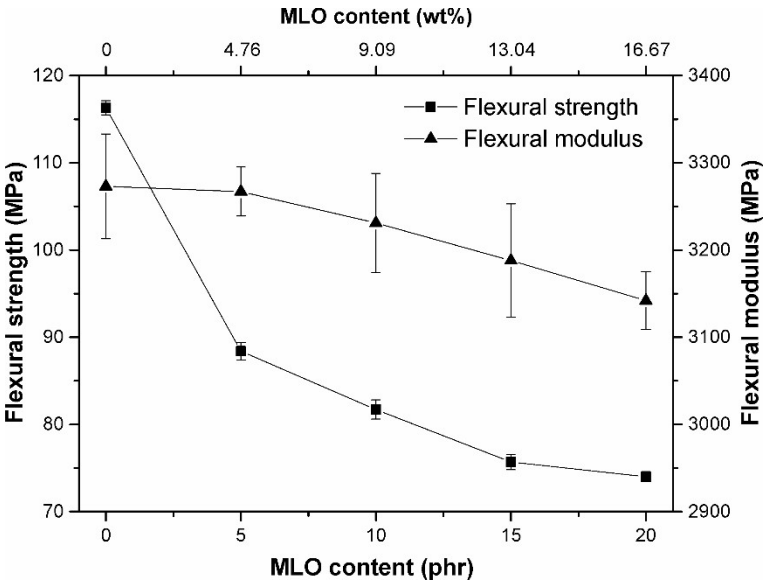

Figure III.4.5. Plot of evolution of flexural mechanical properties of PLA formulations plasticized with various contents of MLO.

Another interesting technique for assessing the plasticization efficiency of MLO is the measurement of the impact-absorbed energy using Charpy's test. This is directly related to toughness. **Table III.4.2** summarizes the impact-absorbed energy of neat PLA and formulations plasticized with MLO. The impact-absorbed energy of neat PLA (30.9 kJ m^{-2}) is relatively low due to intrinsic brittleness. The impact-absorbed energy depends on several factors, i.e. presence of stress concentrators, crack size and growth rate, phase separation, etc. All these factors can influence the overall deformation ability and, subsequently, the total energy absorbed during deformation and fracture. As it has been described previously, plasticization with MLO leads to a marked increase in elongation at break, whilst mechanical resistant properties, such as modulus and strength, are lower compared to neat PLA. The impact-absorbed energy results from the combination of two effects: on the one hand, the deformation ability that is directly related to mechanical ductile properties and, on the other hand, the fracture resistance that is linked to mechanical resistant properties. As evident from **Table III.4.2**, the impact-absorbed energy is increased to twice the value of neat PLA (62.9 kJ m^{-2}) with the addition of 5 phr MLO. Above this value, the impact-absorbed energy decreases slightly, but the values are still much higher than that of

unplasticized PLA. This behavior could indicate that plasticizer saturation occurs for MLO contents between 15 and 20 phr as reported by Mikus et al. for similar systems [66]. Phase separation is one of the main problems related to plasticizer saturation, with a clear negative effect on mechanical ductile properties due to stress concentration and the occurrence of microcracks at the interfaces. Xiong et al. manufactured PLA-starch blends by co-extrusion with ESBO as a reactive plasticizer/compatibilizer. By adding 10 wt% ESBO, the absorbed energy increased by 5.6%. MLO addition leads to toughened materials as the formulation with 10 phr MLO (9.09 wt%) offers an absorbed energy 81% higher than that of neat PLA.

Table III.4.2. Variation of Charpy impact energy, Shore D hardness, Vicat softening temperature (VST) and heat deflection temperature (HDT) of PLA formulations with various contents of MLO.

MLO content (phr)	Hardness Shore D	Charpy impact energy (kJ m^{-2})	VST (°C)	HDT (°C)
0	76.0±0.5	30.9±0.8	52.8	47.6
5	75.7±0.6	62.9±3.1	50.0	47.4
10	75.2±0.7	56.0±5.9	48.8	47.0
15	74.3±0.7	50.3±6.6	47.6	46.8
20	73.4±0.5	48.0±0.9	47.4	47.0

However, Xiong et al. reported a marked increase in toughness by previous starch maleinization, with an increase in absorbed energy of 140% with regard to neat PLA. They concluded the role of maleic anhydride as a compatibilizer between both polymers improving the absorbed energy. In that work, PLA-MLO formulations with a MLO content in the range 5 – 10 phr offer the best balanced properties and optimized toughness. These formulations offer the maximum energy absorption ability. It is important to remark that MLO shows similar results to those observed with epoxidized vegetable oils in terms of ductility and energy absorption [2, 31].

Effect of MLO on thermal properties of plasticized PLA formulations.

Table III.4.3 summarizes the main thermal parameters of PLA formulations plasticized with various MLO contents obtained using DSC. With regard to the glass transition temperature (T_g), a marked decrease with increasing MLO content can be observed. Neat PLA possesses T_g of 65.4 ^oC and the addition of 5 phr MLO promotes a decrease of almost 5 ^oC down to 60.5 ^oC. This is due to the plasticization effect that MLO provides. MLO molecules accommodate between different PLA polymer chains with different effects. On the one hand, the intensity of secondary forces between polymer chains is reduced. On the other hand, the free volume increases and, therefore, chain mobility is favoured along with the lubricity provided by MLO [70, 71]. Over 5 phr MLO, a slight decrease in T_g can be detected but the real change occurs for relatively low MLO content. These results differ slightly from those reported by Santos et al. with PLA formulations plasticized with mixtures of oligoesters obtained from sunflower oil biodiesel as a plasticizer. T_g decreased from 62 ^oC (neat PLA) to 44 ^oC for the blend with 20 wt% of plasticizer. Burgos et al. obtained PLA melt-blended with a bio-based oligomeric lactic acid plasticizer at various concentrations between 15 and 25 wt%. T_g decreased dramatically from 59.2 ^oC (neat PLA) to 25.8 ^oC (25 wt% oligomeric lactic acid). In contrast, Mauck et al. reported negligible changes in T_g of PLA formulations with acrylated ESBO as a plasticizer [72].

The cold crystallization peak also changes with the addition of MLO. The increased chain mobility due to a plasticization effect allows crystallization to occur with lower energy content, thus leading to lower crystallization temperatures as indicated by Li and Huneault [65]. They studied the effect of various nucleants and plasticizers on the crystallization process of PLA during cooling and the effects on the cold crystallization in a subsequent heating. They reported a crystallization peak in PLA plasticized with 5% poly(ethylene glycol) located at 110 ^oC that was reduced to 95 ^oC for a PEG content of 10%, showing that the increase in chain mobility was responsible for the slightly increased ability of PLA chains to crystallize after a previous cooling process. In the present work, the peak temperature for the cold

crystallization process of neat PLA is around 102 ºC. This is markedly reduced to about 87 ºC for MLO contents of 15-20 phr. This indicates that the energetic barrier for crystallization is lower, and PLA polymer chains can form stable crystallites at lower temperatures [65]. In general, the degree of crystallinity is increased due to improved chain mobility as evident from Table 3. Neat PLA possesses a degree of crystallinity (X_{PLA}) of 14.5%, which is increased up to twice this value for plasticized PLA formulations containing 20 phr MLO. Silverajah et al. used EPO as plasticizer for toughened PLA formulations (up to 5 wt% plasticizer) and showed an increase in degree of crystallinity by 10% [64].

Table III.4.3. Main thermal parameters of PLA formulations plasticized with various contents of MLO obtained using DSC.

MLO content (phr)	[a] T_g (ºC)	[b] T_{cc} (ºC)	[c] ΔH_{cc} (J g^{-1})	[d] T_m (ºC)	[e] ΔH_m (J g^{-1})	$\Delta H_m - \Delta H_{cc}$ (J g^{-1})	[f] X_{PLA} (%)
0	65.4	102	26.71	168.3	40.19	13.48	14.5
5	60.5	96.1	21.73	173.3	38.44	16.71	18.9
10	60.1	91.0	19.09	172.1	38.01	18.92	22.4
15	60.8	87.1	19.16	174.3	40.49	21.33	26.4
20	59.0	87.2	18.75	171.5	40.34	21.59	27.9

[a] Glass transition temperature.
[b] Cold crystallization temperature.
[c] Crystallization enthalpy.
[d] Melt peak temperature.
[e] Melt enthalpy.
[f] Degree of crystallinity.

Regarding thermal stability, **Table III.4.4** gives some characteristic thermal parameters of the TGA thermograms for neat PLA and PLA formulations plasticized with various MLO contents. The characteristic thermal parameters are $T_{5\%}$, which stands for the temperature at which a 5% weight loss occurs, and maximum degradation temperature (T_{max}), which corresponds to the highest thermal degradation rate temperature.

Thermal degradation of neat PLA, MLO and PLA-MLO formulations occurs in a one-step process, as can be concluded from their corresponding TGA and DTG

results. As evident from **Table III.4.4**, PLA has a significantly lower thermal stability than MLO. The PLA degradation peak is observed at 363.5 ºC while the maximum degradation rate for neat MLO is located at 424.8 ºC. As expected, the degradation peak temperatures of PLA-MLO formulations are located at about 362 ºC which is very similar to that of neat PLA. Choi and Park reported an absence of interactions between poly[(3-hydroxybutyrate)-co-(3-hydroxyvalerate)] blended with ESBO and soybean oil and both components were degraded separately [73]. We can conclude that MLO also provides negligible effects on the thermal stability of PLA-MLO formulations.

Table III.4.4. Thermal parameters of degradation process of neat PLA and PLA formulations plasticized with various contents of MLO obtained using TGA[a].

MLO content (phr)	$T_{5\%}$ (ºC)	T_{max} (ºC)
0	336.9	363.5
5	333.5	363.6
10	331.8	362.5
15	330.0	361.9
20	328.3	362.2

[a]MLO values: $T_{5\%}$, 349.8ºC; T_{max}, 424.4ºC.

Dynamical mechanical behaviour of plasticized PLA formulations with different content of maleinized linseed oil (MLO).

Figure III.4.6 shows the evolution of the storage modulus (G') as a function of temperature. At room temperature, neat PLA possesses a storage modulus close to 1000 MPa and this value remains almost constant up to 65 ºC. Then the storage modulus undergoes a decrease of three orders of magnitude to 1-2 MPa, which is related to T_g. Above 80 ºC the material behaves as a rubber plastic and then, at 90 ºC, G' increases again up to about 80-90 MPa. This last phenomenon represents the cold crystallization process. At this temperature, the energetic conditions are adequate for

crystallization and polymer chains move to a packed structure, which improves elastic behaviour, thus leading to an increase in G'. With regard to the plasticized PLA formulations, it is possible to observe three main differences compared to neat PLA. Firstly, the initial storage modulus at room temperature is clearly lower for some formulations. Plasticized formulations with 10 and 15 phr MLO possess a storage modulus of 650 and 500 MPa respectively. This indicates the clear plasticization effect that MLO provides. The plasticized formulation with 5 phr MLO is characterized by a storage modulus of 1100 MPa at room temperature, thus indicating that very low plasticizer amounts do not affect the mechanical resistant properties to a great extent.

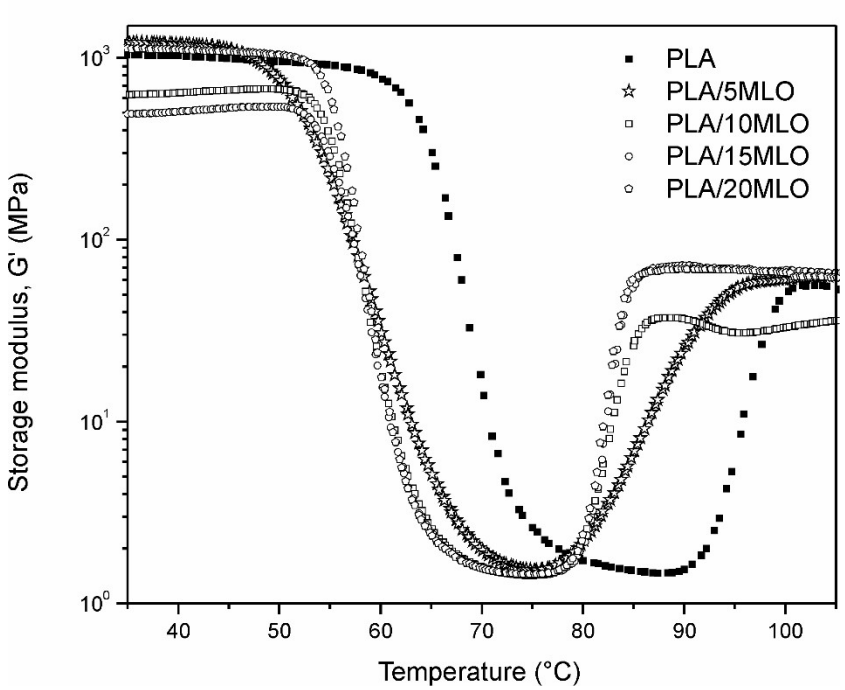

Figure III.4.6. Plot of the evolution of storage modulus (G') in terms of temperature for PLA formulations plasticized with various contents of MLO.

Regarding the PLA formulation with 20 phr, a slight anti-plasticization phenomenon can be observed as the storage modulus is higher compared to formulations with lower MLO content [66]. The second important change is related to T_g. As has been described previously, MLO increases the free volume. In addition to this, the lubricity effect of MLO chains leads to improved chain mobility. This is

evidenced by a decrease in T_g, which indicates that plasticized PLA chains can move with lower energy content than neat PLA chains. T_g is shifted by 10 ºC to lower temperatures, indicating a clear plasticization effect of MLO. Finally, cold crystallization is also moved to lower temperatures as polymer chains can rearrange to a more packed form with less energy content. This decrease in the cold crystallization process is close to 10-15 ºC. All these results are in total agreement with those obtained using DSC.

Figure III.4.7 shows the evolution of the damping factor (*tan δ*) which represents the ratio between loss modulus (G″) and storage modulus (G′).

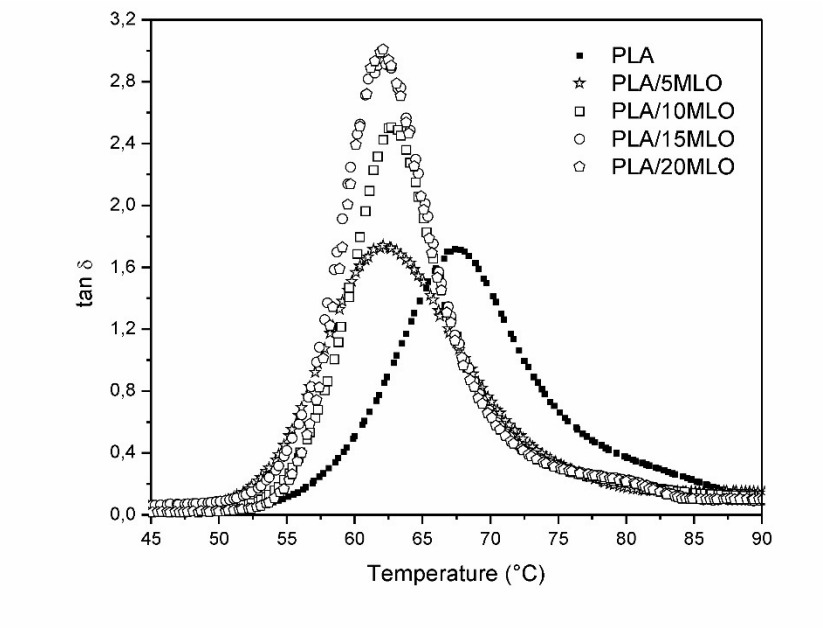

Figure III.4.7. Plot of evolution of damping factor (*tan δ*) in terms of temperature for PLA formulations plasticized with various contents of MLO.

This ratio represents the lost energy (due to viscous behaviour) with regard to the stored energy (due to elastic behaviour). By considering the damping factor peak, T_g of neat PLA is close to 67 ºC, and it is markedly decreased, as expected, to values of 61-62 ºC for all plasticized formulations. Santos et al. observed a similar decrease in T_g with increasing plasticizer content in PLA formulations with oligoesters obtained from sunflower oil biodiesel. They reported a decrease in T_g from 62 ºC (neat PLA) down to

52 and to 44 ºC in formulations containing 10 and 20% plasticizer, respectively [29]. In the same way, Silverajah et al. reported a similar trend. T_g of neat PLA was reduced from 68 to 67 and 62 ºC, for plasticized PLA formulations with 1 and 5 wt% of EPO, respectively [64].

Morphology of PLA formulations plasticized with MLO.

Figure III.4.8 shows FESEM images of fractured surfaces from impact tests. Neat PLA (**Fig. III.4.8(a)**) offers typical brittle fracture with smooth surface which indicates absence (or very low) plastic deformation. With increasing MLO content, clear changes in the fractured surfaces can be observed. Presence of filaments is evident as the MLO content increases. Moreover, the typical smooth surface of brittle fracture changes to a rougher surface with increasing MLO. This rough surface is indicative of plastic deformation and is more intense for PLA formulations plasticized with high MLO content. Silverajah et al. confirmed that neat PLA undergoes brittle fracture, whereas the fractured surface of PLA with 1 wt% EPO was smooth and homogenous, indicating that no phase separation took place. No agglomerates or brittle crack behaviour were observed, which evidenced good interfacial adhesion between PLA matrix and EPO plasticizer [64]. Nevertheless, some kind of plasticizer saturation for MLO contents of 5 phr and above can be observed, which leads to phase separation. It is possible to observe the presence of small cavities and holes that are filled with the excess plasticizer with a negative effect on PLA ductile properties as observed previously. Above 10 phr MLO, the absorbed energy in Charpy's test is noticeable whilst no marked increase in elongation at break can be detected. This agrees with plasticizer saturation and somewhat anti-plasticization effect.

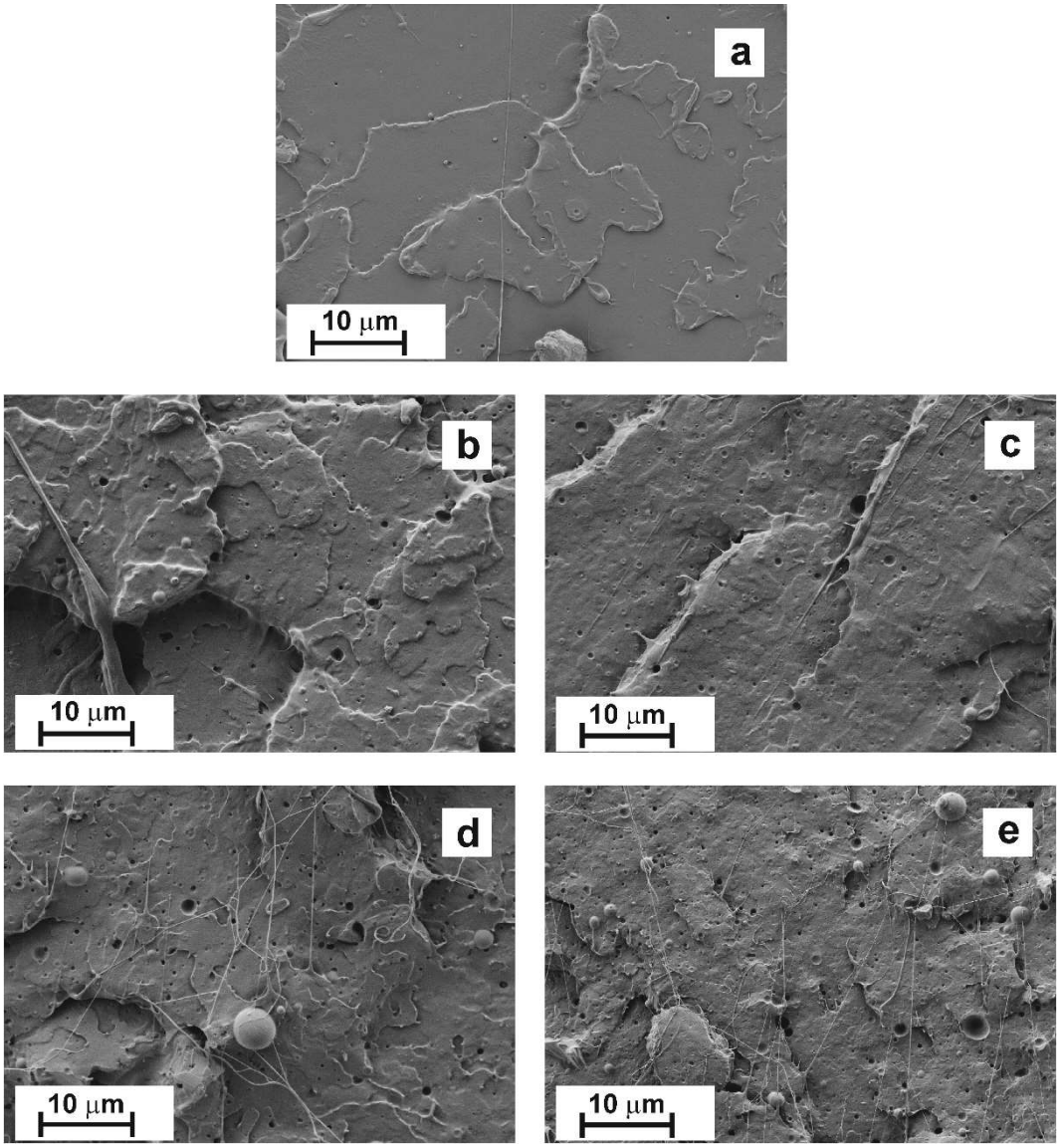

Figure III.4.8. FESEM images of fractured surfaces from impact tests of PLA formulations plasticized with various contents of MLO: (a) neat PLA; (b) 5 phr MLO; (c) 10 phr MLO; (d) 15 phr MLO; (e) 20 phr MLO.

Conclusions.

The present work assesses the effectiveness of a new environmentally friendly plasticizer derived from linseed oil, i.e. MLO for improving the toughness of PLA. MLO content varied in the range 5 – 20 phr that corresponds to a content between 4.76

and 16.67 wt%. Although the plasticization effect of MLO was weak (T_g decreases by 5 ^oC with 5 phr MLO; plasticizer saturation occurs at this content), it is worth noting the great results for impact-absorbed energy with an increase of almost twice the value of neat PLA for the formulation with 5 phr MLO. With regard to elongation at break, maximum values were obtained for formulations plasticized with 15 – 20 phr MLO. MLO leads to increased chain mobility due to reduced intermolecular forces, an increase in free volume and a lubricity effect. All these phenomena have a positive effect on chain mobility with subsequent decrease in T_g by 5-6 ^oC as well as on the cold crystallization process. On the other hand, low MLO content (5 phr) showed a small effect on mechanical properties such as modulus and strength in comparison to other plasticizers thus showing its potential with benefits for both toughness and plasticization. FESEM images revealed clear plasticization with appearance of filaments and a rough surface typical of plastic deformation in contrast to the smooth surface typical of brittle PLA fracture. It is possible to conclude that MLO is a cost-effective eco-friendly solution to PLA plasticization to overcome its low toughness with relatively low plasticizer content.

Acknowledgments.

This research was funded by the Ministry of Economy and Competitiveness - MINECO, Ref: MAT2014-59242-C2-1-R. Authors also thank to "Conselleria d'Educació, Cultura i Esport" - Generalitat Valenciana, Ref: GV/2014/008 for financial support. D. García-García thanks the Spanish Ministry of Education, Culture and Sports for the financial support through an FPU grant (FPU13/06011).

References.

1. Vroman, I., and Tighzert, L, *Biodegradable Polymers*. Materials, 2009. **2**(2): p. 307-344.

2. Garcia-Garcia, D., Ferri, J.M., Boronat, T., Lopez-Martinez, J., and Balart, R., *Processing and characterization of binary poly(hydroxybutyrate) (PHB) and poly(caprolactone) (PCL) blends with improved impact properties*. Polymer Bulletin, 2016. **73**(12): p. 3333-3350.

3. Rhim, J.W. and Kim, J.H., *Properties of poly(lactide)-coated paperboard for the use of 1-way paper cup*. Journal of Food Science, 2009. **74**(2): p. 105-111.

4. van der Harst, E., Potting, J., and Kroeze, C., *Multiple data sets and modelling choices in a comparative LCA of disposable beverage cups*. Science of The Total Environment, 2014. **494-495**: p. 129-143.

5. Bergström, J.S. and Hayman, D., *An Overview of Mechanical Properties and Material Modeling of Polylactide (PLA) for Medical Applications*. Annals of Biomedical Engineering, 2016. **44**(2): p. 330-340.

6. Castro-Aguirre, E., Iñiguez-Franco, F., Samsudin, H., Fang, X., and Auras, R., *Poly(lactic acid)-Mass production, processing, industrial applications, and end of life*. Advanced Drug Delivery Reviews, 2016. **107**: p. 333-366.

7. Sangeetha, V.H., Deka, H., Varghese, T.O., and Nayak, S.K., - *State of the art and future prospectives of poly(lactic acid) based blends and composites*. 2016. DOI: 10.1002/pc.23906.

8. Balart, J.F., Fombuena, V., Fenollar, O., Boronat, T., and Sánchez-Nacher, L., *Processing and characterization of high environmental efficiency composites based on PLA and hazelnut shell flour (HSF) with biobased plasticizers derived from epoxidized linseed oil (ELO)*. Composites Part B, 2016. **86**: p. 168-177.

9. Balart, J.F., García-Sanoguera, D., Balart, R., Boronat, T., and Sánchez-Nacher, L., *Manufacturing and properties of biobased thermoplastic composites from poly(lactid acid) and hazelnut shell wastes*. Polymer Composites, 2017. (In press) DOI: 10.1002/pc.24007.

10. Porras, A., Maranon, A., and Ashcroft, I.A., *Thermo-mechanical characterization of Manicaria Saccifera natural fabric reinforced poly-lactic acid composite lamina*. Composites: Part A, 2016. **81**: p. 105-110.

11. Espino-Pérez, E., Bras, J., Ducruet, V., Guinault, A., Dufresne, A., and Domenek, S., *Influence of chemical surface modification of cellulose nanowhiskers on thermal, mechanical, and barrier properties of poly(lactide) based bionanocomposites*. European Polymer Journal, 2013. **49**(10): p. 3144-3154.

12. Al-Itry, R., Lamnawar, K., and Maazouz, A., *Reactive extrusion of PLA, PBAT with a multi-functional epoxide: Physico-chemical and rheological properties*. European Polymer Journal, 2014. **58**: p. 90-102.

13. Yang, W., Fortunati, E., Dominici, F., Kenny, J.M., and Puglia, D., *Effect of processing conditions and lignin content on thermal, mechanical and degradative behavior of lignin nanoparticles/polylactic (acid) bionanocomposites prepared by melt extrusion and solvent casting*. European Polymer Journal, 2015. **71**: p. 126-139.

14. Tsui, A., Wright, Z.C. and Frank, C.W., *Biodegradable Polyesters from Renewable Resources*, in Annual Review of Chemical and Biomolecular Engineering. 2013. **4**: p. 143-170.

15. Zhang, Y., Rempel, C., and Liu, Q., *Thermoplastic Starch Processing and Characteristics-A Review*. Critical Reviews in Food Science and Nutrition, 2014. **54**(10): p. 1353-1370.

16. Reddy, M., Mohanty, A.K., and Misra, M., *Thermoplastics from Soy Protein: A Review on Processing, Blends and Composites*. Journal of Biobased Materials and Bioenergy, 2010. **4**(4): p. 298-316.

17. Fombuena, V., Sanchez-Nacher, L., Samper, M.D., Juarez, D. and Balart, R., *Study of the Properties of Thermoset Materials Derived from Epoxidized Soybean Oil and Protein Fillers*. Journal of the American Oil Chemists Society, 2012. **90**(3): p. 449-457.

18. Sikorska, W., Musiol, M., Nowak, B., Pajak, J., Labuzek, S., Kowalczuk, M., and Adamus, G., *Degradability of polylactide and its blend with poly (R,S)-3-hydroxybutyrate in industrial composting and compost extract*. International Biodeterioration & Biodegradation, 2015. **101**: p. 32-41.

19. Le Duigou, A., Deux, J.M., Davies, P., and Baley, C., *PLLA/Flax Mat/Balsa Bio-Sandwich Manufacture and Mechanical Properties*. Applied Composite Materials, 2011. **18**(5): p. 421-438.

20. Ferri, J.M., Fenollar, O., Jorda-Vilaplana, A., García-Sanoguera, D., and Balart, R., *Effect of miscibility on mechanical and thermal properties of poly(lactic acid)/ polycaprolactone blends*. Polymer International, 2016. **65**(4): p. 453-463.

21. Yanoso-Scholl, L., Jacobson, J.A., Bradica, G., Lerner, A.L., O'Keefe, R.J., Schwarz, E.M., Zuscik, M.J., and Awad, H.A., *Evaluation of dense polylactic acid/beta-tricalcium phosphate scaffolds for bone tissue engineering*. Journal of Biomedical Materials Research Part A, 2010. **95A**(3): p. 717-726.

22. Ferri, J., Gisbert, I., García-Sanoguera, D., Reig, M.J., and Balart, R., *The effect of beta-tricalcium phosphate on mechanical and thermal performances of poly(lactic acid)*. Journal of Composite Materials, 2016. **50**(30): p. 4189-4198.

23. Gigli, M., Lotti, N., Gazzano, M., Siracusa, V., Finelli, L., Munari, A., and Dalla Rosa, M., *Biodegradable aliphatic copolyesters containing PEG-like sequences for sustainable food packaging applications*. Polymer Degradation and Stability, 2014. **105**: p. 96-106.

24. Navarro-Baena, I., Marcos-Fernández, A., Fernández-Torres, A., Kenny, J.M., and Peponi, L., *Synthesis of PLLA-b-PCL-b-PLLA linear tri-block copolymers and their corresponding poly(ester-urethane)s: Effect of the molecular weight on their crystallization and mechanical properties*. RSC Advances, 2014. **4**(17): p. 8512-8524.

25. Rahman, M. and Brazel, C.S., *The plasticizer market: an assessment of traditional plasticizers and research trends to meet new challenges*. Progress in Polymer Science, 2004. **29**(12): p. 1223-1248.

26. Adeodato Vieira, M.G., da Silva, M.A., dos Santos, L.O., and Beppu, M.M., *Natural-based plasticizers and biopolymer films: A review*. European Polymer Journal, 2011. **47**(3): p. 254-263.

27. Arias, V., Hoglund, A., Odelius, K., and Albertsson, A.-C., *Polylactides with "green" plasticizers: Influence of isomer composition*. Journal of Applied Polymer Science, 2013. **130**(4): p. 2962-2970.

28. Yokesahachart, C. and Yoksan, R., *Effect of amphiphilic molecules on characteristics and tensile properties of thermoplastic starch and its blends with poly(lactic acid)*. Carbohydrate Polymers, 2011. **83**(1): p. 22-31.

29. Santos, E.F., Oliveira, R.V.B., Reiznautt, Q.B., Samios, D., and Nachtigall, S.M.B., *Sunflower-oil biodiesel-oligoesters/polylactide blends: Plasticizing effect and ageing*. Polymer Testing, 2014. **39**: p. 23-29.

30. Fenollar, O., Garcia-Sanoguera, D., Sanchez-Nacher, L., Lopez, J., and Balart, R., *Effect of the epoxidized linseed oil concentration as natural plasticizer in vinyl plastisols*. Journal of Materials Science, 2010. **45**(16): p. 4406-4413.

31. Ferri, J.M., Samper, M.D., García-Sanoguera, D., Reig, M.J., Fenollar, O., and Balart, R., *Plasticizing effect of biobased epoxidized fatty acid esters on mechanical and thermal properties of poly(lactic acid)*. Journal of Materials Science, 2016. **51**(11): p. 5356-5366.

32. Carbonell-Verdu, A., Bernardi, L., Garcia-Garcia, D., Sanchez-Nacher, L., and Balart, R., *Development of environmentally friendly composite matrices from epoxidized cottonseed oil*. European Polymer Journal, 2015. **63**: p. 1-10.

33. Jia, P., Zhang, M., Liu, C., Hu, L., and Zhou, Y.-H., *Properties of poly(vinyl chloride) incorporated with a novel soybean oil based secondary plasticizer containing a flame retardant group*. Journal of Applied Polymer Science, 2015. **132**(25).

34. Jia, P.-Y., Bo, C.-Y., Zhang, L.-Q., Hu, L.-H., Zhang, M., and Zhou, Y.-H., *Synthesis of castor oil based plasticizers containing flame retarded group and their application in poly (vinyl chloride) as secondary plasticizer*. Journal of Industrial and Engineering Chemistry, 2015. **28**: p. 217-224.

35. Mohammed, F.S., Conley, M., Saunders, S.R., Switzer, J., Jha, R., Cogen, J.M., Chaudhary, B.I., Pollet, P., Eckert, C.A., and Liotta, C.L., *Epoxidized linolenic acid salts as multifunctional additives for the thermal stability of plasticized PVC*. Journal of Applied Polymer Science, 2015. **132**(13).

36. Narute, P., Rao, G.R., Misra, S., and Palanisamy, A., *Modification of cottonseed oil for amine cured epoxy resin: Studies on thermo-mechanical, physico-chemical, morphological and antimicrobial properties*. Progress in Organic Coatings, 2015. **88**: p. 316-324.

37. Samper, M.D., Fombuena, V., Boronat, T., Garcia-Sanoguera, D., and Balart, R., *Thermal and Mechanical Characterization of Epoxy Resins (ELO and ESO) Cured with Anhydrides*. Journal of the American Oil Chemists Society, 2012. **89**(8): p. 1521-1528.

38. Shi, Q., Chen, C., Gao, L., Jiao, L., Xu, H., and Guo, W., *Physical and degradation properties of binary or ternary blends composed of poly (lactic acid), thermoplastic starch and GMA grafted POE*. Polymer Degradation and Stability, 2011. **96**(1): p. 175-182.

39. Averous, L., *Biodegradable multiphase systems based on plasticized starch: A review*. Journal of Macromolecular Science-Polymer Reviews, 2004. **C44**(3): p. 231-274.

40. Mittal, V., Akhtar, T., and Matsko, N., *Mechanical, Thermal, Rheological and Morphological Properties of Binary and Ternary Blends of PLA, TPS and PCL*. Macromolecular Materials and Engineering, 2015. **300**(4): p. 423-435.

41. Oromiehie, A.R., Lari, T.T., and Rabiee, A., *Physical and thermal mechanical properties of corn starch/LDPE composites*. Journal of Applied Polymer Science, 2013. **127**(2): p. 1128-1134.

42. Ren, J., Fu, H., Ren, T., and Yuan, W., *Preparation, characterization and properties of binary and ternary blends with thermoplastic starch, poly(lactic acid) and poly(butylene adipate-co-terephthalate)*. Carbohydrate Polymers, 2009. **77**(3): p. 576-582.

43. Sarazin, P., Li, G., Orts, W.J., and Favis, B.D., *Binary and ternary blends of polylactide, polycaprolactone and thermoplastic starch*. Polymer, 2008. **49**(2): p. 599-609.

44. Zhu, C., Zhang, Z., Liu, Q., Wang, Z., and Jin, J., *Synthesis and biodegradation of aliphatic polyesters from dicarboxylic acids and diols*. Journal of Applied Polymer Science, 2003. **90**(4): p. 982-990.

45. Prempeh, N., Li, J., Liu, D., Das, K., Maiti, S., and Zhang, Y., *Plasticizing Effects of Epoxidized Sun Flower Oil on Biodegradable Polylactide Films: A Comparative Study*. Polymer Science Series A, 2014. **56**(6): p. 856-863.

46. Chieng, B.W., Ibrahim, N.A., Then, Y.Y., and Loo, Y.Y., *Epoxidized Vegetable Oils Plasticized Poly(lactic acid) Biocomposites: Mechanical, Thermal and Morphology Properties*. Molecules, 2014. **19**(10): p. 16024-16038.

47. King, J.W., *Determination of the solubility parameter of soybean oil by inverse gas-chromatography*. Food Science and Technology, 1995. **28**(2): p. 190-195.

48. Wang, R. and Schuman, T.P., *Vegetable oil-derived epoxy monomers and polymer blends: A comparative study with review*. Express Polymer Letters, 2013. **7**(3): p. 272-292.

49. Arrieta, M.P., Samper, M.D., Lopez, J., and Jimenez, A., *Combined Effect of Poly(hydroxybutyrate) and Plasticizers on Polylactic acid Properties for Film Intended for Food Packaging*. Journal of Polymers and the Environment, 2014. **22**(4): p. 460-470.

50. Ford, E.N.J., Rawlins, J.W., Mendon, S.K., and Thames, S.F., *Effect of acid value on the esterification mechanism of maleinized soybean oil with cotton*. Journal of Coatings Technology and Research, 2012. **9**(5): p. 637-641.

51. Meier, M.A.R., Metzger, J.O., and Schubert, U.S., *Plant oil renewable resources as green alternatives in polymer science*. Chemical Society Reviews, 2007. **36**(11): p. 1788-1802.

52. Vibhute, B.P., Khotpal, R.R., Karadbhajane, Vijay Y., Kulkarni, A.S., *Preparation of Maleinized Castor oil (MCO) By Conventional Method And It's Application in the Formulation of Liquid Detergent*. International Journal of ChemTech Research, 2013. **5**(4): p. 1886-1896.

53. Ripoll-Seguer, L., Beneito-Cambra, M., Herrero-Martínez, J.M., Simó-Alfonso, E.F., and Ramis-Ramos, G., *Determination of non-ionic and anionic surfactants in industrial products by separation on a weak ion-exchanger, derivatization and liquid chromatography*. Journal of Chromatography A, 2013. **1320**: p. 66-71.

54. Biermann, U., Jungbauer, A., and Metzger, J.O., *Esters of maleinized fatty compounds as plasticizers*. European Journal of Lipid Science and Technology, 2012. **114**(1): p. 49-54.

55. Lligadas, G., Ronda, J.C., Galià, M., and Cádiz, V., *Renewable polymeric materials from vegetable oils: a perspective*. Materials Today, 2013. **16**(9): p. 337-343.

56. Micó-Tormos, A., Collado-Soriano, C., Torres-Lapasió, J.R., Simó-Alfonso, E., and Ramis-Ramos, G., *Determination of fatty alcohol ethoxylates by derivatisation with maleic anhydride followed by liquid chromatography with UV–vis detection*. Journal of Chromatography A, 2008. **1180**(1-2): p. 32-41.

57. Beneito-Cambra, M., Ripoll-Seguer, L., Herrero-Martínez, J.M., Simó-Alfonso, E.F., and Ramis-Ramos, G., *Determination of fatty alcohol ethoxylates and alkylether sulfates by anionic exchange separation, derivatization with a cyclic anhydride and liquid chromatography*. Journal of Chromatography A, 2011. **1218**(47): p. 8511-8518.

58. Ferri, J.M., Garcia-Garcia, D., Sánchez-Nacher, L., Fenollar, O., and Balart, R., *The effect of maleinized linseed oil (MLO) on mechanical performance of poly(lactic acid)-thermoplastic starch (PLA-TPS) blends*. Carbohydrate Polymers, 2016. **147**: p. 60-68.

59. Wiyono, B., Tachibana, S., and Tinambunan, D., *Characteristics and Chemical Composition of Maleo-Pimaric and Fumaro-Pimaric Rosins Made of Indonesian Pinus merkusii Rosin*. Pakistan Journal of Biological Sciences, 2007. **10**(18): p. 3057-3064.

60. Roberts, J.C., *Neutral and alkaline sizing*, in Paper Chemistry. 1996. p. 140-160.

61. Hernández-López, S., López Téllez, G., and Vigueras-Santiago, E., *Characterization of linseed oil epoxidized at different percentages*. Superficies y Vacío, 2009. **22**(1): p. 5 -10.

62. Eren, T., Kusefoglu, S.H., and Wool, R., *Polymerization of maleic anhydride-modified plant oils with polyols*. Journal of Applied Polymer Science, 2003. **90**(1): p. 197-202.

63. Balsamo, V., Gouveia, L.M., Herrera, L., Laredo, E., and Mendez, B., *Miscibilidad en mezclas de poli(estireno-co-anhídrido maleíco) y poli(ε-caprolactona) (sma-pcl)*. Revista Latinoamericana de Metalurgia y Materiales, 2004. **24**(1): p. 17-30.

64. Silverajah, V.S.G., Ibrahim, N.A., Zainuddin, N., Yunus, W.M.Z.W., and Abu Hassan, H., *Mechanical, Thermal and Morphological Properties of Poly(lactic acid)/Epoxidized Palm Olein Blend*. Molecules, 2012. **17**(10): p. 11729-11747.

65. Li, H. and Huneault, M.A., *Effect of nucleation and plasticization on the crystallization of poly(lactic acid)*. Polymer, 2007. **48**(23): p. 6855-6866.

66. Mikus, P.Y., Alix, S., Soulestin, J., Lacrampe, M.F., Krawczak, P., Coqueret, X., and Dole, P., *Deformation mechanisms of plasticized starch materials*. Carbohydrate Polymers, 2014. **114**: p. 450-457.

67. Xu, Y.-Q. and Qu, J.-P., *Mechanical and rheological properties of epoxidized soybean oil plasticized poly(lactic acid)*. Journal of Applied Polymer Science, 2009. **112**(6): p. 3185-3191.

68. Chieng, B.W., Ibrahim, N.A., Yunus, Wan, M.Z.W.Y. and Hussein, M.Z., *Plasticized Poly(lactic acid) with Low Molecular Weight Poly(ethylene glycol): Mechanical, Thermal, and Morphology Properties*. Journal of Applied Polymer Science, 2013. **130**(6): p. 4576-4580.

69. Gutierrez-Villarreal, M.H. and Rodríguez-Velazquez, J., *The effect of citrate esters as plasticizers on the thermal and mechanical properties of poly(methyl methacrylate)*. Journal of Applied Polymer Science, 2007. **105**(4): p. 2370-2375.

70. Vidotti, S.E., Chinellato, A.C., Hu, G.H., and Pessan, L.A., *Effects of low molar mass additives on the molecular mobility and transport properties of polysulfone*. Journal of Applied Polymer Science, 2006. **101**(2): p. 825-832.

71. Moraru, C.I., Lee, T.C., Karwe, M.V., and Kokini, J.L., *Plasticizing and Antiplasticizing Effects of Water and Polyols on a Meat-Starch Extruded Matrix*. Journal of Food Science, 2002. **67**(9): p. 3396-3401.

72. Mauck, S.C., Wang, S., Ding, W., Rohde, B.J., Fortune, C.K., Yang, G., Ahn, S.K., and Robertson, M.L., *Biorenewable Tough Blends of Polylactide and Acrylated Epoxidized Soybean Oil Compatibilized by a Polylactide Star Polymer*. Macromolecules, 2016. **49**(5): p. 1605-1615.

73. Choi, J.S. and Park, W.H., *Thermal and mechanical properties of poly(3-hydroxybutyrate-co-3-hydroxyvalerate) plasticized by biodegradable soybean oils*. Macromolecular Symposia, 2003. **197**(1): p. 65-76.

Research Article

SCI

Received: 6 July 2016 Revised: 4 January 2017 Accepted article published: 11 January 2017 Published online in Wiley Online Library: 23 February 2017

(wileyonlinelibrary.com) DOI 10.1002/pi.5329

The effect of maleinized linseed oil as biobased plasticizer in poly(lactic acid)-based formulations

Jose M Ferri,* Daniel Garcia-Garcia, Nestor Montanes, Octavio Fenollar and Rafael Balart

Abstract

The use of maleinized linseed oil (MLO) as a potential biobased plasticizer for poly(lactic acid) (PLA) industrial formulations with improved toughness was evaluated. MLO content varied in the range 0–20 phr (parts by weight of MLO per hundred parts by weight of PLA). Mechanical, thermal and morphological characterizations were used to assess the potential of MLO as an environmentally friendly plasticizer for PLA formulations. Dynamic mechanical thermal analysis and differential scanning calorimetry revealed a noticeable decrease in the glass transition temperature of about 6.5 °C compared to neat PLA. In addition, the cold crystallization process was favoured with MLO content due to the increased chain mobility that the plasticizer provides. PLA toughness was markedly improved in formulations with 5 phr MLO, while maximum elongation at break was obtained for PLA formulations plasticized with MLO content in the range 15–20 phr. Scanning electron microscopy revealed evidence of plastic deformation. Nevertheless, phase separation was detected in plasticized PLA formulations with high MLO content (above 15–20 phr MLO), which had a negative effect on overall toughness.

Keywords: poly(lactic acid); PLA; plasticizers; environmentally friendly; maleinized linseed oil (MLO); anti-plasticization effects

Chapter III.5

Chapter III.5. The effect of maleinized linseed oil (MLO) on mechanical performance of poly(lactic acid)-thermoplastic starch (PLA-TPS) blends

“The effect of maleinized linseed oil (MLO) on mechanical performance of poly(lactic acid)-thermoplastic starch (PLA-TPS) blends”

J.M. Ferri, D. Garcia-Garcia, l. Sánchez-Nacher, O. Fenollar, R. Balart

Instituto de Tecnología de Materiales (ITM)

Universitat Politècnica de València (UPV)

Plaza Ferrandiz y Carbonell 1, 03801, Alcoy, Alicante (Spain)

Carbohydrate Polymers 147: 60-68 (2016)

Abstract.

In this work, poly(lactic acid), PLA and thermoplastic starch, TPS blends (with a fixed content of 30 wt.% TPS) were prepared by melt extrusion process to increase the low ductile properties of PLA. The TPS used contains an aliphatic/aromatic biodegradable polyester (AAPE) that provides good resistance to aging and moisture. This blend provides slightly improved ductile properties with an increase in elongation at break of 21.5% but phase separation is observed due to the lack of strong interactions between the two polymers. Small amounts of maleinized linseed oil (MLO) can positively contribute to improve the ductile properties of these blends by a combined plasticizing-compatibilizing effect. The elongation at break increases over 160% with the only addition of 6 phr MLO. One of the evidence of the plasticizing-compatibilizing effect provided by MLO is the change in the glass transition temperature (T_g) with a decrease of about 10 ºC. Field emission scanning electron microscopy (FESEM) of PLA-TPS blends with varying amounts of maleinized linseed oil also suggests an increase in compatibility.

Keywords: Poly(lactic acid); Thermoplastic starch; Plasticizing; Maleinized linseed oil.

Introduction.

Due to the high environmental impact, the use of conventional non-biodegradable plastics is being questioned and new environmentally friendly polymers are being demanded and introduced in several industrial sectors. Today, several polymers such as poly(lactic acid)-PLA, poly(hydroxybutyrate)-PHB and thermoplastic starch (TPS), among others, find new and attracting uses in different sectors such as automotive [1] and packaging [2, 3] industries with increasing use. These polymers are characterized by high environmental efficiency along the whole life cycle as they are obtained from renewable resources (PLA is obtained from corn starch and sugar bagasse, PHB is obtained from bacterial fermentation and TPS combines different plant starches with plasticizers) and can be easily disintegrated in compost conditions [4]. In addition to these, some petroleum-based polymers such as poly(caprolactone)-PCL, poly(butylene succinate)-PBS, poly(ester amide)-PEA, etc. offer attracting properties as they can be easily processed and they can biodegrade in different media [5]. Many of the so-called biobased polymers are obtained or derived from different types of starch which plays a key role in their synthesis [6-9].

Poly(lactic acid), PLA is one of the most promising polymers to replace petroleum-based polymers in the packaging industry [10, 11]. This is characterized by balanced mechanical properties, good chemical barrier behavior [12], odorless, biocompatible, bioresorbable [13] and, in the last years its cost has been remarkably reduced. The main synthesis route is ring-opening polymerization from lactides obtained from starch (wheat, corn, sugar bagasse, yucca, tapioca roots, among others) depending on its availability [14, 15]. Some of the main drawbacks of PLA are its sensitiveness to moisture, low flexibility, low elongation at break and low toughness. To overcome these intrinsic properties, copolymers represent an interesting alternative. Nevertheless, copolymers are, in general, costly materials. A cost effective solution is the use of natural plasticizers which are interesting from an environmental point of view and can be an alternative to traditional petroleum-based plasticizers. Some natural vegetable oils [16] and epoxidized vegetable oils (EVOs) find increasing uses in

the plasticization industry [17, 18]. In addition to these, a wide variety of monomeric [19, 20] and polymeric plasticizers have been proposed in the last years [14, 21, 22]. Plasticization mechanisms have been widely studied and the main phenomena are related to the lubricant effect and to the free volume that the plasticizer can provide. Plasticizer molecules placed between two different base polymer chains act as a lubricant with a positive effect on chain mobility. Compatible plasticizers can move into the free volume around the polymer chains. This phenomenon results in several effects: the space between two polymer chains is increased and this reduces the intensity of polymer-polymer interactions. On the other hand, compatibility between the plasticizer and the polymer chains allows entering the plasticizer and this increases intermolecular distance which results in some swelling with a subsequent increase in free volume. As a result of these two phenomena, the plasticizer acts as a lubricant with a remarkable enhancement of polymer chain mobility. A wide variety of plasticizers have been proposed to improve the low intrinsic toughness of neat PLA [23]. In addition, plasticizers can react with hydroxyl groups located at the end groups of PLA polymer chains with a chain extension effect. This is based on the ability of hydroxyl, carbonyl, carboxyl or other polar groups [24] to chemically react with polymer chains to provide a chain extension or a chemical bridge between two polymers in a blend (compatibilization). Some vegetable oil plasticizers act as internal lubricants that allow chain motion and this leads to improved processing conditions, high thermal stability and ductility.

Blending rigid polymers such as PLA with ductile polymers such as poly(caprolactone), thermoplastic starch, polyethylene, etc. is an attracting alternative to overcome the fragility of brittle polymers in a cost effective way. The main problem related to polymer blends is the miscibility between the components. Thermoplastic starch-TPS, has been proposed as a ductile component in different blends to provide toughness and reduce fragility of brittle polymers [14, 25]. TPS addition can lead to increased flexibility and elongation at break [26]. Industrial TPSs are based on different starches (wheat, corn, sorghum, yucca, potato, etc.) [26] and plasticizers (glycerol, sorbitol, maltose, glucose, etc. or a combination of these) [27, 28] that enable easy processing and provide high ductile materials with improved elongation at break,

reduced retrogradation effects and improved thermal stability [29, 30]. Chemically, starch is constituted of two polysaccharides: amylose and amylopectin. Depending on their ratio, mechanical properties can vary in a great extent [21, 22, 31, 32].

One of the main drawbacks of using TPS as co-component in polymer blends is its poor miscibility with polymers such as PLA [33, 34]. For this reason, important efforts are being conducted to improve it by using compatibilizer agents. Maleic anhydride (MA) and other esterifying agents have been successfully used to improve compatibility of immiscible or very low miscible polymers [21, 22, 31, 32, 35, 36]. Maleinization of TPS with 20 wt.% glycerol by using reactive extrusion was revealed as a useful technique to increase the compatibility with a biodegradable polyester [32]. Same results were obtained with chemical modification of starch with an esterifying agent leading to improved blending with poly(lactic acid) [37]. PLA-TPS blends containing 15 wt.% TPS showed improved elongation at break and impact absorbed energy with previous modification with maleic anhydride [38]. Monomeric plasticizers can also provide compatibilization to immiscible or low miscible polymers. Glycidyl methacrylate was successfully used to modify TPS/PEO (TPEO) for improved formulations with poly(lactic acid) [19]. High molecular weight polyethylene glycols have demonstrated to provide good compatibilization properties [39].

PLA/TPS blends and, in particular, the PLA/TPS blend with 30 wt.% TPS show balanced properties in terms of improved toughness but the restricted miscibility between the two components leads to a clear phase separation which gives low mechanical performance. As described previously, the highly reactive acid/anhydride groups in maleinized vegetable oils can potentially provide a dual effect on PLA blends: a plasticizing and a compatibilizing/chain extension effect. The aim of this work is the use of thermoplastic starch to provide improved toughness to rigid-brittle poly(lactic acid). Due to the lack of miscibility of TPS and PLA, maleinized linseed oil (MLO) is used as a natural-derived compatibilizer for PLA-TPS immiscible blends. The influence of MLO on thermal, mechanical, morphological properties and its effect on the compatibility of these two restricted miscibility polymers is evaluated.

Experimental.

Materials.

Poly(lactic acid), PLA IngeoTM Biopolymer commercial grade 6201D was supplied by NatureWorks LLC (Minnetonka, USA). This grade contains 2% D-lactic acid; it is characterized by a density of 1.24 g cm^{-3} and a melt flow index (MFI) in the 15-30 g/(10 min) range measured at 210 ^{o}C. Thermoplastic starch commercial grade Mater-Bi® NF 866 was obtained from Novamont SPA (Novara, Italy) and it is produced from maize starch. It shows a melt flow index of 3.5 g/(10 min) measured at 150 ^{o}C, a density of 1.27 g cm^{-3} and a melt peak located in the 110 ^{o}C – 120 ^{o}C range. This thermoplastic starch is composed of about 15% of an aliphatic/aromatic biodegradable copolyester (AAPE) [40]. The material used as plasticizer-compatibilizer was a maleinized linseed oil (MLO) VEOMER LIN supplied by Vandeputte (Mouscron, Belgium) with a viscosity of 10 dPa s at 20 ^{o}C and an acid value of 105 – 130 mg KOH g^{-1}.

Preparation and compatibilization of PLA-TPS blends.

A constant TPS content of 30 wt.% was used to evaluate the plasticization compatibilization effect provided by maleinized linseed oil (MLO). This composition has given interesting results in terms of toughness improvement as observed by previous results and reported in the literature [41]. 30 wt.% TPS also contributes to lower the cost of the material as it is cheaper than PLA while maintaining the overall properties of PLA. PLA-30 wt.% TPS blends with different maleinized linseed oil (MLO) content as indicated in **Table III.5.1** were manufactured. The MLO range composition varied in the 0-8 phr (per hundred resin) as previous studies with epoxidized vegetable oils and maleinized oils indicated saturation with relatively low contents close to 10 phr. Initially, PLA and TPS were dried at 60 ^{o}C for 24 hours in an air circulating oven. After this, PLA and TPS pellets were mechanically mixed in a zip

bag together with the corresponding amounts of MLO. Subsequently, the mixtures were extruded in a twin-screw co-rotating extruder at a rotating speed of 60 rpm. The temperature profile was set to 167.5 ºC, 170 ºC, 172.5 ºC and 175 ºC from the hopper to the die. After cooling, the extruded materials were pelletized and processed by injection molding in a Meteor 270/75 from Mateu & Solé (Barcelona, Spain) at an injection temperature of 175 ºC. Standard samples for tensile tests and rectangular shapes sizing 80x10x4 mm^3 for other characterizations were obtained.

Table III.5.1. Summary of the compositions and labelling of the PLA-TPS blends with varying amounts of maleinized linseed oil (MLO).

PLA (wt.%)	TPS (wt.%)	MLO (phr)
-	100	-
100	-	-
70	30	-
70	30	2
70	30	4
70	30	6
70	30	8

Mechanical characterization.

Mechanical properties of the blends and individual materials were obtained with standard tensile, flexural, hardness and impact tests. Tensile and flexural properties were obtained in a universal test machine ELIB 30 from S.A.E. Ibertest (Madrid, Spain) at room temperature with the guidelines of the ISO 527-5 and ISO 178 respectively. A 5 kN load cell was used for all tests and the crosshead speed was set to a constant value of 10 mm min^{-1}. At least five different samples were tested in both tensile and flexural tests to obtain average values of the main parameters. In addition, a bi-axial extensometer from Ibertest was used to measure the Young Modulus in a more accurate way.

Shore D hardness was measured in a Shore D durometer 673-D from Instrumentos J. Bot S.A. (Barcelona, Spain) as recommended by the ISO 868. With regard to the energy absorption, a Charpy pendulum (1 J) from Metrotec S.A. (San Sebastián, Spain) was used to measure the absorbed energy in impact conditions as recommended by the ISO 179:1993. Five different notched samples were tested and average values were calculated. The geometry of the notch was type A with a background radius of 0.25 ± 0.05 mm; the remaining width of 8.0 ± 0.2 mm and the notch angle is 45º ± 1º.

Microstructural characterization.

A high-resolution field emission microscope ZEISS ULTRA55 from Oxford Instruments (Oxfordshire, United Kingdom) operated at 2 kV was used to observe the microstructure of cryofractured surfaces. Samples were coated with an ultrathin platinum layer in vacuum conditions in a high vacuum sputter EM MED020 from Leica Microsystems.

Thermal characterization.

Thermal transitions were studied by differential scanning calorimetry (DSC) in a DSC 821 calorimeter from Mettler-Toledo Inc. (Schwerzenbach, Switzerland) with a heating program from 30 ºC to 350 ºC in nitrogen atmosphere (66 mL min^{-1}) at a heating rate of 10 ºC min^{-1}. Degradation at high temperatures was studied by thermogravimetric analysis (TGA) in a TGA/SDTA 851 thermobalance from Mettler-Toledo Inc. (Schwerzenbach, Switzerland). The selected temperature ramp was from 30 ºC to 500 ºC in nitrogen atmosphere (66 mL min^{-1}) at a heating rate of 20 ºC min^{-1}.

Dynamic mechanical thermal analysis (DMTA) in torsion mode was done on rectangular samples sizing 40x10x4 mm^3 in an oscillatory rheometer AR G2 from TA Instruments (New Castle, USA) equipped with a special clamp system for solid

samples. The temperature program was from -80 ºC to 130 ºC at a heating rate of 2 ºC min^{-1} at a frequency of 1 Hz and a maximum deformation (γ) of 0.1%.

Results and discussion.

Effect of MLO on mechanical properties of PLA-TPS blends.

Unblended PLA possesses a tensile strength of 64 MPa and a tensile modulus of 3590 MPa. These values are higher than most commodity plastics. Nevertheless, PLA is a quite brittle polymer with an elongation at break of about 7%. Addition of a high ductile and flexible polymer such as thermoplastic starch provides improved ductile properties but the lack of miscibility of them can lead to lower performance than expected. For this reason, maleinized linseed oil was added at different concentrations to provide plasticization and/or compatibilization effects. **Figure III.5.1a** shows the plot evolution of tensile properties of PLA-30TPS with varying maleinized linseed oil (MLO). PLA-30TPS blend offers a tensile strength of 41.5 MPa and a tensile modulus of 2475 MPa. With the only addition of 2 phr MLO the tensile strength suffers a decrease up to values of 35.7 MPa which represents a percentage decrease of 14%. Higher MLO content such as 8 phr MLO leads to tensile strength values of about 28.2 MPa (percentage decrease of almost 32%). With regard to the tensile modulus, it changes from 2475 for PLA-30TPS blend without MLO to values in the 2200 MPa – 2300 MPa range for MLO content in the 2 – 8 phr range. It is evident that mechanical resistant properties decrease with increasing MLO content. On the other hand, mechanical ductile properties are remarkably improved with MLO. PLA-30TPS is characterized by an elongation at break of 21.5% and we observe an increasing tendency up to 6 phr MLO with noticeable higher elongation at break values of 160%. For an MLO content of 8 phr, the elongation at break is still higher than raw PLA-30TPS blend but this value is lower than that obtained for 6 phr MLO. This could indicate that an optimum is achieved for phr contents close to 6 phr and higher MLO contents do not provide

increased ductile properties. Miscibility of TPS in PLA is poor as referred by some authors [33, 34] and phase separation is the resulting microstructure. Nevertheless, finely rich TPS dispersed phase provides improved toughness and other ductile properties to PLA due to its high flexibility which enables some energy absorption and elongation but in general terms TPS does not act as a plasticizer when blended with PLA.

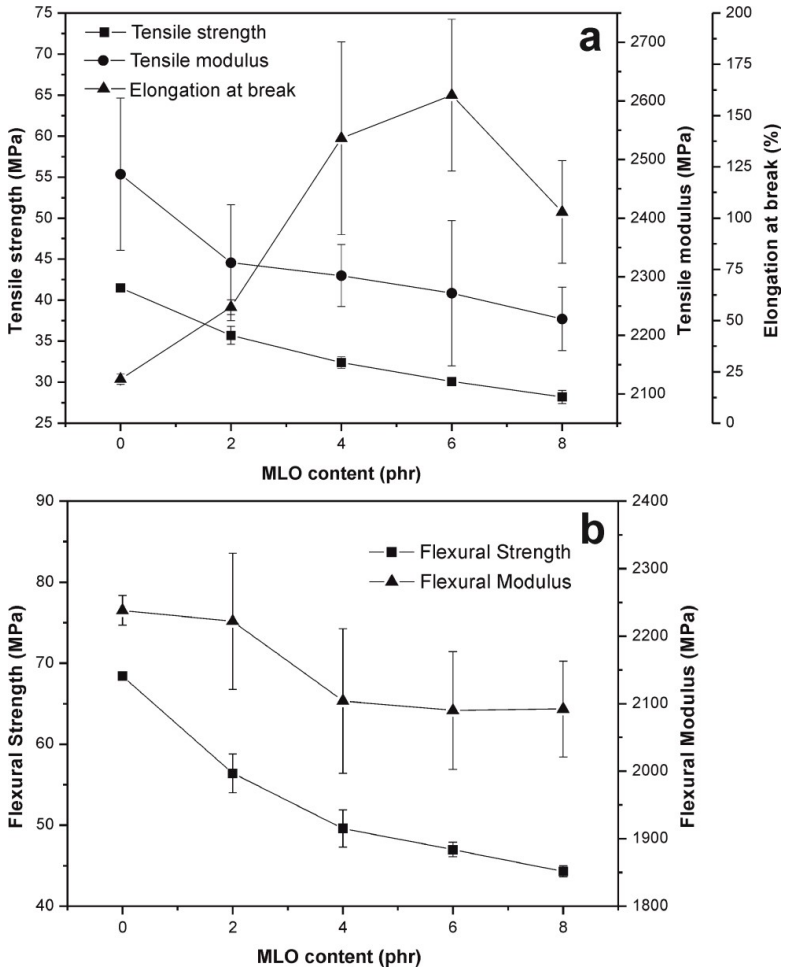

Figure III.5.1. Plot evolution of mechanical tensile (a) and flexural (b) properties of PLA-30TPS blend with varying maleinized linseed oil (MLO) content.

As one can observe, MLO addition leads to a remarkable in elongation at break whilst no remarkable decrease is detected for both tensile strength and tensile modulus. This indicates that MLO provides a clear plasticization effect and the

evidence is the noticeable increase in elongation at break. On the other hand, the tensile strength and modulus do not decrease in a great extent thus giving some evidences that in addition to plasticization, other phenomena could occur. It is expectable that maleic anhydride groups in MLO can react with some hydroxyl groups in PLA end chains (and partially hydrolysed PLA chains during processing) to give a chain extension effect and, on the other hand, MLO can also react with hydroxyl groups in TPS thus leading to a compatibilization effect as observed by the evolution of the mechanical properties.

Figure III.5.1b shows the evolution of the flexural properties as a function of the maleinized linseed oil (MLO) content. The flexural strength and flexural modulus of unblended PLA is 116 MPa and 3273 MPa respectively. We observe a decrease in both flexural strength and flexural modulus with minimum values in the 4 – 6 phr MLO range up to 45-50 MPa and 2100 MPa for flexural strength and modulus respectively. Over 6 phr MLO a decrease in both mechanical resistant and ductile properties is observed and this could be related to a negative effect due to phase separation [42].

One of the main features of PLA-30TPS blends with MLO is the large increase in the impact-absorbed energy as it can be observed in **Table III.5.2**. Unblended PLA is characterized by relatively low energy absorption ability with a Charpy's impact energy of 1.6 ± 0.3 kJ m^{-2}. Physical blend of PLA with TPS leads to a remarkable increase in the energy absorption up to values of 5.3 kJ m^{-2}, which represents a percentage increase of about 230%. Despite this remarkable increase, addition of MLO still improves more the energy absorption up to values of about 9.5 kJ m^{-2} for MLO compositions comprised between 4 and 6 phr MLO, which represents a percentage increase of almost 500% with regard to unblended PLA.

Table III.5.2. Variation of Charpy's impact energy, Shore D hardness, VST and HDT of PLA-30TPS blends with different amounts of maleinized linseed oil (MLO).

MLO content (phr)	Charpy's impact energy (kJ m^{-2})	Shore D hardness	Vicat softening temperature, VST (°C)	Heat deflection temperature, HDT (°C)
0	5.3 ± 0.1	68.2 ± 0.6	50.6	49.4
2	8.7 ± 0.9	67.3 ± 0.6	48.4	44.0
4	9.3 ± 2.0	66.2 ± 0.5	47.8	45
6	9.5 ± 1.3	64.8 ± 0.4	47.4	44.4
8	6.7 ± 0.7	64.1 ± 1.0	46.6	44.8

For an MLO content of 8 phr we observe the same phenomenon described before with a decrease in the energy absorption due to a negative effect as a consequence of MLO saturation and subsequent phase separation.

With regard to the Shore D hardness, we observe similar decreasing tendency as other mechanical resistant properties. The Shore D of unblended PLA is 76 and it is decreased up to 68 by blending with TPS but addition of MLO leads to softer materials due to the plasticization effect clearly observable up to 6 phr MLO.

Evolution of Vicat softening temperature (VST) and heat deflection temperature (HDT) follows typical tendency of a mechanical resistant property such as strength and modulus. The VST and HDT values for unblended PLA are 52.8 °C and 47.6 °C respectively. A blend of PLA with 30 wt.% TPS provides improved deformation properties thus leading to lower VST and HDT values of 50.6 °C and 49.4 °C respectively. Once again, addition of MLO leads to decreased VST and HDT values up to asymptotic values of 47 °C and 44 °C respectively.

Effect of MLO on thermal properties of PLA-TPS blends.

Table III.5.3 shows a summary of the main thermal parameters obtained by differential scanning calorimetry (DSC) on PLA-30TPS blends with different amounts of maleinized linseed oil (MLO). As it can be observed, the melt temperature does not vary in a significant way with regard to the reference PLA-30TPS blend. The glass transition temperature slightly decreases with MLO content due to increased polymer chain mobility. There are two possible effects that MLO can provide: a lubricant effect and a decrease in the intensity between polymer chains. Lubricity and gel theories have been extensively used to explain the effects of plasticizers on polymeric structures. Lubricity theory proposes that the plasticizer can exert a lubricant effect which leads to increased chain mobility as the distance between polymer chains increases thus leading to decreased polymer-polymer interactions.

Table III.5.3. Main thermal parameters of the PLA-30TPS blend with different MLO contents obtained by differential scanning calorimetry (DSC): glass transition temperature (T_g), cold crystallization temperature (T_{cc}) and enthalpy (ΔH_{cc}) and melt temperature (T_m) and enthalpy (ΔH_m).

MLO content (phr)	T_g (°C)	T_{cc} (°C)	ΔH_{cc} (J g^{-1})	T_m (°C)	ΔH_m (J g^{-1})
0	62.8	98.5	16.6	170.3	26.3
2	62.6	97.0	17.6	169.9	27.5
4	62.4	98.0	17.4	169.3	26.6
6	62.0	97.8	16.4	169.3	26.7
8	61.8	95.2	16.4	168.1	29.0
PLA	65.4	102	26.7	168.3	40.2

On the other hand, the gel theory suggests that the plasticizer contributes to lower polymer-polymer interactions (hydrogen bonds, van der Waals or ionic forces, etc.) which has a positive effect on the overall chain mobility. These phenomena could explain the observed decrease in T_g values as MLO is added. In addition, MLO can readily react with hydroxyl groups in both PLA end chains and thermoplastic starch chains leading to a combined effect of compatibilization and chain extension with a subsequent decrease in crystallinity which can also contribute to lower polymer-polymer interactions [43]. It is important to remark that the only addition of 30 wt.% TPS to PLA leads to a decrease in the glass transition temperature from 65.4 °C

(unblended PLA) to 62.8 ºC for the blend. Although these polymers are not fully miscible and phase separation is evident, PLA is able to dissolve a very low amount of TPS chains resulting in a PLA rich phase but the effect of the dissolved TPS chains promotes a decrease in the glass transition temperature. In addition, the cold crystallization temperature follows similar tendency to that observed for T_g. Unplasticized PLA shows a cold crystallization peak at 102 ºC and the blend with 30 wt.% TPS leads to a decrease in the cold crystallization peak to values of 98.5 ºC. Addition of MLO to this blend provides a slight decrease in the cold crystallization temperature up to values of 95.2 ºC for an MLO content of 8 phr. This is directly related to increased chain mobility due to the internal lubrication effect that MLO produces [43].

With regard to the thermal stability of PLA-30TPS, **Figure III.5.2** shows a comparative plot of the TGA thermograms for neat PLA and its blends with 30 wt.% TPS (with and without MLO compatibilizer). We can clearly observe a positive effect of MLO on overall thermal stability with improved thermal degradation temperature as MLO content increases.

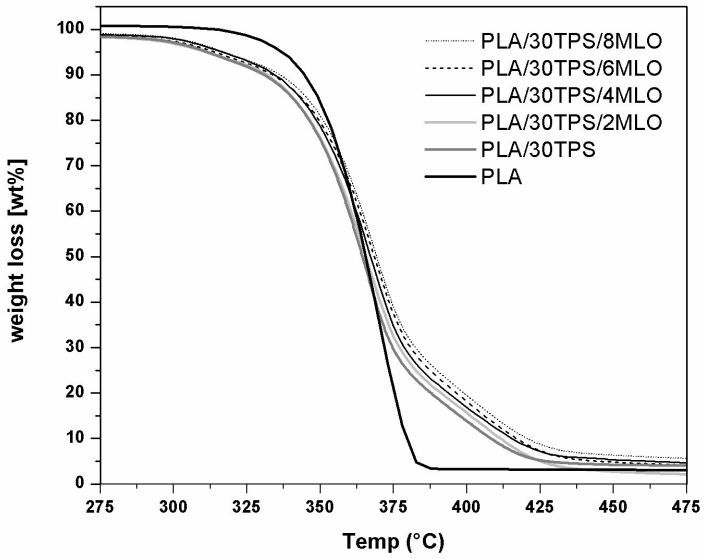

Figure III.5.2. Comparative thermogravimetric curves for unblended PLA, PLA-30TPS and PLA-30TPS with maleinized linseed oil (MLO).

As we can observe, the PLA blend with 30 wt.% TPS offers improved thermal stability with regard to unblended PLA and this thermal stability is still improved with the addition of maleinized linseed oil (MLO) as observed in **Figure III.5.2**. Specifically, the degradation temperature corresponding to 90% weight loss (T_{90}) is 380 °C, whereas for PLA/30TPS is 408 °C. A significant increase in PLA stability is observed when adding TPS, but still it is higher when the blends contains MLO. In fact, a high increase in T_{90} is observed with values of 415 ^{o}C, 411.5 ^{o}C, 416.6 ^{o}C and 420.5 ^{o}C for blends containing 2, 4, 6 and 8 phr MLO, respectively.

Effect of MLO on dynamic mechanical thermal properties of PLA-TPS blends.

Figure III.5.3a & **III.5.3b** represent the evolution of the storage modulus (G′) and the damping factor (*tan δ*) in terms of temperature for different maleinized linseed oil compositions. The storage modulus (G′) at temperatures below T_g (**Figure III.5.3a**) decreases as the MLO content increases. By observing the curve corresponding to the evolution of G′ for the PLA-30TPS blend with 6 phr MLO we see the best ductile properties with minimum G′ values. Over 6 phr MLO a negative effect occurs thus leading to decreased flexibility as it can be seen by G′ values higher than those obtained with an MLO content of 6 phr. This could be related to plasticizer saturation leading to phase separation [42]. In addition, a clear decrease in the cold crystallization process as previously detected by differential scanning calorimetry (DSC) can be observed. The only presence of TPS is responsible for a slight decrease in the cold crystallization temperature with onset values located at lower temperatures. Although PLA and TPS are not completely miscible a PLA rich phase with some TPS polymeric chains can be expected due to the partial (very low) interactions as evidenced by phase separation. This PLA rich phase is characterized by slightly higher mobility which is responsible for some decrease in both cold crystallization onset and glass transition temperature. Addition of MLO provides two phenomena that result in increased chain mobility. On the one hand, MLO acts as typical plasticizer with a lubricant effect and,

on the other hand, MLO contributes to increase PLA-TPS interactions. These two phenomena have a positive effect on overall polymer chain mobility and this results in decreased cold crystallization onset temperature and glass transition temperature as observed in **Figure III.5.3**.

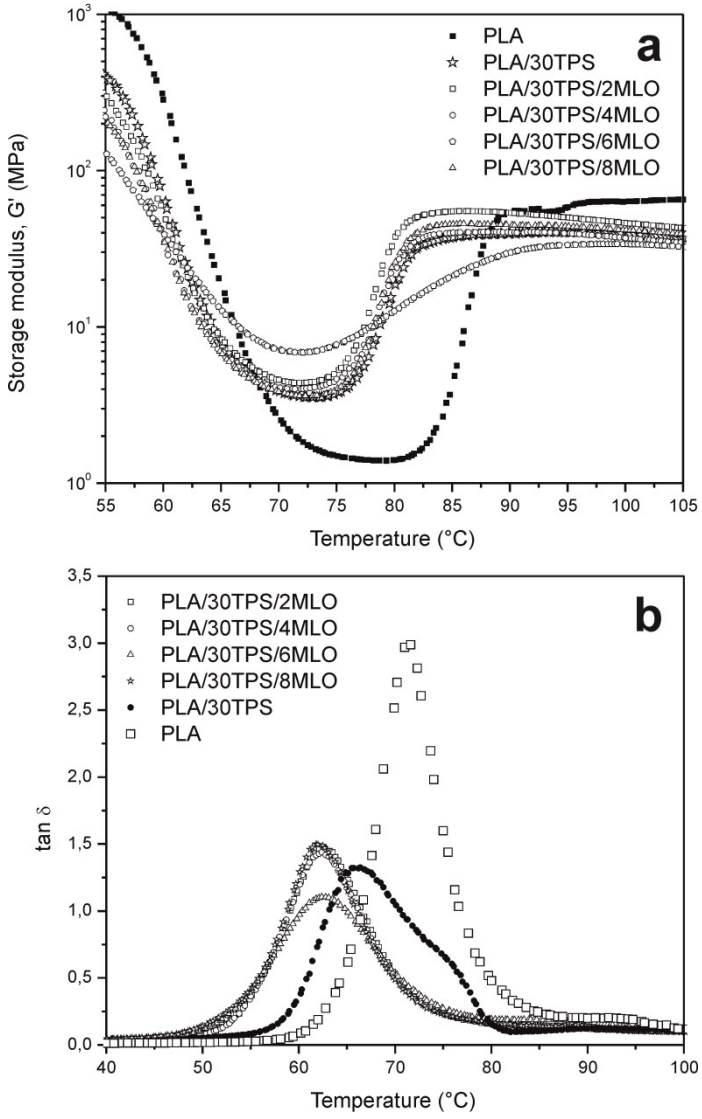

Figure III.5.3. Comparison of the evolution of the storage modulus (G') (a) and damping factor (*tan δ*) (b) for unblended PLA, PLA-30TPS and PLA-30TPS with different maleinized linseed oil (MLO) content.

Figure III.5.3b shows the evolution of the damping factor (*tan δ*) for PLA and PLA-30TPS blends with different MLO content. The peak is directly related to the glass

transition temperature (T_g PLA) and as it can be seen, this peak is moved to lower values thus indicating a decrease in the glass transition temperature of the PLA rich phase. Once again, the initial decrease that TPS provides is accentuated by the synergistic effect of MLO addition.

Effect of MLO on morphology of PLA-TPS blends.

Figure III.5.4 shows FESEM images of fractured samples corresponding to unblended PLA, unblended TPS and the PLA blend with 30 wt.% TPS (PLA-30TPS) (**Figure III.5.4e & III.5.4f**).

These pictures show the typical brittle fracture of PLA (**Figure III.5.4a & II.5.4b**) with smooth fracture surface due to inexistent or very low plastic deformation and a ductile fracture corresponding to a flexible polymer, TPS (**Figure III.5.4c & III.5.4d**) with flake formation. These flakes correspond to crystalline plane growth or "crystalline lamellae" located at the amylopectin branches that are fold up because of fracture. These flake structures form parallel-plane blocks and clusters of these blocks form granules separated by porous of amorphous areas in which amylose and plasticizers can be allocated [44]. The blend with 30 wt.% TPS shows a clear phase separation with a PLA rich phase as the matrix and the TPS rich phase as the dispersed component as detected in **Figure III.5.4e & III.5.4f**. This phase separation is related to the lack of affinity between TPS and PLA and this leads for the need of somewhat compatibilization [45]. PLA is a hydrophobic polymer whilst TPS is a highly hydrophilic polymer (in fact one of the main drawbacks of TPS is its extremely high moisture sensitiveness). This different polarity is responsible of the lack (or very low) affinity between these two polymers and this leads to a phase separation. For this reason, a compatibilization strategy must be applied to PLA-TPS blends to give materials with interesting properties. This effect is provided by MLO as previously described.

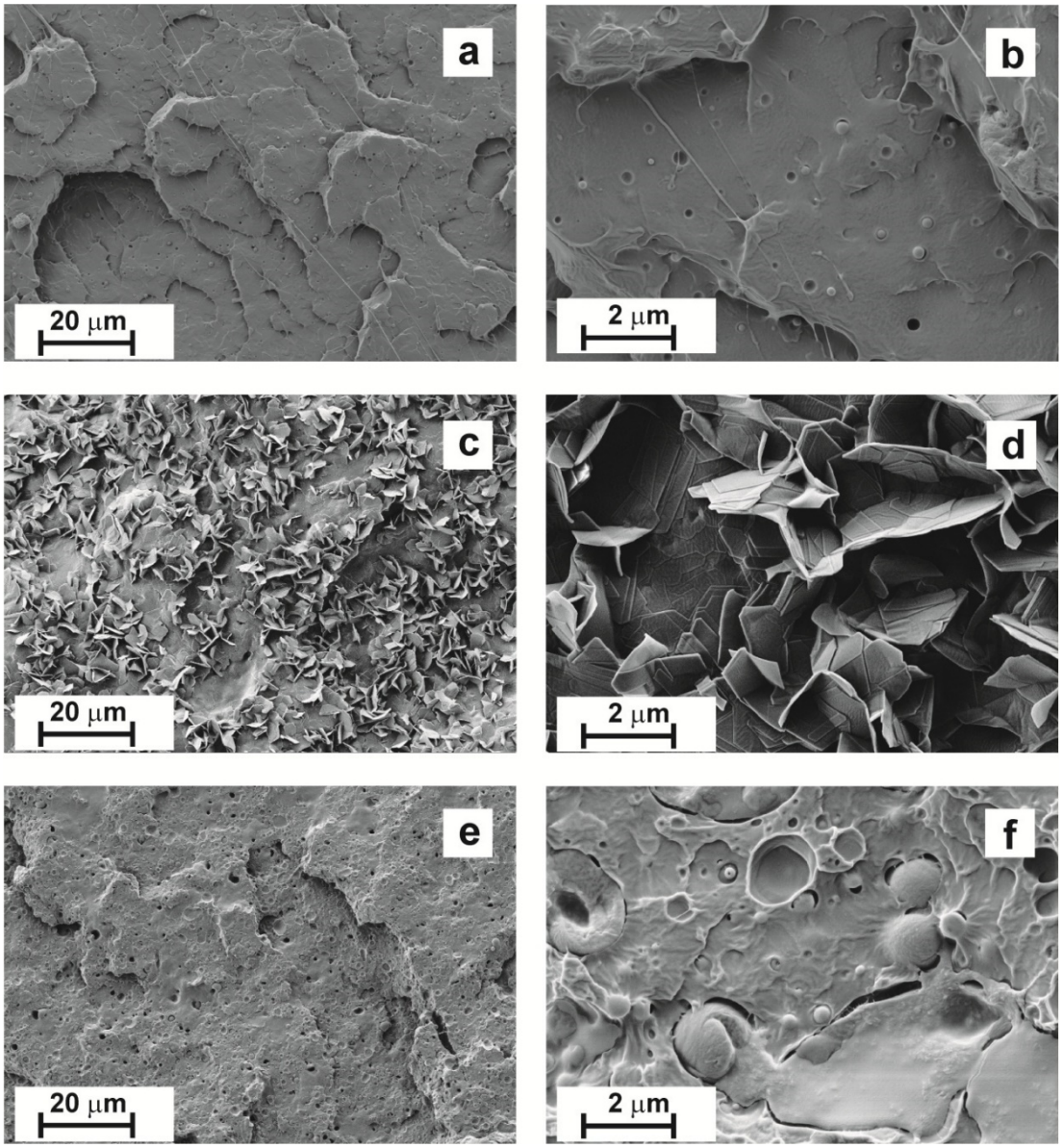

Figure III.5.4. FESEM images from cryofractured surfaces of (a) PLA at 1000x, (b) PLA at 5000x, (c) TPS at 1000x, (d) TPS at 5000x, (e) PLA-30 wt.% TPS at 1000x and (f) PLA-30 wt.% TPS at 5000x.

The effect of maleinized linseed oil (MLO) can be observed in **Figure III.5.5**. The only addition of 2 phr (**Figure III.5.5a & II.5.5b**) leads to improved adhesion/interaction between the two main components in the blend. As the MLO content increases, the compatibility or miscibility between PLA and TPS is improved and it is difficult to observe the dispersed TPS rich phase.

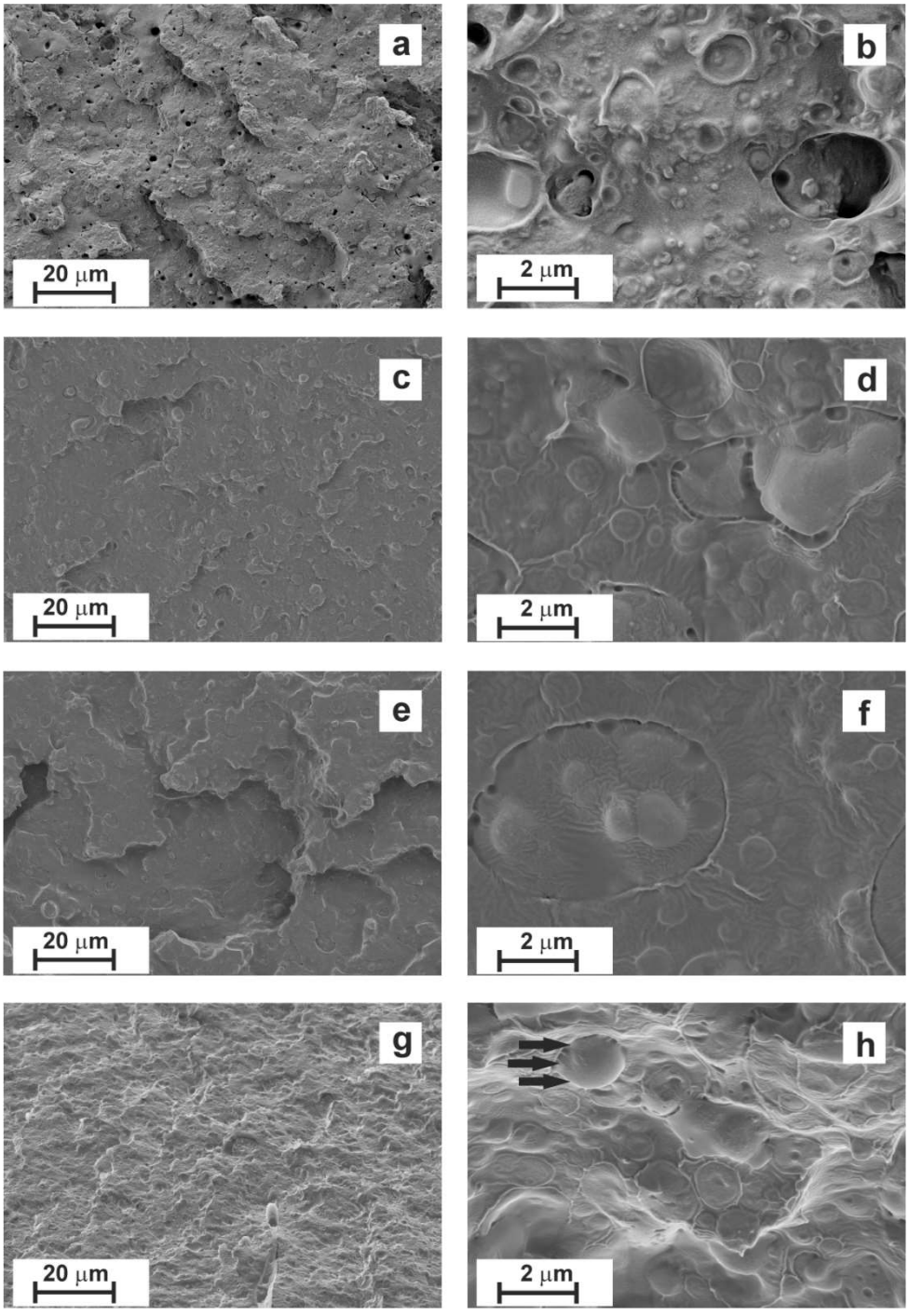

Figure III.5.5. FESEM images of PLA-30TPS blends with different maleinized linseed oil (MLO) content at different magnifications, (a) 2 phr MLO at 1000x, (b) 2 phr MLO at 10000x, (c) 4 phr MLO at 1000x, (d) 4 phr MLO at 10000x, (e) 6 phr MLO at 1000x, (f) 6 phr MLO at 10000x, (g) 8 phr MLO at 1000x, (h) 8 phr MLO at 10000x.

As we have previously described, MLO provides a combined effect on these blends. On the one hand, a clear plasticization effect can be observed by mechanical characterization as MLO increases the free volume. This phenomenon has a positive effect on polymer chain mobility as polymer-polymer interactions are lowered and additionally, the plasticizer provides a lubricant effect. On the other hand, a compatibilization effect is achieved by MLO which can interact with both poly(lactic acid) chain ends and hydroxyl groups in thermoplastic starch thus leading to an overlapped compatibilization and chain extension effect which in turn, is responsible for the observed increase in ductile-flexible properties of PLA-30TPS blends. As the MLO increases the blend becomes saturated and phase separation occurs for MLO content over 6 phr. **Figure III.5.5h** shows some voids that can be related to excess MLO.

Conclusions.

Thermoplastic starch offers very restricted miscibility with PLA as evidenced by FESEM. Addition of TPS leads to an improvement on toughness due to a microstructure composed of a brittle PLA rich phase in which fine TPS rich microspheres are finely dispersed. This particular microstructure results in improved toughness. The lack of strong PLA-TPS interactions does not allow higher ductile properties. To achieve this, a plasticization strategy with maleinized linseed oil (MLO) has been proposed in this research work. Addition of an environmentally friendly plasticizer derived from vegetable oils, maleinized linseed oil (MLO) at relatively low contents in the 2-6 phr leads to a remarkable increase in mechanical ductile properties such as elongation at break and impact-absorbed energy due to a combination of different phenomena. Maleinized linseed oil exerts a typical plasticization effect by increasing the free volume and lowering polymer-polymer interactions and that results in increased chain mobility due to the lubricant effect provided by the plasticizer. On the other hand, the particular chemical structure of maleinized linseed oil, with maleic anhydride groups allows some reactions with hydroxyl groups in both PLA end chains

and starch chains resulting in a chain extension and compatibilization effect respectively. With regard to the elongation at break, unblended and unplasticized PLA shows an elongation at break of about 7%. This value is increased by blending PLA with 30 wt.% TPS up to values of 21% but the addition of 4-6 phr MLO leads to an elongation at break of 140-160% respectively. Similar tendency is detected for energy absorption and other ductile properties. Nevertheless, it is important to note that plasticizer saturation occurs for relatively low MLO content. Over 6 phr MLO a decrease in ductility and ductile properties and an increase in mechanical resistant properties can be detected. This saturation can lead to phase separation which in turn is responsible for stress concentration phenomena thus leading to fracture. The plasticization effect of MLO is clearly evident by a decrease in the glass transition temperature (T_g) of the PLA rich phase as evidenced by differential scanning calorimetry (DSC) and dynamic mechanical thermal analysis (DMTA). On the other hand, MLO also provides a compatibilization effect that allows improving compatibility between PLA and TPS and this also has a positive effect on overall properties. In general terms, maleinized linseed oil (MLO) is an attractive additive to provide plasticization properties to brittle polymers and also improve compatibility in immiscible or partially miscible polymer blends. In addition is natural origin represents an environmental efficient solution to improve industrial formulations based on biopolymers and biopolymer blends.

Acknowledgements.

This research was supported by the Ministry of Economy and Competitiveness - MINECO, Ref: MAT2014-59242-C2-1-R. Authors also thank to "Conselleria d'Educació, Cultura i Esport" - Generalitat Valenciana, Ref: GV/2014/008 for financial support.

References.

1. Mulhaupt, R., *The use of renewable resources: Possibilities and limitations*. Chimia, 1996. **50**(5): p. 191-198.

2. Arrieta, M.P., Samper, M.D., Lopez, J., and Jimenez, A., *Combined Effect of Poly(hydroxybutyrate) and Plasticizers on Polylactic acid Properties for Film Intended for Food Packaging*. Journal of Polymers and the Environment, 2014. **22**(4): p. 460-470.

3. Arrieta, M.P., Lopez, J., Hernandez, A., and Rayon, E., *Ternary PLA-PHB-Limonene blends intended for biodegradable food packaging applications*. European Polymer Journal, 2014. **50**: p. 255-270.

4. Vroman, I. and Tighzert, L., *Biodegradable Polymers*. Materials, 2009. **2**(2): p. 307-344.

5. Arrieta, M.P., Lopez, J., Rayon, E., and Jimenez, A., *Disintegrability under composting conditions of plasticized PLA-PHB blends*. Polymer Degradation and Stability, 2014. **108**: p. 307-318.

6. Bhatia, S.K., Shim, Y.-H., Jeon, J.-M., Brigham, C.J., Kim, Y.-H., Kim, H.-J., Seo, H.-M., Lee, J.-H., Kim, J.-H., Yi, D.-H., Lee, Y.K., and Yang, Y.-H., *Starch based polyhydroxybutyrate production in engineered Escherichia coli*. Bioprocess and Biosystems Engineering, 2015. **38**(8): p. 1479-1484.

7. Liaud, N., Rosso, M.-N., Fabre, N., Crapart, S., Herpoel-Gimbert, I., Sigoillot, J.-C., Raouche, S., and Levasseur, A., *L-lactic acid production by Aspergillus brasiliensis overexpressing the heterologous ldha gene from Rhizopus oryzae*. Microbial Cell Factories, 2015. **14**(1): DOI: 10.1186/s12934-015-0249-x.

8. Pessione, A., Zapponi, M., Mandili, G., Fattori, P., Mangiapane, E., Mazzoli, R., and Pessione, E., *Enantioselective lactic acid production by an Enterococcus faecium strain showing potential in agro-industrial waste bioconversion: Physiological and proteomic studies*. Journal of Biotechnology, 2014. **173**: p. 31-40.

9. Poomipuk, N., Reungsang, A., and Plangklang, P., *Poly-beta-hydroxyalkanoates production from cassava starch hydrolysate by Cupriavidus sp KKU38*. International Journal of Biological Macromolecules, 2014. **65**: p. 51-64.

10. Cheng, H.-Y., Yang, Y.-J., Li, S.-C., Hong, J.-Y., and Jang, G.-W., *Modification and extrusion coating of polylactic acid films*. Journal of Applied Polymer Science, 2015. **132**(35).

11. Sanyang, M.L. and Sapuan, S.M., *Development of expert system for biobased polymer material selection: food packaging application*. Journal of Food Science and Technology, 2015. **52**(10): p. 6445-54.

12. Plackett, D.V., Holm, V.K., Johansen, P., Ndoni, S., Nielsen, P.V., Sipilainen-Malm, T., Sodergard, A., and Verstichel, S., *Characterization of L-polylactide and L-polylactide-polycaprolactone co-polymer films for use in cheese-packaging applications*. Packaging Technology and Science, 2006. **19**(1): p. 1-24.

13. Hutmacher, D.W., Goh, J.C.H., and Teoh, S.H., *An introduction to biodegradable materials for tissue engineering applications*. Annals Academy of Medicine Singapore, 2001. **30**(2): p. 183-191.

14. Averous, L., *Biodegradable multiphase systems based on plasticized starch: A review*. Journal of Macromolecular Science-Polymer Reviews, 2004. **C44**(3): p. 231-274.

15. Lasprilla, A.J.R., Martinez, G.A.R., Lunelli, B.H., Jardini, A.L., and Maciel Filho, R., *Poly-lactic acid synthesis for application in biomedical devices - A review*. Biotechnology Advances, 2012. **30**(1): p. 321-328.

16. Yokesahachart, C. and Yoksan, R., *Effect of amphiphilic molecules on characteristics and tensile properties of thermoplastic starch and its blends with poly(lactic acid)*. Carbohydrate Polymers, 2011. **83**(1): p. 22-31.

17. Mohammed, F.S., Conley, M., Saunders, S.R., Switzer, J., Jha, R., Cogen, J.M., Chaudhary, B.I., Pollet, P., Eckert, C.A., and Liotta, C.L., *Epoxidized linolenic acid salts as multifunctional additives for the thermal stability of plasticized PVC*. Journal of Applied Polymer Science, 2015. **132**(13).

18. Narute, P., Rao, G.R., Misra, S., and Palanisamy, A., *Modification of cottonseed oil for amine cured epoxy resin: Studies on thermo-mechanical, physico-chemical, morphological and antimicrobial properties*. Progress in Organic Coatings, 2015. **88**: p. 316-324.

19. Shi, Q., Chen, C., Gao, L., Jiao, L., Xu, H., and Guo, W., *Physical and degradation properties of binary or ternary blends composed of poly (lactic acid), thermoplastic starch and GMA grafted POE*. Polymer Degradation and Stability, 2011. **96**(1): p. 175-182.

20. Tsui, A., Wright, Z.C., and Frank, C.W., *Biodegradable Polyesters from Renewable Resources*, in Annual Review of Chemical and Biomolecular Engineering, **Vol 4**, J.M. Prausnitz, Editor. 2013. p. 143.

21. Oromiehie, A.R., Lari, T.T., and Rabiee, A., *Physical and thermal mechanical properties of corn starch/LDPE composites*. Journal of Applied Polymer Science, 2013. **127**(2): p. 1128-1134.

22. Ren, J., Fu, H., Ren, T., and Yuan, W., *Preparation, characterization and properties of binary and ternary blends with thermoplastic starch, poly(lactic acid) and poly(butylene adipate-co-terephthalate)*. Carbohydrate Polymers, 2009. **77**(3): p. 576-582.

23. Liu, H. and Zhang, J., *Research Progress in Toughening Modification of Poly(lactic acid)*. Journal of Polymer Science Part B-Polymer Physics, 2011. **49**(15): p. 1051-1083.

24. Niazi, M.B.K., Zijlstra, M., and Broekhuis, A.A., *Influence of plasticizer with different functional groups on thermoplastic starch*. Journal of Applied Polymer Science, 2015. **132**(22).

25. Boonprasith, P., Wootthikanokkhan, J., and Nimitsiriwat, N., *Mechanical, thermal, and barrier properties of nanocomposites based on poly(butylene succinate)/thermoplastic starch blends containing different types of clay*. Journal of Applied Polymer Science, 2013. **130**(2): p. 1114-1123.

26. Sahari, J., Sapuan, S.M., Zainudin, E.S., and Maleque, M.A., *Thermo-mechanical behaviors of thermoplastic starch derived from sugar palm tree (Arenga pinnata)*. Carbohydrate Polymers, 2013. **92**(2): p. 1711-1716.

27. Mahieu, A., Terrie, C., and Youssef, B., *Thermoplastic starch films and thermoplastic starch/polycaprolactone blends with oxygen-scavenging properties: Influence of water content*. Industrial Crops and Products, 2015. **72**: p. 192-199.

28. Chocyk, D., Gladyszewska, B., Ciupak, A., Oniszczuk, T., Moscicki, L., and Rejak, A., *Influence of water addition on mechanical properties of thermoplastic starch foils*. International Agrophysics, 2015. **29**(3): p. 267-273.

29. Schmitt, H., Guidez, A., Prashantha, K., Soulestin, J., Lacrampe, M.F., and Krawczak, P., *Studies on the effect of storage time and plasticizers on the structural variations in thermoplastic starch*. Carbohydrate Polymers, 2015. **115**: p. 364-372.

30. Zhang, Y., Rempel, C., and Liu, Q., *Thermoplastic Starch Processing and Characteristics-A Review*. Critical Reviews in Food Science and Nutrition, 2014. **54**(10): p. 1353-1370.

31. Clasen, S.H., Mueller, C.M.O., and Pires, A.T.N., *Maleic Anhydride as a Compatibilizer and Plasticizer in TPS/PLA Blends*. Journal of the Brazilian Chemical Society, 2015. **26**(8): p. 1583-1590.

32. Raquez, J.-M., Nabar, Y., Srinivasan, M., Shin, B.-Y., Narayan, R., and Dubois, P., *Maleated thermoplastic starch by reactive extrusion*. Carbohydrate Polymers, 2008. **74**(2): p. 159-169.

33. Teixeira, E.d.M., Curvelo, A.A.S., Correa, A.C., Marconcini, J.M., Glenn, G.M., and Mattoso, L.H.C., *Properties of thermoplastic starch from cassava bagasse and cassava starch and their blends with poly (lactic acid)*. Industrial Crops and Products, 2012. **37**(1): p. 61-68.

34. Mittal, V., Akhtar, T., and Matsko, N., *Mechanical, Thermal, Rheological and Morphological Properties of Binary and Ternary Blends of PLA, TPS and PCL*. Macromolecular Materials and Engineering, 2015. **300**(4): p. 423-435.

35. Detyothin, S., Selke, S.E.M., Narayan, R., Rubino, M., and Auras, R.A., *Effects of molecular weight and grafted maleic anhydride of functionalized polylactic acid used in reactive compatibilized binary and ternary blends of polylactic acid and thermoplastic cassava starch*. Journal of Applied Polymer Science, 2015. **132**(28).

36. Zhu, R., Liu, H., and Zhang, J., *Compatibilizing Effects of Maleated Poly(lactic acid) (PLA) on Properties of PLA/Soy Protein Composites*. Industrial & Engineering Chemistry Research, 2012. **51**(22): p. 7786-7792.

37. Shin, B.Y., Jang, S.H., and Kim, B.S., *Thermal, Morphological, and Mechanical Properties of Biobased and Biodegradable Blends of Poly(lactic acid) and Chemically Modified Thermoplastic Starch*. Polymer Engineering and Science, 2011. **51**(5): p. 826-834.

38. Gao, H., Hu, S., Su, F., Zhang, J., and Tang, G., *Mechanical, Thermal, and Biodegradability Properties of PLA/Modified Starch Blends*. Polymer Composites, 2011. **32**(12): p. 2093-2100.

39. Yu, Y., Cheng, Y., Ren, J., Cao, E., Fu, X., and Guo, W., *Plasticizing effect of poly(ethylene glycol)s with different molecular weights in poly(lactic acid)/starch blends*. Journal of Applied Polymer Science, 2015. **132**(16).

40. NOVAMONT. *Copoliéster alifático/aromático biodegradable (AAPE)*. 2010; Available from:http://patentados.com/invento/poliesteres-alifaticos-aromaticos-biodegradables.html.

41. Li, H. and Huneault, M.A., *Effect of Chain Extension on the Properties of PLA/TPS Blends*. Journal of Applied Polymer Science, 2011. **122**(1): p. 134-141.

42. Mikus, P.Y., Alix, S., Soulestin, J., Lacrampe, M.F., Krawczak, P., Coqueret, X., and Dole, P., *Deformation mechanisms of plasticized starch materials*. Carbohydrate Polymers, 2014. **114**: p. 450-457.

43. Chieng, B.W., Ibrahim, N.A., Then, Y.Y., and Loo, Y.Y., *Epoxidized Vegetable Oils Plasticized Poly(lactic acid) Biocomposites: Mechanical, Thermal and Morphology Properties*. Molecules, 2014. **19**(10): p. 16024-16038.

44. Hee-Young Kim, S.S.P., and Seung-Taik, L., *Preparation, characterization and utilization of starch nanoparticles*. Colloids and Surfaces B: Biointerfaces, 2014. **126**: p. 607-620.

45. Huneault, M.A. and Li, H., *Morphology and properties of compatibilized polylactide/thermoplastic starch blends*. Polymer, 2007. **48**(1): p. 270-280.

Carbohydrate Polymers 147 (2016) 60–68

Contents lists available at ScienceDirect

Carbohydrate Polymers

journal homepage: www.elsevier.com/locate/carbpol

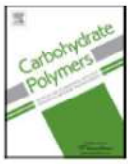

The effect of maleinized linseed oil (MLO) on mechanical performance of poly(lactic acid)-thermoplastic starch (PLA-TPS) blends

J.M. Ferri*, D. Garcia-Garcia, L. Sánchez-Nacher, O. Fenollar, R. Balart

Instituto de Tecnología de Materiales (ITM), Universitat Politècnica de València (UPV), Plaza Ferrandiz y Carbonell 1, 03801 Alcoy, Alicante, Spain

ARTICLE INFO

Article history:
Received 14 January 2016
Received in revised form 24 March 2016
Accepted 27 March 2016
Available online 29 March 2016

Keywords:
Poly(lactic acid)
Thermoplastic starch
Plasticizing
Maleinized linseed oil

ABSTRACT

In this work, poly(lactic acid), PLA and thermoplastic starch, TPS blends (with a fixed content of 30 wt.% TPS) were prepared by melt extrusion process to increase the low ductile properties of PLA. The TPS used contains an aliphatic/aromatic biodegradable polyester (AAPE) that provides good resistance to aging and moisture. This blend provides slightly improved ductile properties with an increase in elongation at break of 21.5% but phase separation is observed due to the lack of strong interactions between the two polymers. Small amounts of maleinized linseed oil (MLO) can positively contribute to improve the ductile properties of these blends by a combined plasticizing-compatibilizing effect. The elongation at break increases over 160% with the only addition of 6 phr MLO. One of the evidence of the plasticizing-compatibilizing effect provided by MLO is the change in the glass transition temperature (T_g) with a decrease of about 10 °C. Field emission scanning electron microscopy (FESEM) of PLA-TPS blends with varying amounts of maleinized linseed oil also suggests an increase in compatibility.

Chapter III.6

Chapter III.6. The effect of beta-tricalcium phosphate on mechanical and thermal performance of poly(lactic acid)

“The effect of beta-tricalcium phosphate on mechanical and thermal performance of poly(lactic acid)”

J.M. Ferri, I. Gisbert, D. García-Sanoguera, M.J. Reig, R. Balart

Instituto de Tecnología de Materiales (ITM)

Universitat Politècnica de València (UPV)

Plaza Ferrandiz y Carbonell 1, 03801, Alcoy, Alicante (Spain)

Journal of Composite Materials 50: 4189-4198 (2016)

Abstract.

Orthophosphates are bioactive crystals with similar structure, in terms of elemental composition and crystal nature, to human bone. In this work, biocomposite materials were prepared with poly(lactic acid) (PLA) as matrix, and beta-tricalcium phosphate (β-TCP) as osteoconductive filler by extrusion-compounding followed by conventional injection molding. The β-TCP load content was varied in the 10-40 wt% range and the influence of the β-TCP load on mechanical performance of PLA/ β-TCP composites was evaluated. Mechanical properties of composites were obtained by standardized tensile, flexural, impact, and hardness tests. Thermal analysis of composites was carried out by means of differential scanning calorimetry; degradation at high temperatures was studied by thermogravimetric analysis; and the effect of the β-TCP load on dynamical response of composites was studied by mechanical thermal analysis in torsion mode. The best-balanced properties were obtained for PLA composites containing 30 wt% β-TCP with a remarkable increase in the Young's modulus. These materials offer interesting properties to be used as base materials for medical applications such as interference screws due to high stiffness and mechanical resistance.

Keywords: Beta-tricalcium phosphate; poly(lactic acid); thermal and mechanical properties; fasteners; bone tissue engineering

Introduction.

The use of joint devices such as screws, fasteners, anchor stitches, etc. for tendon and bone reconstruction or repairing has progressed in the last years; typical biocompatible and biostable materials based on high strength metallic alloys and insoluble ceramics have given way to new resorbable and biocompatible materials based on polymeric matrices. Today, it is possible to find a wide variety of materials that could be potentially used in the biomedical sector. In the last years, important efforts have been done to develop new metallic, ceramics, polymeric, and composite materials [1, 2] thus giving evidence of the need and importance of these materials in medicine.

With regard to metals, titanium based alloys [3-5] are widely used; in particular, Ti6Al4V alloy [6, 7] is one of the most used. Other alloys such as CoCr [8], CoCrMo [6] and stainless steels [9] are used. These metallic alloys are biocompatible but they are not able to induce bone tissue regeneration, so that, these alloys must be subjected to surface treatments to allow osteointegration [10-12]. This costly and arduous procedure plays a key role in bone tissue regeneration among the bone-fixation interface to avoid potential rejection.

On the other hand, calcium phosphate ceramic materials such as hydroxylapatite (HA) are excellent candidates as fillers with osteoconductive properties. HA is a bio crystal that can be found in human bones in combination with collagen. HA and other calcium phosphates can be considered as biomimetic materials with no rejection phenomena when in contact with connective tissue at physiological media pH [13]. Nevertheless, due to its ceramic nature, HA is highly fragile.

For these reasons, the medical sector demands new materials with a balance among mechanical performance, density, and cost. An additional attracting feature for biomaterials (in particular, materials for fixation devices and screws), is biodegradation/resorption in physiologic media. This allows controlled decomposition, gradual resorption and bone growth in the bone-fixation interface thus

leading to total osteointegration. Biodegradable polymeric materials are an interesting choice due to their easy processing and potential degradation in physiological media [14, 15]. An attracting approach is based on the fact that "the best bone substitute is the regenerated bone itself". The polymeric material degrades-dissolves slowly and progressively and it is continuously resorbed and substituted by soft tissue and new specialized connective tissue. This fact leads polymers to an advantageous position if compared to conventional metallic and ceramic materials, since second surgery to remove fixation plates, screws, pins etc. once the bone has regenerated, can be avoided. Biodegradable polymers such as poly(glycolic acid), PGA, poly(butylene succinate), PBS, poly(ester amides), PEA, poly(caprolactone), PCL, poly(lactic acid), and their blends and/or copolymers are increasingly being used in biomedical applications [16-22]. The different biodegradation rates of these polymers and their copolymers, allows tailoring the desired resorption times to ensure optimum recovery.

Formulation of an osteoconductive, biocompatible, resorbable fixation device should be composed of two main components: a biodegradable polymeric matrix and an osteoconductive filler such as those derived from orthophosphates: oxyapatite (OXA), hydroxylapatite (HA), biphasic calcium phosphate (BCP), beta-tricalcium phosphate (β-TCP), or mixtures of all these phosphate materials as all they have similar composition to that of the human bone [23, 24]. Orthophosphates can be classified in terms of their solubility in physiological media from the highest to the lowest [25] and the Ca/P ratio. As β-TCP particles solubilize, they supply calcium and phosphate in a controlled way and this leads to mineralization of the bone-fixation interface thus allowing formation of connective tissue and good osteointegration [26, 27]. Osteointegration allows optimum bony growth and bone healing, which leads to stabilize the fracture of bone defect.

Connective tissue can be soft (cartilaginous) at the beginning and afterwards, hard bone tissue or simply fibrous-cartilaginous tissue if the fracture affected only tendons or ligaments. Several "in vivo" studies with composite materials based on poly(lactic acid) (PLA) matrix and β-TCP showed a remarkable proliferation of mesenchymal stem cells (MSCs), which led to more adipose-derived stem cells

differentiation (ASCs). The potential of rejection or inflammatory process with PLA/β-TCP systems are extremely low. This is due to different phenomena: on the one hand the low degradation rate of PLA and on the other hand, the formation of a buffer solution with dissolved β-TCP particles, which contributes to maintain constant pH. This occurs when alkaline salts such as phosphates (PO_4^{3-}) are present [28].

Manufacturing of polymeric fixation devices, interference screws, fixation pins, etc. by extrusion-injection molding processes is difficult to be substituted by other techniques due to an excellent balance between technical viability, costs and overall properties [29]. Extrusion-injection techniques offer attracting advantages to obtain optimum particle dispersion that leads to high homogeneity [29]. In addition, an increase in the residence time in the screw has a positive effect on particle dispersion. Furthermore, an increase in the applied pressure reduces porosity [30]. Foaming is one of the widely used techniques to mold polymers into shapes. The porous structure favors interaction with human tissues and, subsequently, osteointegration during the resorption process. In this work, PLA/β-TCP composite materials in the form of block materials with potential use as resorbable medical joint devices were prepared by the injection moulding process with previous extrusion-compounding. The extrusion is intended for improved particle dispersion and the injection molding is intended for high quality end and cost-effective products that do not require further processing. The particle aggregation and dispersion has been tested by microscopic techniques by using selective extraction/dissolving of the β-TCP particles with HCl acid solution to reveal the real structure. The load content of β-TCP varied in the 0-40 wt% range and the effects of β-TCP content on mechanical and thermal properties of PLA/β-TCP composites were evaluated.

Experimental.

Materials.

The base polymer was a PLA, commercial grade IngeoTM Biopolymer 6201D supplied by NatureWorks LLC (Minnetonka, USA), which is characterized by a content on D-lactic acid of about 2%. Its density is 1.24 g/cm^3 and the melt flow index is in the 15-30 g/(10 min) range at 210 ^{o}C. The osteoconductive filler was β-TCP supplied by Sigma-Aldrich (Steinheim, Germany).

Composite manufacturing.

Four different compositions based on PLA matrix and β-TCP osteoconductive reinforcement were manufactured by extrusion-compounding and subsequent injection molding. **Table III.6.1** summarizes the compositions and the reference material with their corresponding compositions. The β-TCP load varied in the 0-40 wt% range. PLA was dried at 80 ^{o}C for 24 h to remove moisture. PLA/β-TCP composites were compounded in a twin-screw extruder at 60 rpm/min and a temperature profile of 170 ^{o}C (hopper), 175 ^{o}C, 180 ^{o}C and 185 ^{o}C (die). After cooling, compounds were pelletized and subsequently injected in an injection molding machine Meteor 270/75 (Mateu&Sole, Barcelona, Spain) at an injection temperature of 180 ^{o}C.

Table III.6.1. Compositions and designation of PLA/β-TCP composites.

Reference	wt% PLA	wt% β -TCP
PLA	100	-
PLA / 10 β-TCP	90	10
PLA / 20 β-TCP	80	20
PLA / 30 β-TCP	70	30
PLA / 40 β-TCP	60	40

Mechanical characterization of PLA/β-TCP composites.

Mechanical properties of PLA/β-TCP composites were evaluated in tensile and flexural conditions. Tensile and flexural properties were obtained in a universal test machine ELIB 30 (S.A.E. Ibertest, Madrid, Spain) at room temperature following ISO 527-5 and ISO 178:1993 respectively; a load cell of 5 kN was used and the crosshead rate was set to 10 mm/min (tensile tests) and 5 mm/min (flexural tests). Five different specimens were tested and average values of strength and modulus were calculated.

Shore D hardness was obtained in a Shore durometer mod. 673-D (Instrumentos J. Bot S.A., Barcelona, Spain) as indicated in UNE-EN ISO 868.

The ability for energy absorption was estimated by using a 6 J Charpy's pendulum (Metrotec S.A., San Sebastian, Spain) as recommended in ISO179:1993 standard. Tests were carried out for five different unnotched samples and average values of energy absorption were calculated.

Microscopic characterization of PLA/β-TCP composites.

A scanning electron microscope (SEM) Phenom (FEI Company, Eindoven, Netherlands) was used to characterize fractured surfaces from impact tests as well as raw β-TCP microparticles. Samples were previously subjected to a metallization process in a sputter coater EMITECH SC7620 (Quorum Technologies Ltd., East Suseex, UK) with an Au-Pd alloy. The optimum PLA/β-TCP composite were subjected to a treatment with 6 M HCl for 12 h to selectively remove β-TCP from surface thus leading to detailed observation of the composite morphology and samples were observed in a field emission scanning electron microscope (FESEM) ZEISS ULTRA55 from Oxford Instruments (Oxford, UK) at an acceleration voltage of 2 kV. Samples for FESEM observation were subjected to a sputtering process with platinum to obtain detailed information of the particle dispersion.

Dynamic mechanical characterization of PLA/β-TCP composites.

Dynamic mechanical characterization in torsion mode was conducted in an oscillatory rheometer AR G2 (TA Instruments, New Castle, USA), equipped with a torsion clamp accessory for solid samples. Rectangular samples sizing 40x10x4 mm^3 were subjected to a heating program from -50 ^oC up to 110 ^oC at a constant heating rate of 2 ^oC/min; the frequency and the maximum deformation (γ) were set to 1 Hz and 0.1% respectively.

Thermal analysis of PLA/β-TCP composites.

Thermal properties of raw materials and PLA/β-TCP composites were studied by differential scanning calorimetry (DSC) and thermogravimetric analysis (TGA). TGA was carried out in a TGA/SDTA thermobalance mod. 851 (Mettler-Toledo Inc., Schwerzenbach, Switzerland) with a heating program from 30 ^oC to 700 ^oC at a heating rate of 20 ^oC/min in nitrogen atmosphere (66 mL/min). Thermal transitions were evaluated in a DSC model 821 (Mettler-Toledo Inc., Schwerzenbach, Switzerland); samples sizing 7-10 mg were placed into standard 40 µL aluminum crucibles and subjected to a heating program from 30 ^oC to 350 ^oC at a heating rate of 10 ^oC/min in air atmosphere.

Results and discussion.

Effect of weight % β-TCP on mechanical properties of PLA/β-TCP composites.

Figures III.6.1 and **III.6.2** show the plot evolution of the main parameters obtained from tensile and flexural tests respectively.

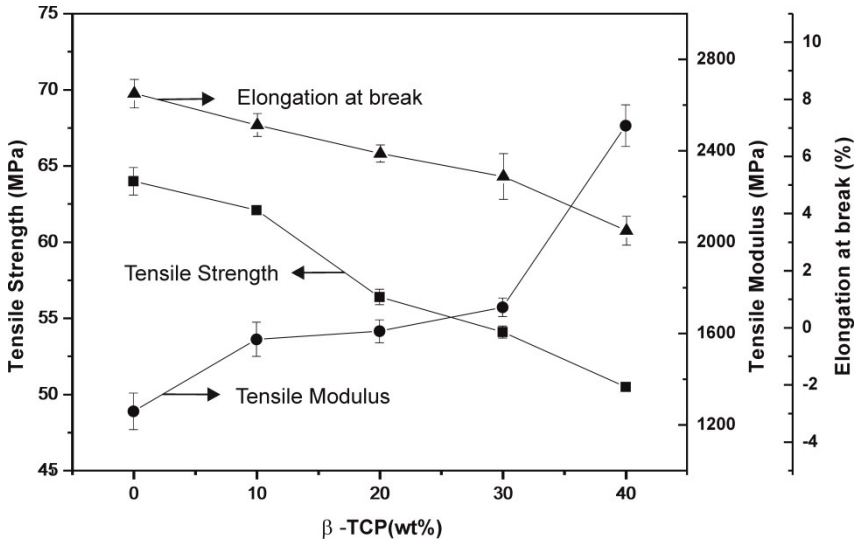

Figure III.6.1. Plot of the evolution of mechanical properties from tensile tests as a function of the weight percent β-TCP.

From observation of tensile test results (**Figure III.6.1**) we see a decrease in tensile strength values with regard to unfilled PLA. The tensile strength of unfilled PLA is close to 64 MPa and decreases up to values of 50.5 MPa for composites containing 40 wt% β-TCP. Nevertheless, for a β-TCP content of 10 wt%, the tensile strength decrease is less than 3%. This is related to low particle-polymer interactions; thus the osteoconductive filler acts as a stress concentrator but the poor interaction makes calcium and phosphate easy available during degradation and this is positive from a biomedical point of view. Intermediate compositions with 20 and 30 wt% β-TCP promote a decrease in tensile strength of about 12% and 15%. With regard to elongation at break the unfilled PLA is characterized by relatively low values around 8%. As the β-TCP content increases, we observe a clear decreasing tendency and minimum values of about 3.4% are obtained for PLA/β-TCP composites with the highest β-TCP content, which represents a percentage decrease of almost 60%. As expected, the elastic modulus increases with β-TCP content thus leading to stiffer materials. This is in total agreement with the evolution of tensile strength and elongation at break. The elastic modulus represents the ratio between the stress and the elongation in the linear region. As abovementioned, we have observed a decrease in

tensile strength but the decrease in elongation at break is still higher so that, the ratio between these values increases due to the lower values of elongation at break.

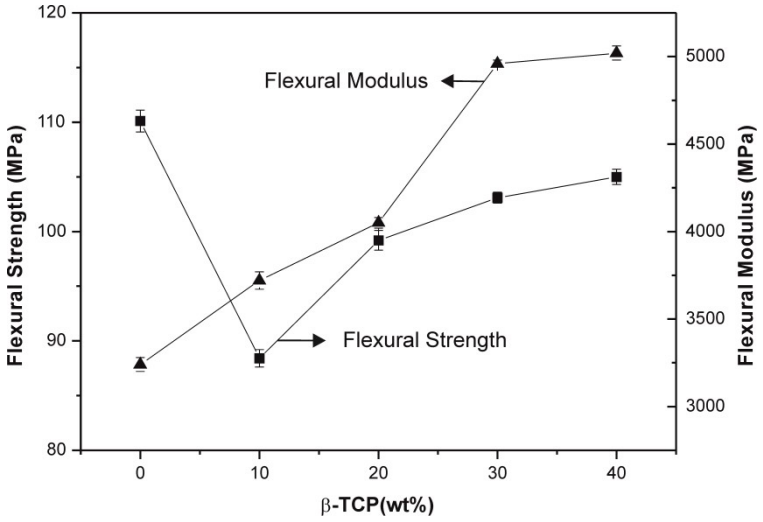

Figure III.6.2. Plot of the evolution of mechanical properties from flexural tests as a function of the weight percent β-TCP.

Different tendency can be observed by following the evolution of the flexural properties of the PLA/β-TCP system. The unfilled PLA is characterized by a flexural strength of about 110 MPa and the flexural strength values in terms of the β-TCP content decreases up to values in the range of 90-100 MPa. It is clear that increasing β-TCP filler increases flexural strength and flexural modulus. However, the resistance is lower in all cases compared to the virgin PLA. The smallest resistance value is obtained for PLA composites containing 10 wt% β-TCP. This may be due to the presence of small particle aggregates that promote crack initiation prematurely thus leading to fracture. However, with increasing β-TCP load we observe stiffer materials and, therefore, an increase in resistance, but always less than virgin PLA due to particle aggregation. On the other hand, the flexural modulus increases in a remarkable way from 3.24 GPa for unfilled PLA up to 5.02 GPa for composites containing 40 wt% β-TCP. Once again, the flexural results indicate that addition of β-TCP provides stiffer materials with slightly lower resistance. Compositions in the 10-20 wt% β-TCP represent a good balance between overall mechanical response as they offer high

stiffness materials with similar resistance and deformation ability to unfilled PLA. The evolution of the Shore D hardness is similar to other mechanical-resistant properties with a clear increase with the β-TCP load.

Another desirable attracting property in materials for fixation devices is the ability to absorb energy during fracture. **Table III.6.2** shows the absorbed energy (Charpy's test) as a function of the β-TCP load content. PLA is a quite fragile material as indicated by the relatively low energy absorption values close to 30.9 kJ/m^2. Addition of β-TCP leads to a slight decrease in absorbed energy. For compositions comprised between 10 and 20 wt% β-TCP, the absorbed energy is reduced up to values of 28.5 kJ/m^2 (percentage decrease of 10%) and 26.0 kJ/m^2 (percentage decrease of about 24%), respectively. These values indicate that the ability of PLA for energy absorption is highly sensitive to presence of stress concentrators such as the case of the osteoconductive β-TCP filler. So that, compositions with more than 20 wt% β-TCP would not be recommended [31] for fixation devices unless additional surface treatments are carried on the filler to minimize the loss on mechanical performance.

Table III.6.2. Shore D hardness values and Charpy's absorbed energy of PLA/β-TCP composites in terms of the β-TCP weight percent.

wt% β-TCP	Shore D hardness	Charpy's impact energy (kJ/m^2)
0	71± 1	30.9± 0.8
10	74± 1	28.5± 0.3
20	75± 1	26.0± 0.9
30	77± 1	21.3± 0.9
40	79± 1	19.3± 1.0

The morphology of the fractured surfaces from impact tests of PLA/β-TCP composites was observed by SEM analysis. **Figure III.6.3(a)** shows typical fracture of unfilled PLA [32]; as the β-TCP content increases we observe more rough surfaces due to presence of filler. Presence of β-TCP leads to a fracture process with a typical flake formation which is representative for a fragile fracture. Increasing flake structure is

representative for more fragile materials as observed in **Table III.6.2** with absorbed energy values.

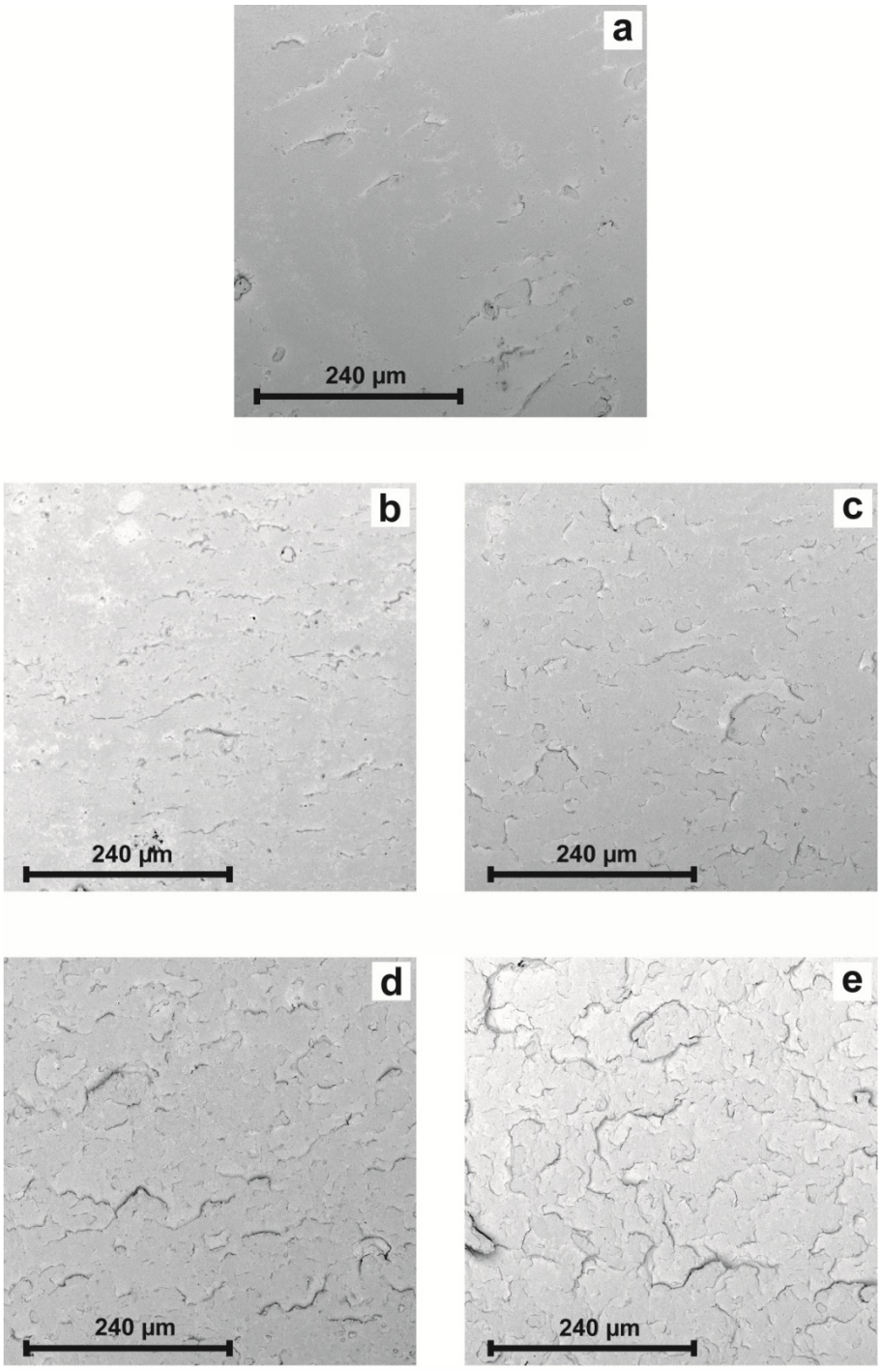

Figure III.6.3. SEM images of fractured surfaces from impact tests corresponding to PLA/β-TCP composites with different weight percent β-TCP: (a) unfilled PLA, (b) 10 wt% β-TCP, (c) 20 wt% β-TCP, (d) 30 wt% β-TCP, (e) 40 wt% β-TCP.

Figure III.6.4 clearly shows the typical distribution β-TCP particles in the PLA matrix. It can be observed good particle dispersion among the PLA matrix. Although some particle-polymer interaction can be observed in **Figure III.6.4(a)** (low particle-polymer gap), in general terms, interaction is not high as previous mechanical characterization has revealed with a decrease in both strength and deformation ability.

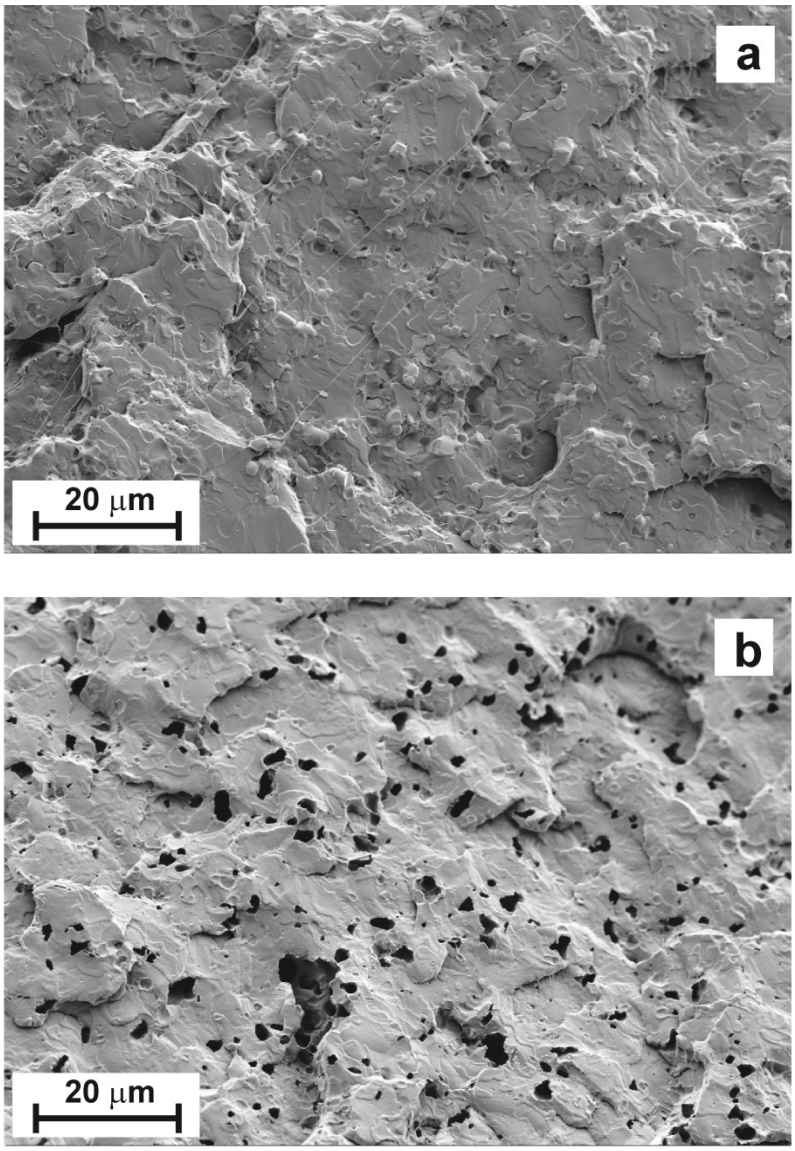

Figure III.6.4. FESEM images of fractured surfaces from impact tests of PLA composite with 30 wt% β-TCP: (a) untreated and (b) treated with 6M HCl for 12 h.

Figure III.6.4(b) shows a field-emission scanning electron microscopic (FESEM) image of a PLA composite containing 30 wt% β-TCP subjected to a treatment with 6 M HCl for 12 h. The voids and holes correspond to removed/dissolved β-TCP and the overall void size and distribution also indicate good particle dispersion.

Effect of weight % β-TCP on thermal properties of PLA/β-TCP composites.

Thermal transitions of PLA/β-TCP composites were evaluated by means of DSC and TGA. **Table III.6.3** shows melt temperature, glass transition temperature (T_g), cold crystallization peaks, and normalized values for the cold crystallization. We observe a slight decrease in the melt peak from 173 ^oC to 170-172 ^oC but it is not relevant. Similar behavior can be observed for the cold crystallization process with a peak at 116 ^oC (unfilled PLA) up to values in the 113-116 ^oC for PLA/β-TCP composites. The crystallization of PLA/β-TCP composites decreases in all formulations compared to the virgin PLA. In addition, the glass transition temperature is slightly lower but it is not relevant as it changes from 65 ^oC (unfilled PLA) to 62-63 ^oC for PLA/β-TCP composites. This could be related to partial hydrolysis of PLA polymer chains due to the presence of a highly hydrophilic filler such as β-TCP which could contribute to hydrolyze [33] some PLA chains and promote a plasticization process with the formed lactic acid olygomers. **Figure III.6.5** shows a comparative plot of the DSC curves for PLA/β-TCP composites with different β-TCP loads in which, the different transitions can be observed. In addition, a double melt peak is detected, which is directly related to a crystalline polymorphism due to presence of small amounts of D-lactide [34]. The change in the peak shape corresponding to PLA with 30 wt% β-TCP is due to increased melting of spherulites D-lactide crystallization. The osteoconductive particles promote this type of crystallization.

Table III.6.3. Summary of the main thermal parameters of PLA/β-TCP composites, obtained by differential scanning calorimetry (DSC).

Sample	Melting temperature (°C)	Glass transition (°C)	Crystalization peak (°C)	Normalized integral (J/g)
PLA	173	65.4	116	40.47
PLA/10β-TCP	172	63.9	113	27.76
PLA/20β-TCP	172	62.2	115	30.23
PLA/30β-TCP	168	63.0	115	34.71
PLA/40β-TCP	172	64.4	116	27.72

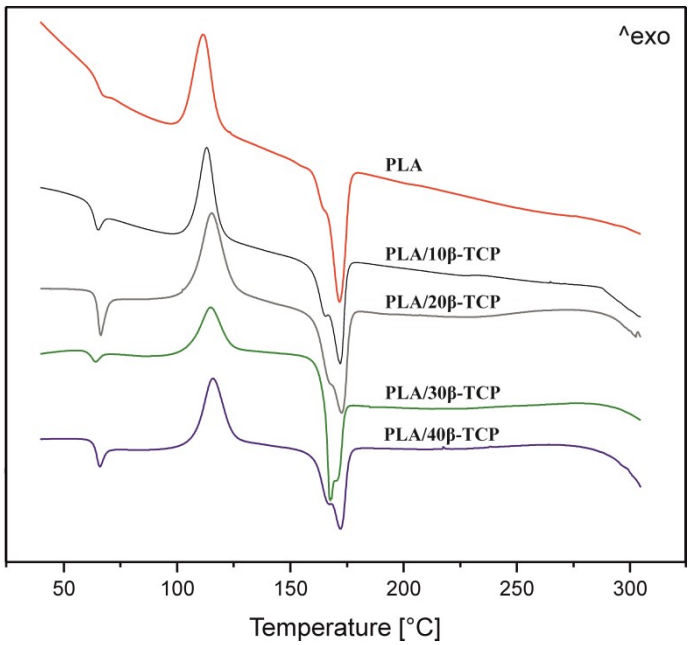

Figure III.6.5. Comparative plot of DSC graphs corresponding to PLA/β-TCP composites with different weight percent β-TCP.

Figure III.6.6 shows thermogravimetric curves (TGA) for PLA/β-TCP composites with different β-TCP content. PLA is highly stable to temperature; nevertheless, PLA/β-TCP composites show a slight decrease in the degradation onset due to hydrolysis processes [35, 36]. As we have described previously, β-TCP is highly hydrophilic and this fact leads to hydrolytic scission of PLA chains thus leading to

formation of lactic acid olygomers. The percentage residue is directly related to the total content on β-TCP inorganic filler; so that, composites with 20 wt% β-TCP show a residual percentage weight of 22% which corresponds to the β-TCP filler plus residual ashes from PLA.

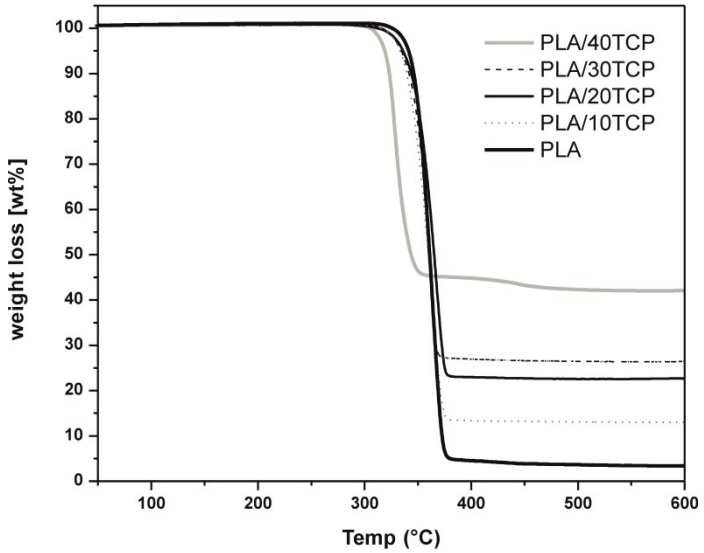

Figure III.6.6. Comparative plot of TGA graphs corresponding to PLA/β-TCP composites with different weight percent β-TCP.

With regard to dynamic mechanical thermal behavior of PLA/β-TCP composites, **Figure III.6.7** shows a comparative plot of the storage modulus (G′) as a function of temperature for different β-TCP loads. As we can see, the storage modulus moves to higher values as the β-TCP content increases which is representative for stiffer materials as described previously. The storage modulus remains almost constant up to values of about 60 ^{o}C. A remarkable decrease in G′ occurs in the 60-80 ^{o}C range which is directly related to the glass transition temperature (T_g). A new increase in storage modulus (G′) is detected at temperatures higher than 90-100 ^{o}C; this is related to the cold crystallization process which leads to increased crystallinity and, subsequently, an increase in stiffness is achieved. As we can clearly detect, the crystallization moves to lower temperatures as the β-TCP content increases due to the nucleating effect of finely dispersed β-TCP into the PLA polymeric matrix [37].

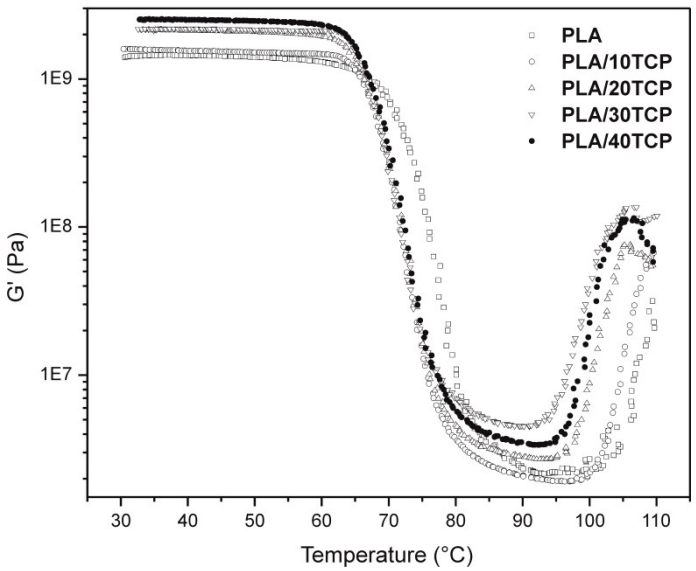

Figure III.6.7. Evolution of the storage modulus (G') of PLA/β-TCP composites with different weight percent β-TCP.

Conclusions.

In this work we developed biocompatible and resorbable composites based on PLA matrix and β-TCP as osteoconductive filler. PLA with 20-30 wt% β-TCP shows an increase in Young's modulus and flexural modulus up to 35% and 53%, respectively. Higher β-TCP loads (>20-30 wt%), produce a significant loss of resilience or ability for energy absorption. A reduction on crystallinity and the degradation onset temperature are observed by adding β-TCP to PLA. Due to the high hydrophilic character of the β-TCP particles, PLA/β-TCP composites are more hydrophilic than neat PLA. This is due to degradation caused by thermal hydrolysis processes. The softening temperature of the composites decreases compared to the polymer without osteoconductive load. This is also due to the lower crystallinity. An increase in the Young's modulus of composites is observed at temperatures below the T_g in comparison with PLA. The Young's modulus increases as the percentage of osteoconductive load rises. Considering that the working temperature of the composites will be lower than the softening point, it can be stated that the PLA composites containing 20-30 wt% β-TCP show a necessary

improvement in mechanical properties to prevent breakage in interference screws made from this material.

Declaration of conflicting interests.

The author(s) declared no potential conflicts of interest with respect to the research, authorship, and/or publication of this article.

Funding.

The author(s) disclosed receipt of the following financial support for the research, authorship, and/or publication of this article: This study was funded by "Conselleria d'Educació, Cultura i Esport" – Generalitat Valenciana ref: GV/2014/008.

References

1. Witte, F., Feyerabend, F., Maier, P., Fischer, J., Stormer, M., Blawert, C., Dietzel, W., and Hort, N., *Biodegradable magnesium-hydroxyapatite metal matrix composites*. Biomaterials, 2007. **28**(13): p. 2163-2174.

2. Jeon, B.J., Jeong, Y.G., Min, B.G., Lyoo, W.S., and Lee, S.C., *Lead Ion Removal Characteristics of Poly(lactic acid)/Hydroxyapatite Composite Foams Prepared by Supercritical CO_2 Process*. Polymer Composites, 2011. **32**(9): p. 1408-1415.

3. Li, Y.H., Yang, C., Zhao, H.D., Qu, S.G., Li, X.Q., and Li, Y.Y., *New Developments of Ti-Based Alloys for Biomedical Applications*. Materials, 2014. **7**(3): p. 1709-1800.

4. Zhu, K.P., Zhu, J.W., and Qu, H.L., *Development and Application of Biomedical Ti Alloys Abroad*. Rare Metal Materials and Engineering, 2012. **41**(11): p. 2058-2063.

5. Geetha, M., Singh, A.K., Asokamani, R., and Gogia, A.K., *Ti based biomaterials, the ultimate choice for orthopaedic implants - A review*. Progress in Materials Science, 2009. **54**(3): p. 397-425.

6. Webster, T.J. and Ejiofor, J.U., *Increased osteoblast adhesion on nanophase metals: Ti, Ti6Al4V, and CoCrMo*. Biomaterials, 2004. **25**(19): p. 4731-4739.

7. Li, J.P., Li, S.H., Van Blitterswijk, C.A., and de Groot, K., *A novel porous Ti6Al4V: Characterization and cell attachment*. Journal of Biomedical Materials Research Part A, 2005. **73A**(2): p. 223-233.

8. Friedman, R.J., Bauer, T.W., Garg, K., Jiang, M., An, Y.H., and Draughn, R.A., *Histological and mechanical comparison of hydroxyapatite-coated cobalt-chrome and titanium implants in the rabbit femur*. Journal of Applied Biomaterials, 1995. **6**(4): p. 231-235.

9. Bordji, K., Jouzeau, E.Y., Mainard, D., Payan, E., Delagoutte, J.P., and Netter, P., *Evaluation of the effect of three surface treatments on the biocompatibility of 316L stainless steel using human differentiated cells*. Biomaterials, 1996. **17**(5): p. 491-500.

10. Choy, M.T., Tang, C.Y., Chen, L., Wong, C.T., and Tsui, C.P., *In vitro and in vivo performance of bioactive Ti6Al4V/TiC/HA implants fabricated by a rapid microwave sintering*

technique. Materials Science & Engineering C-Materials for Biological Applications, 2014. **42**: p. 746-756.

11. Metikos-Hukovic, M., Tkalcec, E., Kwokal, A., and Piljac, J., *An in vitro study of Ti and Ti-alloys coated with sol-gel derived hydroxyapatite coatings*. Surface & Coatings Technology, 2003. **165**(1): p. 40-50.

12. Wang, J., de Boer, J., and de Groot, K., *Preparation and characterization of electrodeposited calcium phosphate/chitosan coating on Ti6Al4V plates*. Journal of Dental Research, 2004. **83**(4): p. 296-301.

13. Melero H, F.J., Guilemany JM., *Recubrimientos bioactivos: Hidroxiapatita y titania*. Biomecánica 2011. **19**: p. 35-48.

14. Hutmacher, D.W., Goh, J.C.H., and Teoh, S.H., *An introduction to biodegradable materials for tissue engineering applications*. Annals Academy of Medicine Singapore, 2001. **30**(2): p. 183-191.

15. Wahit, M.U., Akos, N.I., and Laftah, W.A., *Influence of natural fibers on the mechanical properties and biodegradation of poly(lactic acid) and poly(ε-caprolactone) composites: A review*. Polymer Composites, 2012. **33**(7): p. 1045-1053.

16. Rokkanen, P.U., Bostman, O., Hirvensalo, E., Makela, E.A., Partio, E.K., Patiala, H., Vainionpaa, S., Vihtonen, K., and Tormala, P., *Bioabsorbable fixation in orthopaedic surgery and traumatology*. Biomaterials, 2000. **21**(24): p. 2607-2613.

17. Maurus, P.B. and Kaeding, C.C., *Bioabsorbable implant material review*. Operative Techniques in Sports Medicine, 2004. **12**(3): p. 158-160.

18. Middleton, J.C. and Tipton, A.J., *Synthetic biodegradable polymers as orthopedic devices*. Biomaterials, 2000. **21**(23): p. 2335-2346.

19. Tayton, E., Purcell, M., Aarvold, A., Smith, J.O., Briscoe, A., Kanczler, J.M., Shakesheff, K.M., Howdle, S.M., Dunlop, D.G., and Oreffo, R.O.C., *A comparison of polymer and polymer-hydroxyapatite composite tissue engineered scaffolds for use in bone regeneration. An in vitro and in vivo study*. Journal of Biomedical Materials Research Part A, 2014. **102**(8): p. 2613-2624.

20. Vila, O.F., Bago, J.R., Navarro, M., Alieva, M., Aguilar, E., Engel, E., Planell, J., Rubio, N., and Blanco, J., *Calcium phosphate glass improves angiogenesis capacity of poly(lactic acid) scaffolds and stimulates differentiation of adipose tissue-derived mesenchymal stromal cells to the endothelial lineage*. Journal of Biomedical Materials Research Part A, 2013. **101**(4): p. 932-941.

21. Jiang, L., Xiong, C., Jiang, L., and Xu, L., *Effect of different precipitation procedures on the properties of nano-hydroxyapatite/poly-lactic-co-glycolic acid composite*. Polymer Composites, 2013. **34**(7): p. 1158-1162.

22. Shi, N. and Dou, Q., *Crystallization Behavior, Morphology, and Mechanical Properties of Poly(lactic acid)/Tributyl Citrate/Treated Calcium Carbonate Composites*. Polymer Composites, 2014. **35**(8): p. 1570-1582.

23. Stutzle, H., Hallfeldt, K., Mandelkow, H., Kessler, S., and Schweiberer, L., *Bone substitutes and bone formation*. Orthopade, 1998. **27**(2): p. 118-125.

24. Chae, T., Yang, H., Ko, F., and Troczynski, T., *Bio-inspired dicalcium phosphate anhydrate/poly(lactic acid) nanocomposite fibrous scaffolds for hard tissue regeneration: In situ synthesis and electrospinning*. Journal of Biomedical Materials Research Part A, 2014. **102**(2): p. 514-522.

25. Bohner, M., *Calcium orthophosphates in medicine: from ceramics to calcium phosphate cements*. *Injury*-International Journal of the Care of the Injured, 2000. **31**: p. S37-S47.

26. Navarro, M., Engel, E., Planell, J.A., Amaral, I., Barbosa, M., and Ginebra, M.P., *Surface characterization and cell response of a PLA/CaP glass biodegradable composite material*. Journal of Biomedical Materials Research Part A, 2008. **85A**(2): p. 477-486.

27. Yanoso-Scholl, L., Jacobson, J.A., Bradica, G., Lerner, A.L., O'Keefe, R.J., Schwarz, E.M., Zuscik, M.J., and Awad, H.A., *Evaluation of dense polylactic acid/beta-tricalcium phosphate scaffolds for bone tissue engineering*. Journal of Biomedical Materials Research Part A, 2010. **95A**(3): p. 717-726.

28. Agrawal, C.M. and Athanasiou, K.A., *Technique to control pH in vicinity of biodegrading PLA-PGA implants*. Journal of Biomedical Materials Research, 1997. **38**(2): p. 105-114.

29. Mathieu, L.M., Bourban, P.E., and Manson, J.A.E., *Processing of homogeneous ceramic/polymer blends for bioresorbable composites*. Composites Science and Technology, 2006. **66**(11-12): p. 1606-1614.

30. Dee, G.T. and Sauer, B.B., *The surface tension of polymer liquids*. Macromolecular Symposia, 1999. **139**: p. 115-123.

31. Damadzadeh, B., Jabari, H., Skrifvars, M., Airola, K., Moritz, N., and Vallittu, P.K., *Effect of ceramic filler content on the mechanical and thermal behaviour of poly-l-lactic acid and poly-l-lactic-co-glycolic acid composites for medical applications.* Journal of Materials Science-Materials in Medicine, 2010. **21**(9): p. 2523-2531.

32. Duek, E.A.R., Zavaglia, C.A.C., and Belangero, W.D., *In vitro study of poly(lactic acid) pin degradation*. Polymer, 1999. **40**(23): p. 6465-6473.

33. Carlson, D., Dubois, P., Nie, L., and Narayan, R., *Free radical branching of polylactide by reactive extrusion*. Polymer Engineering and Science, 1998. **38**(2): p. 311-321.

34. Averous, L., *Biodegradable multiphase systems based on plasticized starch: A review*. Journal of Macromolecular Science-Polymer Reviews, 2004. **C44**(3): p. 231-274.

35. Auras, R., Harte, B., and Selke, S., *An overview of polylactides as packaging materials*. Macromolecular Bioscience, 2004. **4**(9): p. 835-864.

36. Carrasco, F., Pages, P., Gamez-Perez, J., Santana, O.O., and Maspoch, M.L., *Processing of poly(lactic acid): Characterization of chemical structure, thermal stability and mechanical properties*. Polymer Degradation and Stability, 2010. **95**(2): p. 116-125.

37. Hu, H.-T., Lee, S.-Y., Chen, C.-C., Yang, Y.-C., and Yang, J.-C., *Processing and properties of hydrophilic electrospun polylactic acid/beta-tricalcium phosphate membrane for dental applications*. Polymer Engineering and Science, 2013. **53**(4): p. 833-842.

Article

JOURNAL OF COMPOSITE MATERIALS

Journal of Composite Materials
0(0) 1–10

DOI: 10.1177/0021998316636205
jcm.sagepub.com
SAGE

The effect of beta-tricalcium phosphate on mechanical and thermal performances of poly(lactic acid)

JM Ferri, I Gisbert, D García-Sanoguera, MJ Reig and R Balart

Abstract

Orthophosphates are bioactive crystals with similar structure, in terms of elemental composition and crystal nature, to human bone. In this work, biocomposite materials were prepared with poly(lactic acid) (PLA) as matrix, and beta-tricalcium phosphate (β-TCP) as osteoconductive filler by extrusion-compounding followed by conventional injection molding. The β-TCP load content was varied in the 10–40 wt% range and the influence of the β-TCP load on mechanical performance of PLA/β-TCP composites was evaluated. Mechanical properties of composites were obtained by standardized tensile, flexural, impact, and hardness tests. Thermal analysis of composites was carried out by means of differential scanning calorimetry; degradation at high temperatures was studied by thermogravimetric analysis; and the effect of the β-TCP load on dynamical response of composites was studied by mechanical thermal analysis in torsion mode. The best-balanced properties were obtained for PLA composites containing 30 wt% β-TCP with a remarkable increase in the Young's modulus. These materials offer interesting properties to be used as base materials for medical applications such as interference screws due to high stiffness and mechanical resistance.

Keywords

Beta-tricalcium phosphate, poly(lactic acid), thermal and mechanical properties, fasteners, bone tissue engineering

Chapter III.7

Chapter III.7. Manufacturing and characterization of poly(lactic acid) composites with hydroxyapatite

“Manufacturing and characterization of poly(lactic acid) composites with hydroxyapatite”

J.M. Ferri, J. Jordá, N. Montanes, O. Fenollar, R. Balart

Instituto de Tecnología de Materiales (ITM)

Universitat Politècnica de València (UPV)

Plaza Ferrandiz y Carbonell 1, 03801, Alcoy, Alicante (Spain)

Journal of Thermoplastic Composite Materials (Enviado)

Abstract.

Hydroxyapatite (HA), a naturally occurring calcium orthophosphate, possesses the most similar chemical composition to human bone. In this research work, composite materials were prepared by using poly(lactic acid), PLA as a polymer matrix and hydroxyapatite as osteoconductive filler for potential uses in medical applications. Composites with varying hydroxyapatite content comprised in the 10-30 wt% range were obtained by extrusion-compounding followed by injection moulding. The effect of the HA loading on overall properties was assessed by mechanical characterization using tensile, flexural, impact and hardness standard tests. Main thermal transitions of PLA-HA composites were obtained by differential scanning calorimetry (DSC) and degradation/decomposition at high temperatures was followed by thermogravimetric analysis (TGA). Dynamical behavior was assessed by dynamical mechanical thermal analysis (DMTA) and the dimensional stability was studied by thermomechanical analysis (TMA). As per the results, PLA-HA composites with 20-30 wt% HA offer the best-balanced properties with a remarkable increase in the Young's modulus. The glass transition temperature (T_g) remained almost constant with slight changes of less than 1 ^oC as measured by both differential scanning calorimetry (DSC) and thermomechanical analysis (TMA). TMA also revealed a remarkable decrease in the coefficient of linear thermal expansion. The overall results confirm the usefulness of these materials from a mechanical point of view for biomedical applications as they are characterized by high stiffness, tensile strength and dimensional stability.

Keywords: hydroxyapatite; poly(lactic acid); thermal and mechanical properties; screws; bone tissue engineering

Introduction.

Some of the technical requirements for many fixation systems such as screws, fasteners, anchor stitches, etc. are related to mechanical performance and biocompatibility. Research in this field has been intense and today it is possible to find a wide variety of materials (metallic, ceramic, polymeric and composites) [1, 2] for these purposes. Among metals, Ti-based alloys [3, 4] such as Ti6Al4V, CoCr alloys, CoCrMo [5] and stainless steels [6] own an advantageous position because of their high biocompatibility and excellent mechanical performance. However these metallic alloys do not induce the regeneration of the broken bone tissue and needs somewhat surface treatment and/or finishing to promote new tissue proliferation on these materials to give total embedment [7, 8]. The existing treatments are quite laborious, complex and expensive but they play a key role in enabling bone tissue regeneration in the fixing area and avoiding post-surgical rejection of plates and screws. For these reasons, research on new resorbable materials is being conducted with the main aim of avoiding a second surgery to remove the plate and/or screw and obtaining a complete bone tissue integration.

Orthophosphates belong to a family of inorganic phosphates that present a chemical composition that resembles to human bone. Hydroxyapatite (HA) offers the most similar chemical structure to human bone, which is constituted by almost 70 wt% of a hydroxyapatite-type carbonated phosphate. For this reason, hydroxyapatite can be considered a biomimetic material that can avoid any rejection in contact with bone-tissue under typical physiological medium pH conditions [9]. Nevertheless, hydroxyapatite, as other orthophosphates, is extremely brittle and this makes it impossible to use it alone, mainly in medical applications that could be subjected to mechanical stresses or impact. For these reasons, these ceramic materials are used as coating of metallic prostheses, fixation plates, screws, etc. A. Stoch et al. developed hydroxyapatite coatings on Ti6Al4V alloys using the sol-gel method [10]. Jaiswal et al. created new biomimetic nanocomposite scaffolds by electrospinning of poly(l-lactic acid) and a blend of poly(L-lactic acid)/gelatin. The scaffolds were mineralized via

alternate soaking in calcium and phosphate solutions leading to formation on homogeneous hydroxyapatite nanoparticles. The mineralization process remarkably improved the tensile modulus and the tensile strength whilst the brittleness was not increased [11]. Rakmae et al. used bovine bone-based hydroxyapatite (b-HA) as bioactive filler in a poly(lactic acid)-PLA matrix. Calcined bovine powder revealed the typical form of a highly aggregated crystalline carbonated HA. In addition, HA powder was silanized to promote strong polymer matrix-filler interactions. As a consequence, an increase in the overall thermal stability was obtained [12].

The use of polymeric materials in medical devices such as fasteners, fixation plates, screws, etc. has increased in a remarkable way in the last few years as some of them are bioresorbable. Zhou et al. reviewed a variety of materials composed of poly(lactic acid)-PLA, poly(lactic acid-co-glycolic acid)-PLGA and calcium phosphates. They paid special attention to manufacturing methods, bioactivity, cytotoxicity and their potential uses in orthopedic applications [13]. Poly(lactic acid)-PLA and hydroxyapatite scaffolds were successfully obtained by Zhang et al. by combining high-pressure compression-molding and salt-leaching techniques. The obtained scaffolds offered an interconnected open pore structure with a storage modulus almost three times higher regarding to neat PLA scaffolds [14]. Manufacturing of these devices with resorbable materials reduces the probability of rejection and the overall costs as only one surgery is needed [15]. In addition to this, manufacturing processes make attractive the use of polymeric materials for their quick and easy processability by conventional processes such as hot press molding, injection molding, etc. Moreover, with the recent rise of 3D printing technologies, a wide range of possibilities has been expanded with additive manufacturing. Among the wide variety of polymers for medical devices, it is worth to note the use of poly(ester amides)-PEA that have been successfully used as coatings in cardiovascular stents with the additional feature of promoting natural healing [16]. Poly(glycolic acid)-PGA was used to manufacture felts combined with fibrin sealant to prevent leakage in different surgeries thus contributing to a better sealing process [17]. Poly(caprolactone)-PCL offers a wide range of applications as described by Woodruff et al. [18]. Although PCL is a petroleum-derived polymer, its polyester-type chemical structure allows hydrolytic degradation and has

been used for controlled drug release in tissue engineering. Despite this, one of the most promising material for medical applications is poly(lactic acid)-PLA which is also used in several industrial applications [19, 20] due to its excellent balance between cost, processability and overall properties together with biodegradation. Castro-Aguirre at al. collected some of the main uses of PLA in medical devices or implants, in the packaging industry and serviceware components, base material for 3D printing, plasticulture and others [21] thus showing the high potential of this material. It is worth to note that the degradation rate of these biodegradable polymers highly depends on their chemical structure. It is possible to tailor degradation rates for particular uses by polymer blending, chemical modification, etc.

Orthophosphates can also be added as osteoconductive filler in these polymers with two main features: on one hand, it represents the bioactive component in the polymer composite and on the other hand, the organic filler positively contributes to improve mechanical performance of neat polymers. Depending on the medical purpose, polymers can be loaded with different orthophosphates [22]. Rojbani et al. evaluated the osteoconductivity of α-tricalcium phosphate (α-TCP), β-TCP and HA, combined with or without simvastatin as bone regeneration promoter. Their results confirmed that all three particles were osteoconductive materials by acting as space maintainers for bone formation. On the other hand, they also revealed the synergistic effect of simvastatin which stimulates bone regeneration and affects degradation rate of α-TCP and β-TCP [23]. Yamada et al. evaluated the osteoclastic resorption of HA, β-TCP and biphasic calcium phosphate (BCP). The main findings of this work was that β-TCP offers higher solubility rate that the other in acid medium [24]. Hiromoto et al. obtained Mg alloys coated with an octacalcium phosphate and hydroxyapatite which resulted in improved biocompatibility and corrosion resistance [25]. All these particles are soluble in physiological medium [26]. The dissolution rate depends on the Ca/P ratio, which ranges from 0.5 to 2. Ca/P ratios equal to or less than 0.5, as in monocalcium phosphate (MCP) or in monocalcium phosphate monohydrate (MCPM), indicate high dissolution rate; then, the risk of possible inflammation in the body is high. The Ca/P ratio for hydroxyapatite is 1.67, which indicates a moderate to low dissolution rate in physiological serum media. This contributes to provide calcium and

phosphate ions in a progressive and controlled way, which has a positive effect on the mineralization, process among the bone-medical device zone with the subsequent formation of connective tissue and ensuring good osseointegration. Zhang et al. carried out a study with poly(amide)-PA, poly(ethylene)-PE and poly(lactic acid)-PLA with hydroxyapatite particles. The best particle-polymer interaction was observed for PLA and hydroxyapatite due to the higher polarity of PLA [27]. Danoux et al. studied PLA and PLA with 50 wt% HA degradation in physiologic serum. The study revealed the higher degradation rate for neat PLA with regard to the HA-filled formulation [28]. Persson et al. showed excellent cell proliferation in PLA with a hydroxyapatite content of 5 - 20 wt% [29].

The main aim of this work is to assess the potential usefulness of poly(lactic acid)-PLA composites with varying amounts of hydroxyapatite (HA) as osteoconductive filler. The work is mainly focused on the effect of different filler amounts on mechanical and thermal performance of PLA-HA composites. The work also explores the usefulness of conventional extrusion-injection molding techniques to manufacture plastic parts for medical purposes.

Experimental.

Materials.

Poly(lactic acid), PLA IngeoTM Biopolymer 6201D was supplied in pellet form by NatureWorks LLC (Minnetonka, USA) in pellet form. This PLA grade contains a D-lactic acid content of 2%. Its density is 1.24 g cm^{-3} and its melt flow index (MFI) is 15-30 g/(10 min) measured at 210 ^{o}C which allows both injection and extrusion processes. The osteoconductive filler was hydroxyapatite supplied by Sigma Aldrich (Steinheim, Germany) with 35-40% Ca.

Manufacturing of PLA-HA composites.

PLA pellets were previously dried overnight at 60 ºC to remove residual moisture and minimize hydrolysis effects during processing. PLA composites with different HA content specifically between 0-30 wt% HA content (see **Table III.7.1** for detailed compositions and labelling) were manufactured by extrusion in a twin-screw co-rotating extruder at a rotating speed of 60 rpm. The temperature profile was set to 170 ºC (hopper), 175 ºC, 180 ºC and 185 ºC (die). After cooling, PLA-HA composites were pelletized and further processed by injection molding in a Meteor 270/75 from Mateu & Solé (Barcelona, Spain) at an injection temperature of 180 ºC. Rectangular samples 80 x 10 x 4 mm^3 in size were obtained to characterize them, both mechanically and thermally.

Table III.7.1. Compositions and labelling of PLA-HA composites.

Code	wt% poly(lactic acid), PLA	wt% hydroxyapatite, HA
PLA	100	-
PLA-10HA	90	10
PLA-20HA	80	20
PLA-30HA	70	30

Mechanical characterization of PLA-HA composites.

Mechanical properties (tensile and flexural) of PLA-HA composites were obtained in a universal test machine ELIB 30 from S.A.E. Ibertest (Madrid, Spain) at room temperature as recommended by the ISO 527-5 and ISO 178 respectively. A load cell of 5 kN was used for both tests and the crosshead rate was set to 5 mm min^{-1}. A series of five different specimens were tested and the average values of different mechanical properties were calculated. Shore D hardness of PLA-HA composites was obtained in a Shore durometer 673-D from Instrumentos J. Bot S.A. (Barcelona, Spain) following ISO 868. The toughness of PLA-HA composites was measured by the Charpy's impact test in a 1 J Charpy's pendulum from Metrotec S.A. (San Sebastian,

Spain) as indicated in the ISO 179:1993 standard. Five different unnotched samples were subjected to impact conditions and the average values of the impact-absorbed energy were calculated. All the values obtained in each mechanical test were subjected to the statistical outlier rejection "Dixon's Q-Test" with a confidence level of 95%.

Microscopic characterization of PLA-HA composites.

A scanning electron microscope, SEM mod. Phenom from FEI Company (Eindhoven, Netherlands) was used to characterize the surface morphology of fractured samples from impact tests. Samples were subjected to a metallization process with an aurum-palladium (Au-Pd) alloy by sputtering in a sputter-coater mod. EMITECH SC7620 from Quorum Technologies Ltd. (East Sussex, UK). Moreover, PLA-HA composites were subjected to a cryofracture process with liquid N_2. The surface of cryofractured samples was covered with a palladium metallizing layer and subsequently was observed in a field emission scanning electron microscope (FESEM) ZEISS ULTRA55 from Oxford Instruments.

Thermal analysis of PLA-HA composites.

Dynamic mechanical thermal characterization was conducted in an oscillatory rheometer AR G2 from TA Instruments (New Castle, USA), equipped with a torsion clamp accessory for solid samples. Rectangular samples sizing 40x10x4 mm^3 were subjected to a temperature sweep from -50 ^oC to 110 ^oC at a constant heating rate of 2 $^oC\ min^{-1}$. The frequency and the maximum percentage deformation (γ) were set to 1 Hz and 0.1% respectively.

Thermogravimetric analysis (TGA) was carried in a TGA/SDTA thermobalance mod. 851 by Mettler-Toledo Inc. (Schwerzenbach, Switzerland). Samples with an average weight of 10 mg were placed in alumina crucibles and subjected to a heating

program from 30 ºC to 700 ºC at a heating rate of 20 ºC min^{-1} in nitrogen atmosphere with a flow rate of 66 mL min^{-1}.

Main thermal transitions i.e. glass transition temperature (T_g), melt peak temperature (T_m) and enthalpy (ΔH_m) and cold crystallization peak temperature (T_{cc}) and the corresponding enthalpy (ΔH_{cc}) were evaluated in a differential scanning calorimeter (DSC) mod. 821 from Mettler-Toledo Inc. (Schwerzenbach, Switzerland). Samples with an average weight comprised between 7 and 10 mg were placed into standard 40 µL aluminum crucibles and subjected to a heating ramp from 30 ºC to 350 ºC at a constant rate of 10 ºC min^{-1} in air atmosphere. The percentage crystallinity of PLA was calculated using Equation 1.

$$\boldsymbol{X_c}\ (\%) = \frac{\boldsymbol{\Delta H_m - \Delta H_{cc}}}{\boldsymbol{w\ \Delta H_m^0}} 100 \qquad \textbf{Equation 1}$$

where ΔH_m and ΔH_{cc} represent the experimental melting and cold crystallization enthalpies of PLA respectively, and w is the weight fraction of PLA in PLA-HA composites. ΔH_m^0 represents the theoretical melting enthalpy for a fully (100%) crystalline PLA and was assumed to be 93 J g^{-1} as reported in literature [30].

Dimensional stability of PLA-HA composite materials was studied in a thermomechanical analyzer (TMA) working in expansion mode, Q400 V7.4 build 93 from TA Instruments (New Castle, USA). Samples with a size of 7x7x4 mm^3 were subjected to a heating program from 0 to 150 ºC at a heating rate of 2 ºC min^{-1} in nitrogen atmosphere with a flow rate of 50 mL min^{-1} and a static force of 0.02 N. The coefficient of linear thermal expansion (CLTE), α, was determined from the slope of the linear expansion and the glass transition temperature (T_g) was estimated as the temperature range in which the slope of the linear expansion changes.

Results and Discussion.

Effect of hydroxyapatite content on mechanical properties of PLA-HA composites.

PLA/HA composites were manufactured by extrusion followed by injection moulding which is an interesting issue due to the easiness and availability of both manufacturing techniques [31]. Combination of these two techniques allows good particle dispersion which gives high homogeneous materials [31]. In addition, the use of high pressures during injection moulding remarkably reduces the inner porosity of the molded parts. On the other hand, an increase in the processing temperature (below the degradation temperature) allows a decrease in viscosity which has a positive effect on particle wetting [32].

Fig. III.7.1 and **Fig. III.7.2** show the plot evolution of the main parameters obtained from tensile and flexural tests respectively. By considering the results of the tensile tests (**Fig. III.7.1**) it is possible to detect a proportional increase in stiffness with regard to unfilled PLA as the HA loading increases. This increase is more pronounced for 10 wt% HA. At the same time, the tensile strength decreases from 45.3 MPa (2.56 kN (unfilled PLA)) to 32.6 MPa (1.6 kN) for composites containing 30 wt% HA which represents a percentage decrease of about 28%. It is possible to expect somewhat interaction between the filler particles and the polymer matrix. The osteoconductive filler has a porous structure and this contributes to stablish some interactions with the polar groups present in PLA (-COO, -OH, $-CH_3$ and -C=O) and HA (-OH) as reported by Zhang, H.-P., et al. [27]. With regard to elongation at break, neat PLA is characterized by relatively low values around 6.4%. As the HA content increases, a clear decreasing tendency can be observed down to minimum values of about 2.5% for PLA-HA composites with the highest HA content in this study, which represents a percentage decrease of almost 61%. As expected, the elastic modulus, which is representative for the stiffness, increases with HA content thus leading to more rigid materials. This is in total agreement with the evolution of tensile strength and

elongation at break. The elastic modulus represents the ratio between the stress and the elongation in the linear deformation region. Although both parameters decrease with increasing HA content, the decrease is more pronounced for elongation at break, thus leading to stiffer materials.

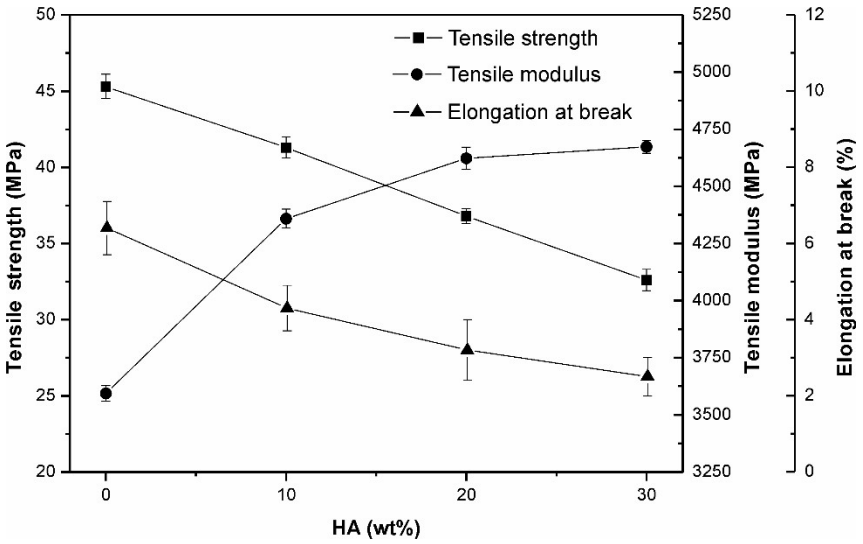

Figure III.7.1. Plot evolution of mechanical properties, tensile strength, tensile modulus and elongation at break from tensile tests as a function of the weight % hydroxyapatite.

Similar tendency can be observed for the flexural properties of PLA-HA composites (**Fig. III.7.2**). Flexural modulus increases (the stiffness increase greatly) as the HA content increases. As expected, the flexural modulus changes in a remarkable way from 3.24 GPa for unfilled PLA up to 4.90 GPa for composites containing 30 wt% HA. In contrast, neat PLA possesses a flexural strength of about 108 MPa and the flexural strength values in terms of the HA content decreases until 54 MPa for composites containing 30 wt% HA. With increasing HA loading, stiffer materials are obtained. In a previous work, similar results were obtained for PLA composites with varying amounts of β-TCP [22]. However, both the elongation at break and the strength were lower for the PLA-β-TCP system compared to their corresponding counterparts in the PLA-HA system. This is due to the fact that HA particles are highly porous (compared to β-TCP particles) and this provides a high surface area which is able to establish interactions with the polar groups in PLA polymer chains [33].

Different polar groups appear in PLA polymer chains such as -OH, -C=O, -COO and -CH_3. These groups and the -OH groups in commercial HA can react or interact to provide improved interactions between both components as demonstrated by Zhang, H.-P., et al. [27]. Once again, the flexural results are much like those reported for the tensile tests. PLA-HA composites containing 10-20 wt% HA represent a good balance between overall mechanical responses as they offer high stiffness materials with slightly lower resistance and deformation ability to neat PLA. It is due a several reasons, first because the degree of crystallinity is higher with lower content of HA (10wt% HA in this study). The HA particles are distributed without aggregates and the effect of nucleating is important in comparison to composites with higher contents. As the content of HA increases, the particle aggregation is more likely to occur and the nucleating effect is not as pronounced. However, the probability of crack is higher because hydroxyapatite aggregates act as crack initiator.

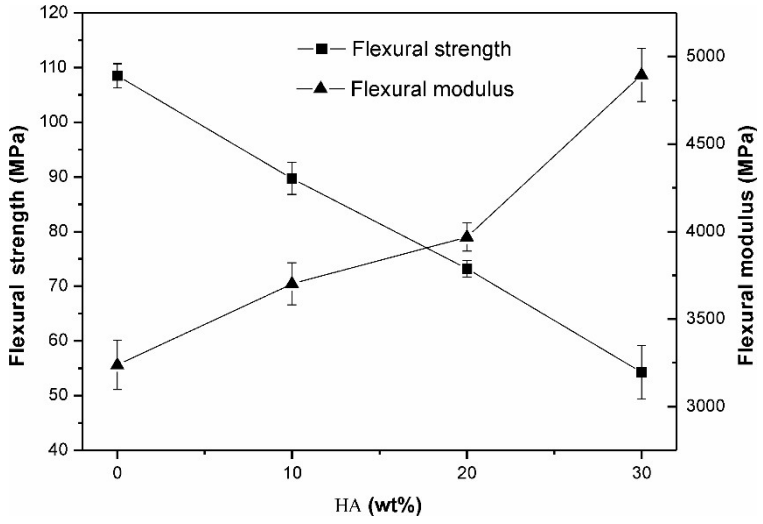

Figure III.7.2. Plot evolution of mechanical properties, tensile strength, tensile modulus and elongation at break from flexural tests as a function of the weight % hydroxyapatite.

Other mechanical properties are represented by the hardness, impact- absorbed energy and the softening point. The evolution of the Shore D hardness (**Table III.7.2**) is similar to other mechanical resistant properties with a clear increase with the HA load.

Table III.7.2. Summary of some mechanical properties i.e. Shore D hardness, Charpy's impact-absorbed energy, Vicat softening temperature (VST) and heat deflection temperature (HDT) for PLA-HA composites with varying hydroxyapatite content.

Property	wt% hydroxyapatite			
	0	10	20	30
Charpy impact energy (KJ m^{-2})	30.9 ± 0.8	11.0 ± 2.6	8.4 ± 3.1	5.7 ± 1.0
Shore D hardness	73.9 ± 0.5	74.3 ± 0.3	77.6 ± 0.6	78.4 ± 0.4
VST (°C)	52.8	52.6	51.4	51.8
HDT (°C)	47.6	53.4	53.8	53.2

Another desirable attracting property in materials for fixation devices is the ability to absorb energy during fracture. **Table III.7.2** summarizes the impact-absorbed energy (Charpy's test) as a function of the hydroxyapatite content. PLA is a quite fragile material as indicated by the relatively low energy absorption values close to 30.9 KJ m^{-2}. It means PLA is not able to absorb energy for deformation before fracture occurs. Addition of hydroxyapatite leads to a considerable decrease in the absorbed energy. For compositions comprised between 10 and 30 wt% hydroxyapatite, the absorbed energy is reduced up to values of 11.0 KJ m^{-2} (percentage decrease of 64%), 8.4 KJ m^{-2} (percentage decrease of about 73%) and 5.7 KJ m^{-2} (percentage decrease of about 81%) respectively. These values indicate that the ability of PLA for energy absorption is highly sensitive to the presence of stress concentrators such as the case of the osteoconductive hydroxyapatite filler. So that, composite materials with HA particles are not the best option for fixation devices that could be subjected to high impacts, although it is excellent for a stiffness pieces like screws. These drawbacks can be overcome by using different strategies. Hasan et al. studied the compatibilizing effect of three different chemical agents, i.e. aminopropyl triethoxysilane (APS), sorbitol ended PLA oligomer (SPLA) and hexamethylene diisocyanate (HDI) between a phosphate glass fiber and poly(lactic acid) polymer. They concluded that the hydrophobic coupling agents (HDI, APS) helped retain mechanical properties for a long period since hydrolysis at interface was delayed [34]. Nainar et al. studied the effect of maleic anhydride compatibilizer on mechanical properties of hydroxyapatite

poly(lactic acid) composites. Maleic anhydride was grafted onto PLA polymer chains and the overall interaction with hydroxyapatite was improved due to reaction of maleic anhydride groups with hydroxyl groups in HA [35].

Table III.7.2 also shows the evolution of the Vicat softening temperature (VST) and the heat deflection temperature (HDT) of PLA-HA composites with varying HA content. Hydroxyapatite particles provide higher rigidity to PLA-HA composites and this is evidenced by a clear increase in HDT by 5-6 ^{o}C. Regarding VST values, they remain almost invariable with different hydroxyapatite content.

The morphology of the cryofractured surfaces of PLA-HA composites was observed by FESEM analysis. **Fig. III.7.3** gathers some FESEM pictures with varying HA loading.

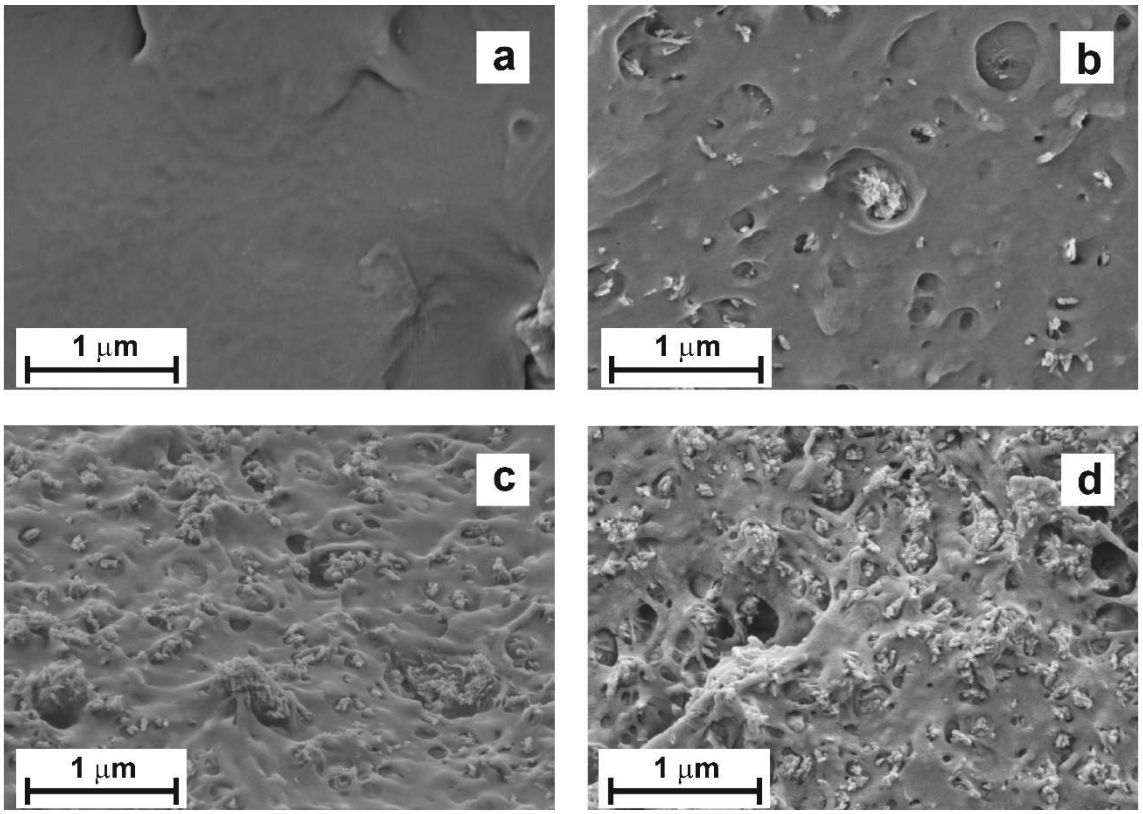

Figure III.7.3. FESEM images at 25000x of cryofractured surfaces corresponding to PLA-HA composites with different wt% hydroxyapatite, a) unfilled PLA, b) 10 wt% HA, c) 20 wt% HA, d) 30 wt% HA.

Fig. III.7.3a shows typical fracture of unfilled PLA with a soft surface, which is representative for fragile fracture with very low deformation. As the HA content increases a rougher surface due to presence of a porous filler can be observed. FESEM images are also useful to assess good particle dispersion after extrusion compounding plus injection moulding. Presence of HA leads to a fracture process characterized by a typical fragile fracture. Increasing the filler content also increases the porosity of the composite and, in consequence, the ability to absorb energy is remarkably reduced as previously described. HA particles seem to be embedded in the PLA matrix for all compositions. **Fig. III.7.4** shows a detailed view of the polymer-particle dispersion and interaction. As it can be seen, the particle dispersion is quite good whilst the particle size range cover a wide span. In general, a very small gap between HA particles and the surrounding PLA matrix can be detected and this leads to a synergistic effect due to somewhat interaction between both components that leads to stiffer materials [13, 27].

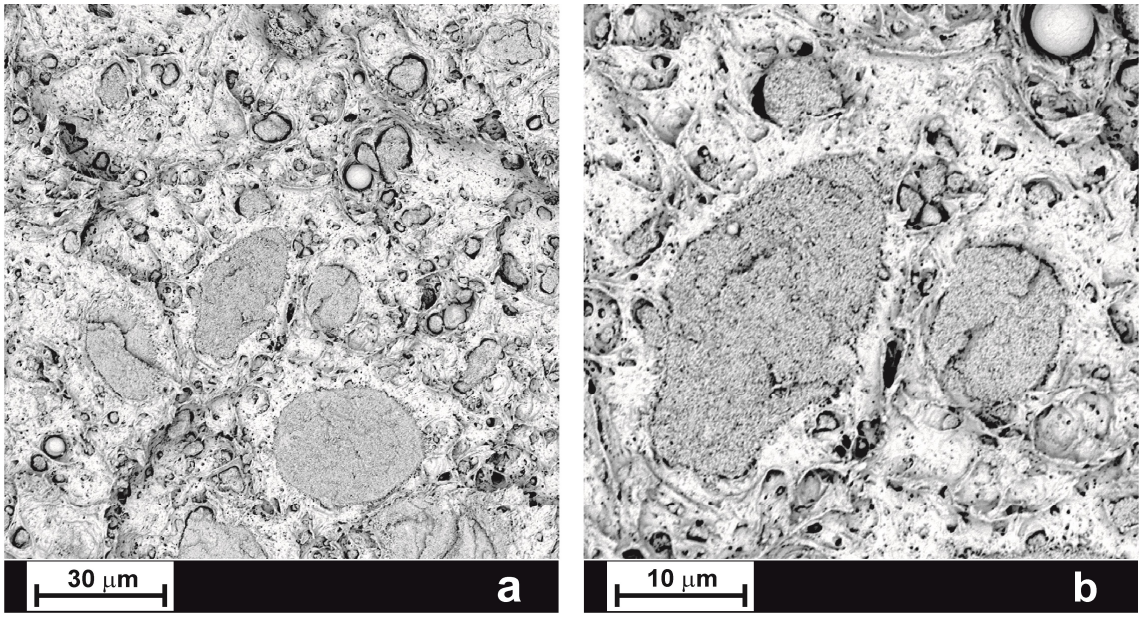

Figure III.7.4. SEM images at 2000X (a) and 5000X (b) of fractured surfaces from Charpy's impact test corresponding to PLA-HA composites with 20 wt% HA.

Effect of hydroxyapatite content on thermal properties of PLA-HA composites.

Thermal transitions of PLA-HA composites were evaluated by differential scanning calorimetry (DSC) and decomposition at high temperatures was assessed by thermogravimetric analysis (TGA). **Table III.7.3** shows a summary of the main thermal transitions of PLA-HA composites obtained by differential scanning calorimetry (DSC).

Table III.7.3. Summary of the main thermal parameters of PLA-HA composites, obtained by differential scanning calorimetry (DSC).

wt% HA	[a]Tg (°C)	[b]T_{cc} (°C)	[c]ΔH_{cc} (J g^{-1})	[d]T_m (°C)	[e]ΔH_m (J g^{-1})	[f]χ (%)
0	64.3	109.7	28.17	172.6	41.19	14.0
10	63.9	99.1	26.78	170.8	46.19	23.2
20	61.7	98.3	25.12	171.2	39.69	19.6
30	59.4	97.5	21.73	169.6	33.28	17.7

[a]T_g is the glass transition temperature of PLA.
[b]T_{cc} is the cold crystallization peak temperature of PLA.
[c]ΔH_{cc} is the crystallization enthalpy of PLA.
[d]T_m is the melting peak temperature of PLA.
[e]ΔH_m is the melting enthalpy of PLA.
[f]χ is the percentage crystallinity of PLA.

A slight decrease in the melt peak from around 173 °C to 170-171 °C can be detected but the overall change is not relevant. Nevertheless, a clear different behavior can be observed for the cold crystallization process with a peak at 110 °C for neat PLA. The cold crystallization process is remarkably shifted to lower temperatures in the 97-99 °C for all PLA-HA composites, which represents a decrease of 10-12 °C with regard to neat PLA. This behavior is mainly due to two overlapping phenomena. On one hand, it is worth to note the strong nucleating effect that crystal HA particles provide to the overall formation of stable spherulites at lower temperatures. In addition, the glass transition temperatures (T_g) of PLA in PLA-HA composites is slightly lower due

to hydrolysis during manufacturing and interaction with a highly hydrophilic filler such as hydroxyapatite. As indicated in Table 3, the T_g for PLA changes from 64 ºC for neat PLA to values lower values up to 59 ºC for the PLA-HA composite containing 30 wt% HA. This could be related to partial hydrolysis of PLA polymer chains due to the presence of a highly hydrophilic filler such as hydroxyapatite which could contribute to hydrolyze some poly(lactic acid) chains and promote a plasticization process with the formed lactic acid oligomers [36]. The difference between the melting and cold crystallization enthalpies increases for all the PLA-HA compositions, although the largest difference is found for PLA/10HA (10 wt% HA). As the HA content increases, the crystallization degree decreases, but in all cases is higher than virgin PLA.

Fig. III.7.5 shows thermogravimetric curves (TGA) for PLA-HA composites with different HA content. PLA is rather stable to temperature; nevertheless, PLA-HA composites show a slight decrease in the degradation onset due to hydrolysis processes. In a similar work, Liu et al. showed that the onset degradation temperature decreased when hydroxyapatite or talc were added to PLA [37]. Siqueira et al. found a remarkable decrease in the onset and the maximum degradation temperature of PLA/β-TCP fiber composites obtained by electrospinning processes [38]. This is more pronounced with increasing the β-TCP content. As it has been reported in literature, hydroxyapatite is a highly hydrophilic inorganic compound and its tendency to moisture gain can affect PLA as this polyester-type polymer is highly sensitive to hydrolysis. Chain scission of poly(lactic acid) molecules leads to formation of lactic acid oligomers (OLAs) which offer less thermal stability at high temperatures than long PLA chains. The percentage residue is directly related to the total hydroxyapatite content. So that, composites containing 20 wt% HA show a residual percentage weight of 19% which corresponds to the HA inorganic filler content. As it can be observed, although the onset degradation temperature is lower for PLA-HA composites with regard to neat PLA, PLA degrades in a narrow temperature range while PLA-HA composites degrade in a broader temperature range.

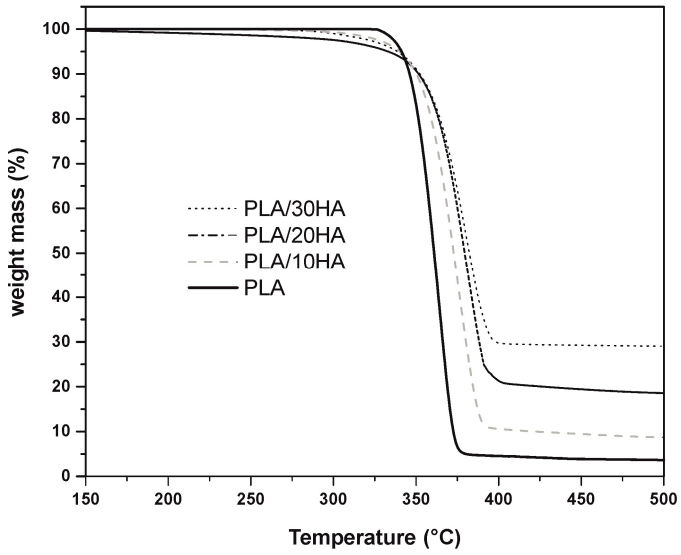

Figure III.7.5. Comparative plot of thermogravimetric (TGA) curves corresponding to PLA-HA composites with different wt% HA.

With regard to dynamic mechanical thermal behavior of PLA-HA composites, **Fig. III.7.6** shows a comparative plot of the storage modulus (G′) as a function of temperature for different HA loads. As one can see, the storage modulus moves to higher values as the HA content increases which is representative for more rigid materials as described previously with regard to tensile properties of PLA-HA composites. The storage modulus remains almost constant up to values of about 60 ^{o}C. A remarkable decrease in G′ (almost three orders of magnitude) occurs in the 60-80 ^{o}C range which is directly related to the glass transition temperature (T_g) of the amorphous phase in poly(lactic acid). A new increase in storage modulus (G′) is detected at temperatures comprised between 85 ^{o}C and 100 ^{o}C. This phenomenon is related to the cold crystallization process which leads to increased crystallinity and, subsequently, an increase in stiffness is achieved. Poly(lactic acid) chains tend to arrange in a packed way as a consequence if its chemical structure. Sometimes, the cooling process at industrial level is very quick and this restricts polymer chain motions thus avoiding crystallization to occur. Nevertheless, the tendency of PLA chains to arrange in a packed way is high and the only action of heat is enough to increase chain mobility. Heating PLA above its T_g allows crystallization to occur and

the packed structure achieved with this is responsible for an increase in the stiffness. In addition, as it can be seen, the typical crystallization temperature range moves to lower temperatures as the HA content increases due to the nucleating effect of finely dispersed HA into the PLA polymeric matrix. As reported by Liuyun et al. the morphology of several hydroxyapatite fillers added to poly(lactic acid-*co*-glycolic acid) composites had a significant effect on dispersion [39]. They demonstrated that the best results were obtained with hydroxyapatite nanoparticle (n-HA) instead of whisker shape hydroxyapatite (w-HA).

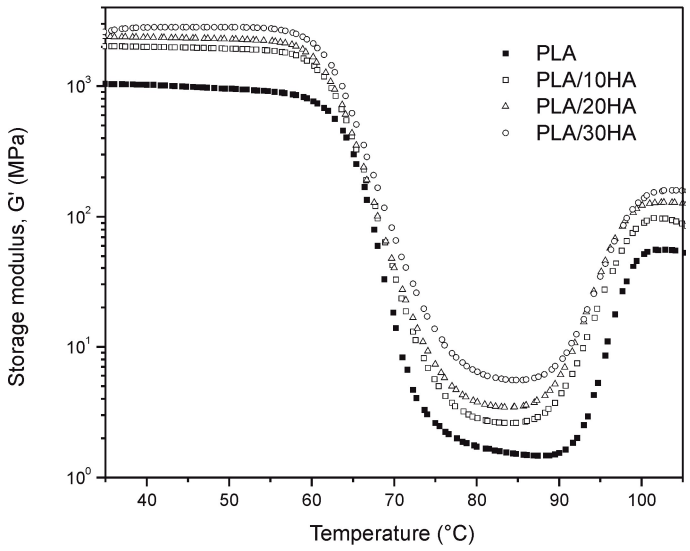

Figure III.7.6. Comparative plot of the evolution of the storage modulus (G') of neat PLA and PLA-HA composites with different wt% HA.

The dimensional stability of PLA-HA composites in terms of the HA loading was assessed by thermomechanical analysis (TMA) and the corresponding plots are shown in **Fig. III.7.7**. It is known that PLA is one of the most stable biodegradable polymers and this plot shows how the osteoconductive filler affects in terms of dimensional stability.

As it can be observed, an increase in the HA content in PLA-HA composites provides increased dimensional stability regarding neat PLA. This is evidenced by the coefficient of linear thermal expansion (CLTE or α) which decreases with the HA

content. This behavior is typical of polymer systems with inorganic fillers. The inorganic filler is characterized by a remarkably lower sensitiveness to temperature and this contributes positively to improved dimensional stability on composites with polymer matrices. These resultas are in accordance to those reported by Hossan et al. They developed gelatin-hydroxyapatite composites and revealed a dramatic increase in dimensional stability with 20 wt% [40]. The PLA-HA composites with the highest dimensional stability is, as expected, the one with 30 wt% HA. Furthermore, thermomechanical analysis (TMA) gives information about the glass transition temperature, T_g. The glass transition represents the change in behavior from a glassy state (below T_g) to a plastic state (above T_g). For this reason, the linear expansion is higher above the T_g as polymer chain mobility is remarkably increased. So that, the temperature range in which a change in the slope of the linear expansion occurs, can be considered as the glass transition temperature range and as it can be observed in **Fig. III.7.7**, follows similar tendency as that observed by DMTA and DSC.

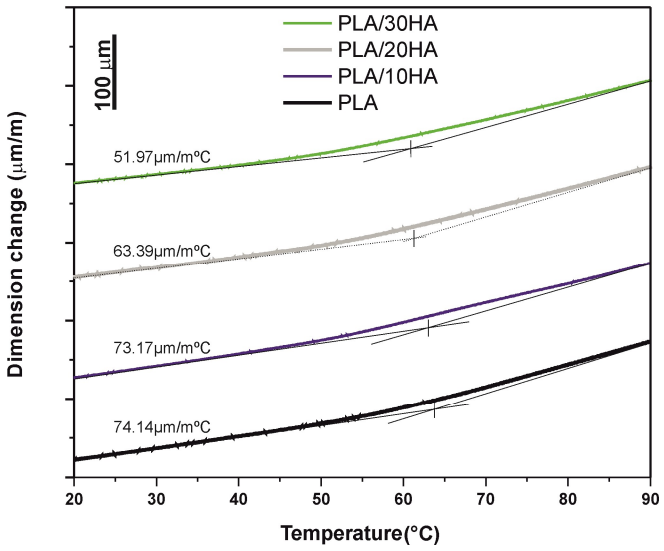

Figure III.7.7. Comparison plot of the dimension changes as a function of temperature obtained by thermomechanical analysis (TMA) for neat PLA and PLA-HA composites with different wt% HA.

Conclusions.

In this work, biocompatible and resorbable composites based on PLA matrix and hydroxyapatite as osteoconductive filler were obtained by extrusion-compounding and subsequent injection moulding. PLA-HA composites with 20-30 wt% HA show the maximum Young's modulus which is 28% higher regarding neat PLA demonstrating a clear increase in stiffness. However, high HA loads (above 20 wt%), produce a significant decrease in toughness and the ability to absorb energy in impact conditions is considerably reduced. Due to the high hydrophilic nature of the HA particles, PLA-HA composites are more hydrophilic than neat PLA and this could be responsible for somewhat hydrolytic degradation of PLA chains. Considering that the working temperature of PLA-HA composites in medical devices is the body temperature 37 ^{o}C, it can be stated that PLA-HA composites containing 20-30 wt% HA show balanced properties in terms of stiffness, toughness and dimensional stability to prevent breakage in medical devices. Nevertheless, it is important to remark that increasing HA leads to highly rigid composites with reduced ability for energy absorption in impact conditions which will have to be considered when designing medical devices with these materials.

Acknowledgments

Authors want to acknowledge the Ministry of Economy and Competitiveness - MINECO, for financial support through the grant number MAT2014-59242-C2-1-R.

References.

1. Duek, E.A.R., Zavaglia, C.A.C., and Belangero, W.D., *In vitro study of poly(lactic acid) pin degradation*. Polymer, 1999. **40**(23): p. 6465-6473.

2. Lewandrowski, K.-U., Bondre, S.P., Shea, M., Untch, C.M., Hayes, W.C., Hile, D.D., Wise, D.L., and Trantolo, D.J., *Composite polylactide-hodroxylapatite screws for fixation of osteochondral osteotomies. A morphometric, histologic and radiographic study in sheep*. Journal of Biomaterials Science, Polymer Edition, 2002. **13**(11): p. 1241-1258.

3. Zhu, K.P., Zhu, J.W., and Qu, H.L., *Development and Application of Biomedical Ti Alloys Abroad*. Rare Metal Materials and Engineering, 2012. **41**(11): p. 2058-2063.

4. Geetha, M., Singh, A.K., Asokamani, R., and Gogia, A.K., *Ti based biomaterials, the ultimate choice for orthopaedic implants - A review*. Progress in Materials Science, 2009. **54**(3): p. 397-425.

5. Webster, T.J. and Ejiofor, J.U., *Increased osteoblast adhesion on nanophase metals: Ti, Ti6Al4V, and CoCrMo*. Biomaterials, 2004. **25**(19): p. 4731-4739.

6. Bordji, K., Jouzeau, E.Y., Mainard, D., Payan, E., Delagoutte, J.P., and Netter, P., *Evaluation of the effect of three surface treatments on the biocompatibility of 316L stainless steel using human differentiated cells*. Biomaterials, 1996. **17**(5): p. 491-500.

7. Choy, M.T., Tang, C.Y., Chen, L., Wong, C.T., and Tsui, C.P., *In vitro and in vivo performance of bioactive Ti6Al4V/TiC/HA implants fabricated by a rapid microwave sintering technique*. Materials Science & Engineering C-Materials for Biological Applications, 2014. **42**: p. 746-756.

8. Metikos-Hukovic, M., Tkalcec, E., Kwokal, A., and Piljac, J., *An in vitro study of Ti and Ti-alloys coated with sol-gel derived hydroxyapatite coatings*. Surface & Coatings Technology, 2003. **165**(1): p. 40-50.

9. Melero H, F.J., Guilemany JM., *Recubrimientos bioactivos: Hidroxiapatita y titania*. Biomecánica 2011. **19**: p. 35-48.

10. Stoch, A., Jastrzebski, W., Dlugon, E., Lejda, W., Trybalska, B., Stoch, G.J., and Adamczyk, A., *Sol-gel derived hydroxyapatite coatings on titanium and its alloy Ti6Al4V*. Journal of Molecular Structure, 2005. **744**: p. 633-640.

11. Jaiswal, A.K., Chandra, V., Bhonde, R.R., Soni, V.P., and Bellare, J.R., *Mineralization of nanohydroxyapatite on electrospun poly(l-lactic acid)/gelatin by an alternate soaking process: A biomimetic scaffold for bone regeneration*. Journal of Bioactive and Compatible Polymers, 2012. **27**(4): p. 356-374.

12. Rakmae, S., Ruksakulpiwat, Y., Sutapun, W., and Suppakarn, N., *Physical properties and cytotoxicity of surface-modified bovine bone-based hydroxyapatite/poly(lactic acid) composites*. Journal of Composite Materials, 2011. **45**(12): p. 1259-1269.

13. Zhou, H.L., J.G.; Bhaduri, S.B., *Fabrication aspects of PLA-CaP/PLGA-CaP composites for orthopedic applications: A review*. Acta Biomaterialia, 2012. **8**: p. 1999-2016.

14. Zhang, J.Y., Hua-Mo.; Hsiao, Benjamin S.; Zhong, Gan-Ji.; Li, Zhong-Ming., *Biodegradable poly(lactic acid)-hydroxyl apatite 3D porous scaffolds using high-pressure molding and salt leaching*. Journal of Materials Science, 2014. **49**(4): p. 1648-1658.

15. Hutmacher, D.W., Goh, J.C.H., and Teoh, S.H., *An introduction to biodegradable materials for tissue engineering applications*. Annals Academy of Medicine Singapore, 2001. **30**(2): p. 183-191.

16. DeFife, K.M., Grako, K., Cruz-Aranda, G., Price, S., Chantung, R., Macpherson, K., Khoshabeh, R., Gopalan, S., and Turnell, W.G., *Poly(ester amide) Co-polymers Promote Blood and Tissue Compatibility*. Journal of Biomaterials Science, Polymer Edition, 2009. **20**(11): p. 1495-1511.

17. Liu, Y., Xie, D., Chi, C., Lin, X., and Lin, C., *Combined application of fibrin sealant and polyglycolic acid felt in surgery for pneumothorax due to emphysema*. International Journal of Clinical and Experimental Medicine, 2016. **9**(2): p. 4182-4185.

18. Woodruff, M.A. and Hutmacher, D.W., *The return of a forgotten polymer: Polycaprolactone in the 21st century*. Progress in Polymer Science, 2010. **35**(10): p. 1217-1256.

19. Le Duigou, A., Deux, J.-M., Davies, P., and Baley, C., *PLLA/Flax Mat/Balsa Bio-Sandwich Manufacture and Mechanical Properties*. Applied Composite Materials, 2011. **18**(5): p. 421-438.

20. Le Duigou, A., Deux, J.-M., Davies, P., and Baley, C., *PLLA/Flax Mat/Balsa Bio-Sandwich – Environmental Impact and Simplified Life Cycle Analysis*. Applied Composite Materials, 2012. **19**(3): p. 363-378.

21. Castro-Aguirre, E., Iñiguez-Franco, F., Samsudin, H., Fang, X., and Auras, R., *Poly(lactic acid)-Mass production, processing, industrial applications, and end of life*. Advanced Drug Delivery Reviews, 2016. **107**: p. 333-366.

22. Ferri, J., Gisbert, I., García-Sanoguera, D., Reig, M.J., and Balart, R., *The effect of beta-tricalcium phosphate on mechanical and thermal performances of poly(lactic acid)*. Journal of Composite Materials, 2016. **50**(30): p. 4189-4198.

23. Rojbani, H., Nyan, M., Ohya, K., and Kasugai, S., *Evaluation of the osteoconductivity of a-tricalcium phosphate, β-tricalcium phosphate, and hydroxyapatite combined with or without simvastatin in rat calvarial defect*. Journal of Biomedical Materials Research. Part A, 2011. **98A**(4): p. 488-498.

24. Yamada, S., Heymann, D., Bouler, J.M., and Daculsi, G., *Osteoclastic resorption of calcium phosphate ceramics with different hydroxyapatite/β-tricalcium phosphate ratios*. Biomaterials, 1997. **18**(15): p. 1037-1041.

25. Hiromoto, S., Inoue, M., Taguchi, T., Yamane, M., and Ohtsu, N., *In vitro and in vivo biocompatibility and corrosion behaviour of a bioabsorbable magnesium alloy coated with octacalcium phosphate and hydroxyapatite*. Acta Biomaterialia, 2015. **11**: p. 520-530.

26. Bohner, M., *Calcium orthophosphates in medicine: from ceramics to calcium phosphate cements*. Injury-International Journal of the Care of the Injured, 2000. **31**: p. S37-S47.

27. Zhang, H.-p., Lu, X., Leng, Y., Fang, L., Qu, S., Feng, B., Weng, J., and Wang, J., *Molecular dynamics simulations on the interaction between polymers and hydroxyapatite with and without coupling agents*. Acta Biomaterialia, 2009. **5**: p. 1169-1181.

28. Danoux, C.B., Barbieri, D., Yuan, H., de Bruijn, J.D., van Blitterswijk, C.A., and Habibovic, P., *In vitro and in vivo bioactivity assessment of a polylactic acid/hydroxyapatite composite for bone regeneration*. Biomatter, 2014. **4**: p. e27664.

29. Persson, M., Lorite, G.S., Kokkonen, H.E., Cho, S.-W., Lehenkari, P.P., Skrifvars, M., and Tuukkanen, J., *Effect of bioactive extruded PLA/HA composite films on focal adhesion*. Colloids and Surfaces B: Biointerfaces, 2014. **121**: p. 409-416.

30. Russias, J.S.E., Nalla, R.K., Gryn, K., Ritchie, R.O., and Tomsia, A.P., *Fabrication and mechanical properties of PLA/HA composites-A study of in vitro degradation*. Materials Science and Engineering: C, 2006. **26**(8): p. 1289-1295.

31. Mathieu, L.M., Bourban, P.E., and Manson, J.A.E., *Processing of homogeneous ceramic/polymer blends for bioresorbable composites*. Composites Science and Technology, 2006. **66**(11-12): p. 1606-1614.

32. Dee, G.T. and Sauer, B.B., *The surface tension of polymer liquids*. Macromolecular Symposia, 1999. **139**: p. 115-123.

33. Zhang, R. and Ma, P.X., *Porous poly(L-lactic acid) apatite composites created by biomimetic process*. Journal of Biomedical Materials Research, 1999. **45**(4): p. 285-293.

34. Hasan, M., Ahmed, I., Parsons, A., Walker, G., and Scotchford, C., *Cytocompatibility and Mechanical Properties of Short Phosphate Glass Fibre Reinforced Polylactic Acid (PLA) Composites: Effect of Coupling Agent Mediated Interface*. Journal of Functional Biomaterials, 2012. **3**(4): p. 706-725.

35. Nainar, S.M., Begum, S., Hasan, Z., Ansari, M.N.M., and Anuar, H., *Influence of maleic anhydride on mechanical properties and morphology of hydroxyapatite/poly-(lactic acid) composites*. Regenerative Research, 2012. **1**(2): p. 32-38.

36. Carlson, D., Dubois, P., Nie, L., and Narayan, R., *Free radical branching of polylactide by reactive extrusion*. Polymer Engineering and Science, 1998. **38**(2): p. 311-321.

37. Liu, X., Wang, T., C. Chow, L., Yang, M., and W. Mitchell, J., *Effects of Inorganic Fillers on the Thermal and Mechanical Properties of Poly(lactic acid)*. International Journal of Polymer Science, 2014. **1:** p. 1-8.

38. Siqueira, L., Passador, F.R., Costa, M.M., Lobo, A.O., and Sousa, E., *Influence of the addition of β-TCP on the morphology, thermal properties and cell viability of poly (lactic acid) fibers obtained by electrospinning*. Materials Science and Engineering: C, 2015. **52**: p. 135-143.

39. Liuyun, J., Chengdong, X., Lixin, J., and Lijuan, X., *Effect of hydroxyapatite with different morphology on the crystallization behavior, mechanical property and in vitro degradation of hydroxyapatite/poly(lactic-co-glycolic) composite*. Composites Science and Technology, 2014. **93**: p. 61-67.

40. Hossan, M.J., Gafur, M.A., Karim, M.M., and Rana, A.A., *Mechanical properties of Gelatin –Hydroxyapatite composite for bone tissue engineering*. Bangladesh Journal of Scientific and Industrial Research, 2015. **50**(1): p. 15-20.

Journal of Thermoplastic Composite Materials JTCM-16-0217 Recibidos x

Journal of Thermoplastic Composite Materials <onbehalfof+pod+udel.edu@manuscriptcentral.com> 7/12/16

para joferaz

inglés › español Traducir mensaje Desactivar para: inglés ×

07-Dec-2016

Dear Mr. Ferri Azor:

Your manuscript entitled "Manufacturing and characterization of poly(lactic acid) composites with hydroxyapatite" has been successfully submitted online and is presently being given full consideration for publication in Journal of Thermoplastic Composite Materials.

Your manuscript ID is JTCM-16-0217.

Please mention the above manuscript ID in all future correspondence or when calling the office for questions. If there are any changes in your street address or e-mail address, please log in to ScholarOne Manuscripts at https://mc.manuscriptcentral.com/jtcm and edit your user information as appropriate.

You can also view the status of your manuscript at any time by checking your Author Center after logging in to https://mc.manuscriptcentral.com/jtcm.

Thank you for submitting your manuscript to Journal of Thermoplastic Composite Materials.

Sincerely,
Journal of Thermoplastic Composite Materials Editorial Office

IV. CONCLUSIONES

CONCLUSIONES

IV. Conclusiones

Las principales conclusiones obtenidas en la presente tesis doctoral se resumen a continuación:

Se han estudiado los efectos de plastificación que conlleva el mezclado físico de de polímeros biodegradables dúctiles (TPS y PCL) con el PLA. En dicho análisis se ha observado que la miscibilidad (solubilidad entre polímeros) es un factor decisivo para que dichas mezclas experimenten un incremento en su ductilidad. El TPS y la PCL muestran pobre o nula miscibilidad con el PLA y es por eso que las principales transiciones térmicas (T_g, T_{cc} y T_m) del PLA experimentan cambios insignificantes. De igual forma, la estabilidad térmica también experimenta cambios leves. Además, las mezclas PLA/PCL experimentan una pérdida en la absorción de energía a impacto, tanto mayor según aumenta el contenido de PCL.

Sin embargo, las mezclas PLA/TPS si experimentan un aumento significativo de la absorción de energía a impacto Charpy. La miscibilidad parcial conseguida entre ambos componentes se atribuye al poliéster alifático/aromático biodegradable (AAPE) contenido en el TPS, que muestra una mayor interacción con el PLA y aumenta la solubilidad de la mezcla binaria.

A pesar de esto, dichas mezclas binarias muestran un aumento en la ductilidad del PLA. Concretamente, las mezclas PLA/TPS y PLA/PCL consiguen aumentar su alargamiento a la rotura un 21.5% (PLA/30wt%TPS) y un 85% (PLA/22.5wt%PCL), respectivamente.

Por otra parte, en los estudios de degradación en compost se observó que pequeñas cantidades de PCL aceleran la degradación del PLA.

En un segundo bloque se han analizado los aceites vegetales modificados que ejercen un gran efecto sobre la plastificación del PLA. La adición de OES a la matriz de PLA aumenta el alargamiento a la rotura en torno a un 40% (5phr OES) y sobre un 75%

mas, la absorción de energía a impacto. A mayores contenidos se experimenta un efecto de antiplastificación.

El OES permite un mayor movimiento de las cadenas poliméricas y en consecuencia, un aumento de la cristalinidad y un descenso de la T_g y T_{cc} importante (en torno a 10°C). En consecuencia, sus propiedades barrera mejoran. La permeabilidad a oxígeno medida a los films de la formulación PLA/5phr OES disminuye de forma considerable comparándose con los films de PLA. El aumento de cristalinidad ofrece mayor resistencia a la difusión del oxígeno.. Además, la adición de OES al PLA aumenta su hidrofobicidad al agua.

El MLO presenta niveles de alargamiento a la rotura superiores a los obtenidos con el plastificante OES, así como una mejora en las propiedades a impacto sin llegar a comprometer la rigidez (el módulo de Young se ve levemente afectado) de los materiales plastificados. El incremento de movilidad de las cadenas poliméricas que aporta el MLO permite reducir el valor de la T_g y la T_{cc} (en torno a 7°C) y ello repercute en un incremento de la cristalinidad dando lugar a una serie de materiales con ductilidad mejorada y con un gran potencial para su uso en el sector del envase y embalaje.

Cabe destacar que el MLO actúa de agente compatibilizador en las mezclas binarias PLA/TPS, aumentando la miscibilidad entre ambos de forma muy notoria como se observa en FESEM. El alargamiento a la rotura pasa de un 21.5% (PLA/30TPS) a un 160% para la misma mezcla añadiendo tan solo un 6 phr MLO. Además, la absorción de energía a impacto también aumenta considerablemente, pasando de 5,3 kJ/m^{-2} de la formulación PLA/30TPS a 9,5 kJ/m^{-2} para la formulación PLA/30TPS con un 6 phr MLO.

El resultado del efecto de compatibilización repercute en un aumento de la estabilidad térmica del PLA y en un descenso importante de la T_g y T_{cc} con respecto a los valores obtenidos para las mezclas sin MLO.

En el tercer bloque, las cargas biocompatibles/bioabsorbibles de la familia de los ortofosfatos (β-TCP y HA) utilizadas aportan un efecto rigidizante importante al PLA para su uso en la fabricación de determinadas prótesis, tornillos, fijaciones, etc. aumentando su potencial uso en el sector médico.

El método de fabricación de extrusión e inyección presenta buenas dispersiones de las partículas osteoconductoras en el seno de PLA. Desde el punto de vista de las propiedades mecánicas, se consigue alta rigidez con composiciones en β-TCP y HA de hasta un 30% en peso. Ambos tipos de partículas muestran un efecto nucleante aumentando la cristalinidad y aportando, en consecuencia, una mayor rigidez a dichos composites.

En términos de estabilización térmica, la HA tiene un efecto positivo sobre el PLA, mientras que el β-TCP empeora la estabilidad debido a su carácter higroscópico. Las principales transiciones térmicas (T_g y T_{cc}) se ven afectadas ligeramente, aunque mayormente para el caso de los composites PLA/HA.

Como conclusión global del presente trabajo, se puede indicar que la plastificación del PLA mediante los mecanismos llevados a cabo en esta tesis demostraron su potencial como materiales destinados al envasado de alimentos principalmente por las mejoras conseguidas sobre la ductilidad y en determinados casos sobre la mejora de la biodegradabilidad y propiedades barrera. Además, los composites realizados aportan una mejora en la rigidización que es necesaria para la fabricación de determinados sistemas de fijaciones utilizadas en el sector médico.